Morphometric properties and bone mineral density of the lumbar spine in a South African population: surgical considerations for spinal fusion

Submitted by:

Anya König

BSc (Hons) Anatomy,

University of Pretoria, 2016

Master's Thesis

A thesis submitted to the Department of Anatomy, School of Medicine, Faculty of Health Sciences, University of Pretoria, in fulfilment of the requirements for the degree

of

Master of Science in Anatomy

Pretoria

2018

Supervisor: Dr N Keough

Co-supervisor: Dr J Myburgh

DECLARATION

I, Anya König, declare that this thesis is my own work. It is being submitted for the degree of MSc in Anatomy at the University of Pretoria. It has not been submitted before for any other degree or examination at this or any other Institution.

Sign: _____

This ____ Day of _____ __ _____, 2018

TABLE OF CONTENTS

LIST OF FIGURES

LIST OF TABLES

ABSTRACT

The raised prevalence of lumbar spine pathologies and injuries, has lead to the investigation into more efficient and less invasive treatments for these diseases. In order to establish more specialised techniques, various authors have turned their attention to the morphometrics and material properties of the lumbar spine. Some of these properties might be considered as population specific, however possible trends have not yet been investigated in certain population groups. This study aimed to determine which factors, if any, might be specific to South African population groups.

Twenty white adult (age > 20) cadaver specimens were obtained from the University of Pretoria (n = 12) and the University of Witwatersrand (n = 8), of which nine were male and eleven female. The lumbar spines were dissected to measure parameters of Kambin's triangle (a safety zone used to avoid the dorsal nerve root and ganglion during microdiscectomies), and record the position of the dorsal root ganglion (DRG) in relation to the caudal pedicle. Computed Tomography (CT) scans, obtained from Steve Biko Academic Hospital (SBAH), were used to determine the lumbar lordosis angle (LLA), bone mineral density (BMD), and morphometrics of healthy lumbar spines. The sample consisted of eighty-two adult scans of which forty-six were male (33 black; 13 white) and thirty-six female (22 black; 14 white). Magnetic Resonance Imaging (MRI) scans, also from SBAH, were used to measure the neural foramen, and map the position of the nerve root and ganglion within. The sample consisted of twenty-six black adult scans (9 female; 17 male).

The DRG's were generally seen at the midline of the caudal pedicle. The dimensions of Kambin's triangle showed little variation between sexes. The lordosis angles, most morphometric parameters, and most BMD parameters varied greatly between groups and sexes. The neural foramen and nerve root measurements indicated little variation between sexes. When comparing measurements between vertebral levels for all three components, patterns of increase, decrease, or combinations thereof were seen when moving caudally in the spine.

Population differences were seen for some parameters. Also, some differences were evident when comparing results from the current study to previous studies, however the exact reason for variation was not established. Therefore, further investigation is needed into the cause of variation in trends between and within the population groups.

Keywords: Lumbar spine; South African; Population trends; BMD; CT; Hounsfield Units; Morphometrics; Kambin's triangle; Cadavers; Dorsal nerve root

ACKNOWLEDGEMENTS

Firstly, I would like to thank our Heavenly Father for the opportunity and means to perform research on the remarkably intricate human body. A body designed by Him so we as anatomists can appreciate the complexities thereof.

I would also like to thank Dr Keough and Dr Myburgh for all their support, knowledge, and guidance throughout this research journey. Words could not express my gratitude for their seemingly endless patience, and their steadfast faith in my abilities. They have cultivated important research and life skills in me, in order to produce the researcher I am today.

Next, I would like to thank the University of Pretoria for allowing me the opportunity to utilise their facilities in order to perform my postgraduate research. I would like to thank the staff of the Department of Anatomy and Prof. Bosman for allowing me to use the departmental cadaver material and specialised equipment. I would also like to thank Mr Lewis for all his technical advice and for always being willing to lend a helping hand. I would like to thank Marinda Pretorius for her graphical input in the project, and for creating the images used.

I would like to acknowledge the Biostatistical Unit of the Medical Research Council and Charl Janse van Rensburg for their extensive contribution towards the statistical analyses.

I would also like to thank Steve Biko Academic Hospital, its radiology department and Dr Joseph, Prof Lockhat and Prof Suleman for allowing me to use the radiographic material (MRI and CT) for this study, and for taking the time to obtain patient demographics.

The University of Witwatersrand also deserves thanksgiving, as they provided me with the additional cadaver specimens needed to complete my sample and obtain a reasonable sample size. Special thanks to Dr Brits and Mr Nicholas Bacci for making this opportunity possible.

I would also like to thank my family for all the support and understanding you have given me. Your unending encouragement has not gone unnoticed. Thank you for enduring the more difficult times with me, and for showing me that staying focused and never giving up, will result in success.

I would like to thank my God through Jesus Christ, for all the people and opportunities He has put on my life path. Without the necessary individuals and the necessary skills learnt in certain circumstances, I would not have been able to achieve the goals I have set.

CHAPTER 1: INTRODUCTION

The incidence of lumbar spine or lower back problems is rapidly increasing in our modern-day society (Manchikanti, 2000, Hoy *et al.*, 2010). This is mostly a result of evolving lifestyle factors such as poor posture and greater longevity (O'Sullivan *et al.*, 2002, Pope *et al.*, 2002, Adams and Roughley, 2006, Bjorck-van Dijken *et al.*, 2008, Manchikanti *et al.*, 2014). Lower back pain is not the only disorder of the lumbar spine that has shown an increase in prevalence over the years. Lumbar spine surgery has also shown a raised incidence due to degenerative disorders associated with longevity and lifestyle effects on posture, which can lead to pathological changes in intervertebral discs and muscle support (Jones *et al.*, 1998, Liuke *et al.*, 2005, Lee *et al.*, 2006, Schumann *et al.*, 2010, Magee, 2014, Zampolin *et al.*, 2014, Barr *et al.*, 2016, Coric *et al.*, 2017, Gardocki and Park, 2017, Lund and de Moraes, 2017).

The increase in surgical intervention has led to a higher frequency of post-operative complications (Kumar *et al.*, 2001, Hilibrand and Robbins, 2004, Park *et al.*, 2004, Rampersaud *et al.*, 2006, Martin *et al.*, 2007, Radcliff *et al.*, 2013, Hu *et al.*, 2014). The rise in post-operative complications is not due to poor interventions, but present due to the increasing amount of surgical procedures resulting in larger samples of patients, meaning that the chance of encountering complications will be greater. The number of revisit rates for these surgeries has sparked the investigation into patient specific preoperative screening, in order to determine the best preventative methods. Researchers have been investigating the material and morphometric properties and the variation of the human spine within individual populations to assist with refining patient and population specific screening (Fehily, 1989, Mosner *et al.*, 1989, Schnitzler *et al.*, 1990, Gilsanz *et al.*, 1991, McCormick *et al.*, 1991, O'Neill *et al.*, 1994, Seeman, 1997, Norton *et al.*, 2002, Tan *et al.*, 2004, Looker *et al.*, 2009, Vialle *et al.*, 2015, Zengin *et al.*, 2016, Hurday *et al.*, 2017). The use of anatomical considerations in order to either improve existing techniques, or establish new approaches, have been the main subject of investigation (Perese and Fracasso, 1959, Merloz *et al.*, 1998, Rampersaud *et al.*, 2006, Benglis Jr. *et al.*, 2009, Uribe *et al.*, 2010, Hu *et al.*, 2014, Lehmen and Gerber, 2015, Choi *et al.*, 2016a). Understanding how these anatomical considerations are affected by population specifics, may aid in this goal to customise surgical techniques to optimise the outcome.

Surgeons from various disciplines have been utilising less invasive techniques with the hope of improving post-operative recovery time and to reduce certain risks during surgery. One of these minimally invasive techniques is known as arthroscopic surgery. This is performed using an arthroscope (an optical instrument), television cameras and surgical tools, which are inserted through portals separate from the one made for the arthroscope (Phillips, 2017). This technique enables surgeons to perform certain surgical procedures without having to create a large incision to access the area where the procedure needs to be performed. However, because the field of view is limited, a sound knowledge of the location of important structures in relation to the surgical field should be established. Kambin's triangle is an anatomical region defined and investigated by previous authors, which allows safe arthroscopic access to damaged intervertebral discs (IVDs) without injuring the important posterior or dorsal nerve root and ganglion (DNR and DRG) exiting the neural foramen (Mirkovic *et al.*, 1995, Matuoka and Basile Júnior, 2002, Hulme *et al.*, 2007). Knowing whether differences in the parameter exist between and within population groups, will enable specialists to be aware of potential variations present within or between groups. If variations or differences are present, then the knowledge of them will assist in avoiding damage to the essential structures, which might be in a different location than anticipated.

Determining the position of the DNR and DRG within the neural foramen is also important, as this could not only aid in arthroscopic disc procedures, but also those involving the correction of stenosis due to osteophyte formation or disc bulging (Lee *et al.*, 2006, Magee, 2014, Barr *et al.*, 2016). Determining the position of the DNR, will then aid in reconstructing the foramen, thereby avoiding damage to the root. However, the neural foramen is not the only important skeletal structure to consider. The rest of the vertebral osteology is also important for surgical considerations. Knowing how morphology and dimensions change between levels, and whether specific population trends exist between or within population groups, can greatly improve surgical approaches and influence the customisation of procedures for specific patients from different population groups (Eisenstein, 1977, Gilsanz *et al.*, 1994, Lee *et al.*, 1995, Tan *et al.*, 2004, Shaw *et al.*, 2015).

Bone mineral density (BMD) is the measure of the amount of calcium in bone, and can be used to determine or understand the integrity of bone (Celenk and Celenk, 2012). Determining the integrity of lumbar vertebrae can aid in understanding how alterations (either pathological, idiopathic, or iatrogenic) in the structural properties of the bone can affect the outcome of certain

treatment modalities involving bone-altering techniques. Determining whether normal BMD ranges are specific to certain population groups, will enable specialists to optimise their surgical approaches with regards to patients from different groups. If standard normal ranges do vary between populations and population groups, then comparing an individual from theoretical population X, to theoretical population Y's standards, could result in either misdiagnosing a healthy individual as diseased, or a diseased individual as healthy. Furthermore, different treatment modalities (pre- and postoperatively) and surgical approaches are employed in certain situations for patients with diseased bone, as opposed to those with healthy bone (Coe *et al.*, 1990, Halvorson *et al.*, 1994, Lim *et al.*, 2001, Cook *et al.*, 2004, Burval *et al.*, 2007, Becker *et al.*, 2008, Ponnusamy *et al.*, 2011, Yagi *et al.*, 2011). Therefore, determining possible population specificity will also avoid potential misdiagnoses, and subsequent mistreatments.

The current study is comprised of two components, a cadaver dissection component, and a radiographic imaging component, which was further subdivided into a CT (Computed Tomography) and an MRI (Magnetic Resonance Imaging) component. The primary objective of the cadaver component was to determine the ranges of the parameters of Kambin's triangle for the cadaver sample. The secondary objective was to record the position of the DRG on the left – and right-hand sides of each vertebral level. Both these objectives were achieved through dissection of cadaver specimens obtained from the University of Pretoria and the University of Witwatersrand. The CT component aimed to determine the material and morphometric properties of the vertebrae, whereas the MRI component aimed to determine the morphometric properties of the neural foramen and the DNR and DRG within the foramen. These objectives were achieved through the use radiographic images obtained from the Steve Biko Academic Hospital (SBAH).

CHAPTER 2: LITERATURE REVIEW

2.1 Anatomy of the lumbar spine

The lumbar spine has two important functional roles, namely strength and flexibility. It provides support and protection to the spinal canal and its contents, as well as flexibility for positioning of the lower limbs. The spine receives it strengthening properties from vertebrae, muscles, and ligaments, while its flexibility can be owed to the large number of joints placed close to each other. Each of the vertebral segments can be divided into three parts: one intervertebral disc (IVD) with the vertebral endplates and two zygapophyseal joints. The characteristic lordotic curvature of the lumbar spine not only assists with its flexibility, but also enhances the shock-absorbing properties of the spine (Barr *et al.*, 2016).

In order to understand the material properties and the biomechanical functionality of the lumbar spine, a background knowledge of the anatomy (osteology and soft tissue) should be established.

2.1.1 Osteology of the lumbar spine

The lumbar spine consists of five lumbar vertebrae. Each vertebra is formed by a vertebral body and the posterior elements (Figure 2.1). The bodies increase in size as the position moves more caudally in the spine. The lumbar curvature or lumbar lordosis angle (LLA) (Figure 2.2) is formed by the wedge-shaped bodies of the lower three vertebrae, which generally display larger anterior heights as opposed to posterior heights (Magee, 2014).

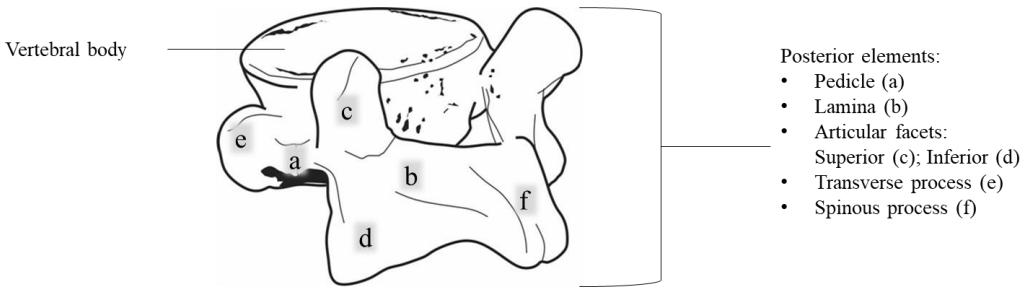

Figure 2.1: Figure showing the posterior view of a typical lumbar vertebra with the body and posterior elements

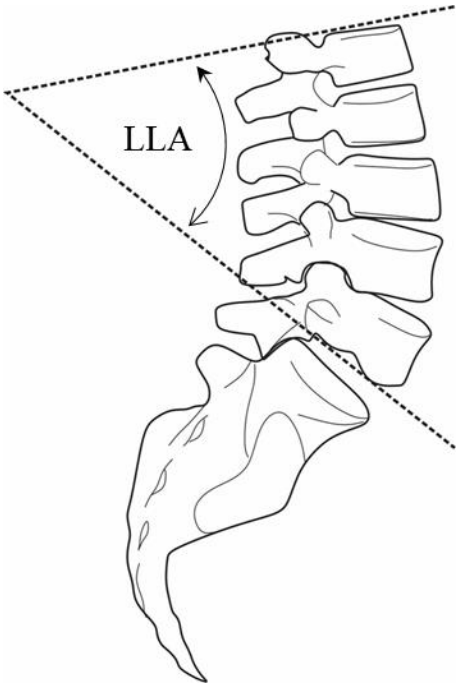

Figure 2.2: Image indicating the lumbar spine lordosis or lumbar lordosis angle (LLA). Adapted from Ghandhari *et al.* (2013)

An important skeletal landmark on the vertebrae is the neural foramen. It is an aperture formed by the superior – and inferior vertebral notches of the two adjacent vertebrae, providing a route for the exiting segmental spinal nerves and the entering vessels and nerves supplying the bone and soft tissue structures (Parke *et al.*, 2011).

The load bearing capacity of the vertebral bodies mainly depend on their bone mineral density (BMD), geometry, mass, and architecture (Kurutz, 2010). The posterior elements consist of the pedicles, laminae, and the articular –, transverse –, and spinous processes. The superior – and inferior articular processes of adjacent vertebrae form the zygapophyseal (facet) joints. These joints generally do not carry excessive weight, but the weight distributed onto the joint increases as the extension angle increases (Magee, 2014). With a normal intact disc, the facet joints carry only around 20% to 25% of the axial load, but disc degeneration may lead to an increase of up to 70% (Magee, 2014). The regions on the laminae between the superior – and inferior articular processes are known as the pars interarticularis and is the site where stress fractures (spondylolysis) commonly occur (Barr *et al.*, 2016). The superior articular processes (facets) face

posteromedially and are usually concave, while the inferior articular processes face anterolaterally and are usually convex (Magee, 2014).

2.1.2 Soft tissue of the lumbar spine

Muscles and ligaments

The muscles of the lumbar spine can be divided into anterior – and posterior groups. The posterior muscles can be further subdivided into a superficial and deep group. The deep muscles are known as the paramedian transversospinales group and includes: the polysegmental multifidus muscles, short intersegmental interspinales, intertransversarii, and short rotatores. The more superficial muscles include the erector spinae muscles (iliocostalis, longissimus and spinalis) (Waldman and Campbell, 2011, Kim and Garfin, 2018). Figure 2.3 displays the important erector spinae and multifidus muscles. The main function of the posterior back muscles is to extend the spine whilst maintaining stability and aiding in proprioception (Magee, 2014). The anterior muscle group includes psoas major and minor and quadratus lumborum. The psoas muscles aid with accentuating the lordosis of the lumbar spine while quadratus lumborum mainly causes lumbar flexion (Barr *et al.*, 2016).

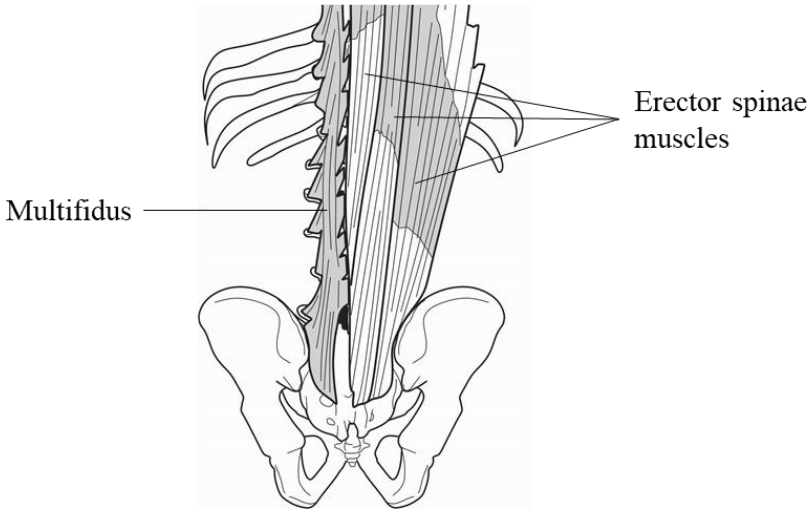

Figure 2.3: Image of the lumbar spine musculature indicating the erector spinae and multifidus muscles. Adapted from Barr *et al.* (2016) and Standring (2016)

Seven distinct stabilising ligaments are present in the lumbar spine, including the anterior – and posterior longitudinal ligaments (PLL), ligamentum flavum, supra – and interspinous ligaments and intertransverse ligaments (Figure 2.4). The iliolumbar ligament (Figure 2.5) is limited to the lumbar spine and is important for stabilisation of L5 by providing a connection between the transverse process of L5 and the posterior border of the ilium (Magee, 2014).

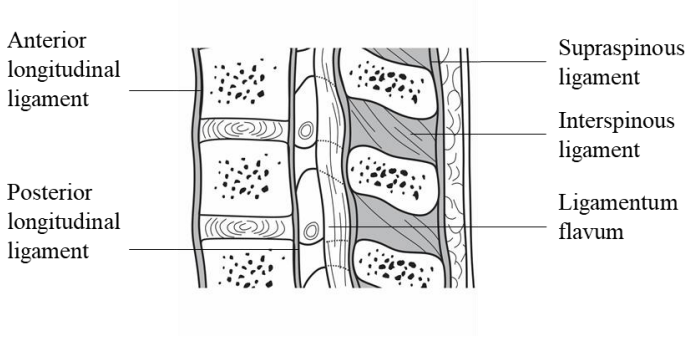

Figure 2.4: Sagittal section through the lumbar spine indicating five characteristic ligaments. Adapted from Magee (2014)

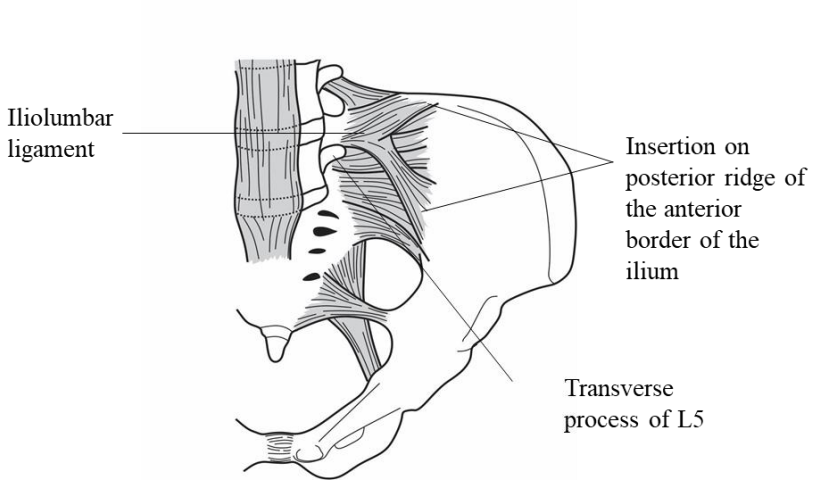

Figure 2.5: Anterior view of the pelvis and lumbar spine indicating the iliolumbar ligament. Image adapted from Magee (2014)

Intervertebral discs

The IVDs consist of two divisions. An outer laminated portion called the annulus fibrosus (AF) and an inner portion called the nucleus pulposus (NP). The AF further consists of three zones, all

three of which are comprised out of fibrocartilage. The important outer zone attaches to the peripheral part of the vertebral body by means of a cartilaginous endplate. This endplate allows for movement of fluid between the IVD and the vertebral body (Magee, 2014). Figure 2.6 shows a diagram of a typical, healthy IVD.

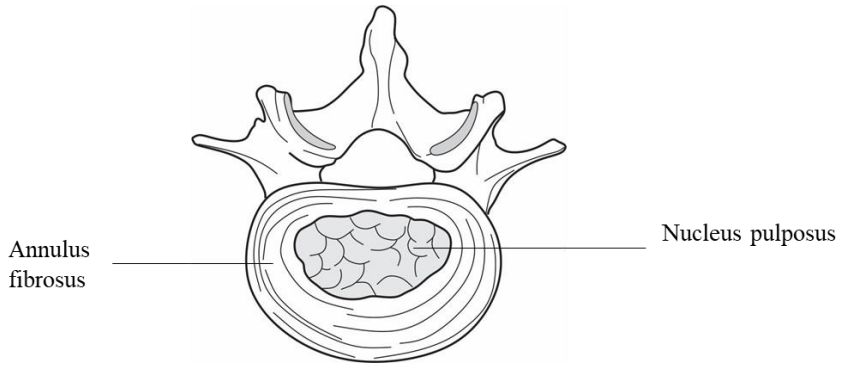

Figure 2.6: Transverse view of a typical, healthy intervertebral disc. Image adapted from Mayfield Clinic (2016)

Neurovascular structures

The posteriorly located dorsal root ganglion (DRG) lies at the level of the neural foramen (the space between the two vertebrae) and extends as the sinuvertebral nerve (spinal nerve). This nerve then branches into a ventral – and a dorsal ramus (Figure 2.7). The sinuvertebral nerve innervates the IVD, the anterior part of the vertebral bodies and the PLL. The ventral ramus is the largest branch, supplying all the structures lying anterior to the neural canal. The dorsal ramus pierces the intertransverse ligament close to the pars interarticularis and innervates all the structures lying posterior to the neural canal. The pedicle is an important landmark when attempting to understand the surgical neural anatomy of the lumbar region. In the lumbar spine, the named root exits below the named pedicle. When lateral recess pathology such as stenosis or posterolateral disc herniation occurs, the nerve root exiting inferior to the disc is affected. For example: an L3/L4 posterolateral disc herniation would typically cause L4 nerve root complications or symptoms (Gardocki and Park, 2017).

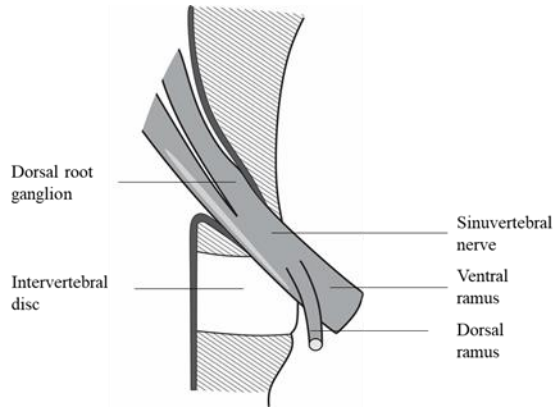

Figure 2.7: Branches of a typical spinal/sinuvertebral nerve. Image adapted from Barr *et al.* (2016)

Each vertebral body receives several nutritional vessels coming from a segmental artery. These arteries are branches of the aorta which follow a posterolateral course (Figure 2.8). As the artery reaches the transverse process, it divides into two branches (one lateral and one posterior). The posterior part of each vertebral body also receives blood from four arteries derived from the upper and lower vertebral levels. The spinal artery runs along the inner surface of the vertebral arch, giving off several radicular arteries (Figure 2.8). The largest radicular artery, known as the artery of Adamkiewicz, is a tributary of the upper lumbar and lower thoracic segmental arteries (Parke *et al.*, 2011).

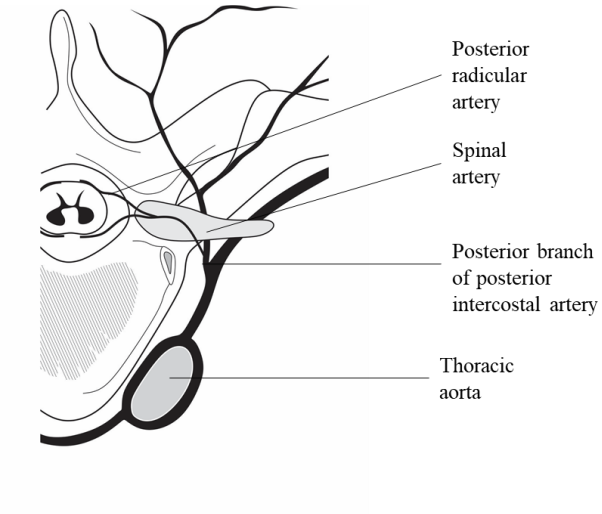

Figure 2.8: Typical arterial supply of a segment the lumbar spine. Image adapted from Reina *et al.* (2010)

2.2 Biomechanics of the lumbar spine

2.2.1 Terminology and concepts

In order to understand the more complex biomechanics of the lumbar spine, a base knowledge of how the fundamental biomechanics operate should be established. Some terms and concepts are explained to better understand the biomechanical properties which follow.

Scalars and vectors

Scalars are quantities defined by their magnitudes and are independent of the direction of the scalar. Vectors, however, consist of both a magnitude and a direction. Forces applied to any structures (in this case the spine) can be broken down into components of vectors, which leads to the establishment of a reference system. A load or force vector is when a force is applied in a direction in order to change the state of rest of the body to which the force is applied. Due to the flexibility of the spine, forces often result in deformation (Yoganandan *et al.*, 2017).

Deformation and Poisson's ratio

Deformation is often used to define the change in normal morphology. It can either be translational (change in the length of the body) or rotational (change in the angle of the body). Deformations often result in strain which is the change in unit length (linear) or change in unit angle (shear) in the body which is subjected to a force vector. When load is applied to a deformable body, strains occur either along the direction of the force (axial/longitudinal) or transverse to the direction of application of force (transverse/lateral). The ratio of lateral to longitudinal strain is known as Poisson's ratio (Yoganandan *et al.*, 2017).

Force deformation response

The energy of a force is defined as the area under the force deformation curve and is often used to relate force with deformation. This energy represents the amount of work done on the body by the force. Stiffness, however, is defined by the ratio of deformation. The most linear portion on the usually non-linear force deformation curve of the spine is chosen to obtain the maximum stiffness of the body. In the spine, there is a nonlinear response – meaning that the force does not increase linearly with the deformation and/or vice versa (Yoganandan *et al.*, 2017).

The biomechanical load deflection response has been classified into the: physiologic loading phase, traumatic loading phase, and failure/posttraumatic loading phase (Figure 2.9). In the spine,

the physiological phase, is where the spinal structure performs as an integral unit where the stiffness gradually increases to reach a maximum value. This means that the structure obtains its highest level of stiffness, leading to an increased resistance to external forces. This is the region of the highest mechanical efficiency and is the least likely place for trauma to occur. At the onset of decrease in stiffness, yielding of the structures start to take place and the traumatic loading phase starts. As this too comes to an end, changes in stiffness occur which correspond to the ultimate load-carrying capacity of the structure. Once the peak is reached during the physiological phase, the stiffness starts to decrease to zero (the end of the traumatic loading phase). This indicates that the structure has reached its ultimate load-carrying capacity. In the subsequent posttraumatic loading phase, an increase in deformation occurs, resulting in a decrease in load. Trauma is identified as when the structure has been loaded to this phase (Yoganandan *et al.*, 2017).

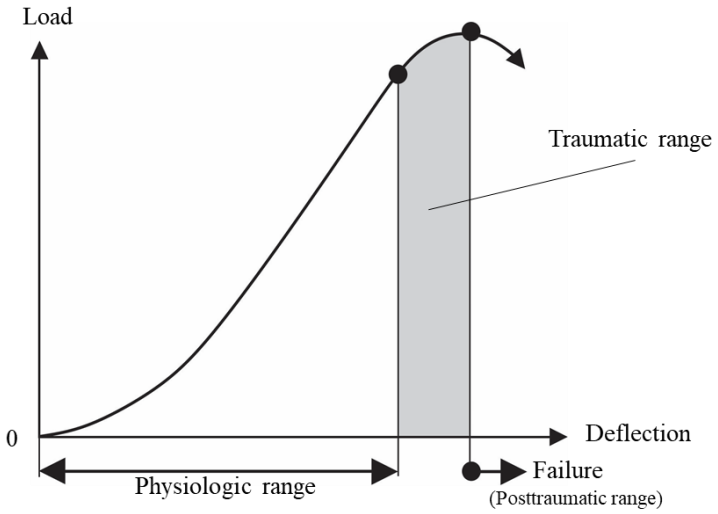

Figure 2.9: Graph indicating the biomechanical load deflection curve. Image adapted from Yoganandan *et al.* (2017)

Coupling

Motions of the spine are coupled due to the three-dimensional structure of the spine. Coupling can be defined as the capacity of the spine to move in motions (such as translations or rotations) other that the primary motion. The primary or principal motion is that which is associated with the

direction of application of the external force and any out-of-phase motion is the coupled motion (Yoganandan *et al.*, 2017).

2.2.2 Loads on the lumbar spine

The human spine undergoes deformation in order to resist internal and external loads. The lumbar spine mainly endures two types of loads; physiological and traumatic. Physiological loads are due to normal, everyday movements of the spine and are divided into four classes: short-term (during flexion and extension), long-term (during sitting and standing), cyclic (during gait or walking) and dynamic (during running and jumping). Traumatic loads are due to sudden, intense forces such as whiplash injuries (Kurutz, 2010, Yoganandan *et al.*, 2017).

The loads can also be divided according to their source (gravity, muscles, ligaments, intra-abdominal pressure, and ergonomics). Each part of the body is subject to loading due to gravity, which is proportional to the mass of the element in question. This means that the centre of support of the body carries the highest gravitational load. During the standing position, this will be the lumbar spine. It is important to realise that muscles and ligaments also create load on the spine. The muscles result in active loading and ligaments result in passive loading. Dynamics inside the abdominal cavity also have a unique influence on the loading patterns (Kurutz, 2010).

When considering intra-abdominal pressure, it is evident that an increase thereof causes a decrease in spinal pressure (loading due to the action of the abdominal muscles). Therefore, holding one's breath (increasing intra-abdominal pressure) will increase spinal stability. Ergonomic loads also affect the lumbar spine, and include heavy lifting and whole body vibration, both of which lead to increase in spinal compression (Kurutz, 2010).

2.2.3 Internal forces in the lumbar spine

Compressive forces

The main force inside the lumbar spine is a compression force, which acts in the midline of the spine leading to high compression on the IVDs (Kurutz, 2010, Warren *et al.*, 2012). For an individual with a standard body mass of 70kg (700N), it has been calculated that the normal physiologic compression force in the lumbar spine is around 400N. This force will increase as the weight, height, muscle forces, dynamic loads, and hip flexion increases (Kurutz, 2010). The lumbar spine's vertebral bodies are thicker and wider than the cervical and thoracic and can

therefore withstand higher compression forces. For adults of around 45 years of age and younger, the cortical and cancellous (or medullary) layers of bone share the load transmitted through the body, with a ratio of 45:55, respectively. For subjects over 40 years of age, the cortical shell carries approximately 65% of the load exerted on the body as a result of the increased porosity (Warren *et al.*, 2012).

Shear forces

Shear forces, clinically termed subluxation forces (Yoganandan *et al.*, 2017), also work on the spine in the sagittal and lateral planes and are responsible for the angles observed between the discs. The concept of moment components/arms are best described as the distance between the joint or pivot axis and the line of the force acting in on the joint. These moments of the shear forces include sagittal and lateral bending moments, which cause flexion/extension and lateral flexion respectively; and torque moments, which cause rotation along the long axis (Kurutz, 2010). The spine must constantly balance itself by maintaining a homeostasis between the different forces acting in on it. For example: while standing, the centre of gravity is passing through L4, causing activation of postural muscles. Thus, the extensors of the back need to provide tensile forces to counteract torque. Another example is flexion: when the body is flexed, the moment increases anteriorly due to the increase in distance. Therefore, the extensor muscles of the back need to increase their tension forces to prevent the individual from falling over. It is important to note that flexion also affects the IVDs, as it causes an anterior protrusion and posterior retraction of the IVD, changing its loads and forces (Avallone *et al.*, 2007).

Posture and gait

Posture also affects the magnitude of the force, for example: laying down will decrease the magnitude, whereas sitting erect will result in an increased magnitude if no back support is provided (Kurutz, 2010). If a seated back support is provided, however, then the loads will decrease, as parts of the upper body are supported. The abdominal muscles can now focus on supporting the spine. During walking, the loads on the spine increase with an increase in walking speed (Avallone *et al.*, 2007). Cappozzo (1984) showed in his study that the maximum load occurred at the point where the toe is off of the ground (toe-off) or during the left and right heel strikes (heels touching the ground).

2.2.4 Individual components

Facet joint

Facet joints support axial or transverse compressive loads when the spine is in extension. When the orientation of the joint changes, the mobility and load-carrying capacity of the spine will change under different force vectors. This is particularly seen in the sagittal orientation of the lumbar spine where the orientation between T12/L1 (approximately 25°) is significantly different from L5/S1 (approximately 50°). Due to its sagittal plane orientation, the lumbar spine is able to resist great amounts of rotational forces, but is unable to resist major flexion or translational movements (Yoganandan *et al.*, 2017).

Spinal cord

Due to movements of the spine, the spinal cord also has to change its configuration with the body's positioning. Injury susceptibility changes as abnormalities in the spine vary. Its physical properties are a result of its structural elements such as nerve roots, dentate ligaments and pia – and dura mater. Due to the elasticity of the cord, small movements and forces cause large displacements of the cord. However, this flexibility can be followed by stiffening which could lead to injury (Yoganandan *et al.*, 2017).

During flexion, elongation of the cord occurs and decreases in its anteroposterior (AP) diameter, increasing axial tension within the axon cylinders of the white matter tracts. This can result in lesions of the spinal cord. During extension, shortening of the spinal cord occurs in the AP diameter along with relative relaxation of the axon cylinders. If the cord experiences bending motions, an increase in compressive forces on the concave side occurs along with distractive forces on the convex side. Increased incidence of such forces can lead to spinal cord injury (Figure 2.10). Shear forces result in maximal force towards the centre of the cord and act in a perpendicular plane to the tensile and compressive forces (Yoganandan *et al.*, 2017).

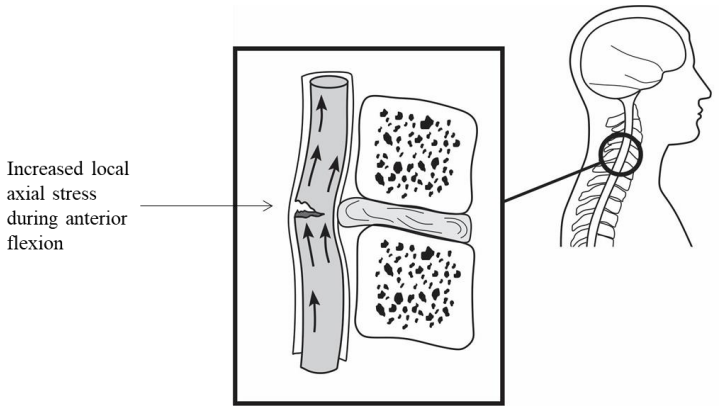

Figure 2.10: Diagram indicating the increased local axial stress on the spinal cord during anterior flexion of the spine. Adapted from Yoganandan *et al.* (2017)

Ligaments

Ligaments can be seen, in a biomechanical sense, as uniaxial components responding to direct tensile forces, even though they possess a three-dimensional geometry. Ligamentous efficacy is dependent on morphology, anatomical location, strength, and the acting moment arm of the individual ligament. Strong ligaments may contribute less to stability than weaker ligaments if the former possesses a shorter lever arm than the latter. For example: the PLL is strong but has little resistance to flexion due to the anterior attachment. This is because the ligament is closer to the axis of rotation, resulting in a short lever arm (Yoganandan *et al.*, 2017).

Muscles

The muscle length at the initiation of muscle contraction contributes greatly to its ability to resist forces. Electromyographic (EMG) studies are used to determine the action of a muscle. However, during flexion, the majority of the back muscles are active. EMG activity in the back muscles occur at the beginning and completion of full extension. In contrast, the abdominal muscles show activity with increased flexion and extension and usually occur on the ipsilateral side (Yoganandan *et al.*, 2017)

2.2.5 Lumbar spine mobility

The initial 50° to 60° of axial flexion is due to flexion of the lower motion segments (two vertebral bodies and interlaying IVD) of the lumbar spine (Avallone *et al.*, 2007). The lumbar spine has six movement components: three degrees of flexion and three degrees of rotation. The spinal motions are characterised into three parameters: (1) a neutral zone where there is no resistance; (2) an elastic zone where spinal resistance is present; (3) the range of motion (ROM) which is the sum of the previous two parameters. A typical lumbar segment has an ROM of around 12° to 16° for flexion/extension increasing from L1 to L5; 6° for lateral bending and approximately 2° for axial rotation (torsion). Spinal mobility depends on the state and geometry of the IVDs, ligaments, facet joints and posterior skeletal elements (Kurutz, 2010).

2.3 Factors influencing the integrity of the lumbar spine

Skeletal and soft tissue changes will affect the integrity of the lumbar spine, as one of its important characteristics is its large contribution to the weight-bearing role of the axial skeleton. It therefore endures large amounts of stresses and strains, which over time may lead to spine-related diseases. Common diseases of the lumbar spine include osteoporosis, spinal stenosis, spondylolisthesis, disc herniation and degeneration, endplate changes, scoliosis, kyphosis, osteomyelitis, rheumatoid arthritis and osteo-arthritis (Zampolin *et al.*, 2014, Coric *et al.*, 2017).

Osteoporosis affects the entire skeleton and is the result of bone loss (Woodward *et al.*, 2011). It is characterised by low bone mass and particularly affects cancellous/medullay and cortical bone. Determining BMD can therefore aid in determining which individuals are at risk of osteoporosis-related fractures. Due to the complex movements of the spinal column, spinal stenosis may also result over time. It is a condition where narrowing of the spinal canal and foramina occurs either due to spinal degeneration with age, spinal disc herniation, a tumour, or a synovial cyst. This leads to compression of the enclosed neurovascular structures (Woodward *et al.*, 2011). The other diseases mentioned are discussed in more detail in section 2.3.2.

2.3.1 Bone mineral density

BMD is the measurement of the amount of calcium in a specific region of the bone. It is therefore an ideal measurement of bone quality but is not sufficient by itself. It might then be used to describe bone quality when there are alterations in the density of the bone in the regions

representing the structure of the cortical/trabecular bone (Celenk and Celenk, 2012). BMD can be measured using a wide variety of radiographic methods. These include T-scores determined by Dual Energy X-ray Absorptiometry (DEXA), Hounsfield units (HU) number obtained from Computed Tomography (CT) or Quantitative Computed Tomography (QCT), Ultrasound, Single Energy X-ray Absorptiometry (SXA), Peripheral Dual Energy X-ray Absorptiometry (PXA), Radiographic Absorptiometry (RA), Dual Photon Absorptiometry (DPA), Single Photon Absorptiometry (SPA) and Magnetic Resonance Imaging (MRI). DEXA with T-scores is the most commonly used as it is easy to perform, widely available and, relatively cost-effective. It also produces less radiation than CT or QCT. However, studies have shown that DEXA tends to provide an over-estimate of the T-score of patients with bone mineral disease, despite the patients having low BMD (Celenk and Celenk, 2012, Choi *et al.*, 2016b).

HU has subsequently been investigated by previous authors and was found to be more reliable than DEXA with T-scores (Schreiber *et al.*, 2011, Celenk and Celenk, 2012, Choi *et al.*, 2016b). HU is a linear transformation of the original linear attenuation (the reduction of value) coefficient measurement. It is used in medical imaging techniques to describe the X-ray attenuation of each voxel (volume and element) in the created 3D image. The HU number of a tissue is directly proportional to the density of that tissue. In order to provide perspective for HU tissue values, it is relevant to mention that the normative radiodensity for distilled water and air at standard temperature and pressure (STP) are 0 HU and -1000 HU, respectively (Celenk and Celenk, 2012). The typical HU value for bone ranges between 300 and 3000 HU (Schreiber *et al.*, 2011). Previous researchers have established a fracture threshold value for all the BMD methods; for CT and QCT it is around 100-110 mg/cm^3 (Schreiber *et al.*, 2011). A patient with a BMD above this threshold is unlikely to present with osteoporotic fractures while patients with BMD values below this threshold are more likely to present with such fractures.

It is of great importance to be aware of the predisposing factors leading to weakening of the lumbar vertebrae when considering lumbar spinal surgery, as it regularly involves bone-altering procedures. Normal HU values have been calculated for different populations, but no standardised values are available for the South African population. Table 2.1 shows a selection of standard DEXA BMD values determined for a number of other population groups.

Table 2.1: Table summarising the DEXA BMD values (g/cm^2) of other global population groups

Country / region	P	VL	N	Age group					
				20 - 29	30 - 39	40 - 49	50 - 59	60 - 69	70 - 79
Lebanon[a]	**AM**		**165**	1.14 ± 0.13	1.10 ± 0.14	1.12 ± 0.14	1.09 ± 0.18	1.06 ± 0.15	1.06 ± 0.15
	AF		**858**	1.10 ± 0.13	1.11 ± 0.12	1.10 ± 0.13	1.02 ± 0.13	0.95 ± 0.13	0.94 ± 0.15
Saudi Arabia [b]	**AM**		**915**	1.14 ± 0.09	1.12 ± 0.15	1.01 ± 0.18	0.98 ± 0.13	0.97 ± 0.22	0.73 ± 0.09
	AF	**2-4**	**1065**	1.12 ± 0.12	1.13 ± 0.11	1.11 ± 0.15	0.99 ± 0.17	0.88 ± 0.15	0.76 ± 0.09
Iran [c]	**AF**		**2340**	1.19 ± 0.14	1.16 ± 0.15	1.12 ± 0.16	1.07 ± 0.15	1.07 ± 0.18	1.09 ± 0.18
	AM		**2861**	1.19 ± 0.13	1.17 ± 0.14	1.14 ± 0.15	1.05 ± 0.16	1.00 ± 0.18	0.99 ± 0.19
Italy [d]	**EF**		**1622**	1.03 ± 0.10	1.04 ± 0.10	1.03 ± 0.13	0.95 ± 0.14	1.00 ± 0.14	0.86 ± 0.15
Turkey [e]	**EM**	**1-4**	**119**	0.97 ± 0.10	1.00 ± 0.11	0.93 ± 0.14	0.91 ± 0.12	0.86 ± 0.15	0.77 ± 0.09
	EF		**347**	0.96 ± 0.10	0.96 ± 0.14	0.93 ± 0.11	0.88 ± 0.12	0.81 ± 0.14	0.76 ± 0.15
Croatia [f]	**EM**		**249**	1.26 ± 0.05	1.26 ± 0.16	1.20 ± 0.12	1.12 ± 0.19	1.12 ± 0.10	1.12 ± 0.11
	EF		**292**	1.18 ± 0.08	1.19 ± 0.12	1.15 ± 0.14	1.08 ± 0.16	1.01 ± 0.20	1.03 ± 0.23
USA [g]	**WF**	**2-4**	**1487**	1.24 ± 0.14	1.23 ± 0.14	1.19 ± 0.14	1.11 ± 0.15	1.02 ± 0.15	0.97 ± 0.16
Mexico [h]	**MF**		**4460**	1.19 ± 0.13	1.18 ± 0.14	1.14 ± 0.16	1.05 ± 0.16	0.98 ± 0.16	0.95 ± 0.17
SE Mexico [h]	**MF**		**925**	1.14 ± 0.13	1.14 ± 0.15	1.13 ± 0.17	1.00 ± 0.18	0.92 ± 0.15	0.93 ± 0.17

Key: P = Population group; VL = Vertebral levels (lumbar); N = Number of individuals per group; AM = Asian males; AF = Asian females; EM = European male; EF = European female; MF = Mexican females; WF = White females; SE = South-east; a = (Maalouf et al., 2000); b = (Ardawi et al., 2005); c = (Larijani et al., 2006); d = (Pedrazzoni et al., 2003); e = (Manisali et al., 2003); f = (Cvijetic and Korsic, 2004); g = (Mazess and Barden, 1999); h = (Deleze et al., 2000)

The average DEXA BMD values of the two most common diseases are summarised in Table 2.2. Various degenerative spine diseases lead to complications such as osteophyte formation, bone sclerosis, disk space narrowing, and spondylolisthesis, which are known to affect the BMD value of the lumbar spine (Muraki *et al.*, 2004). Of these degenerative diseases, rheumatoid arthritis and Crohn's disease have a characteristic contribution to loss in BMD, leading to osteoporosis (Haderslev *et al.*, 2000, Orstavik *et al.*, 2003). According to the literature, post-menopausal women are at higher risk of decreased BMD due to a decrease in their free oestradiol index (Kanis *et al.*, 1994, Melton *et al.*, 2003, Torstveit and Sundgot-Borgen, 2005, Chain *et al.*, 2017). Certain drugs and therapeutic agents such as tetraperatide and chemoradiation therapy are also known for

decreasing the BMD value of the lumbar spine (Chen *et al.*, 2006, Wei *et al.*, 2016). Lifestyle is another factor which plays a role in the BMD quality of a patient. Both male and female endurance runners have a decreased BMD, with males in this category being at the same risk of bone diseases as female endurance runners (Hind *et al.*, 2006).

Table 2.2: Known BMD values for certain bone-related diseases

Disease	BMD value (HU)
Osteoporosis	80.6 – 103.4 [a, d]
Osteopenia	78.8 – 132.9 [a, b, c, d]
Key: a = (Alacreu et al., 2017); b = (Schreiber et al., 2011); c = (Lee et al., 2013); d = (Choi et al., 2016b). These values are equivalent to the traditional T-score values where a score of ≥ −1.0 is considered healthy and < −1.0 is considered unhealthy or diseased bone (with T-score ≤ −2.5 representing osteopenia, and −2.5 < T-score < −1.0 representing osteoporosis) (Alacreu et al., 2017)	

2.3.2 Pathologies and injuries

Deformities and degeneration

Most degenerative diseases lead to deformities, but deformities are not purely a result of degeneration. Degenerative spine disease (spondylosis) affects everyone and occurs throughout the entire spine, but is more prevalent in the lumbar region due to the main axial loading function in this region. The three main degenerative diseases and deformations of the spine include scoliosis, lumbar stenosis and intervertebral disc disease (Lee *et al.*, 2006).

Scoliosis is the lateral deviation of the spine from the normal midsagittal plane. The lateral curvature is also associated with rotation of the vertebrae. The result is a three-dimensional deformity occurring in the sagittal, frontal and coronal planes (Warner and Sawyer, 2017). Lumbar stenosis is the narrowing of either the central canal or the neural foramina(e) (Figure 2.11). Symptoms include lower back pain (axial), radiating lower limb pain (radicular), paraesthesia (partial loss of sensation), weakness of muscles and gait instability. The symptoms mostly present as chronic, but may, in traumatic cases, present as acute symptoms. Central canal stenosis is most commonly caused by multiple factors which include ligamentous hypertrophy, osteophyte hypertrophy, spondylolisthesis, hypertrophic facets, and disc herniation. Less common causes are

tumours, abscesses, and postoperative lesions. Compromise of the canal leads to compensation due to pain, causing a spinal imbalance and functional instability over time (Lee *et al.*, 2006).

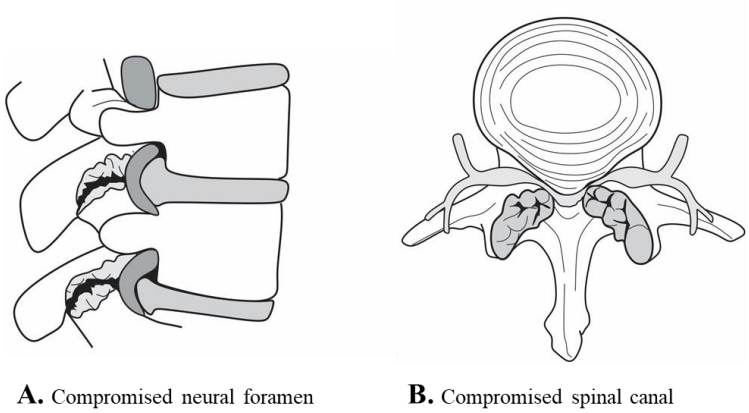

Figure 2.11: The two most common types of spine stenosis. Image adapted from Ratish *et al.* (2018)

Spondylosis, which is the defective arching of the vertebrae and decrease in water concentration in the discs with age, may cause the IVDs to lose some of their height (Magee, 2014, Barr *et al.*, 2016). The AF contains fibres that run concentrically at oblique angles to each other, allowing them to endure stresses and strains in any direction. The AF provides the primary shock absorption properties of the IVDs, since the liquid properties of the NP makes it nearly incompressible. As axial loading on the spine occurs, there is an increase in the pressure in the nucleus, which then pushes on the annulus, causing its fibres to stretch. If the fibres break, the result is a herniated NP. Flexion causes loading on the anterior part of the IVD, displacing the nucleus posteriorly. Forces which are too high will result in a nuclear herniation through the posterior annular fibres, and due to the thin lateral fibres, the prevalence of this type of herniation is relatively high (Barr *et al.*, 2016). Injury to the IVD can lead to one or more possible complications such as protrusion, prolapse, extrusion and sequestration (Figure 2.12) (Magee, 2014).

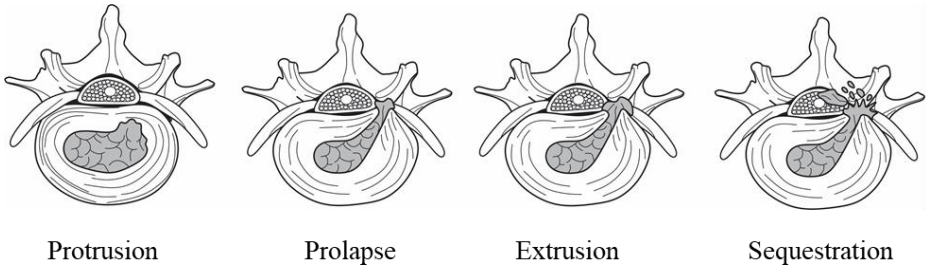

Figure 2.12: Diagram showing the four main types of disc injury. Image adapted from Magee (2014)

Vertebral injuries/fractures

There are many different injuries which influence the lumbar spine. For practical purposes, these injuries will be divided into three groups: distraction –, compression –, and translation injuries. Figures 2.13 to 2.18 illustrate the fracture patterns described below.

Distraction injuries/fractures include those which are characterised by flexion injuries. These often involve primary distractive forces rather than crushing forces as seen in compression fractures. The injuries can be classified as Chance fractures and Chance fracture variants. The Chance injuries may include only osseous sections (Figure 2.13 A), only discoligamentous sections (Figure 2.13 B), or both mentioned segments (Figure 2.13 C) and may occur on the anterior – or posterior border of the vertebral body. Anterior injuries are known as hyperextension injuries and often only include the discoligamentous sections. Posterior injuries can be monosegmental (purely osseous) or osseoligamentous. These injuries cause either moderate or severe instability of the spinal column, depending on the type of Chance fracture which occurred, and the elements involved (Williams, 2011, Schnake *et al.*, 2017).

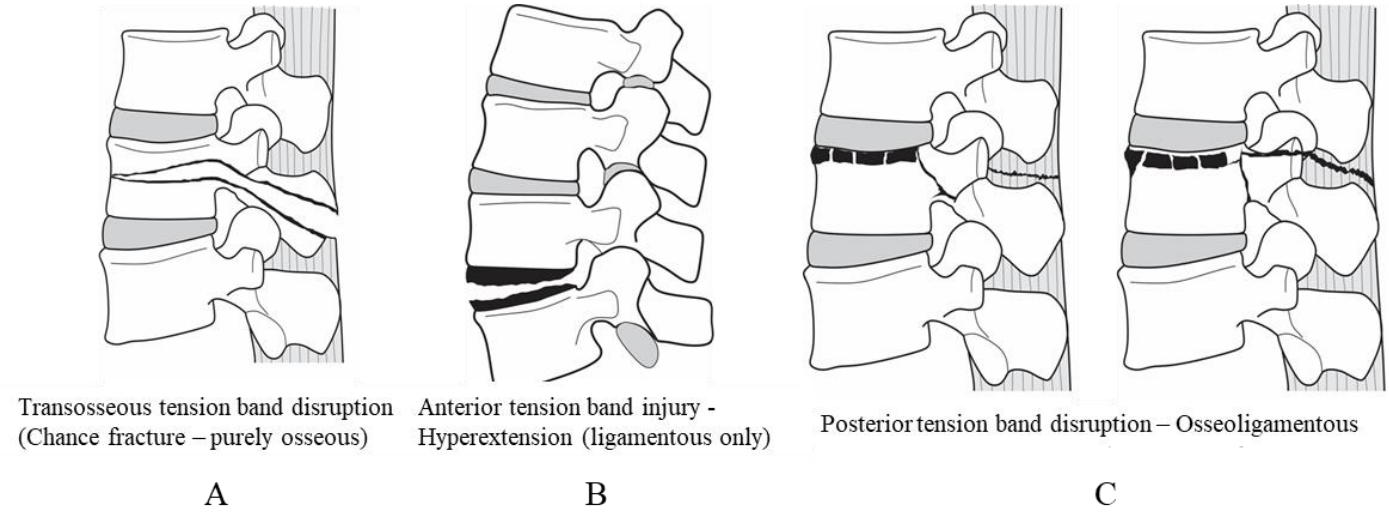

Figure 2.13: Figure depicting the three main types of distraction injuries. Adapted from Schnake *et al.* (2017)

Compression injuries/fractures often result from axial compression through the vertebral body, with failure through the anterior column and include minor non-structural, wedge-compression, and burst fractures or injuries (Figures 2.14 to 2.17). Minor, non-structural fractures are where the spinous or transverse processes are fractured or injured, resulting in no damage to the vertebral body or spinal canal. The injuries are usually insignificant and cause low levels of spinal instability. Wedge-compression fractures usually involves the superior end plate and is mostly stable. However, significant posterior ligamentous disruption can cause instability. Burst fractures can either be complete (both endplates are involved) or incomplete (only one or no endplates are involved) and are caused by axial compression through the vertebral body with the posterior wall of the vertebral body involved in the fracture – unlike split or wedge fractures (Williams, 2011, Go, 2016, Schnake *et al.*, 2017).

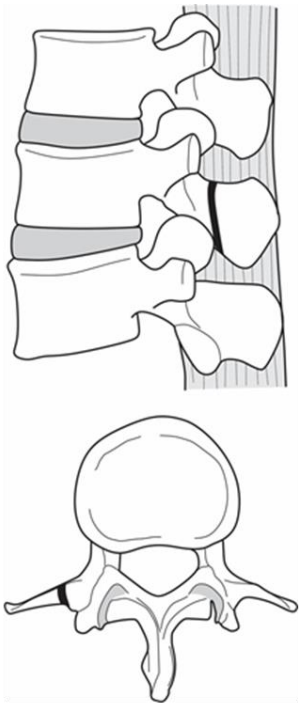

Figure 2.14: Image showing a type of compression injury involving the vertebral processes. Adapted from Schnake *et al.* (2017)

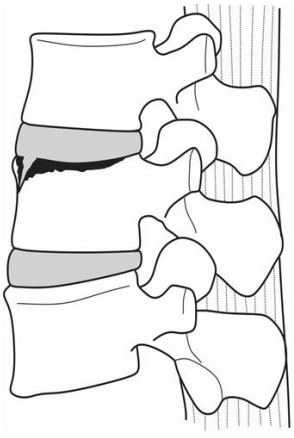

Figure 2.15: Image showing a type of vertebral body compression injury involving neither the posterior wall (posterior elements), nor both endplates. Adapted from Schnake *et al.* (2017)

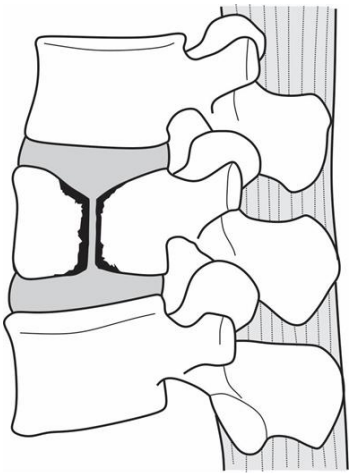

Split fracture

Figure 2.16: A type of compression injury involving both endplates, but not the posterior wall. Adapted from Schnake *et al.* (2017)

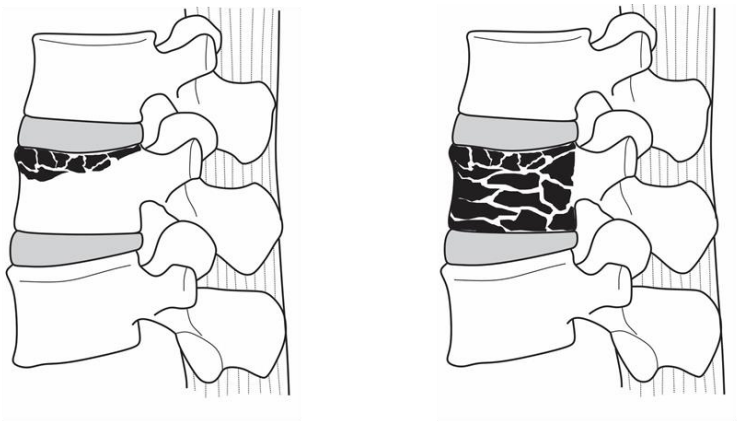

A. Incomplete burst fracture B. Complete burst fracture

Figure 2.17: Two variations of a compression injury known as a burst fracture. Adapted from Schnake *et al.* (2017)

Translation injuries involve displacement or dislocation of vertebral segments in relation to each other. These types of injuries or fractures are usually caused by one or more of the following force vectors: shear, rotation, distraction, flexion, and extension (Figure 2.18). The injuries are therefore classified according to the high degree of spinal instability resulting from the fracture or injury (Williams, 2011).

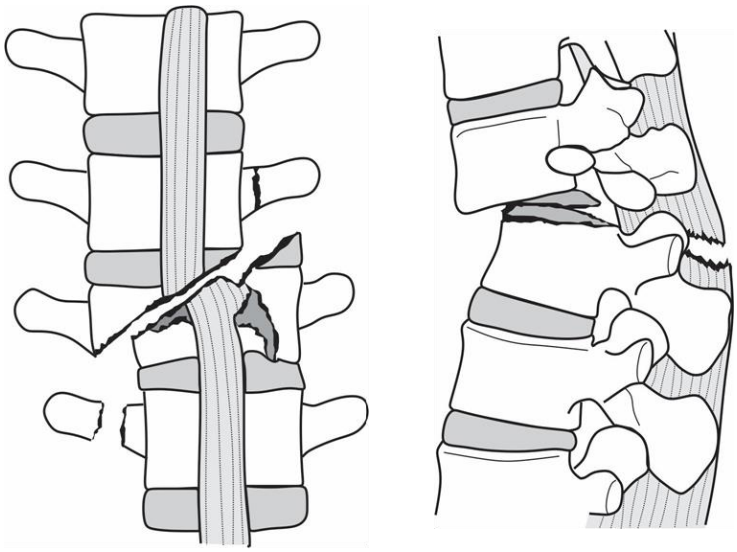

Figure 2.18: Figure showing a translation injury. Adapted from Schnake *et al.* (2017)

2.4 Surgical procedures of the lumbar spine

2.4.1 Decompression

Lumbar disc disease often requires surgical intervention when nonoperative or conservative treatment fails. Most of these IVD diseases present in patients who are otherwise healthy and usually in their third or fourth decade of life, and present with severe back pain. The back pain is generally related to a traumatic event and can often also be associated with leg pain. Episodes of back pain are intermittent, and the onset of leg pain may only occur much later in the disease stage. Over-exertion can often aggravate the pain and rest usually helps with relieving the pain. Dermatomal buttock pain may commonly be present as the nerve roots are affected in disc disease. These signs and symptoms are due to the compression of neural structures (specifically the nerve roots) as a result of herniated or torn IVDs, which compress the spinal cord. Decompression surgery is then needed (Gardocki and Park, 2017).

Discectomy or microdiscectomy

The decompression surgical technique related to disc disease is known as a discectomy or microdiscectomy, where the IVD and the leaked annular substance are removed. The surgery is performed under anaesthesia and is usually aided by an operating microscope. Radiographic

confirmation of positioning is also necessary. After disc excision, the space between the two adjacent vertebral bodies is now void and needs to be filled. This is either done by fusion or disc replacement surgery (Gardocki and Park, 2017).

Laminotomy and foraminotomy

Laminotomy and foraminotomy procedures involve the partial removal of the laminae and enlargement of the neural foramina, usually due to spinal stenosis. One of the more common procedures is known as a bilateral laminotomy. In this procedure, the spinous process and supra- and interspinous ligaments are preserved, whilst the paraspinal muscles are elevated from the spinous processes and laminae bilaterally. Each side is then separately decompressed (the bone is removed) under microscopy (endoscopic procedure). Both the proximal and distal laminae are resected and the ligamentum flavum is detached from its attachment sites. The ligamentum flavum is carefully resected, keeping the neural structures intact. If it is deemed necessary by the surgeon, the decompression is finalised by a foraminotomy, where the facet joint is undercut and resected in order to enlarge the neural foramen (Lund and de Moraes, 2017).

Laminectomy

Unlike laminotomies, laminectomies involve the entire removal of the vertebral lamina(e) and spinous processes and are also usually not performed endoscopically (Gupta *et al.*, 2012). The surgery aims to decompress the stenotic spinal canal through total removal of the posterior ligamentous and laminar complex and limited undercutting of the facet joints. Even though it provides sufficient decompression, it is more invasive and carries a higher risk than laminotomies, as it risks injury to structures affecting spinal stability and sagittal profiles (Jeon *et al.*, 2015). Figure 2.19 shows the difference between laminectomies and laminotomies.

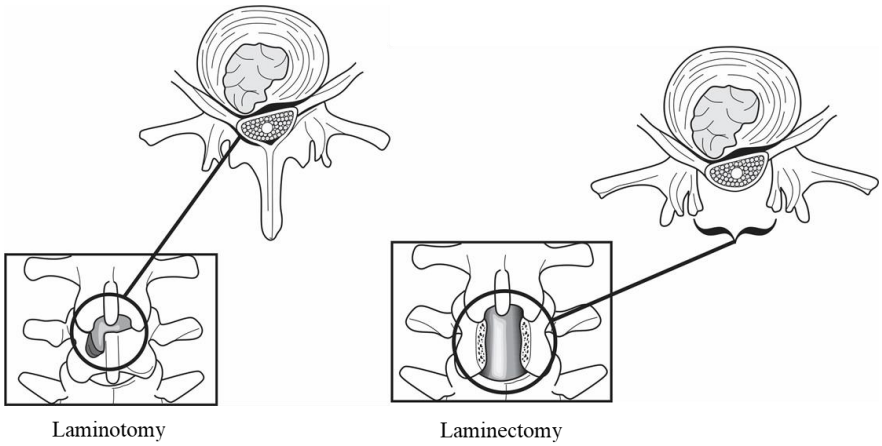

Figure 2.19: Figure demonstrating the difference between a laminotomy and a laminectomy. Iamge adapted from Alvarado Hospital Medical Center (2018)

Corpectomy

A corpectomy is a procedure in which the vertebral body is removed along with the superior and inferior adjoining IVDs. The resulting spinal defect is corrected by reconstructing the body with an anterior bone graft and/or fusion cage. This is usually stabilised by anterior and/or posterior spinal instrumentation. The procedure aims to relieve anterior neural compression that extends behind the vertebral body or to remove a structurally compromised vertebral body (infection, tumour, fracture, etc.) (Gupta *et al.*, 2012).

2.4.2 Spine fusion

Spinal stenosis is one of the most common diseases of the lumbar spine and is commonly associated with disc-related problems. To treat this disease, decompression (often involving the removal of IVDs) and spinal fusion of two or more vertebrae is performed. Spinal fusion is the process where the vertebral bodies and/or spinous processes are fused together with bone grafts and surgical implants. The result is immobilisation of the vertebral segments (arthrodesis), relieving the pain, but may result in pressure on the spinal nerves. Decompression is subsequently performed in order to eliminate the pressure on the spinal nerves by distracting and fusing the spinous processes (Woodward *et al.*, 2011).

There are five commonly used lumbar fusion techniques: (1) posterolateral lumbar fusion (PLF) (Figure 2.20); (2) posterolateral lumbar interbody fusion (PLIF) (Figure 2.21); (3) transforaminal lumbar interbody fusion (TLIF) (Figure 2.22); (4) anterior lumbar interbody fusion (ALIF) (Figure 2.23); (5) extreme lateral lumbar interbody fusion (XLIF) (Figure 2.24). Each of the techniques have their own indications. Anterior and lateral approaches are mostly used in cases of disc herniation, endplate changes and disc degeneration, without the use of decompression and fusion. The posterior approach is used when a patient presents with severe posterior or lateral disc herniation or severe spinal stenosis (Zampolin *et al.*, 2014). The most common indications for lumbar interbody fusion is spondylolisthesis, multiple disc rupture and failed fusion, scoliosis, kyphosis, osteomyelitis and discitis (Coric *et al.*, 2017). These procedures are not without risk and due to their complex nature, postoperative complications are often encountered. Table 2.3 provides a summary of the complications associated with the various approaches used in lumbar fusion.

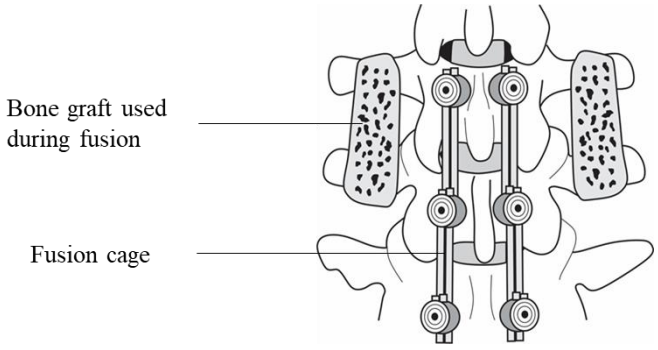

Figure 2.20: Figure demonstrating the posterolateral fusion (PLF) procedure. Adapted from Bone and Spine (2018)

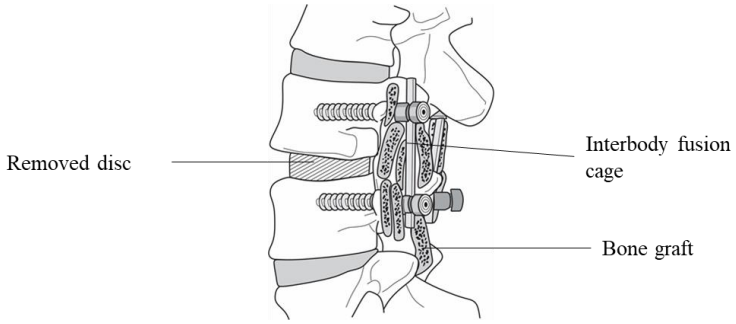

Figure 2.21: Figure demonstrating the posterior lumbar interbody fusion (PLIF) procedure. Adapted from Houston Methodist (2018)

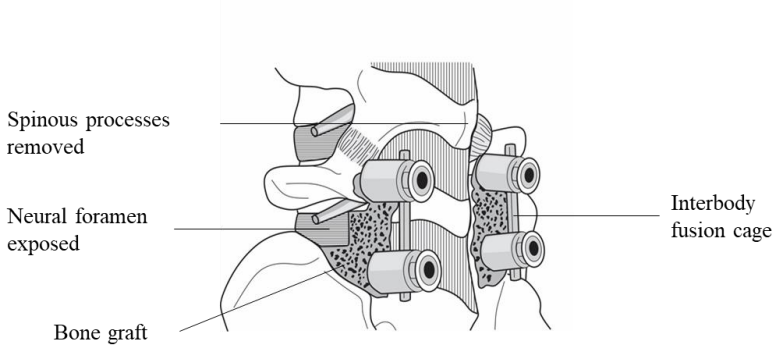

Figure 2.22: Figure demonstrating the transforaminal lumbar interbody fusion (TLIF) procedure. Adapted from Montgomery (2018)

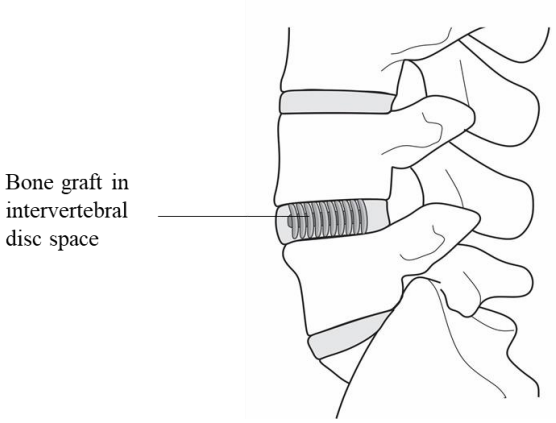

Figure 2.23: Figure demonstrating the anterior lumbar interbody fusion (ALIF) procedure. Adapted from Spine Center Atlanta (2017)

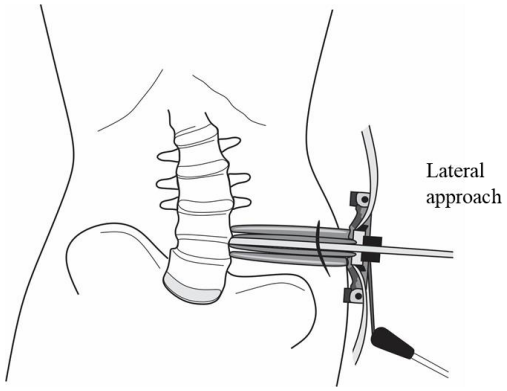

Figure 2.24: Figure demonstrating the extreme lumbar/lateral intebody fusion (XLIF) procedure. Adapted from Billinghurst and Akbarnia (2009)

Table 2.3: Table indicating the indications and complications of the five common lumbar fusion techniques

Fusion technique	Known complications
PLF (Figure 2.20)	• Fibrosis occurring at the nerve roots and/or thecal sac [a, b] • Hardware or bone-graft material causing impingement of neurological structures [a] • Dural tears [a]
PLIF (Figure 2.21)	• Damage to the conus or exiting nerves, leading to retraction of these structures [a, b] • Dural tears [a] • Fibrosis resulting in chronic pain [a, b] • Postoperative radiculopathy [a, b] • Postoperative instability [a, b] • Postoperative failure of fusion device (such as a broken screw) • Posterior migration of the fusion device [a, b]
TLIF (Figure 2.22)	• Fusion cage migration [a] • Fibrosis due to retraction [a, b] • Migration of fusion implant through transforaminal space [a, b]
ALIF (Figure 2.23)	• Vascular damage [a, b] • Damage to viscera (perforation) [a] • Lumbar plexus damage [a] • Incontinence [a] • Retrograde ejaculation [a, b] • Abdominal wall hernias [a] • Deep vein thrombosis [a, b]
XLIF (Figure 2.24)	• Vascular damage [a] • Psoas major hematoma [a] • Lumbar plexus damage [a] • Abdominal wall hernias [a] • Deep vein thrombosis [a]
Key: PLF = Posterolateral fusion; PLIF = Posterior lumbar interbody fusion; TLIF = Transforaminal interbody fusion; ALIF = Anterior lumbar interbody fusion; XLIF = Extreme lateral/lumbar interbody fusion; a = (Zampolin et al., 2014); b = (Coric et al., 2017)	

2.4.3 Novel techniques for spinal surgeries

Due to the complications associated with traditional spinal fusion, there is a need to improve current techniques. If current techniques cannot be improved, new methods of surgical intervention, such as the interspinous fusion device (IFD), need to be addressed. In a systematic review performed by Zhu and Yin (2016), a classification system was established to divide the IFDs into two categories: (1) interspinous fixation without situ fusion (or rigid IFD) and (2) interspinous fixation with situ fusion (or fused IFD). The authors discovered that IFD procedures (both rigid and fused) are less invasive than traditional fusion procedures, result in decreased estimated blood loss, length of hospital stay and surgical time. They also reduce the occurrence of adjacent vertebral segment degeneration and have resulted in an increase in foraminal height, which helps relieve neurogenic symptoms. However, rigid IFDs tend to result in occult spinous process fractures due to the structural weakness of spinous processes. This makes them largely incompatible with patients suffering from advanced degenerative spondylolisthesis, osteoporosis, or osteopenia due to the characteristic compromise in bone material strength of these diseases. In most cases, IFD constructs provide adequate flexion-extension stability, but are inferior to the other, routinely used fusion constructs when considering lateral bending and axial rotation. There are a few devices which have managed to overcome this problem by providing sufficient rigidity in all planes of movement. The fused IFD type seems to provide more stability and strength in the eventual fusion due to the extra interspinous fusion (Zhu and Yin, 2016).

2.5 Anatomical considerations

2.5.1 Soft tissue

Understanding the variations of soft tissue structures is important during any surgery, as surgeons need to consider that there are individuals whom have variant anatomy. This could lead to alternative procedures and protocols having to be followed.

Nerve root anomalies have been documented in various anatomical studies but are not considered often enough in clinical practice. The lack of consideration of these anomalies may explain the amount of complications and poor results of lumbar disc surgery, as roots may be injured during procedures when they are located in abnormal locations. This is especially important when performing minimally invasive surgery where nerve visualisation is not as direct

(Gardocki and Park, 2017). The most common anomalies of the lumbar region are those of the lumbosacral region (Parke *et al.*, 2011). The four main types of variations defined by Kadish and Simmons (1984) are: (1) intradural connections, (2) anomalous origins of roots, (3) extradural connections, and (4) extradural divisions. It is always important to consider the position of the nerve root within the neural foramen in order to avoid injury of the root during surgical procedures, and to aid with the selection of incision site (Taylor *et al.*, 2001).

Neurological variation is not the only troublesome aspect of spine surgery. Variation in blood supply can also lead to complications. An example would be the sacroiliolumbar system formed below the region where the aorta divides into the common iliac arteries at around the level of L4. This is where the arterial complex no longer branches off the aorta, but rather from other origins. The derivatives are mostly from the internal iliac arteries (hypogastric arteries) and consist of the fourth lumbar, iliolumbar, middle –, and lateral sacral arteries. It is seldom that vertebromedullary branches (branches supplying the spinal cord) are found below the level of L4, but when they do occur, they originate from the internal iliac arteries, which means ligation of both internal iliac arteries can result in spinal cord ischaemia (Parke *et al.*, 2011).

2.5.2 Osteology

Understanding how the osteological factors affect spine surgery is very important, as spine surgery often involves bony disfiguration, pathology, and surgical alteration. Pedicle screw loosening and high pull-out rates are common among patients with low BMD values since the bone mineral density of the spine determines the successful anchorage of pedicle screws (Burval *et al.*, 2007, Cho *et al.*, 2010, Schwaiger *et al.*, 2014). Therefore, the BMD value of a patient's spine should be thoroughly analysed before performing spine fusion. Alternative techniques for the placement of the pedicle screws have been investigated to minimise the rate of screw loosening and pullout. A novel screw placement technique using the cortical bone trajectory (CBT) pathway has proven to provide a stronger and more stable method of screw implantation than the traditional trajectory pathway, especially in patients with osteoporotic bone (Santoni *et al.*, 2009, Mai *et al.*, 2016). The BMD of different regions of the vertebrae have also been investigated to find an alternative location for screw placement due to the high prevalence of pullout rates of pedicle screws. A study done by Hohn *et al.* (2017) has found that the densest parts of the vertebrae are in fact the lamina and the inferior articular processes.

Another anatomical consideration is the morphology and position of the spine segments. The main difference between the cervical, thoracic, and lumbar spine is the presence or absence of rib-attachment to the vertebral bodies. This is a common obstacle in thoracic spine surgery, as the rib attaching to the vertebral body is usually a structure restricting access (Kalra *et al.*, 2017). Any injury, degeneration or trauma to the motion segments may lead to a number of morphologically-altering pathologies such as: spondylosis, spondylolysis (defective arch of the vertebra), spondylolisthesis (forward displacement of a vertebral body in relation to another) and/or retrolisthesis (backwards displacement of the vertebral body). Abnormalities or tropisms of the superior articular facets can also occur and are most common at the L5/S1 level (Figure 2.25). It is important to note that the first sacral vertebra is often included in discussions of the lumbar spine, as it is at this point where the mobile lumbar spine joins the fixed sacral spine. In some instances, it has been found that the first sacral vertebra is mobile. This is referred to as lumbarization of S1, and some clinicians refer to the presence of a sixth lumbar vertebra. The opposite may also occur where the fifth lumbar vertebra fuses with the first sacral vertebra. This is then referred to as sacralization of L5 (Magee, 2014).

Vertebral body morphology should be considered when performing surgical procedures such as corpectomies and spinal fusions. Knowledge of the patient's vertebral body and posterior element dimensions and extrapolation with standard normal population values will aid with the reconstruction of the vertebral body into the original or normal functional state. Vertebral body morphology also plays a role in the placement of trajectory screws during ALIF procedures (Prakash *et al.*, 2007, Nuket *et al.*, 2010). Certain morphometric characteristics of the vertebral body can also be indications of possible diseases in patients, and establishing normative values are therefore important for accurate diagnosis (Hayashi *et al.*, 1998, Roux *et al.*, 2016).

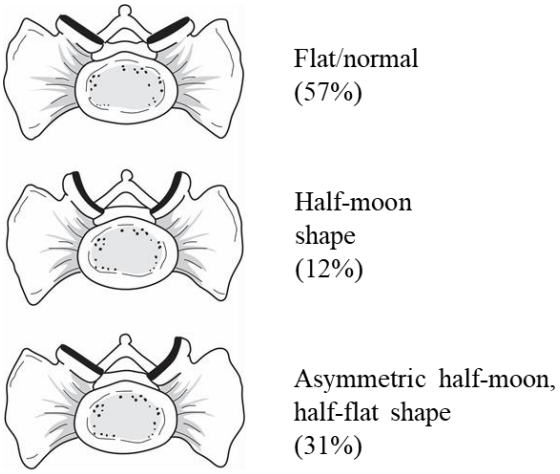

Figure 2.25: Image showing the three most common tropisms and their incidence (%). Adapted from Magee (2014)

2.5.3 Guidelines and suggestions

According to Singh *et al.* (2017) there are ten main anatomical and biomechanical principles to consider when performing any spine surgery. Only the main lumbar spine related principles (6 of the 10) are listed along with their implications in clinical practice:

- Principle 1: Posterior distraction tends to produce a flattened back and is therefore not desirable. The flattened back can lead to chronic lower back pain, as it alters the sagittal balance of the spine
- Principle 2: A spine brace has an inversely proportional relationship to the axial distance between the spine and the inner shell of the brace, and a direct proportionality to the length of the brace above and below the immobilised segments
- Principle 3: An anteriorly placed short-segment fixation device should be applied in a compression mode as it allows the device to share the axial load with an interbody strut
- Principle 4: Circumferential injury (three-column injury), is an indication for spinal instability and requires spinal stabilisation
- Principle 5: Spinal instrumentation will almost certainly fail without concomitant bone fusion. This often leads to the "race between spinal implant failure and the acquisition of a bony fusion"

- Principle 6: Spinal stability is usually lost during decompression surgery and should therefore always be taken into consideration when planning and performing decompression surgeries

Due to the many complications that can result from spine surgery, it is of great importance that clinicians and researchers should understand the various factors involved during these procedures. Having a thorough background knowledge of the mechanisms and structures of the lumbar spine will aid in this regard. It is not only important to have a sound knowledge of these concepts, but to also understand that these may vary between population groups, as variability might affect the ultimate decision on the best course of action and in order to optimise the surgical outcome.

CHAPTER 3: MATERIALS AND METHODS

A quantitative approach was used to investigate the morphological and structural properties of the lumbar vertebrae and related neural structures. CT (Computed Tomography) scans, obtained from the Steve Biko Academic Hospital (SBAH), were used to determine the bone mineral density (BMD) in Hounsfield Units (HU), and skeletal morphometrics of healthy lumbar spines. MRI (Magnetic Resonance Imaging) scans, also obtained from SBAH, were used to measure parameters of the neural foraminae of each level and map the position of the neural structures within the lumbar neural foramen. Cadaveric specimens were dissected to establish the parameters of a triangular safety zone (Kambin's triangle) used by Orthopaedic surgeons to avoid damaging the DRG (dorsal root ganglion) when performing arthroscopic procedures such as discectomies of diseased intervertebral discs (IVDs). Data was recorded using various data sheets.

3.1 Materials

3.1.1 Cadaver component

The sample comprised of twenty white adult, cadaveric lumbar spines (mean age > 70 years) from both the University of Pretoria (n = 12) and the University of Witwatersrand (n = 8) (Table 3.1). The spinal specimens from University of Pretoria were selected from the cadavers used for medical – and dental dissection modules within the Department of Anatomy, University of Pretoria. The spinal specimens from University of Witwatersrand were selected from the cadavers used for medical and dental dissection modules within the School of Anatomical Sciences, University of Witwatersrand.

Any spines that displayed prominent pathology such as ossified ligaments, severe osteoporosis and scoliosis, signs of surgical procedures or any morphological anomalies were excluded from the sample. Within these parameters however, an attempt was made to obtain an equally distributed sample with the available cadavers.

Table 3.1: Cadaver sample demographics

Sex	N	Age (years)	
		Mean ± SD	95% CI
Male	9	78.7 ± 8.7	73.0 – 84.4
Female	11	71.0 ± 16.8	61.1 – 80.9
Key: N = Number of individuals; SD = Standard deviation; CI = Confidence interval			

3.1.2 Imaging component

The sample comprised of eighty-two lumbar CT scans and twenty-six MRI scans. The imaging material was obtained from the Department of Radiology, SBAH with permission from the hospital CEO. Only scans of adult patients (age > 20) were included. Images were excluded if the patient files (CT – and MRI scans) presented with trauma, pathology or surgical intervention affecting the neural structures and skeletal properties of the lumbar spine. The demographics of the samples for the CT – and MRI scans that were used in this study are summarised in Tables 3.2 and 3.3:

Table 3.2: Table indicating the mean age for the entire sample and for each individual population group for the CT scans

Sex	N	Population group (mean age ± SD)				Mean age ± SD	95% CI
		Black	N	White	N		
Male	46	32.56 ± 8.45	33	38.46 ± 11.91	13	34.24 ± 9.78	31.4 – 37.1
Female	36	31.96 ± 9.38	22	37.93 ± 12.78	14	34.28 ± 11.05	30.7 – 37.9
Key: N = Number of individuals; SD = Standard deviation; CI = Confidence interval							

Table 3.3: Table indicating the demographic spread and mean age for each section of the MRI scans

Section	Sex	N	Mean age ± SD	95% CI
Sagittal	**Male**	17	37.1 ± 10.7	31.5 – 42.6
	Female	9	39.2 ± 9.7	31.8 – 46.7
Coronal	**Male**	9	39.1 ± 12.3	29.6 – 48.6
	Female	1	47	N/A
Transverse	**Male**	10	37.0 ± 13.2	27.5 – 46.5
	Female	3	44.0 ± 2.6	37.4 – 50.6
Key: N = Number of cases; SD = Standard deviation; N/A = Not applicable; CI = Confidence interval. All individuals were black				

3.2 Ethics

This research study falls under the National Health Act (Act 61 of 2003). A proposal was submitted, and the project was approved by the Faculty of Health Sciences Research Ethics Committee (320/2017). See the Ethics documentation section at the end of this document.

3.3 Methods

3.3.1 Cadaver component

Dissection

The cadavers were placed in a prone position. The posterior skeletal elements were exposed by removing the overlying soft tissue, which included the skin, subcutaneous tissue, muscles (erector spinae, multifidus, and deep muscles of the back) and ligaments. This was done by creating two incisions on each side of the back: one directly adjacent to the spinous processes and the next approximately 10 to 15cm lateral to the spinous processes (Figure 3.1). Once the spinous processes were exposed and clear of any attaching soft tissue, they were removed. Laminectomies were then performed on the L1 to L4 vertebrae. L5 was not included due to the difficulty of accessing the vertebral body for the dissection without destroying important anatomical landmarks and the high variability of the position of the L5 nerve root (Hogan, 1996, Chen *et al.*, 2013). Laminectomies

involved the removal of the entire bony lamina, a portion of the facet joints and ligaments overlying the spinal cord and nerves. The removal of the spinous processes and the laminectomies were performed using a Makita Multi Tool TM3000CX2 saw. The pedicles were trimmed to the level of the ganglia to ensure maximum exposure of the DNRs (dorsal or posterior nerve roots), DRGs, pedicles, and spinal cord. Care was taken not to damage underlying structures during the dissection.

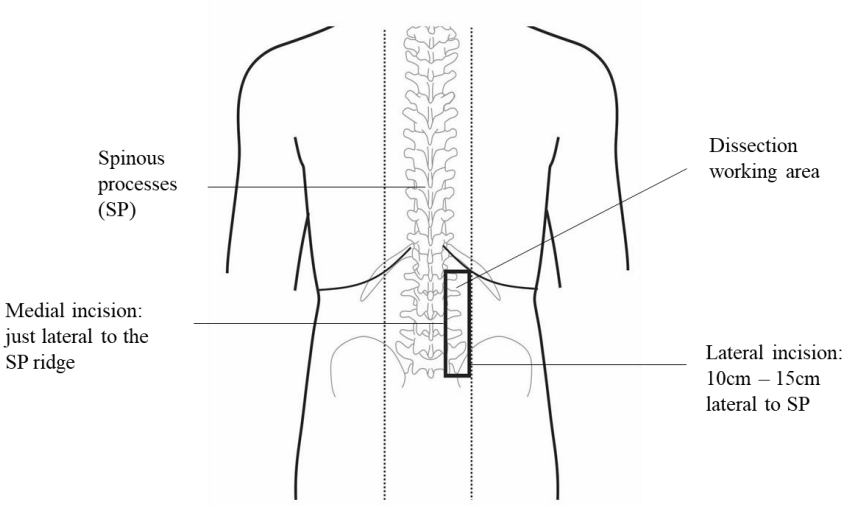

Figure 3.1: Posterior view of the back explaining the incisions made in order to expose the posterior elements of the vertebrae in the cadaver specimens

Measurements:

All measurements were recorded in metric units on a Microsoft Excel spreadsheet alongside the demographics (age, sex, and population group) of each of the cadaver specimens. Measurements were taken using a calibrated electronic sliding calliper; the calliper was zeroed after each measurement was recorded. The roots of the nerves were measured in relation to the pedicles, DRGs, and spinal cord using the following descriptions:

a) Triangle measurements (Figure 3.2 A) were taken by placing a string between pins placed at the points defined below. The measurements were defined according to those used by Matuoka and Basile Júnior (2002):

- Spinal nerve length (SNL): this measurement was defined as the distance from the nerve's appearance from the dura mater to the upper vertebral endplate of the body of the adjacent, inferior vertebra, and was essentially the diagonal measurement or border
- Dura-mater length (DML): this measurement was defined as the distance on the dura mater from the point where the nerve root exited the dura mater to the upper endplate of the body of the inferior vertebra and was essentially the vertical measurement or border
- Distance from dura-mater to the nerve (DDMN): this measurement was defined as the distance between the lateral edge of the dura-mater, at the upper vertebral endplate of the body of the inferior vertebra to the medial edge of the spinal nerve in the transverse axis and was essentially the horizontal measurement or border

The triangle is known as the triangular safety zone or Kambin's triangle and was calculated based on the above measurements. This triangle is used in the clinical setting when deciding on the safest location of access for the IVDs of the lumbar spine, without putting the neural structures at risk. This zone was first defined by Mirkovic *et al.* (1995) and is formed by the SNL, DML and DDMN.

b) Dorsal root ganglion location: The location of the DRG was recorded as being in one of three positions (Figure 3.2 B). These positions were modified versions of a study done by Matuoka and Basile Júnior (2002):
   - Position A (medial foraminal): this position was defined as the area bordered medially by the medial edge of the pedicle and laterally by the sagittal line dividing the pedicle into two halves (midline of the pedicle)
   - Position B (lateral foraminal): this position was defined as the area bordered medially by the sagittal line dividing the pedicle into two halves (midline of the pedicle), and laterally by the lateral edge of the pedicle
   - Position C (extra-foraminal): this position was defined as the area bordered medially by the lateral edge of the pedicle

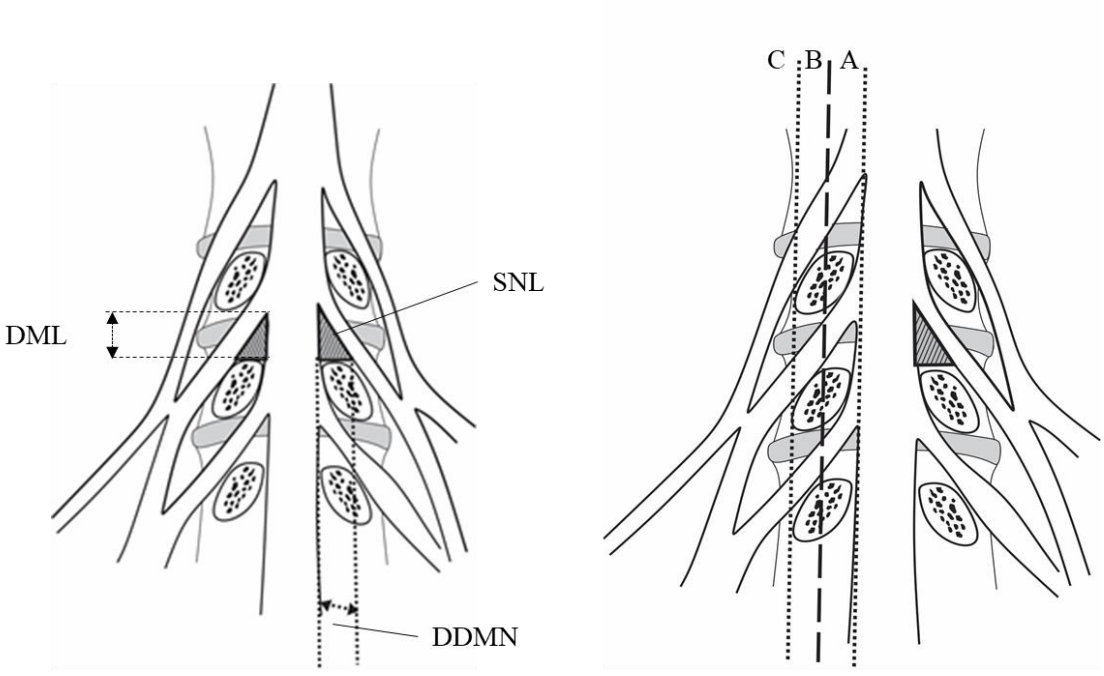

A. Kambin's triangle B. Ganglion position

Figure 3.2: Image of Kambin's triangle (A), and the possible position of the DRG. Adapted from Matuoka and Basile Júnior (2002)

Key: In A: DML = Dura-mater length (the vertical length); SNL = Spinal nerve length (the diagonal length); DDMN = Distance from dura-mater to nerve (the horizontal length). In B: A = The medial position in relation to the pedicle; B = The middle position in relation to the pedicle; C = The lateral position in relation to the pedicle

3.3.2 Radiographic material analysis

All MRI – and CT analyses were performed on vertebral levels L1 through to L5. For the transverse CT scans, the level of L1 was determined by finding the level where the last costal articulation could be seen (which should be the level of T12). The vertebral level below this was estimated to be that of L1.

Measurements

The skeletal morphology of the vertebrae was measured on the CT scans while the position and relations of the neural foramina was examined on the MRI scans. All measurements were recorded in metric units on a Microsoft Excel spreadsheet alongside the demographics (age, sex, and population) of each patient file. All patient files received a unique reference number to maintain anonymity. Measurements were taken using IMPAX CD Viewer (for the MRI – and CT scans).

CT scan measurements:

a) Lumbar lordosis angle (LLA): the lumbar lordosis angle was measured on the CT scans using the traditional Cobb method. This method uses the angle between the intersection of two lines drawn from the superior endplate of L1 and the inferior endplate of L5 (Figure 3.3) (Hwang *et al.*, 2010, Ghandhari *et al.*, 2013)

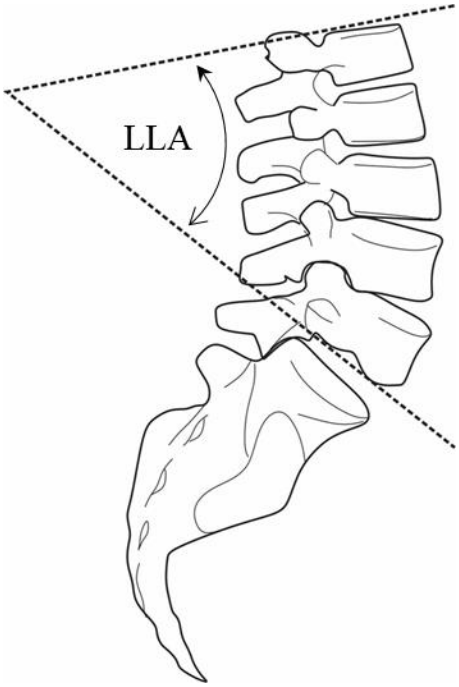

Figure 3.3: Image indicating the lumbar spine lordosis or lumbar lordosis angle (LLA). Adapted from (Ghandhari *et al.*, 2013)

b) BMD: the BMD was determined using the HU method. Firstly, the cortical BMD was measured at the anterior – (AB) and posterior (PB) borders, and superior – (SEP) and inferior (IEP) endplates of the vertebral bodies. A line was drawn from the two furthest points of each border or endplate (most anterior and posterior points for the endplates; most superior and inferior points for AB and PB), and the average BMD measurement was recorded. Taking the cortical BMD on the anterior margin was somewhat difficult due to the irregular surface. After cortical BMD was measured, the medullary BMD was determined using regions of interest (ROIs) within the vertebral body. This was done

according to a method described by Schreiber *et al.* (2011), where an elliptical or circular shape was drawn on three regions of the vertebral body confined to the medullary space. The first (ROI1) being below the superior endplate, the second (ROI2) halfway down the vertebral body, and the third (ROI3) being just above the inferior endplate. Computer software was used to calculate the average HU value. The ROIs were measured on transverse CT images at L1 through L5:

- ROI1: the region inferior to the superior endplate
- ROI2: the region in the centre of the vertebral body
- ROI3: the region superior to the inferior endplate

The level of the intervertebral disc was first established and was the point where the pedicles and transverse processes were no longer visible, and an obscurity on the vertebral body could be seen (Figure 3.4). Moving inferiorly from the intervertebral disc level, ROI1 was determined as the point where the pedicles became visible (but not the transverse processes) (Figure 3.5). Care was taken not to measure the superior endplate. This was avoided by referring to the BMD values, as the value of the superior endplate should be significantly higher than the BMD value below the endplate (Figure 3.6). ROI2 was defined as the level at which most of the posterior elements (pedicles, transverse processes, beginning of laminas and part of the spinous process) were visible (Figure 3.7). When moving inferiorly from ROI2 until the transverse processes were no longer visible, the point of ROI3 was found. Note that no facet joints were visible on ROI3, but only on the level of the intervertebral disc (inferior to ROI3). Care was taken not to measure the inferior endplate. This was avoided by referring to the BMD values, as the value of the inferior endplate should be significantly higher than the BMD value above the endplate. This meant that a value might have to be taken just superior to the defined level (i.e.: pedicles might still have been visible) (Figure 3.8).

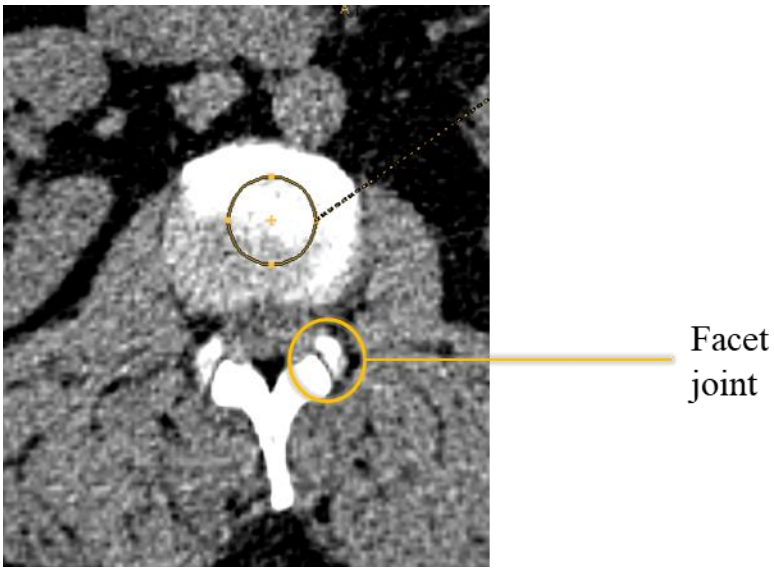

Figure 3.4: Transverse CT scan at the level of the IVD at level L2/L3

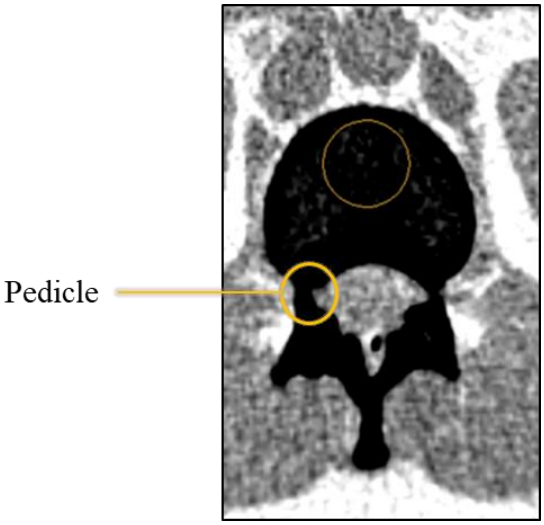

Figure 3.5: Transverse CT scan at the level of L1 showing the level of ROI1

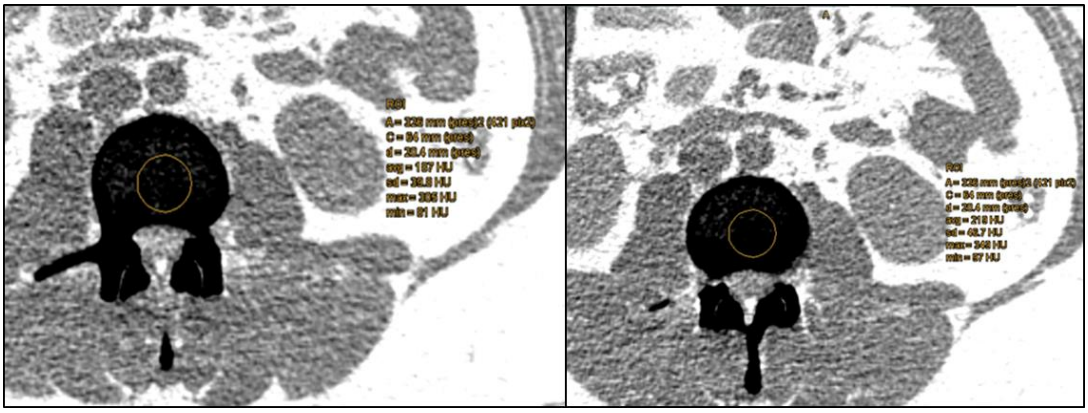

Figure 3.6: Transverse slice at the level of L3 showing the difference between ROI1 (on the left, with HU = 187) and the superior endplate (on the right, with HU = 218)

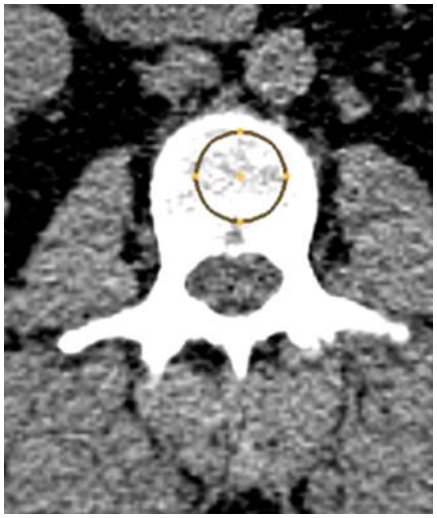

Figure 3.7: Transverse slice at the level of L3 showing ROI2

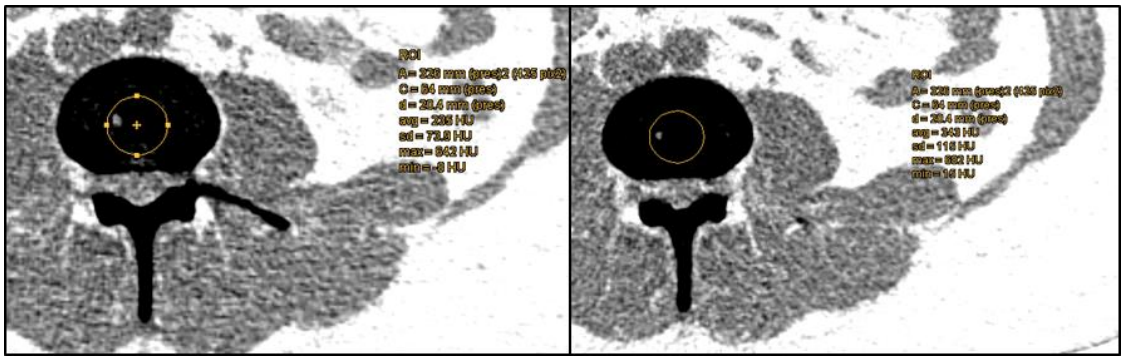

Figure 3.8: Transverse slice at the level of L3 showing the difference between ROI3 (on the left, with HU = 235) and the inferior endplate (on the right, with HU = 343)

c) Skeletal measurements were performed on the CT scans using IMPAX CD Viewer. Figure 3.9 indicates the parameters which were determined for the bony vertebrae. The parameters were defined as follows:

- VDMaxL (maximum vertebral body diameter from lateral to lateral): largest distance between the lateral borders of the vertebral body (at the level of the superior endplate)
- VDMinL (minimum vertebral body diameter from lateral to lateral): smallest distance between the lateral borders of the vertebral body (midway down the vertebral body)
- VDMaxAP (maximum vertebral body diameter from anterior to posterior): largest distance between the anterior and posterior borders of the vertebral body (at the level of the SEP)
- VDMinAP (minimum vertebral body diameter from anterior to posterior): smallest distance between the anterior and posterior borders of the vertebral body (midway down the vertebral body)
- SCDL (spinal canal lateral diameter): distance between the inner borders or the pedicles at the level where the pedicles, laminae, transverse –, and spinous process were visible
- SCDAP (spinal canal AP diameter): distance from the posterior border of the vertebra to the lamina at the midline at the level where the pedicles, laminae, transverse –, and spinous process were visible
- PDDL (pedicle lateral diameter): distance from the medial to the lateral border of the pedicle at the level where the pedicles, laminae, transverse –, and spinous process were visible
- VHa and VHp (vertebral body height anterior and posterior): distance between the superior – and inferior endplates of the vertebral body at the anterior – or posterior borders respectively
- TPL (transverse process length): distance between the tips of the transverse processes
- PDH (pedicle height): distance from the superior – to the inferior border of the pedicle
- SPL (spinous process length): length of spinous process from a sagittal view in the middle of the process

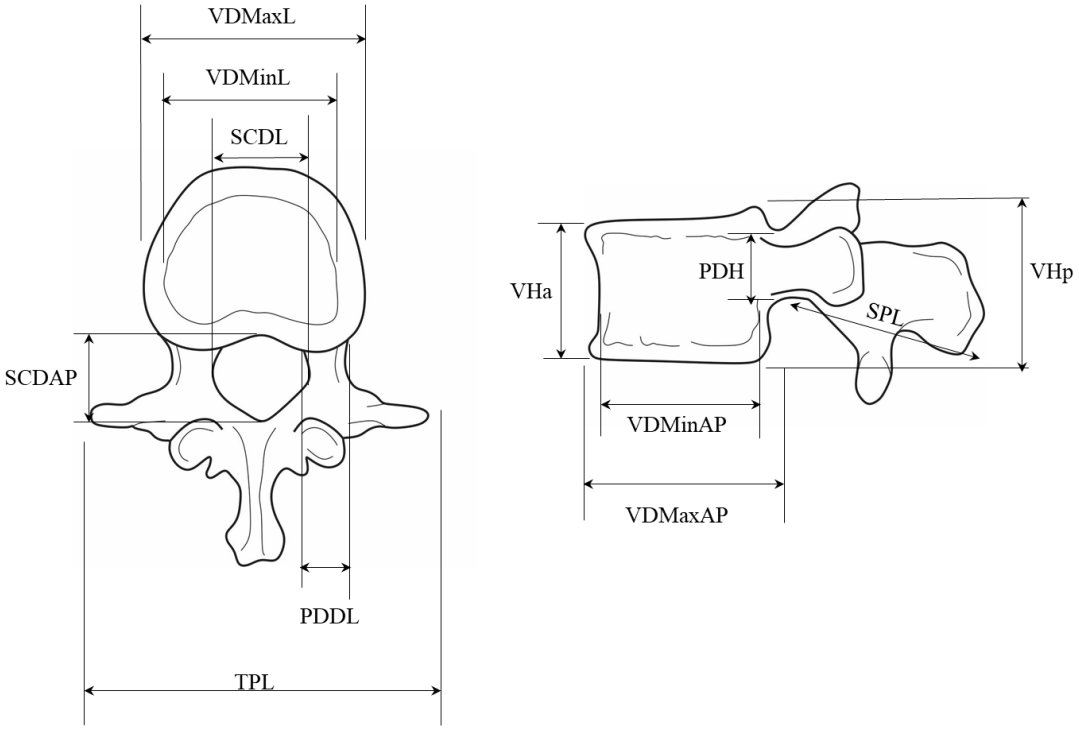

Figure 3.9: Figure showing the skeletal measurements taken on the CT scans

Key: In the transverse view on the left: VDMaxL = Maximum vertebral body lateral diameter (at the superior endplate); VDMinL = Minimum vertebral body lateral diameter (halfway down the vertebral body); SCDL = Spinal canal lateral diameter; SCDAP = Spinal canal anteroposterior diameter; PDDL = Pedicle lateral diameter; TPL = Distance between the two transverse processes. In the sagittal view on the right: VDMaxAP = Maximum vertebral body anteroposterior diameter (at the superior endplate); VDMinAP = Minimum vertebral body anteroposterior diameter (halfway down the vertebral body); VHa = Anterior vertebral body height; VHp = Posterior vertebral body height; PDH = Pedicle height; SPL = Spinous process length

MRI scan measurements:

Neural foramen and nerve root measurements were performed on the MRI scans using IMPAX CD viewer. These measurements are shown in Figures 3.10 to 3.12 and were defined according to those used by Hurday *et al.* (2017) and taken on sagittal –, transverse – and coronal sections:

a) Sagittal section measurements (Figure 3.10):

- Foraminal height (FH): distance between inferior border of the superior pedicle and superior border of the inferior pedicle

- Foraminal diameters:
    - Superior foraminal diameter (SFD): distance between the most postero-superior edge of the IVD and the anterior surface of the facet
    - Middle foraminal diameter (MFD): distance between the most postero-middle point of the IVD and the anterior surface of the facet
    - Inferior foraminal diameter (IFD): distance between the most postero-inferior point of the IVD and the anterior surface of the facet
- Nerve root-to-disc distance (RD): distance between the superior margin of the disc and the inferior margin of the DNR. Distances measured above the superior margin of the IVD were considered as negative readings (-mm) and below as positive readings (+mm)
- Nerve root-to-pedicle distance (RP): distance between the inferior margin of the DNR and the superior margin of the pedicle

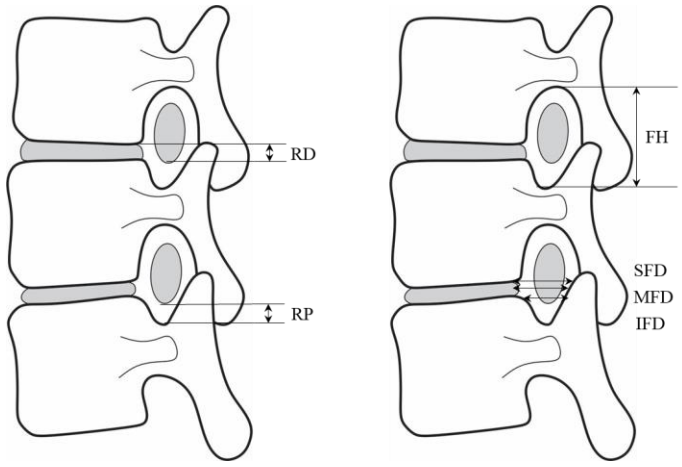

Figure 3.10: Graphic representation of the sagittal measurements taken. Adapted from Hurday *et al.* (2017)

Key: In the figure on the left: RD = Distance between the dorsal nerve root and the superior border of the intervertebral disc; RP = Distance between the dorsal nerve root and the superior border of the pedicle. In the figure on the right: FH = Foraminal height; SFD = Superior foraminal diameter; MFD = Middle foraminal diameter; IFD = Inferior foraminal diameter

b) On the transverse sections (Figure 3.11):

- Superior margin of the IVD:
    - Foraminal transverse AP diameter (FDTS): shortest distance between the posterior surface of vertebral body and the anterior surface of the facet
    - Nerve root-to-disc distance (RDS): shortest distance between the DNR and the posterior surface of the IVD
    - Nerve root-to-facet distance (RFS): shortest distance between the DNR and the anterior surface of the facet
    - Target angle (TAS): angle between a horizontal line along the posterior surface of the IVD and a line crossing the anterior surface of the facet to posterio-middle corner of the disc (target line)
- Inferior margin of the IVD (similar descriptions as for the superior margin were applied to the inferior margin):
    - Foraminal width (FDTI)
    - Nerve root-to-disc distance (RDI)
    - Nerve root-to-facet distance (RFI)
    - Target angle (TAI)

All distances and angles anterior to the posterior vertebral line were considered as negative readings (-mm) and those posterior as positive readings (+mm).

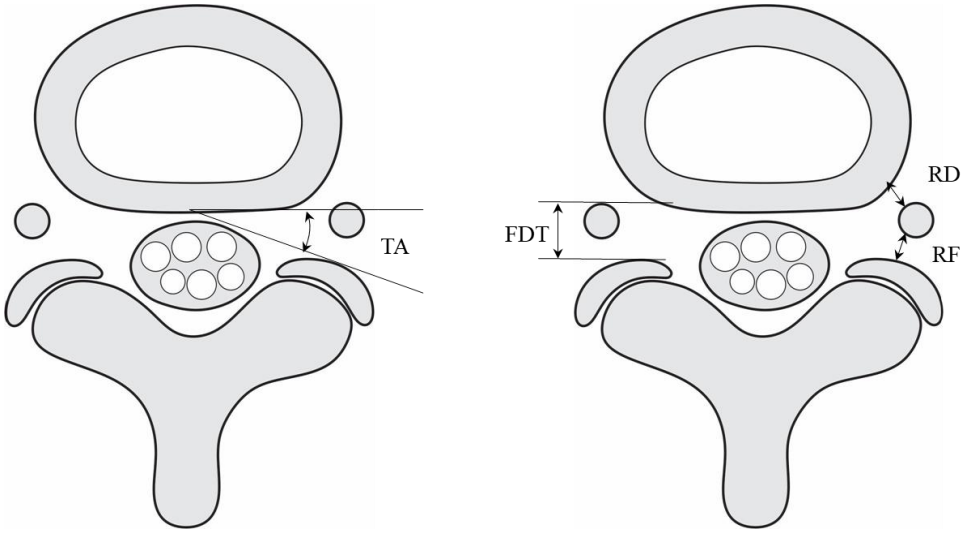

Figure 3.11: Figure indicating the measurements taken on the transverse sections. Adapted from Hurday *et al.* (2017)

Key: Image on the left: TA = Target angle. Image on the right: FDT = Foraminal transverse anteroposterior diameter; RD = Distance from the nerve root to the intervertebral disc; RF = Distance from the nerve root to the facet joint. Note that these measurements are the same for the levels superior and inferior to the IVD

c) On the coronal sections (Figure 3.12):

- Nerve root-to-disc measurements (distances):
  - Medial border of the pedicle (MedD): distance from the DNR to the IVD at the medial border of the pedicle
  - Middle of the pedicle (MidD): distance from the DNR to the IVD at the midline of the pedicle
  - Lateral border of the pedicle (LatD): distance from the DNR to the IVD at the lateral border of the pedicle
- Nerve root-to-pedicle measurements (distances):
  - Medial border of the pedicle (MedP): distance from the DNR to the pedicle at the medial border of the pedicle
  - Middle of the pedicle (MidP): distance from the DNR to the pedicle at the midline of the pedicle
  - Lateral border of the pedicle (LatP): distance from the DNR to the pedicle at the lateral border of the pedicle

For the root-to-disc measurements that crossed inferior to the superior margin of the IVD, the readings were considered as positive (+mm) and those above as negative (-mm).

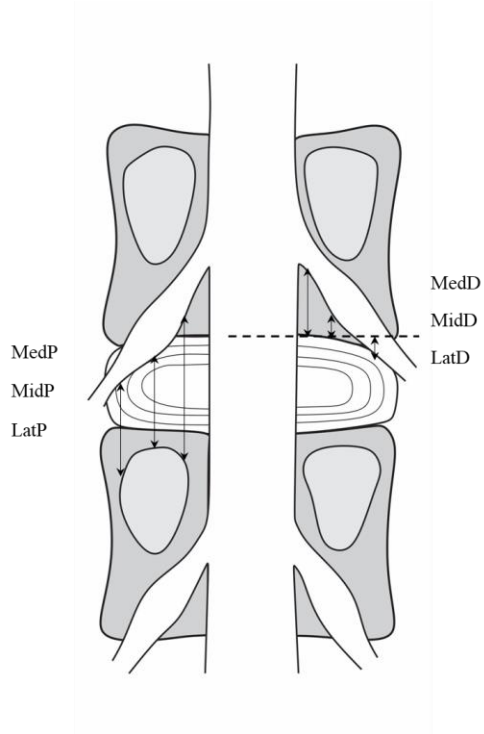

Figure 3.12: Figure showing the measurements taken on the coronal scans. Adapted from Hurday *et al.* (2017)

Key: MedP = Medial root-to-pedicle distance; MidP = Midline root-to-pedicle distance; LatP = Lateral root-to-pedicle distance; MedD = Medial root-to-disc distance; MidD = Midline root-to-disc distance; LatD = Lateral root-to-disc distance. The dashed line indicates the superior border of the IVD

3.4 Statistical analysis

Statistical analyses were performed by guidance of biostatisticians. Tests were evaluated at 5% level of significance and all analyses were done using STATA 14 and SPSS.

3.4.1 Descriptive statistics

Similar descriptive statistical methods were used in all three components of the study. The descriptive statistics such as mean, standard deviation and 95% confidence intervals (with the lower and upper limits), were used to describe continuous variables. Continuous variables were

those which were expressed as values between a minimum and a maximum on a predefined measurement scale (D'Agostino *et al.*, 2006a), including BMD and morphological parameters of the vertebrae and soft tissue elements. This provided an idea of the spread, trends, and distribution of the data. Frequencies and proportions were used to describe categorical variables, to illustrate the distribution of the sample. Categorical variables were those which took on an unordered, limited number of categories (D'Agostino *et al.*, 2006a) such as sex and population.

3.4.2 Comparative statistics

Parametric tests

T-tests

The t-test, or non-parametric alternative, is used in statistics in order to test for mean differences of continuous outcome variables between groups of categorical variables which are normally distributed. T-tests work on the basis of hypothesis testing. This involves creating a null – and alternative hypothesis, where the null hypothesis (written as H_0) is a statement or speculation of a characteristic of the distribution. The aim of the t-test is to determine whether H_0 is true or not, and this is accomplished through creating an alternative, contradicting statement: the alternative hypothesis (H_1). If H_0 is rejected, then H_1 is accepted. For example: If H_0: $\mu \geq 50$, then H_1: $\mu < 50$. T-tests are generally used in normal distributions to test the hypotheses when the standard deviation (σ) of the population is not known, but the standard deviation of the sample (s) is known. This is achieved through determining the distribution of T (Formula 3.4.1) (Wilcox, 2003a):

$$T = \frac{\bar{X} - \mu_0}{s/\sqrt{n}}$$

With the critical value determined using a standard critical value table and the degrees of freedom set to $v = n - 1$. The decision rules for testing the hypotheses are as follows (Wilcox, 2003a):

- For H_0: $\mu \geq \mu_0$, reject if $T \leq c$, where c is the α quantile of Student's T distribution with $v = n - 1$ degrees of freedom and T is given by Formula 3.4.1.
- For H_0: $\mu \leq \mu_0$, reject if $T \geq c$, where c is the $1 - \alpha$ quantile of Student's T distribution with $v = n - 1$ degrees of freedom

- For H_0: $\mu = \mu_0$, reject if $T \geq c$ or $T \leq -c$, where c is the $1 - \alpha/2$ quantile of Student's T distribution with $v = n - 1$ degrees of freedom. Equivalently, reject if $|T| \geq c$.

Pearson's Correlation

Correlation analyses takes into account the relationship between two different continuous variables. The goal of the analysis in statistics is to determine if any relationship exists between variables, and how strong this relationship is. Pearson's correlation coefficient (r) depicts the nature of a linear relationship between variables, meaning that one variable decreases as the other increases, and vice versa. It takes on a value ranging from -1 to 1, where negative values indicate an inverse linear relationship, and a positive value a direct linear relationship (D'Agostino *et al.*, 2006b). The r^2 value is the coefficient of determination and is the squared value of the previously determined r-value. This value determines the strength of the relationship, whereas the r-value shows the directionality of the relationship (through the sign of the value), as well as indicating whether a linear relationship exists. An r^2 value between 0.85 and 1, shows a strong correlation or relationship. A value between 0.65 and 0.84 is usually moderate, and anything below 0.65 is usually considered weak or poor (Wilcox, 2003b).

Often times an important correlation can be overlooked because it is only of moderate strength. However, when looking at scatter plots generated for correlation analyses, a very clear curved relationship can be seen, which means the linear correlation coefficient will not depict a strong relationship, even though a clearly important one exists. Other factors can also affect the r value such as: outliers, the slope of the line around which the points are clustered and the magnitude of the residuals. Therefore, correlation coefficients should be interpreted alongside their scatterplots (Wilcox, 2003b). If a non-linear relationship is observed, an appropriate formula can be applied to the data in order to transform the data from non-linear to linear. The test can then be repeated, and a new, relevant value can be observed, allowing the interpretation of initially non-linear data using linear techniques. Transforming data using logarithms is known as an exponential model (used when an exponential relationship is observed on the scatter-plot), using square roots or the reciprocal (if the r-value is negative) is known as a quadratic or reciprocal model (used when a quadratic or reciprocal relationship is observed on the scatterplot), and using cubic terms is known as a cubic model (when a cubic relationship is observed in the scatterplot) (Hazarika, 2013).

Nonparametric tests

The Sign test

The Sign test compares two dependent groups of continuous variables or samples by focusing on the differences between measurements. The sign test works on the null hypothesis that the median difference is zero. It is usually applied to a small sample of binomially distributed data. A p-value of less than 0.05 is considered as significant in this test, and the data will then be considered to be significantly different (the null hypothesis is rejected). This test does not focus on the magnitude of the differences, but merely on the direction. The direction is used to describe whether the one measurement is larger (a positive sign/direction) or smaller (a negative sign/direction) than the other. In other words, the Sign test indicates whether a difference exists and whether the one variable is larger than the other, but does not specify by how much (D'Agostino *et al.*, 2006c).

Kruskal-Wallis Test

The Kruskal-Wallis test is also used when comparing multiple groups of continuous variables/measurements. It is the nonparametric analogue to ANOVA (analysis of variance) testing. This test works on the basis of assigning ranks to values which are observed in the measurements. It then sums the observed ranks and compares it to what would be expected if no difference existed among the groups (D'Agostino *et al.*, 2006c). The main goal is to determine whether any difference exists between the distribution of multiple groups. The null hypothesis being that no such difference exists. If a p-value of less than 0.05 is obtained, the null hypothesis is rejected, and a significant difference exists between the groups (Wilcox, 2003c).

McNemar's test

McNemar's test is a test for correlated proportions of categorical data and aims to determine whether two sample proportions on the same individuals are equal. It is based on the Chi-squared distribution with 1 degree of freedom (Salkind, 2010b).

Fisher's Exact test

The Fisher's exact test is a nonparametric test used when comparing categorical data. It is used to analyse the difference between the proportion of two groups (Routledge, 2005). It tests for associations between variables.

Mann-Whitney U test

This test is used to compare the means of two independent variables or samples which do not have a normal distribution. It is nonparametric in that it uses analyses done on the rank order of the scores of the data. It tests whether the mean ran scores of the one sample is the same as the mean rank scores of the other sample within the population (Salkind, 2010a).

Shapiro-Wilk test for normality

Shapiro-Wilk test tests for the normality of the distribution of the data. It is a highly complex test which basically generates the ratio between the square of the linr combination of standard normal statistics to the sample variance (Lewis-Beck *et al.*, 2004).

Linear Regression

Linear regression is used to determine whether one variable influences another and is basically the linear method used during Pearson's correlation analyses. Regression analysis is a useful technique for determining relationships between two variables. Linear regression assumes that the mean of a response variable (Y) is related to the regressor or predictor variable (x) by the following straight-line relationship (Formula 3.4.2) (Montgomery and Runger, 2007):

$$E(Y|x) = \beta_0 + \beta_1 x$$

Where:

β_0 = the intercept

β_1 = the slope

When both the slope and the intercept are unknown regression coefficients, we assume that each observation, Y, can be expressed as (Formula 3.4.3) (Montgomery and Runger, 2007):

$$Y = \beta_0 + \beta_1 + \epsilon$$

Where:

ϵ = a random error with mean zero and variance σ^2

This model is simple as it only contains one independent variable or regressor. The true regression model (Formula 3.4.4):

$$\mu_{(Y|x)} = \beta_0 + \beta_1 x$$

is essentially a line of mean values; meaning that the height of the regression line at any value of x is the same as the expected value of Y for that x. The slope is the change in the mean of Y for a unit change in x (Montgomery and Runger, 2007).

3.4.3 Inter – and intra-observer error

Intra – and interobserver agreement can be tested for by using the intraclass correlation coefficient (ICC). This coefficient tests for relative similarity between numerical measurements (LaVange and Koch, 2006). The ICC is a method that measures relative reliability. This is due to it being a unitless value which is derived from ANOVA and is easier to understand than the commonly used r-value and Pearson's correlation tests. The ICC can range between 0 and 1.0, where 0 shows no reliability and 1.0 indicates 100 percent reliability. An ICC less than 0.5 is weak; between 0.50 and 0.75 is average; between 0.75 and 0.9 is good; and greater than 0.9 is excellent. It is important to understand that the ICC is a context specific value, in that its magnitude depends on between-subjects variability (Weir, 2005).

The ICC is applicable for both intra – and interobserver tests. With intra-observer, the measurements were performed by the primary investigator on two separate occasions. With interobserver, the measurements were performed by two independent investigators.

CHAPTER 4: RESULTS

In order to determine whether any population specific trends existed for material and morphometric properties of the South African lumbar spine, five statistical procedures were used for the cadaver component, and seven statistical procedures were used for the imaging component.

4.1 Cadaver component

The cadaver component included measurements taken of the three sides of Kambin's triangle on both the left – and right-hand sides for L1 to L4, as well as the recorded ganglion position for each of these levels on either side. The aim was to add possible population specific data unique to our South African population to existing databases of other populations. The reason for this was to optimise the understanding in terms of the variation of Kambin's triangle and the ganglion position between various population groups. This is essential, as it is a common anatomical consideration used during lumbar spine surgery.

Descriptive statistics were generated first for the qualitative – (dorsal root ganglion position) and quantitative continuous (Kambin's triangle measurements) data. Descriptive statistics involved determining the means, standard deviations, and upper – and lower limits of the 95% confidence intervals. Comparative analyses were performed on the continuous (triangle dimensions) and categorical (ganglionic position) data. When comparing sexes, a Kruskal-Wallis test was used (non-parametric test), which tested for distribution agreement between the males and females for specific variables. For categorical variables, a Fisher's exact test was used in order to determine whether an association existed between sex and the outcome variable. When comparing the left – and right-hand sides, a Sign test was used for continuous variables, and the two-sided p-value was reported. Categorical variables were tested using McNemar's test, in which a null hypothesis is used which stated that the variables agree. The raw data used to perform statistical analyses can be accessed in Appendix A.1.

4.1.1 Cadaver descriptive statistics

Descriptive statistics were calculated for the three sides of Kambin's triangle and are presented in Tables 4.1 to 4.3. The general position of the dorsal root ganglion (DRG) is also seen in Table 4.4. The results indicated that the diagonal border (SNL) was the longest in both males and females (Table 4.2). The vertical and horizontal borders (DML and DDMN, respectively) indicated similar lengths for both males and females, with the horizontal border being slightly shorter than the vertical (Tables 4.1 and 4.3).

Table 4.4 shows a clear trend in DRG position, where the majority of the ganglia were found in Position B for both sexes, followed by C for females and A for males, and then A for females and C for males. The only exception lies at L4, where the majority of DRGs were found in Position C. The total ganglia found in Position A were 25 (14 in males and 11 in females), Position B were 104 (47 in males and 57 in females), and in Position C were 30 (10 in males and 20 in females).

Table 4.1: Table showing the descriptive statistics of the vertical border (DML) of Kambin's triangle for the left – and right-hand sides of each vertebral level

Level	Sex	Left				Right			
		N	Mean	SD	95%CI	N	Mean	SD	95%CI
L1	Male	8	17.1	1.0	16.5 – 17.8	9	15.6	1.7	14.5 – 16.7
	Female	11	15.7	2.6	14.2 – 17.3	11	15.8	2.0	14.6 – 17.0
L2	Male	9	17.5	1.7	16.4 – 18.7	9	17.4	0.6	17.0 – 17.8
	Female	11	16.4	1.4	15.6 – 17.2	11	15.5	1.8	14.5 – 16.6
L3	Male	9	17.0	0.8	16.4 – 17.5	9	17.1	1.2	16.3 – 17.8
	Female	11	16.2	1.8	15.2 – 17.3	11	15.7	2.4	14.2 – 17.1
L4	Male	9	17.0	1.4	16.0 – 17.9	9	16.8	0.9	16.2 – 17.4
	Female	10	16.2	1.9	15.0 – 17.3	10	15.8	1.9	14.7 – 17.0

Key: N = Number of individuals per group; SD = Standard deviation; CI = Confidence interval. Measurements are in millimetres

Table 4.2: Table showing the descriptive statistics of the diagonal border (SNL) of Kambin's triangle for the left – and right-hand sides of each vertebral level

Level	Sex	Left				Right			
		N	Mean	SD	95%CI	N	Mean	SD	95%CI
L1	Male	8	21.4	2.1	19.9 – 22.8	9	22.1	3.5	19.8 – 24.4
	Female	11	20.7	1.9	19.6 – 21.8	11	21.7	1.5	20.9 – 22.6
L2	Male	9	21.6	1.5	20.7 – 22.6	9	22.2	1.5	21.3 – 23.2
	Female	11	21.3	1.8	20.2 – 22.4	11	21.8	1.2	21.2 – 22.5
L3	Male	9	21.1	1.1	20.4 – 21.9	9	22.1	2.1	20.8 – 23.5
	Female	11	19.9	2.0	18.7 – 21.0	11	20.9	2.0	19.7 – 22.1
L4	Male	9	22.6	2.8	20.7 – 24.4	9	23.7	3.2	21.6 – 25.8
	Female	10	21.5	2.3	20.1 – 23.0	10	22.9	1.9	21.7 – 24.1

Key: N = Number of individuals per group; SD = Standard deviation; CI = Confidence interval. Measurements are in millimetres

Table 4.3: Table showing the descriptive statistics of the horizontal border (DDMN) of Kambin's triangle for the left – and right-hand sides of each vertebral level

Level	Sex	Left				Right			
		N	Mean	SD	95%CI	N	Mean	SD	95%CI
L1	Male	8	15.3	2.1	13.9 – 16.7	9	16.2	2.3	14.7 – 17.7
	Female	11	15.6	2.3	14.2 – 16.9	11	15.0	2.3	13.6 – 16.4
L2	Male	9	15.4	2.3	14.0 – 16.9	9	15.1	2.4	13.6 – 16.7
	Female	11	15.7	1.6	14.7 – 16.7	11	15.3	2.3	14.0 – 16.7
L3	Male	9	16.2	2.0	14.9 – 17.6	9	16.5	1.9	15.2 – 17.7
	Female	11	15.2	1.8	14.2 – 16.3	11	15.0	1.7	14.0 – 16.0
L4	Male	9	17.4	2.6	15.7 – 19.1	9	17.1	3.3	14.9 – 19.3
	Female	10	16.8	1.5	15.8 – 17.7	10	17.2	1.8	16.1 – 18.3

Key: N = Number of individuals per group; SD = Standard deviation; CI = Confidence interval. Measurements are in millimetres

Table 4.4: The distribution of the position of the DRG on both the left – and right-hand sides of the four vertebral levels.

Level	Sex	Position A			Position B			Position C		
		Left	**Right**	**Total**	**Left**	**Right**	**Total**	**Left**	**Right**	**Total**
L1	**Male**	2	5	7	4	2	6	2	2	4
	Female	0	5	5	10	6	16	1	0	1
	Total	**2**	**10**	**12**	**14**	**8**	**22**	**3**	**2**	**5**
L2	**Male**	1	2	3	8	7	15	0	0	0
	Female	2	1	3	9	10	19	0	0	0
	Total	**3**	**3**	**6**	**17**	**17**	**34**	**0**	**0**	**0**
L3	**Male**	1	1	2	7	6	13	1	2	3
	Female	1	2	3	9	9	18	1	0	1
	Total	**2**	**3**	**5**	**16**	**15**	**31**	**2**	**2**	**4**
L4	**Male**	1	1	2	7	6	13	1	2	3
	Female	0	0	0	2	2	4	9	9	18
	Total	**1**	**1**	**2**	**9**	**8**	**17**	**10**	**11**	**21**
TOTAL		**8**	**17**	**25**	**56**	**48**	**104**	**15**	**15**	**30**

Key: Position A = Between the medial border and the midline of the caudal pedicle; Position B = Between the midline and the lateral border of the caudal pedicle; Position C = Lateral to the lateral border of the caudal pedicle

4.1.2 Cadaver comparative statistics

When comparing sexes using the Kruskal-Wallis test, differences were seen at L2 on the right-hand side at the vertical border (DML) ($p = 0.010$), where the females showed significantly shorter lengths than males (Tables 4.1 and 4.5). Fisher's exact test showed that a relationship existed between sex and the DRG position on both sides at L4 ($p = 0.003$ – left; $p = 0.020$ – right) where males showed ganglia situated more centrally (position B), and females more laterally (position C) for both sides (Tables 4.4 and 4.6). The male and female groups were pooled for the left – and right-hand measurement comparisons due to only one significant difference between sexes (Table 4.5). When using the Sign test to compare the measurements for left – and right-hand sides, differences were observed for measurements at the diagonal border (SNL) at L4 ($p = 0.030$), where the right-hand side was significantly longer than the left (Tables 4.2 and 4.7). The male and female groups were pooled for DRG comparisons between sides, due to only one level showing

differences between sexes (Table 4.6). When using McNemar's test to compare the position of the ganglia for left – and right-hand sides, the results indicated that at L1 (p = 0.040) the left ganglion was situated more centrally and, on the right, more medially (position A) (Tables 4.4 and 4.8).

Table 4.5: Table depicting the p-values obtained from the Kruskal-Wallis tests for comparing male and female border measurements

Measurement	VL	Side	
		Left	Right
SNL	L1	0.248	0.732
	L2	0.790	0.382
	L3	0.382	0.518
	L4	0.462	0.683
DML	L1	0.216	0.621
	L2	0.184	0.012*
	L3	0.305	0.224
	L4	0.369	0.270
DDMN	L1	0.216	0.271
	L2	0.518	0.732
	L3	0.342	0.119
	L4	0.462	0.624

*Key: VL = Vertebral level; SNL = Spinal nerve length or diagonal border; DML = Dura mater length or vertical border; DDMN = Distance from dura mater to the nerve or horizontal border; * = Significant p-value*

Table 4.6: Table depicting the two-sided p-values obtained from Fisher's exact tests for comparing male and female DRG positions

VL	Side	
	Left	Right
L1	0.177	0.142
L2	1.000	0.566
L3	1.000	0.361
L4	0.003*	0.022*

*Key: VL = Vertebral level; * = Significant p-value*

Table 4.7: Table depicting the two-sided p-value obtained from the Sign-test for comparing left – and right-hand border measurements

Measurement	VL	p-value
SNL	**L1**	1.000
	L2	0.503
	L3	0.263
	L4	0.031*
DML	**L1**	0.648
	L2	0.263
	L3	1.000
	L4	1.000
DDMN	**L1**	1.000
	L2	0.824
	L3	0.824
	L4	0.167
*Key: VL = Vertebral level; SNL = Spinal nerve length; DML = Dura mater length; DDMN = Distance from dura mater to nerve; * = Significant p-value*		

Table 4.8: Table depicting the two-sided p-value obtained from the McNemar's test for comparing left – and right-hand DRG position

VL	p-value
L1	0.039*
L2	1.000
L3	1.000
L4	1.000
*Key: VL = Vertebral level; * = Significant p-value*	

4.1.3 Inter – and intra-observer analysis

ICC (Interclass Correlation Coefficient) could not be determined for the cadaver section of the study, as the maceration of remains occurred almost immediately after the initial dissection. Only two cadavers out of the entire sample were available for inter – and intra-observer testing. This

small sample size was not sufficient for meaningful statistical analyses. This is one of the major limitations of the cadaver component of the study.

4.2 CT component

The aim of the CT (Computed Tomography) component was to identify possible population specific trends for the material and morphological properties considered during lumbar spine procedures. The CT component consisted of measurements taken for the bone mineral density (BMD) of the vertebral bodies of L1 to L5, as well as morphometric measurements taken on each of these levels for skeletal components. The lumbar lordosis angle (LLA) was also recorded and analysed. Descriptive statistics were generated for all measurements, and involved determining the means, standard deviations, and upper – and lower limits of the 95% confidence intervals. Pearson's correlation, linear regression, and non-linear regression analyses were used in order to determine if any relationship existed between the LLA and either the BMD or the morphometric data. The data was first tested for normality using Shapiro-Wilk tests. Values less than 0.05 were considered significant and was evidence for non-normally distributed data. Normally distributed data was compared using two-sided t-tests, and comparisons between non-normal data was tested using Mann-Whitney U tests. These methods were applied when comparing males and females and the different population groups to one another. Paired t-tests were used to compare the left – and right-hand; anterior – and posterior measurements; and maximum – and minimum measurements to each other where applicable.

The repeatability and reproducibility of the measurements were evaluated with ICC determination. The raw data used to obtain the results can be accessed in Appendices A.2 to A.4.

4.2.1 CT descriptive statistics

Lumbar lordosis angle (LLA)

The LLA for the four sample groups (black males, black females, white males, and white females) are presented in Table 4.9. The results indicated that white females had the largest mean angle (37.0° ± 8.2°) when compared to other groups, while black females presented with the smallest LLA (29.2° ± 9.9°). In general, the results showed that the white population group had larger LLA's across both sexes when compared to the black population group.

Table 4.9: Descriptive statistics of the lumbar lordosis angle (LLA) taken

Population group	Lumbar Lordosis Angle (LLA) (degrees)	
	Mean ± SD	**95% CI**
BM	29.4 ± 8.8	26.3 – 32.5
BF	29.2 ± 9.9	24.9 – 33.6
WM	32.2 ± 7.1	27.9 – 36.5
WF	37.0 ± 8.2	32.3 – 41.8
Key: SD = Standard deviation; CI = Confidence interval; BM = Black males; BF = Black females; WM = White males; WF = White females		

Bone mineral density (BMD)

The BMD of both endplates increased when moving caudally with each level up until L4 then a slight decrease was noted from L4 to L5 for both male groups. The inferior endplates of the black females, and the superior endplates of white females showed the same increase and subsequent decrease in BMD observed in both endplates of males. The BMD at the inferior endplate of white females increased from L1 to L3, before decreasing from L3 to L4, and subsequently increasing from L4 to L5. The superior endplate in black females demonstrated an increase in BMD from L1 to L2, a decrease from L2 to L3, a subsequent increase from L3 to L4, before finally decreasing again from L4 to L5. This created a unique alternating pattern. Black males exhibited higher endplate BMD than white males and black females for both endplates. White males had lower BMD than white females for most endplate measurements except at the superior endplate of L2 to L4 and the inferior endplate of L4 (Table 4.10).

Table 4.10: Descriptive statistics of the superior – and inferior endplates

VL	P	SEP (HU)			IEP (HU)		
		Mean	SD	95% CI	Mean	SD	95% CI
L1	BM	453.1	58.7	430.4 – 475.9	503.2	76.6	473.5 – 532.9
	BF	446.4	76.5	410.6 – 482.1	467.3	85.4	427.3 – 507.2
	WM	426.6	45.0	396.3 – 456.8	439.6	82.3	384.4 – 494.9
	WF	445.2	83.1	389.4 – 501.0	476.4	109.4	402.9 – 549.9
L2	BM	482.2	61.8	458.2 – 506.2	514.1	76.6	484.4 – 543.9
	BF	446.9	80.4	409.3 – 484.6	500.9	70.1	468.0 – 533.7
	WM	455.7	67.3	410.5 – 500.9	470.2	69.1	423.8 – 516.6
	WF	449.1	112.6	373.4 – 524.8	486.1	102.5	417.3 – 554.9
L3	BM	497.9	78.8	457.4 – 528.4	558.9	87.7	524.9 – 592.9
	BF	445.1	77.8	408.7 – 481.5	507.9	91.6	465.0 – 550.7
	WM	469.4	90.2	408.7 – 530.0	484.6	88.6	425.1 – 544.0
	WF	458.6	96.1	394.1 – 523.2	510.2	84.8	453.2 – 567.2
L4	BM	513.5	55.6	491.9 – 535.0	593.0	79.9	562.0 – 624.0
	BF	454.2	78.5	417.4 – 490.9	537.9	104.4	489.0 – 586.8
	WM	478.6	60.5	437.9 – 519.2	522.4	94.7	458.7 – 586.0
	WF	462.4	116.1	384.4 – 540.3	501.9	98.1	436.0 – 567.8
L5	BM	481.8	78.2	451.4 – 512.1	568.6	81.2	537.1 – 600.1
	BF	431.7	102.5	383.7 – 479.7	503.1	106.7	453.2 – 553.1
	WM	421.5	73.0	372.4 – 470.5	503.2	92.8	440.8 – 565.6
	WF	458.4	107.7	386.0 – 530.7	519.3	108.7	446.2 – 592.3

Key: HU = Hounsfield Units; P = Population group; VL = Vertebral level; SD = Standard deviation; CI = Confidence interval; BM = Black males; BF = Black females; WM = White males; WF = White females; SEP = Superior endplate; IEP = Inferior endplate

The BMD of the posterior border showed a clear increase from L1 to L4, before decreasing from L4 to L5, in black males and both female groups. White males started showing a decrease in BMD at the posterior border from L3 to L5. Black males exhibited a gradual incline in BMD at the anterior border when moving caudally in the spine, with a small dip at L3. Black females had an increase in BMD at the anterior border from L1 to L2 before gradually decreasing from L2 to L4, and subsequently increasing again from L4 to L5. White females showed a similar pattern,

with the second increase occurring at L3 rather than L4 as in the black female group. White males produced an alternating pattern (as described previously) for the BMD at the anterior border, showing an initial decline from L1 to L2. Black females had lower BMD than black males for most border (anterior – and posterior border) measurements, except for the anterior border of L1 to L3. White females had greater BMD values than white males for all border measurements (Table 4.11).

Table 4.11: Descriptive statistics of the anterior – and posterior borders

VL	P	AB (HU)			PB (HU)		
		Mean	SD	95% CI	Mean	SD	95% CI
L1	BM	445.2	46.9	427.0 – 463.4	566.3	111.5	523.1 – 609.5
	BF	445.9	76.8	410.0 – 481.8	546.4	135.3	483.1 – 609.7
	WM	422.6	37.2	397.6 – 447.6	515.4	107.4	443.2 – 587.5
	WF	453.7	72.6	405.0 – 502.5	562.5	98.8	469.1 – 628.8
L2	BM	451.2	54.0	430.2 – 472.1	665.4	116.5	620.2 – 710.6
	BF	455.9	73.8	421.4 – 490.4	589.6	145.3	530.6 – 666.6
	WM	410.1	51.4	375.6 – 444.6	637.3	97.8	571.5 – 703.0
	WF	484.6	58.7	445.1 – 524.0	650.1	146.8	551.4 – 748.7
L3	BM	448.9	45.4	431.3 – 466.5	680.2	113.2	636.3 – 724.1
	BF	450.3	56.7	423.8 – 476.8	600.9	150.5	530.4 – 671.3
	WM	428.9	65.7	384.8 – 473.0	664.6	116.7	586.2 – 742.9
	WF	470.9	65.9	426.6 – 515.2	694.7	136.5	603.1 – 786.4
L4	BM	460.0	53.2	439.3 – 480.6	711.8	106.7	670.4 – 753.2
	BF	439.6	72.8	405.5 – 473.6	625.1	139.1	560.0 – 690.2
	WM	426.1	73.4	376.8 – 475.4	630.9	105.1	560.3 – 701.5
	WF	497.2	71.1	499.4 – 545.0	723.9	129.0	637.2 – 810.6
L5	BM	523.6	58.2	501.1 – 546.2	665.9	106.6	624.5 – 707.2
	BF	467.0	78.7	430.2 – 503.8	564.9	122.6	507.5 – 622.2
	WM	456.0	37.4	430.9 – 481.1	607.6	92.4	545.5 – 669.6
	WF	532.5	77.8	480.2 – 584.7	616.2	185.5	491.6 – 740.8

Key: HU = Hounsfield Units; P = Population group; VL = Vertebral level; SD = Standard deviation; CI = Confidence interval; BM = Black males; BF = Black females; WM = White males; WF = White females; AB = Anterior border; PB = Posterior border

Cortical BMD results showed that the inferior endplate was generally denser than the superior endplate, and the posterior border more so than the anterior border for all measurements. The overall maximum and minimum cortical BMD measurements were summarised as follows (the first value represents the minimum, the second value the maximum) (Tables 4.10 and 4.11):

- SEP: L5 of white males (421.5 ± 73.0 HU); L4 of black males (513.5 ± 55.6 HU)
- IEP: L1 of white males (439.6 ± 82.3 HU); L4 of black males (593.0 ± 79.9 HU)
- AB: L2 of white males (410.1 ± 51.4 HU); L5 of white females (532.5 ± 77.8 HU)
- PB: L1 of white males (515.4 ± 107.4 HU); L4 of white females (723.9 ± 129.0 HU)

Table 4.12 depicts the descriptive statistics for the medullary BMD. For ROI1, the BMD in black males exhibited an increase when moving inferiorly per level up until L4, before decreasing from L4 to L5. White males demonstrated a similar trend but started showing a decline in BMD from L3. White females showed an initial increase in BMD from L1 to L2, and then a decline from L2 to L4, after increasing again from L4 to L5. Black females' BMD initially decreased from L1 to L2, then suddenly increased from L2 to L3, and subsequently declined from L3 to L5 (similar to white males). A decrease in BMD from L1 to L3, and a subsequent increase from L3 to L5 was observed for ROI2 in both male groups. The female groups both displayed an initial increase in BMD from L1 to L2 and a subsequent decrease from L2 to L3. In black females the decline from L3 to L4 continued, which then inclined sharply from L4 to L5. The BMD in white females however, immediately started increasing in density from L3 to L5. For ROI3, the two male groups indicated an alternating pattern with an initial decrease in BMD from L1 to L2. White female BMD also initially decreased from L1 to L2, but gradually increased from L2 to L5. Black female BMD showed a gradual decrease in density from L1 through to L5. The medullary BMD results indicated that ROI2 exhibited the lowest density and ROI3 the highest for most groups, except for L3 to L5 in white males, and L5 in black females. The overall maximum and minimum medullary BMD measurements were summarised as follows:

- ROI1: L1 of white females (209.7 ± 34.7 HU): L4 of black males (248.3 ± 19.3HU)
- ROI2: L3 of white males (166.2 ± 21.5 HU); L5 of black males (222.3 ± 33.6 HU)
- ROI3: L5 of black females (213.2 ± 42.7 HU); L5 of black males (255.7 28.6 HU)

Table 4.12: Descriptive statistics of the three regions of interest

VL	P	ROI1 (HU)			ROI2 (HU)			ROI3 (HU)		
		Mean	SD	95% CI	Mean	SD	95% CI	Mean	SD	95% CI
L1	BM	238.2	20.9	230.1 – 246.3	219.9	24.8	210.2 – 229.5	255.2	24.7	245.6 – 264.8
	BF	217.5	30.1	203.2 – 231.8	187.6	37.1	170.2 – 204.9	235.6	43.1	215.4 – 255.8
	WM	210.0	12.0	201.9 – 218.1	180.7	33.8	158.0 – 203.5	221.8	26.7	203.9 – 239.7
	WF	209.7	34.7	186.4 – 233.0	194.5	27.0	176.4 – 212.7	227.6	18.9	215.0 – 240.3
L2	BM	239.3	23.9	230.0 – 248.6	215.5	27.1	205.0 – 226.0	250.8	25.4	240.9 – 260.6
	BF	217.3	28.2	203.8 – 230.7	188.7	40.8	169.6 – 207.8	232.7	54.5	207.2 – 258.2
	WM	214.3	19.0	201.5 – 227.1	176.2	25.9	158.8 – 193.6	217.0	29.6	197.1 – 236.9
	WF	216.1	35.4	192.3 – 239.9	194.7	29.5	174.9 – 214.6	221.9	27.0	203.8 – 240.0
L3	BM	242.6	21.1	234.4 – 250.8	207.9	25.0	198.2 – 217.6	252.7	24.0	243.4 – 262.0
	BF	223.3	28.0	210.2 – 236.4	180.6	41.4	161.2 – 200.0	230.1	51.3	206.1 – 254.1
	WM	232.0	26.8	214.0 – 250.0	166.2	21.5	151.7 – 180.6	223.5	16.6	212.4 – 234.7
	WF	214.8	33.5	192.3 – 237.3	185.4	31.7	164.1 – 206.7	227.1	24.0	211.0 – 243.2
L4	BM	248.3	19.3	240.8 – 255.8	211.5	25.3	201.7 – 221.4	249.7	30.7	237.7 – 261.6
	BF	223.4	37.0	206.1 – 240.7	177.9	47.2	155.8 – 199.9	222.5	46.2	200.8 – 244.1
	WM	231.6	33.8	208.8 – 254.3	175.7	18.8	163.1 – 188.3	219.9	13.3	210.9 – 228.8
	WF	214.3	31.0	193.4 – 235.1	193.7	31.6	172.5 – 215.0	231.7	33.1	209.5 – 254.0
L5	BM	242.1	25.5	232.3 – 252.0	222.3	33.6	209.2 – 235.3	255.7	28.6	244.6 – 266.8
	BF	216.0	41.3	196.7 – 235.3	185.5	42.3	165.7 – 205.2	213.2	42.7	193.2 – 233.1
	WM	225.4	34.1	202.5 – 248.3	179.3	20.7	165.4 – 193.2	220.7	26.9	202.7 – 238.8
	WF	219.8	31.1	198.9 – 240.7	200.4	29.4	180.6 – 220.1	232.8	37.9	207.3 – 258.3

Key: HU = Hounsfield Units; P = Population group; VL = Vertebral level; SD = Standard deviation; CI = Confidence interval; BM = Black males; BF = Black females; WM = White males; WF = White females; ROI1 = Region of interest 1; ROI2 = Region of interest 2; ROI3 = Region of interest 3

Morphometrics

Table 4.13 shows that the males of both population groups had longer transverse process –, and spinous process lengths than either of the females. Also, in general, the white population had longer measurements for these features than the black population. The exception for sexes was at L5, where the spinous processes of the white females had longer process lengths than those of white

males. In contrast, the transverse process lengths of L3 in black females and L4 in black males, and the spinous process lengths of L3 to L5 in black males, were larger in black individuals than those of white individuals. Across all groups, the transverse process lengths increased from L1 to L3, then decreased from L3 to L4, followed by an increase in length from L4 to L5. A similar trend was seen across groups for the spinous process lengths, except that after the increase from L1 to L3, there is a constant decrease in length from L3 to L5.

Table 4.13: Descriptive statistics for the posterior element measurements

VL	P	TPL (mm)			SPL (mm)		
		Mean	SD	95% CI	Mean	SD	95% CI
L1	BM	75.4	6.7	72.8 – 77.9	33.2	3.7	31.7 – 34.5
	BF	65.3	5.7	62.6 – 67.9	31.5	3.5	29.8 – 33.1
	WM	77.3	4.1	73.6 – 81.1	34.8	2.4	32.6 – 37.0
	WF	71.2	6.1	67.7 – 74.7	32.7	2.8	31.0 – 34.3
L2	BM	85.5	6.9	82.9 – 88.0	37.2	3.3	35.9 – 38.4
	BF	76.7	6.8	73.5 – 79.8	34.6	3.4	33.0 – 36.2
	WM	85.1	4.7	80.8 – 89.5	38.9	2.3	36.8 – 41.0
	WF	79.9	5.6	76.6 – 83.1	36.4	2.9	34.7 – 38.1
L3	BM	96.0	7.1	93.3 – 98.7	39.1	3.1	37.9 – 40.2
	BF	86.6	8.9	82.5 – 90.8	35.8	3.3	34.2 – 37.3
	WM	97.5	5.5	92.4 – 102.5	39.0	3.9	35.4 – 42.6
	WF	86.2	8.4	81.3 – 91.0	37.6	3.1	35.8 – 39.4
L4	BM	90.5	6.6	88.0 – 92.9	37.4	3.8	36.0 – 38.9
	BF	81.8	7.9	78.1 – 85.4	34.3	4.4	32.2 – 36.3
	WM	90.3	6.7	84.1 – 96.5	36.0	3.3	32.9 – 39.0
	WF	83.8	8.2	79.1 – 88.6	35.1	3.4	33.1 – 37.0
L5	BM	92.5	5.3	90.5 – 94.5	31.5	3.7	30.1 – 32.9
	BF	85.8	8.9	81.6 – 90.0	29.5	4.4	27.4 – 31.5
	WM	95.9	5.1	91.2 – 100.7	29.7	4.1	25.9 – 33.4
	WF	90.2	9.0	85.0 – 95.4	30.1	4.5	27.5 – 32.7

Key: P = Population group; VL = Vertebral level; SD = Standard deviation; CI = Confidence interval; BM = Black males; BF = Black females; WM = White males; WF = White females; TPL = Transverse process length; SPL = Spinous process length

Table 4.14 shows that males displayed larger lateral diameters and heights for pedicles than females, and white females displayed noticeably smaller measurements than the other three groups. Black males and females demonstrated larger lateral pedicle diameters than white males and females except at L5 where white males had larger measurements than black males. The heights appeared to have minor differences between the two population groups.

Table 4.14: Descriptive statistics for the pedicle measurements

VL	P	PDDL (mm)			PDH (mm)		
		Mean	SD	95% CI	Mean	SD	95% CI
L1	BM	10.7	1.6	10.1 – 11.3	18.0	1.5	17.5 – 18.6
	BF	9.2	1.8	8.3 – 10.0	16.3	1.2	15.8 – 16.9
	WM	8.9	1.0	7.9 – 9.8	18.0	1.7	16.4 – 19.5
	WF	7.5	1.3	6.7 – 8.3	16.3	1.6	15.4 – 17.2
L2	BM	10.8	1.5	10.2 – 11.3	18.0	1.5	17.4 – 18.5
	BF	9.6	1.7	8.8 – 10.4	15.9	1.5	15.3 – 16.6
	WM	10.2	1.4	10.0 – 11.5	18.1	1.8	16.4 – 19.8
	WF	8.2	1.5	7.3 – 9.0	16.0	1.4	15.1 – 16.8
L3	BM	12.2	1.3	11.7 – 12.7	18.0	1.5	17.4 – 18.4
	BF	10.9	1.5	10.2 – 11.6	15.9	1.4	15.3 – 16.6
	WM	11.9	1.3	10.7 – 13.2	17.8	1.5	16.4 – 19.2
	WF	9.9	2.0	8.7 – 11.1	16.1	2.0	14.9 – 17.2
L4	BM	14.2	1.7	13.6 – 14.8	17.0	1.6	16.4 – 17.6
	BF	12.5	1.7	11.7 – 13.3	14.9	1.1	14.4 – 15.5
	WM	13.8	0.8	13.1 – 14.5	16.9	1.6	15.4 – 18.4
	WF	11.8	2.0	10.6 – 12.9	15.2	1.9	14.1 – 16.4
L5	BM	17.4	2.4	16.5 – 18.3	15.3	1.8	14.6 – 15.9
	BF	15.7	2.2	14.7 – 16.7	13.5	1.6	12.9 – 14.1
	WM	17.7	1.7	16.1 – 19.3	15.4	1.2	14.3 – 16.5
	WF	15.5	2.5	14.0 – 16.9	14.0	1.6	13.1 – 14.9

Key: P = Population group; VL = Vertebral level; SD = Standard deviation; CI = Confidence interval; BM = Black males; BF = Black females; WM = White males; WF = White females; PDDL = Pedicle lateral diameter; PDH = Pedicle height

White females showed longer AP spinal canal diameters than the other three groups, who had similar measurements. Black females displayed narrower lateral diameters across all levels when compared to the other three groups, who again had similar measurements. In general, the AP diameters were narrowest at L2 and L3, while the lateral diameters were observed to be narrower at L1 and L2, followed by a steady increase in diameter from L3 to L5 (Table 4.15).

Table 4.15: Descriptive statistics for the spinal canal measurements

VL	P	SCDAP (mm)			SCDL (mm)		
		Mean	SD	95% CI	Mean	SD	95% CI
L1	BM	15.5	1.7	14.9 – 16.2	21.9	1.9	21.2 – 22.6
	BF	15.3	2.3	14.5 – 16.0	20.3	1.9	19.4 – 21.2
	WM	15.3	0.8	14.5 – 16.0	22.9	1.3	21.6 – 24.1
	WF	17.1	1.6	16.1 – 18.0	22.2	1.2	21.5 – 22.9
L2	BM	15.1	1.7	14.5 – 15.7	22.0	1.7	21.3 – 22.6
	BF	14.3	1.4	13.7 – 15.0	20.3	1.9	19.4 – 21.2
	WM	14.3	0.4	13.9 – 14.7	22.3	1.5	20.9 – 23.6
	WF	16.4	2.1	15.2 – 17.7	22.4	1.2	21.7 – 23.1
L3	BM	14.5	1.7	13.8 – 15.1	23.5	2.3	22.6 – 24.3
	BF	14.1	1.6	13.4 – 14.9	21.5	2.1	20.5 – 22.4
	WM	14.2	1.9	12.5 – 15.9	23.9	2.2	21.9 – 26.0
	WF	16.5	2.6	15.0 – 18.0	23.4	2.3	22.1 – 24.7
L4	BM	14.8	2.0	14.1 – 15.6	25.2	2.7	24.2 – 26.3
	BF	14.3	1.8	13.5 – 15.1	22.7	2.5	21.6 – 23.9
	WM	15.3	2.4	13.1 – 17.5	24.6	2.0	22.7 – 26.4
	WF	16.4	2.6	14.9 – 17.9	25.0	3.5	23.0 – 27.0
L5	BM	16.3	2.2	15.4 – 17.1	27.6	3.4	26.3 – 28.8
	BF	15.2	2.2	14.1 – 16.2	25.9	3.2	24.4 – 27.4
	WM	17.0	2.2	14.9 – 19.0	28.1	2.9	25.4 – 30.8
	WF	16.6	2.6	15.0 – 18.1	27.3	3.8	25.1 – 29.5

Key: P = Population group; VL = Vertebral level; SD = Standard deviation; CI = Confidence interval; BM = Black males; BF = Black females; WM = White males; WF = White females; SCDAP = Spinal canal anteroposterior diameter; SCDL = Spinal canal lateral diameter

The minimum and maximum lateral and AP diameters were larger in the male group than in the female group (Tables 4.16 and 4.17). In the males, it was noted that the white population showed slightly larger maximum lateral diameters, while the black population showed slightly larger minimum lateral diameters. The minimum and maximum lateral diameters exhibited a gradual increase when moving caudally in the spine for all individuals (Table 4.16).

Table 4.16: Descriptive statistics for the lateral diameter measurements

VL	P	VDMinL (mm)			VDMaxL (mm)		
		Mean	SD	95% CI	Mean	SD	95% CI
L1	BM	41.3	2.7	40.3 – 42.3	45.7	3.0	44.5 – 46.8
	BF	36.5	3.3	35.0 – 38.1	40.0	3.7	38.2 – 41.7
	WM	39.3	2.9	36.6 – 41.9	45.0	2.5	42.6 – 47.3
	WF	35.4	2.4	34.0 – 36.8	39.7	2.0	38.5 – 40.8
L2	BM	42.6	3.4	41.3 – 43.8	48.0	2.7	47.0 – 49.0
	BF	37.8	3.5	36.2 – 39.5	42.4	3.5	40.7 – 44.0
	WM	40.5	2.8	37.9 – 43.1	46.1	2.4	43.9 – 48.3
	WF	36.7	3.2	34.8 – 38.5	42.6	2.7	41.0 – 44.1
L3	BM	44.4	2.9	43.3 – 45.5	50.2	3.1	49.1 – 51.4
	BF	39.7	3.7	38.0 – 41.4	44.3	4.1	42.4 – 46.2
	WM	42.7	1.7	41.1 – 44.3	49.2	2.5	46.9 – 51.5
	WF	39.0	3.3	37.2 – 40.9	44.0	2.6	42.5 – 45.5
L4	BM	46.2	3.2	45.0 – 47.5	52.0	3.1	50.9 – 53.2
	BF	42.0	4.1	40.1 – 43.9	47.0	4.0	45.1 – 48.8
	WM	44.1	2.2	42.1 – 46.1	50.6	2.6	48.2 – 52.9
	WF	40.5	3.8	38.3 – 42.7	46.6	2.9	45.0 – 48.3
L5	BM	45.6	3.2	44.4 – 46.8	54.3	3.9	52.8 – 55.8
	BF	41.2	4.9	38.9 – 43.5	48.7	4.5	46.7 – 50.8
	WM	43.0	2.4	40.8 – 45.2	53.7	3.1	50.8 – 56.6
	WF	40.1	3.2	38.3 – 42.0	48.9	4.1	46.5 – 51.3

Key: P = Population group; VL = Vertebral level; SD = Standard deviation; CI = Confidence interval; BM = Black males; BF = Black females; WM = White males; WF = White females; VDMaxL = Maximum vertebral body lateral diameter; VDMinL = Minimum vertebral body lateral diameter

In general, white males had the largest AP diameters compared to the other groups, while black females showed the smallest AP diameters. A gradual increase in AP diameter was observed from L1 to L3, after which L4 diameters closely mimicked those of L3, followed by an increase in AP diameters at L5 (Table 4.17).

Table 4.17: Descriptive statistics for the AP diameter measurements

VL	P	VDMinAP (mm)			VDMaxAP (mm)		
		Mean	SD	95% CI	Mean	SD	95% CI
L1	BM	29.8	2.7	28.8 – 30.8	32.1	2.5	31.2 – 33.0
	BF	25.6	2.0	24.7 – 26.5	28.0	1.8	27.1 – 28.8
	WM	31.3	1.8	29.6 – 32.9	33.9	2.8	32.4 – 35.5
	WF	28.2	2.2	27.0 – 29.5	31.0	2.7	29.5 – 32.6
L2	BM	31.7	2.5	30.8 – 32.7	33.8	2.4	32.9 – 34.7
	BF	27.5	2.3	26.4 – 28.5	29.4	2.3	28.3 – 30.5
	WM	32.4	1.8	30.7 – 34.0	35.3	2.1	33.4 – 37.3
	WF	30.1	2.0	28.9 – 31.3	32.3	2.7	30.7 – 33.8
L3	BM	33.1	2.3	32.3 – 34.0	35.2	2.5	34.2 – 36.1
	BF	29.0	2.1	28.0 – 30.0	31.2	2.2	30.1 – 32.2
	WM	33.0	1.6	31.6 – 34.5	35.7	1.4	34.4 – 37.0
	WF	30.5	2.2	29.3 – 31.8	32.6	2.1	31.4 – 33.9
L4	BM	33.8	1.7	33.1 – 34.4	35.7	2.0	35.0 – 36.4
	BF	30.4	2.3	29.3 – 31.5	32.4	2.4	31.2 – 33.5
	WM	33.3	1.8	31.6 – 35.0	35.7	1.6	34.2 – 37.1
	WF	30.8	1.8	29.7 – 31.8	32.8	2.4	31.3 – 34.2
L5	BM	35.3	1.9	35.3 – 36.1	37.2	1.7	36.6 – 37.8
	BF	31.9	2.5	30.7 – 33.0	33.7	2.9	32.3 – 35.0
	WM	35.3	2.9	32.6 – 38.0	37.8	2.6	35.4 – 40.2
	WF	32.6	2.6	31.1 – 34.0	34.5	2.7	33.0 – 36.1

Key: P = Population group; VL = Vertebral level; SD = Standard deviation; CI = Confidence interval; BM = Black males; BF = Black females; WM = White males; WF = White females; VDMaxAP = Maximum vertebral body anteroposterior diameter; VDMinAP = Minimum vertebral body anteroposterior diameter

Males displayed larger anterior – and posterior vertebral body heights compared to females, except at L4 where white females showed a slightly larger height anteriorly compared to white males (Table 4.18). Overall, the anterior height gradually increased when moving caudally from L1 to L3, with L4 and L5 levelling out with similar values to that of L3. The posterior height initially increased from L1 to L2 for both female groups and black males, before decreasing from L2 to L5. White males displayed an overall decrease in height when moving caudally in the spine.

Table 4.18: Descriptive statistics for the vertebral body heights

VL	P	VHa (mm)			VHp (mm)		
		Mean	SD	95% CI	Mean	SD	95% CI
L1	BM	29.5	2.2	28.6 – 30.3	31.2	1.8	30.5 – 31.8
	BF	27.2	1.5	26.5 – 27.9	28.1	2.1	27.1 – 29.1
	WM	28.5	2.3	26.4 – 30.7	31.6	2.5	29.3 – 33.9
	WF	27.8	1.9	26.7 – 28.9	29.9	1.8	28.9 – 30.9
L2	BM	30.6	2.0	29.8 – 31.3	31.8	2.2	31.0 – 32.6
	BF	28.0	1.7	27.3 – 28.8	29.1	1.6	28.4 – 29.9
	WM	30.6	2.2	28.6 – 32.6	31.2	1.3	30.1 – 32.5
	WF	29.5	1.8	28.5 – 30.5	30.1	1.7	29.1 – 31.1
L3	BM	31.4	2.3	30.6 – 32.3	31.3	2.6	30.4 – 32.3
	BF	28.9	1.6	28.2 – 29.7	29.0	1.9	28.1 – 29.9
	WM	31.2	2.0	29.4 – 33.1	31.0	1.6	29.5 – 32.5
	WF	30.2	1.6	29.3 – 31.1	29.9	1.8	28.9 – 30.9
L4	BM	31.3	2.0	30.6 – 32.0	30.7	2.3	29.8 – 31.5
	BF	29.0	2.0	28.0 – 29.9	28.3	1.7	27.5 – 29.1
	WM	30.3	1.5	28.9 – 31.7	29.4	2.1	27.4 – 31.3
	WF	30.4	1.9	29.3 – 31.5	28.3	1.6	27.4 – 29.3
L5	BM	31.8	2.3	31.0 – 32.7	28.8	2.1	28.0 – 29.5
	BF	29.5	2.3	28.4 – 30.5	26.1	1.5	25.4 – 26.8
	WM	31.0	1.8	29.3 – 32.7	27.0	1.9	25.3 – 28.7
	WF	30.8	1.8	29.8 – 31.8	26.1	1.7	25.1 – 27.1

Key: P = Population group; VL = Vertebral level; SD = Standard deviation; CI = Confidence interval; BM = Black males; BF = Black females; WM = White males; WF = White females; VHa = Anterior vertebral body height; VHp = Posterior vertebral body height

The overall maximum and minimum values of the morphometrics were summarised as follows (with the first number being the smallest value, and the second the largest value) (Tables 4.13 to 4.18):

- TPL: L1 of black females (65.3 ± 5.7 mm); L3 of white males (97.5 ± 5.5 mm)
- SPL: L5 of black females (29.5 ± 4.4 mm); L3 of black males (49.1 ± 3.1 mm)
- PDDL: L1 of white females (7.5 ± 1.3 mm); L5 of white males (17.7 ± 1.7 mm)
- PDH: L5 of black females (13.5 ± 1.6 mm); L2 of white males (18.1 ± 1.8 mm)
- SCDL: L1 and L2 of black females (20.3 ± 1.9 mm each); L5 of white males (28.1 ± 2.9 mm)
- SCAP: L3 of black females (14.7 ± 1.6 mm); L1 of white females (17.1 ± 1.6 mm)
- VDMinL: L1 of white females (35.4 ± 2.4 mm); L4 of black males (46.2 ± 3.2 mm)
- VDMaxL: L1 of white females (39.7 ± 2.0 mm); L5 of black males (54.3 ± 3.9 mm)
- VDMinAP: L1 of black females (25.6 ± 2.0 mm); L5 of black and white males (35.3 ± 1.9 mm and 35.3 ± 2.9 mm, respectively)
- VDMaxAP: L1 of black females (28.0 ± 1.8 mm); L5 of white males (37.8 ± 2.6 mm)
- VHa: L1 of black females (27.2 ± 1.5 mm); L5 of black males (31.8 ± 2.3 mm)
- VHp: L5 of black and white females (26.1 ± 1.5 mm and 26.1 ± 1.7 mm, respectively); L2 of black males (31.8 ± 2.2 mm)

4.2.2 CT comparative statistics

Lumbar lordosis angle (LLA)

Lumbar lordosis correlation with age, BMD and morphometric measurements was determined using Pearson's correlation.

The only correlation with age was seen for black females. A quadratic correlation was seen with an r^2 value of 0.430 and a p-value of 0.010. The LLA initially decreased with age but started to increase after the fourth decade of life. Appendix B.1 shows the scatterplot generated for the regression analysis. No correlation (neither linear nor non-linear) was seen with BMD. Appendix C.1 shows the Pearson's correlation values as well as the non-linear correlation values obtained.

Some moderate linear correlations were observed for angle and morphometrics. However, when considering the scatterplots, r^2 values and p-values, some results appeared to have a cubic and/or quadratic relationship which showed an r^2 value that was better than the linear results. Therefore, a curve fit analysis was performed, and relevant curves were generated with their corresponding r^2 values for the data which was non-linearly distributed. Appendix D.1 contains the results from the linear analysis. Table 4.19 shows the significant r^2 values which were strong enough to indicate notable correlations. Scatterplots of the data can be found in Appendix B.2. Most of the correlations were seen for the white group, with only one being for black females. The variables showing these non-linear relationships were either the uppermost – (L1) or lower two (L4 and L5) levels. The transverse process length of black females decreased in a cubic relationship as the lumbar lordosis angle increased. For the white female group, the lateral diameter of the spinal canal increased slightly before decreasing as the angle increased. The opposite relationship was seen for the spinous process length. The maximum and minimum AP diameters of the vertebral body at L5 showed a slight initial decrease, with a subsequent increase as the angle increases.

Table 4.19: Significant r^2 values and associated two-sided p-values for the correlation between lordosis angle and morphometric measurements (variable column)

Variable	Population group	r^2	p-value
TPL L4	**BF**	0.440	0.010
SCDL L1	**WF**	0.500	0.020
SPL L1		0.470	0.030
VDMaxAP L5	**WM**	0.540	0.020
VDMinAP L5		0.550	0.020

Key: BF = Black females; WF = White females; WM = White males; TPL = Transverse process length; SPL = Spinous process length; SCDL = Spinal canal lateral diameter; VDMaxAP = Maximum vertebral body anteroposterior diameter; VDMinAP = Minimum vertebral body anteroposterior diameter. Light grey cells depict a cubic regression. Dark grey cells depict a quadratic regression

Bone mineral density (BMD)

Between sex – and population group comparisons were made for BMD using two-sided independent t-tests. For the endplate component, the only significant difference was found between black and white males at the superior endplate of L5, where black males exhibited significantly higher densities than white males (p = 0.030) (Table 4.10). Black males also had higher densities than white males at the anterior border of L5, and at the posterior border of L4 (p = 0.050 and 0.020, respectively). Black males had higher densities than black females at both the anterior – and posterior borders of L5 (p = 0.020 and 0.030, respectively), however white females had denser values than white males at the anterior border of L2 (p = 0.010) (Table 4.11). For medullary BMD (Table 4.20), black males showed the highest densities of all groups. This was especially evident when black males were compared to: black females at L1, L2 and L4 of ROI1, L5 of ROI2 and ROI3; and white males at L1 and L2 of ROI1, and all levels of ROI2 and ROI3 (Table 4.12).

Table 4.20: Significant p-values for group comparisons

Comparison	Vertebral level	ROI	p-value
BM vs BF	**L1**	**ROI1**	0.010
	L2	**ROI1**	0.030
	L5	**ROI2**	0.030
		ROI3	0.010
BM vs WM	**L1**	**ROI1**	0.000
		ROI2	0.001
		ROI3	0.020
	L2	**ROI1**	0.030
		ROI2	0.000
		ROI3	0.010
	L3	**ROI2**	0.000
		ROI3	0.010
	L4	**ROI2**	0.001
		ROI3	0.004
	L5	**ROI2**	0.000
		ROI3	0.004

Key: vs = Versus; BM = Black males; BF = Black females; WM = White males; ROI = Region of interest

Simple linear regression analysis was used to determine the linear correlation between age and BMD for both cortical – and medullary measurements. When considering the results from the regression analysis, some linear relationships were observed for the correlation analysis between BMD and age. However, when performing non-linear correlations using the data, stronger and more significant results were observed. This was especially evident when considering the r^2 values and associated scatterplots. Appendix D.2 provides the output of the linear regression analyses. The majority of variables showing non-linear relationships were mostly observed in the white female population group. The results revealed that only one variable correlated with age in the white male population group, and only two variables showed correlations/relationships in the black female population group.

For medullary BMD, ROI1 and ROI2 indicated substantially more correlations with age than ROI3, with ROI1 showing the most cases of correlation. For cortical BMD, border analysis demonstrated that the anterior border had two times the amount of correlations compared to the posterior border. The medullary correlations were seen in the female group only, and predominantly for the white population group. An overall decrease was observed in BMD with age for all the variables. The majority of the correlations were cubic –, followed by quadratic –, and finally exponential regressions. Table 4.21 shows the r^2 values and associated two-sided p-values obtained from the cortical – and medullary BMD correlation with age which were strong enough to indicate notable non-linear correlations. Scatterplots of the data can be found in Appendix B.3.

For the superior – versus inferior endplate comparisons using paired t-tests, the superior endplate was less dense than the inferior endplate in all four groups for all lower and upper-most levels (Table 4.6). The posterior border was also denser than the anterior border for all groups and at all levels (Table 4.7). The significant p-values calculated using paired t-tests can be seen in Table 4.22.

Table 4.21: Significant r^2 values and associated two-sided p-values for correlation between age and BMD (variable column)

Variable	VL	Population group	r^2	p-value
ROI1	**L1**	**BF**	**0.61**	**0.000**
	L1	**WF**	0.77	0.002
	L2		0.75	0.001
	L3		0.76	0.002
	L4		0.72	0.004
	L5		0.77	0.002
ROI2	**L2**	**WF**	0.65	0.003
	L3		0.71	0.004
	L4		0.65	0.003
	L5		0.81	0.000
ROI3	**L1**	**WF**	0.64	0.010
AB	**L1**	**WF**	**0.52**	**0.004**
	L1	**WM**	0.56	0.020
	L4	**WF**	0.62	0.010
	L5	**BF**	**0.61**	**0.000**
PB	**L3**	**WF**	0.64	0.010
	L4		0.56	0.040

Key: ROI = Region of interest; AB = Anterior border; PB = Posterior border; VL = Vertebral level; BF = Black females; WF = White females; WM = White males. Light grey cells depict a cubic regression. Dark grey cells depict a quadratic regression. Light grey bolded cells depict an exponential regression

Table 4.22: Significant p-values for the comparisons between the superior – and inferior endplates, and anterior – and posterior borders

Comparison	VL	P	p-value	Comparison	VL	P	p-value
SEP vs IEP	L1	BM	0.010	AB vs PB	L1	WF	0.010
	L2	BM	0.010		L2	BM	0.000
		BF	0.001			BF	0.000
	L3	BM	0.000			WM	0.000
		BF	0.000			WF	0.020
		WF	0.003		L3	BM	0.000
	L4	BM	0.000			BF	0.000
		BF	0.000			WM	0.000
		WM	0.020			WF	0.001
		WF	0.047		L4	BM	0.000
	L5	BM	0.000			BF	0.000
		BF	0.000			WM	0.000
		WM	0.010			WF	0.000
		WF	0.010		L5	BM	0.000
AB vs PB	L1	BM	0.000			BF	0.001
		BF	0.002			WM	0.010
		WM	0.010				

Key: P = Population group; BM = Black males; BF = Black females; WM = White males; WF = White females; vs = Versus; VL = Vertebral level; SEP = Superior endplate; IEP = Inferior endplate; AB = Anterior border; PB = Posterior border

The cortical BMD of the vertebral levels were compared to each other using paired t-tests. Results showed that the inferior endplate of L2 was less dense than that of L3 for white females ($p = 0.030$) (Table 4.10). Comparisons indicated that in black females, the inferior endplate of L1 was less dense than those of all other levels (Table 4.10). For both male groups, both endplates almost always increased in density when moving caudally. The only variation was when comparing the density of the superior endplate of L5 to L4 in both male groups, and L5 to L3 in the white males, where L5 was less dense than L3 (in white males) and L4 (in both male groups) (Table 4.10). Table 4.23 depicts the significant p-values resulting from the paired t-tests.

Table 4.23: Significant p-values for vertebral level comparisons for the superior – and inferior endplate

Variable	Comparison	P	p-value	Variable	Comparison	P	p-value
SEP	L1 vs L3	BM	0.030	IEP	L1 vs L4	BM	0.000
	L1 vs L4	BM	0.004			BF	0.000
		WM	0.010			WM	0.001
	L2 vs L4	BM	0.010		L1 vs L5	BM	0.000
	L3 vs L5	WM	0.010			BF	0.003
	L4 vs L5	BM	0.040			WM	0.040
		WM	0.001		L2 vs L3	BM	0.001
IEP	L1 vs L2	BF	0.020			WF	0.030
		WM	0.010		L2 vs L4	BM	0.000
	L1 vs L3	BM	0.000			WM	0.001
		BF	0.001		L3 vs L4	BM	0.020
		WM	0.030			WM	0.040

Key: SEP = Superior endplate; IEP = Inferior endplate; P = Population group; vs = Versus; BM = Black males; BF = Black females; WM = White males; WF = White females

Paired t-tests were used in order to compare the cortical BMD of the anterior – and posterior borders of the vertebral levels to each other. For the anterior border, there was an increase in density when moving caudally in the spine, as the lower levels showed higher densities than the upper levels (Table 4.11). The posterior border increased from L1 to L4, before decreasing from L4 to L5 for the black group and white females and increased from L1 to L3, before decreasing from L3 to L5 in white males (Table 4.11). Table 4.24 demonstrates the significant p-values obtained from paired t-tests when comparing the vertebral levels to each other.

Table 4.24: Significant p-values for vertebral level comparisons for the anterior border and posterior border

Variable	Comparison	P	p-value	Variable	Comparison	P	p-value
AB	L1 vs L4	WF	0.020	PB	L1 vs L3	BF	0.010
	L1 vs L5	BM	0.000			WM	0.001
		WM	0.020			WF	0.020
		WF	0.000		L1 vs L4	BM	0.000
	L2 vs L5	BM	0.000			BF	0.002
		WM	0.010			WM	0.004
		WF	0.030			WF	0.004
	L3 vs L5	BM	0.000		L1 vs L5	BM	0.000
		WM	0.040			WM	0.020
		WF	0.001		L2 vs L4	BM	0.002
	L4 vs L5	BM	0.000			WF	0.020
		WM	0.030		L3 vs L4	BM	0.002
		WF	0.010			WM	0.040
PB	L1 vs L2	BM	0.000		L3 vs L5	WF	0.020
		BF	0.020		L4 vs L5	BM	0.030
		WM	0.000			BF	0.010
	L1 vs L3	BM	0.000			WF	0.010

Key: P = Population group; AB = Anterior border; PB = Posterior border; vs = Versus; BM = Black males; BF = Black females; WM = White males; WF = White females

For medullary BMD, vertebral levels of the four sample groups were compared to each other for each separate region of interest, using paired t-tests. For white males, the upper levels were less dense than the middle level at ROI1, and for black males, L1 was less dense than L4 at ROI1 (Table 4.12). At ROI3, BMD gradually declined from L1 to L5 in black females. The ROI comparisons showed that ROI2 was the least dense, and ROI3 the most (Table 4.12). Significant p-values for the tests are summarised in Table 4.25.

Table 4.25: Significant p-values for vertebral level comparisons of the three medullary regions of interest

Variable	Comparison	P	p-value	Variable	Comparison	P	p-value
ROI1	**L1 vs L3**	**WM**	0.010	**ROI2**	**L2 vs L3**	**WM**	0.046
	L1 vs L4	**BM**	0.020		**L2 vs L4**	**BF**	0.003
	L2 vs L3	**WM**	0.020		**L3 vs L4**	**WF**	0.040
ROI2	**L1 vs L2**	**BM**	0.020		**L3 vs L5**	**BM**	0.003
	L1 vs L3	**BM**	0.000			**WM**	0.030
		BF	0.010		**L4 vs L5**	**BM**	0.010
		WM	0.040	**ROI3**	**L1 vs L4**	**BF**	0.040
	L1 vs L4	**BM**	0.001		**L1 vs L5**		0.004
		BF	0.010		**L2 vs L5**		0.010
	L2 vs L3	**BM**	0.002		**L3 vs L5**		0.030
		BF	0.010		**L4 vs L5**		0.030

Key: P = Population group; vs = Versus; BM = Black males; BF = Black females; WM = White males; WF = White females; ROI = Region of interest

Morphometrics

Simple regression analysis was used to determine the linear relationship between age and the morphometrics. Appendix D.3 provides the output of the linear analyses. Table 4.26 shows the r^2 values which were strong enough to indicate notable correlations. Scatterplots of the data can be found in Appendix B.4. The variables showing these non-linear relationships were only found in the white population groups. The majority of the correlations were seen at the superior – and middle levels for the posterior elements and the spinal canal correlations with age. The vertebral body correlations were found at the lowest level only (L5). The majority of correlations were seen for the female group. The AP – and lateral spinal canal diameters demonstrated an increase with an increase in age. The spinous process length of L3 in white males showed an increase with an increase in age, whereas the spinous process lengths of L1 and L2 in white females, showed an overall decrease with an increase in age. The pedicle height of L4 also decreased in white males as age increased. The lateral vertebral body diameters increased as age increased.

Table 4.26: Table indicating the r^2 and associated two-sided p-values for correlations between age and morphometrics (variable column)

Variable	VL	P	r^2	p-value
SCDAP	**L1**	**WF**	0.68	0.010
	L3		0.66	0.010
SCDL	**L2**	**WF**	0.54	0.020
	L3		0.69	0.010
SPL	**L1**	**WF**	0.68	0.010
	L2		0.66	0.010
	L3	**WM**	0.61	0.010
PDH	**L4**	**WM**	0.59	0.010
VDMaxL	**L5**	**WF**	0.62	0.020
VDMinL	**L5**	**WF**	0.55	0.010

Key: SCDAP = Spinal canal anteroposterior diameter; SCDL = Spinal canal lateral diameter; VDMaxL = Maximum vertebral body lateral diameter; VDMinL = Minimum vertebral body lateral diameter; SPL = Spinous process length; PDH = Pedicle height; VL = Vertebral level; P = Population group; WF = White females; WM = White males. Dark grey cells show a quadratic relationship, and light grey a cubic relationship

Paired t-tests were used to compare the maximum and minimum values to each other for vertebral body width and depth. The maximum and minimum vertebral body lateral – and AP diameters differed across population – and sex groups for all levels, where the maximum values were larger than the minimum values (Tables 4.16 and 4.17). This is clearly seen in Table 4.27.

Table 4.27: Significant p-values of comparisons between the minimum and maximum AP – and lateral vertebral body diameters

Comparison	VL	P	p-value	Comparison	VL	P	p-value
VDMaxL vs VDMinL	L1	BM	0.000	VDMaxAP vs VDMinAP	L1	BM	0.000
		BF	0.000			BF	0.000
		WM	0.000			WM	0.000
		WF	0.000			WF	0.000
	L2	BM	0.000		L2	BM	0.000
		BF	0.000			BF	0.000
		WM	0.000			WM	0.000
		WF	0.000			WF	0.000
	L3	BM	0.000		L3	BM	0.000
		BF	0.000			BF	0.000
		WM	0.000			WM	0.000
		WF	0.000			WF	0.000
	L4	BM	0.000		L4	BM	0.000
		BF	0.000			BF	0.000
		WM	0.000			WM	0.000
		WF	0.000			WF	0.000
	L5	BM	0.000		L5	BM	0.000
		BF	0.000			BF	0.000
		WM	0.000			WM	0.000
		WF	0.000			WF	0.000

Key: P = Population group; vs = Versus; VL = Vertebral level; BM = Black males; BF = Black females; WM = White males; WF = White females; VDMaxL = Maximum vertebral body lateral diameter; VDMinL = Minimum vertebral body lateral diameter; VDMaxAP = Maximum vertebral body anteroposterior diameter; VDMinAP = Minimum vertebral body anteroposterior diameter

Using paired t-tests to compare the anterior – and posterior vertebral body heights, significant differences were seen for almost all groups at almost all levels. The exceptions were seen at L2 for white females, L3 for all groups, and L4 for black females and white males (Table 4.18). The posterior height was larger than the anterior for L1 and L2, but smaller for L4 and L5. The p-values obtained are seen in Table 4.28.

Table 4.28: Significant p-values of comparisons between the anterior – and posterior vertebral body heights

Comparison	VL	P	p-value
VHa vs VHp	L1	BM	0.000
		BF	0.001
		WM	0.001
		WF	0.000
	L2	BM	0.000
		BF	0.000
		WM	0.040
	L4	BM	0.020
		WF	0.000
	L5	BM	0.000
		BF	0.000
		WM	0.000
		WF	0.000

Key: P = Population group; vs = Versus; VL = Vertebral level; BM = Black males; BF = Black females; WM = White males; WF = White females; VHa = Anterior vertebral height; VHp = Posterior vertebral height

Independent two-sided t-tests were used to determine if any significant differences exist between the population groups and between sexes within the population groups. The anterior – and posterior heights; and minimum and maximum measurements were analysed separately due to significant differences found between these measurements. For comparisons between sexes, the black population groups showed that males had larger measurements than females for all variables. The white population groups showed that males also had greater values than females in most measurements, with the exception of the AP spinal canal diameters of L1 to L4, where females had larger measurements (Table 4.15). Comparisons between population groups indicated that, for females: the white group had larger values than the black group for most measurements except for the pedicle lateral diameters of L1 and L2; and for males: the white group had larger values than the black group in most measurements except at the pedicle lateral diameter of L1 and the spinal

canal AP diameter of L2 (Table 4.15). Tables 4.29 and 4.30 show the relevant p-values for the posterior element and spinal canal group comparisons.

Table 4.29: Significant p-values of comparisons made between groups for posterior element measurements

Variable	VL	Comparison	p-value	Variable	VL	Comparison	p-value
TPL	L1	BM vs BF	0.000	PDH	L1	BM vs BF	0.000
		WM vs WF	0.020			WM vs WF	0.020
		BF vs WF	0.004		L2	BM vs BF	0.000
	L2	BM vs BF	0.000			WM vs WF	0.020
		WM vs WF	0.045		L3	BM vs BF	0.000
	L3	BM vs BF	0.000			WM vs WF	0.040
		WM vs WF	0.001		L4	BM vs BF	0.000
	L4	BM vs BF	0.000			WM vs WF	0.020
		WM vs WF	0.010		L5	BM vs BF	0.000
	L5	BM vs BF	0.001	PDDL	L1	BM vs BF	0.001
		WM vs WF	0.040			WM vs WF	0.010
		BM vs WM	0.030			BM vs WM	0.003
SPL	L1	WM vs WF	0.010			BF vs WF	0.010
		BM vs WM	0.040		L2	BM vs BF	0.004
	L2	BM vs BF	0.004			WM vs WF	0.001
		WM vs WF	0.002			BF vs WF	0.010
		BM vs WM	0.010		L3	BM vs BF	0.000
	L3	BM vs BF	0.000			WM vs WF	0.010
		WM vs WF	0.020		L4	BM vs BF	0.001
	L4	BM vs BF	0.003			WM vs WF	0.001
		WM vs WF	0.010		L5	BM vs BF	0.010
	L5	BM vs BF	0.040			WM vs WF	0.010

Key: VL = Vertebral level; BM = Black males; BF = Black females; WM = White males; WF = White females; vs = Versus; TPL = Transverse process length; PDH = Pedicle height; SPL = Spinous process length; PDDL = Pedicle lateral diameter

Table 4.30: Significant p-values of comparisons made between groups for spinal canal measurements

Variable	VL	Comparison	p-value	Variable	VL	Comparison	p-value
SCDAP	L1	WM vs WF	0.002	SCDL	L1	BM vs BF	0.002
		BF vs WF	0.020			BF vs WF	0.003
	L2	WM vs WF	0.002		L2	BM vs BF	0.000
		BM vs WM	0.010			BF vs WF	0.001
		BF vs WF	0.020		L3	BM vs BF	0.001
	L3	WM vs WF	0.010			BF vs WF	0.020
		BF vs WF	0.010		L4	BM vs BF	0.001
						BF vs WF	0.040

Key: VL = Vertebral level; BM = Black males; BF = Black females; WM = White males; WF = White females; vs = Versus; SCDAP = Spinal canal anteroposterior diameter; SCDL = Spinal canal lateral diameter

For vertebral body comparisons between sexes within groups (Tables 4.31 and 4.32), both populations showed that males had larger values than females. Comparisons between population groups indicated that the white group had greater values than the black group (Tables 4.16 to 4.18).

Table 4.31: Significant p-values of comparisons made between groups for vertebral height measurements

Variable	VL	Comparison	p-value	Variable	VL	Comparison	p-value
VHa	L1	BM vs BF	0.000	VHp	L1	BM vs BF	0.000
	L2	BM vs BF	0.000			BF vs WF	0.010
		BF vs WF	0.010		L2	BM vs BF	0.000
	L3	BM vs BF	0.000			WM vs WF	0.030
		BF vs WF	0.030		L3	BM vs BF	0.001
	L4	BM vs BF	0.000			WM vs WF	0.030
		BF vs WF	0.030		L4	BM vs BF	0.000
	L5	BM vs BF	0.001			WM vs WF	0.010
					L5	BM vs BF	0.000

Key: VL = Vertebral level; BM = Black males; BF = Black females; WM = White males; WF = White females; vs = Versus; VHa = Anterior vertebral body height; VHp = Posterior vertebral body height

Table 4.32: Significant p-values of comparisons made between groups for vertebral body diameter measurements

Variable	VL	Comparison	p-value	Variable	VL	Comparison	p-value
VDMaxL	L1	BM vs BF	0.000	VDMaxAP	L2	BM vs BF	0.000
		WM vs WF	0.000			WM vs WF	0.002
	L2	BM vs BF	0.000			BM vs WM	0.010
		WM vs WF	0.000			BF vs WF	0.002
	L3	BM vs BF	0.000		L3	BM vs BF	0.000
		WM vs WF	0.000			WM vs WF	0.000
	L4	BM vs BF	0.000		L4	BM vs BF	0.000
		WM vs WF	0.000			WM vs WF	0.002
	L5	BM vs BF	0.000		L5	BM vs BF	0.000
		WM vs WF	0.001			WM vs WF	0.010
VDMinL	L1	BM vs BF	0.000	VDMinAP	L1	BM vs BF	0.000
		WM vs WF	0.000			WM vs WF	0.000
	L2	BM vs BF	0.000			BM vs WM	0.010
		WM vs WF	0.000			BF vs WF	0.000
	L3	BM vs BF	0.000		L2	BM vs BF	0.000
		WM vs WF	0.001			WM vs WF	0.002
	L4	BM vs BF	0.000			BF vs WF	0.001
		WM vs WF	0.001		L3	BM vs BF	0.000
	L5	BM vs BF	0.000			WM vs WF	0.001
		WM vs WF	0.002		L4	BM vs BF	0.000
VDMaxAP	L1	BM vs BF	0.000			WM vs WF	0.000
		WM vs WF	0.001		L5	BM vs BF	0.000
		BM vs WM	0.002			WM vs WF	0.010
		BF vs WF	0.000				

Key: VL = Vertebral level; BM = Black males; BF = Black females; WM = White males; WF = White females; vs = Versus; VDMaxL = Maximum vertebral body lateral diameter; VDMinL = Minimum vertebral body lateral diameter; VDMaxAP = Maximum vertebral body anteroposterior diameter; VDMinAP = Minimum vertebral body anteroposterior diameter

Paired t-tests were used to compare the vertebral levels to each other for all measurements. The four groups were analysed separately due to differences between sexes and populations. When comparing the transverse process measurements of the vertebral levels, differences were found in all groups between L1 and all other levels, L2 and all other levels, and L4 and L5, with the upper levels indicating shorter lengths than the lower levels (Table 4.13). Differences were also seen between L3 and all other levels for the male groups, with L3 having longer lengths than the other levels (Tables 4.13 and 4.33).

Table 4.33: Significant p-values of the transverse process length comparisons made between vertebral levels

Comparison	P	p-value	Comparison	P	p-value
L1 vs L2	**BM**	0.000	**L2 vs L3**	**WM**	0.000
	BF	0.000		**WF**	0.003
	WM	0.000	**L2 vs L4**	**BM**	0.002
	WF	0.000		**WM**	0.010
L1 vs L3	**BM**	0.000		**BF**	0.020
	BF	0.000		**WF**	0.020
	WM	0.000	**L2 vs L5**	**BM**	0.000
	WF	0.000		**BF**	0.000
L1 vs L4	**BM**	0.000		**WM**	0.001
	BF	0.000		**WF**	0.000
	WM	0.000	**L3 vs L4**	**BM**	0.001
	WF	0.000		**WM**	0.006
L1 vs L5	**BM**	0.000	**L3 vs L5**	**BM**	0.000
	BF	0.000		**WM**	0.020
	WM	0.000	**L4 vs L5**	**BM**	0.030
	WF	0.000		**BF**	0.040
L2 vs L3	**BM**	0.000		**WM**	0.020
	BF	0.000		**WF**	0.010

Key: P = Population group; BM = Black males; BF = Black females; WM = White males; WF = White females; vs = Versus

In all four groups, the lengths of the spinous processes of L1 were much shorter than all other levels except when compared to L5. The spinous processes of L2 to L4 were larger than those of L5 for all four groups as well (Table 4.13). The spinous process of L3 was longer than L2 and L4 for all groups (Tables 4.13 and 4.34).

In all four groups, the pedicle lateral diameter gradually increased while the pedicle height decreased when moving caudally (Table 4.14). Tables 4.35 and 4.36 shows the significant p-values.

Table 4.34: Significant p-values of the spinous process length comparisons made between vertebral levels

Comparison	P	p-value	Comparison	P	p-value
L1 vs L2	**BM**	0.000	**L2 vs L5**	**BM**	0.000
	BF	0.000		**BF**	0.000
	WM	0.000		**WM**	0.000
	WF	0.000		**WF**	0.000
L1 vs L3	**BM**	0.000	**L3 vs L4**	**BM**	0.001
	BF	0.000		**BF**	0.010
	WM	0.000		**WM**	0.040
	WF	0.000		**WF**	0.010
L1 vs L4	**BM**	0.010	**L3 vs L5**	**BM**	0.000
	BF	0.030		**BF**	0.000
	WM	0.010		**WM**	0.000
	WF	0.030		**WF**	0.000
L1 vs L5	**BF**	0.040	**L4 vs L5**	**BM**	0.000
	WM	0.010		**BF**	0.000
L2 vs L3	**BM**	0.001		**WM**	0.000
	BF	0.030		**WF**	0.000
	WF	0.030			

Key: P = Population group; BM = Black males; BF = Black females; WM = White males; WF = White females; vs = Versus

Table 4.35: Significant p-values of vertebral level pedicle height comparisons

Comparison	P	p-value
L1 vs L2	**BF**	0.040
L1 vs L3	**BF**	0.020
L1 vs L4	**BM**	0.010
	BF	0.000
	WM	0.030
	WF	0.020
L1 vs L5	**BM**	0.000
	BF	0.000
	WM	0.000
	WF	0.000
L2 vs L4	**BM**	0.001
	BF	0.000
	WF	0.040
L2 vs L5	**BM**	0.000
	BF	0.000
	WM	0.001
	WF	0.002
L3 vs L4	**BM**	0.010
	BF	0.000
	WF	0.020
L3 vs L5	**BM**	0.000
	BF	0.000
	WM	0.000
	WF	0.001
L4 vs L5	**BM**	0.000
	BF	0.000
	WM	0.001
	WF	0.010

Key: P = Population group; BM = Black males; BF = Black females; WM = White males; WF = White females; vs = Versus

Table 4.36: Significant p-values of the pedicle lateral diameter comparisons made between vertebral levels

Comparison	P	p-value	Comparison	P	p-value
L1 vs L2	**WM**	0.000	**L2 vs L4**	**BF**	0.000
	WF	0.020		**WM**	0.000
L1 vs L3	**BM**	0.000		**WF**	0.000
	BF	0.000	**L2 vs L5**	**BM**	0.000
	WM	0.000		**BF**	0.000
	WF	0.000		**WM**	0.000
L1 vs L4	**BM**	0.000		**WF**	0.000
	BF	0.000	**L3 vs L4**	**BM**	0.000
	WM	0.000		**BF**	0.000
	WF	0.000		**WM**	0.000
L1 vs L5	**BM**	0.000		**WF**	0.000
	BF	0.000	**L3 vs L5**	**BM**	0.000
	WM	0.000		**BF**	0.000
	WF	0.000		**WM**	0.000
L2 vs L3	**BM**	0.000		**WF**	0.000
	BF	0.000	**L4 vs L5**	**BM**	0.000
	WM	0.000		**BF**	0.000
	WF	0.000		**WM**	0.000
L2 vs L4	**BM**	0.000		**WF**	0.000

Key: P = Population group; BM = Black males; BF = Black females; WM = White males; WF = White females; vs = Versus

For the AP diameter of the spinal canal, L1 was larger than all levels for black females. It was also larger than that of L2 and L3 in white males, and L2 to L4 in black males. The AP diameter of the spinal canal of L5 was larger than L3 and L4 in black females, and black males and white males. The AP diameters of L2 and L4 were greater than L3 in black males. The spinal canal of L2 was smaller than L5 in both male groups for the AP diameter (Table 4.15). The lateral diameter of the spinal canal increased caudally with each level in the spine for all four groups (Table 4.15). Spinal canal AP and lateral diameter comparison results are depicted in Table 4.37.

Table 4.37: Significant p-values of the spinal canal AP – and lateral diameter comparisons made between vertebral levels

Variable	Comparison	P	p-value	Variable	Comparison	P	p-value	Variable	Comparison	P	p-value
SCDAP	L1 vs L2	BF	0.000	SCDL	L1 vs L3	BM	0.000	SCDL	L2 vs L4	WM	0.000
		WM	0.001			BF	0.010			WF	0.010
	L1 vs L3	BM	0.010			WF	0.030		L2 vs L5	BM	0.000
		BF	0.000		L1 vs L4	BM	0.000			BF	0.000
		WM	0.030			BF	0.000			WM	0.000
	L1 vs L4	BF	0.040			WM	0.000			WF	0.000
	L1 vs L5	BM	0.040			WF	0.010		L3 vs L4	BM	0.000
	L2 vs L3	BM	0.020		L1 vs L5	BM	0.000			BF	0.003
	L2 vs L5	BM	0.002			BF	0.000			WM	0.030
		WM	0.004			WM	0.000		L3 vs L5	BM	0.000
	L3 vs L4	BM	0.030			WF	0.000			BF	0.000
	L3 vs L5	BM	0.000		L2 vs L3	BM	0.000			WM	0.000
		BF	0.020			BF	0.001			WF	0.000
		WM	0.000			WM	0.030		L4 vs L5	BM	0.000
	L4 vs L5	BM	0.000			WF	0.050			BF	0.000
		BF	0.030		L2 vs L4	BM	0.000			WM	0.000
		WM	0.000			BF	0.000			WF	0.001

Key: P = Population group; SCDAP = Spinal canal anteroposterior diameter; SCDL = Spinal canal lateral diameter; BM = Black males; BF = Black females; WM = White males; WF = White females; vs = Versus

The anterior vertebral heights of L1 and L2 were significantly smaller than the other three levels for all groups. The posterior vertebral height of L1 was smaller than L2 for black males and females, and smaller than L3 in black females (Table 4.18). The posterior height of L1 was larger than L4 for black males and white females, and larger than L5 for all groups. The posterior vertebral height then decreased caudally with each level for all groups (Table 4.18). The anterior – and posterior vertebral height comparison results are depicted in Table 4.38.

Table 4.38: Significant p-values of the vertebral height comparisons made between vertebral levels

Variable	Comparison	P	p-value	Variable	Comparison	P	p-value	Variable	Comparison	P	p-value
VHa	L1 vs L2	BM	0.000	VHa	L2 vs L3	WF	0.020	VHp	L2 vs L4	BF	0.010
		BF	0.000		L2 vs L4	BM	0.030			WM	0.020
		WM	0.000			BF	0.002			WF	0.003
		WF	0.000			WF	0.010		L2 vs L5	BM	0.000
	L1 vs L3	BM	0.000		L2 vs L5	BM	0.001			BF	0.000
		BF	0.000			BF	0.001			WM	0.000
		WM	0.000			WM	0.040			WF	0.000
		WF	0.000			WF	0.010		L3 vs L4	BM	0.001
	L1 vs L4	BM	0.000	VHp	L1 vs L2	BM	0.040			BF	0.000
		BF	0.000			BF	0.001			WM	0.040
		WM	0.000		L1 vs L3	BF	0.020			WF	0.001
		WF	0.000		L1 vs L4	BM	0.030		L3 vs L5	BM	0.000
	L1 vs L5	BM	0.000			WF	0.010			BF	0.000
		BF	0.000		L1 vs L5	BM	0.000			WM	0.001
		WM	0.000			BF	0.000			WF	0.000
		WF	0.000			WM	0.010		L4 vs L5	BM	0.000
	L2 vs L3	BM	0.010			WF	0.000			BF	0.000
		BF	0.001		L2 vs L3	BM	0.030			WM	0.010
		WM	0.010		L2 vs L4	BM	0.000			WF	0.000

Key: P = Population group; VHa = Anterior vertebral body height; VHp = Posterior vertebral body height; BM = Black males; BF = Black females; WM = White males; WF = White females; vs = Versus

The maximum and minimum vertebral lateral – and AP diameters increased caudally with each vertebral level for all four population groups (Tables 4.16 and 4.17). Tables 4.39 and 4.40 show the results from the paired t-tests.

Table 4.39: Significant p-values of the vertebral body lateral diameter comparisons made between vertebral levels

Variable	Comparison	P	p-value	Variable	Comparison	P	p-value	Variable	Comparison	P	p-value
VDMaxL	L1 vs L2	BM	0.000	VDMaxL	L2 vs L5	BF	0.000	VDMinL	L1 vs L4	WM	0.000
		BF	0.000			WM	0.000			WF	0.000
		WM	0.000			WF	0.000		L1 vs L5	BM	0.000
		WF	0.000		L3 vs L4	BM	0.000			BF	0.000
	L1 vs L3	BM	0.000			BF	0.000			WM	0.000
		BF	0.000			WM	0.010			WF	0.000
		WM	0.000			WF	0.000		L2 vs L3	BM	0.000
		WF	0.000		L3 vs L5	BM	0.000			BF	0.000
	L1 vs L4	BM	0.000			BF	0.000			WM	0.000
		BF	0.000			WM	0.000			WF	0.000
		WM	0.000			WF	0.000		L2 vs L4	BM	0.000
		WF	0.000		L4 vs L5	BM	0.000			BF	0.000
	L1 vs L5	BM	0.000			BF	0.000			WM	0.000
		BF	0.000			WM	0.002			WF	0.000
		WM	0.000			WF	0.002		L2 vs L5	BM	0.000
		WF	0.000	VDMinL	L1 vs L2	BM	0.000			BF	0.000
	L2 vs L3	BM	0.000			BF	0.000			WM	0.010
		BF	0.000			WM	0.002			WF	0.000
		WM	0.000			WF	0.020		L3 vs L4	BM	0.000
		WF	0.002		L1 vs L3	BM	0.000			BF	0.000
	L2 vs L4	BM	0.000			BF	0.000			WM	0.010
		BF	0.000			WM	0.000			WF	0.003
		WM	0.000			WF	0.000		L3 vs L5	BM	0.010
		WF	0.000		L1 vs L4	BM	0.000			BF	0.020
	L2 vs L5	BM	0.000			BF	0.000		L4 vs L5	WM	0.030

Key: P = Population group; VDMaxL = Maximum vertebral body lateral diameter; VDMinL = Minimum vertebral body lateral diameter; BM = Black males; BF = Black females; WM = White males; WF = White females; vs = Versus

Table 4.40: Significant p-values of the vertebral body AP diameter comparisons made between vertebral levels

Variable	Comparison	P	p-value	Variable	Comparison	P	p-value	Variable	Comparison	P	p-value
VDMaxAP	L1 vs L2	BM	0.000	VDMaxAP	L2 vs L5	WF	0.010	VDMinAP	L1 vs L5	BF	0.000
		BF	0.000		L3 vs L4	BF	0.002			WM	0.001
		WM	0.002		L3 vs L5	BM	0.000			WF	0.000
		WF	0.040			BF	0.000		L2 vs L3	BM	0.000
	L1 vs L3	BM	0.000			WM	0.040			BF	0.000
		BF	0.000			WF	0.020		L2 vs L4	BM	0.000
		WM	0.000		L4 vs L5	BM	0.000			BF	0.000
		WF	0.010			BF	0.001		L2 vs L5	BM	0.000
	L1 vs L4	BM	0.000			WF	0.010			BF	0.000
		BF	0.000	VDMinAP	L1 vs L2	BM	0.000			WM	0.030
		WM	0.001			BF	0.000			WF	0.003
		WF	0.010			WM	0.000		L3 vs L4	BM	0.020
	L1 vs L5	BM	0.000			WF	0.000			BF	0.000
		BF	0.000		L1 vs L3	BM	0.000		L3 vs L5	BM	0.000
		WM	0.001			BF	0.000			BF	0.000
		WF	0.001			WM	0.001			WM	0.030
	L2 vs L3	BM	0.001			WF	0.000			WF	0.010
		BF	0.000		L1 vs L4	BM	0.000				
	L2 vs L4	BM	0.000			BF	0.000		L4 vs L5	BM	0.000
		BF	0.000			WM	0.000			BF	0.000
	L2 vs L5	BM	0.000			WF	0.000			WF	0.010
		BF	0.000		L1 vs L5	BM	0.000				

Key: P = Population group; VDMaxAP = Maximum vertebral body anteroposterior diameter; VDMinAP = Minimum vertebral body anteroposterior diameter; BM = Black males; BF = Black females; WM = White males; WF = White females; vs = Versus

4.2.3 Inter – and Intra-observer analysis

The raw data for the observer analysis for all CT measurements can be found in Appendix E.1 and E.2. No weak ICC values were found for LLA or BMD. Medullary BMD indicated better ICC values than cortical BMD. The lowest ICC was seen at the anterior border of L2 for the interobserver (ICC = 0.58). Table 4.41 provides the ICC values.

Table 4.41: Table showing the interclass correlation coefficients calculated for the lumbar lordosis angle (LLA) and BMD measurements (variables)

Variable	IAO	IEO	Variable	IAO	IEO
LLA	0.996	0.99	**SEPL3**	0.97	0.96
ROI1L1	0.97	0.71*	**SEPL4**	0.94	0.68*
ROI1L2	0.96	0.90	**SEPL5**	0.95	0.69*
ROI1L3	0.96	0.71*	**IEPL1**	0.71*	0.87
ROI1L4	0.97	0.83	**IEPL2**	0.69*	0.69*
ROI1L5	0.99	0.70*	**IEPL3**	0.98	0.91
ROI2L1	0.99	0.96	**IEPL4**	0.91	0.81
ROI2L2	0.995	0.99	**IEPL5**	0.96	0.74*
ROI2L3	0.99	0.99	**ABL1**	0.96	0.94
ROI2L4	0.99	0.99	**ABL2**	0.97	0.58*
ROI2L5	0.99	0.98	**ABL3**	0.71*	0.90
ROI3L1	0.99	0.69*	**ABL4**	0.83	0.94
ROI3L2	0.98	0.95	**ABL5**	0.96	0.84
ROI3L3	0.94	0.87	**PBL1**	0.90	0.99
ROI3L4	0.99	0.92	**PBL2**	0.79	0.98
ROI3L5	0.98	0.88	**PBL3**	0.78	0.98
SEPL1	0.94	0.73*	**PBL4**	0.76	0.97
SEPL2	0.92	0.90	**PBL5**	0.76	0.99

*Key: IAO = Intra-observer ICC results; IEO = Interobserver ICC results; LLA = Lumbar lordosis angle; ROI1 = Region of interest 1; ROI2 = Region of interest 2; ROI3 = Region of interest 3; SEP = Superior endplate; IEP = Inferior endplate; AB = Anterior border; PB = Posterior border. Values with * are moderate*

The intra-observer analyses indicated better ICC values than the interobserver tests. The pedicle lateral diameters of the upper and lower levels, and the pedicle height of the middle level seem to be the least repeatable for the interobserver. The pedicle height of L3 showed a weak ICC value for the interobserver, meaning that it should be interpreted with care. Table 4.42 provides the ICC values obtained.

The observer analyses indicated good to excellent ICC values for most measurements. The transverse process lengths appeared to have lower repeatability as opposed to the spinous process length. The AP diameter of the spinal canal also seemed to be less repeatable than the spinal canal

lateral diameter measurements. The spinal canal dimensions proved more difficult to repeat, especially for the interobserver, as three of the ten values were weak values Table 4.43 provides the ICC values for all the measurements tested.

Table 4.42: Table showing the interclass correlation coefficients calculated for the various pedicle measurements (variables)

Variable	IAO	IEO	Variable	IAO	IEO
PDDL L1	0.92	0.63*	**PDHL1**	0.95	0.58*
PDDL L2	0.95	0.81	**PDHL2**	0.91	0.66*
PDDL L3	0.86	0.75	**PDHL3**	0.90	0.38**
PDDL L4	0.84	0.73*	**PDHL4**	0.96	0.68*
PDDL L5	0.84	0.66*	**PDHL5**	0.96	0.79
*Key: IAO = Intra-observer ICC results; IEO = Interobserver ICC results; PDDL = Pedicle lateral diameter; PDH = Pedicle height. Values with * are moderate and with ** are weak*					

Table 4.43: Table showing the interclass correlation coefficients calculated for the various posterior element – and spinal canal measurements (variables)

Variable	IAO	IEO	Variable	IAO	IEO
TPLL1	0.997	0.64*	**SCDLL1**	0.95	0.80
TPLL2	0.98	0.71*	**SCDLL2**	0.72*	0.88
TPLL3	0.997	0.83	**SCDLL3**	0.82	0.39**
TPLL4	0.99	0.70*	**SCDLL4**	0.79	0.90
TPLL5	0.99	0.68*	**SCDLL5**	0.87	0.78
SPLL1	0.82	0.92	**SCDAPL1**	0.43**	0.61*
SPLL2	0.97	0.89	**SCDAPL2**	0.61*	0.56*
SPLL3	0.98	0.74*	**SCDAPL3**	0.97	0.45**
SPLL4	0.99	0.92	**SCDAPL4**	0.99	0.75
SPLL5	0.95	0.84	**SCDAPL5**	0.96	0.56*
*Key: IAO = Intra-observer ICC results; IEO = Interobserver ICC results; TPL = Transverse process length; SPL = Spinous process length; SCDAP = Spinal canal anteroposterior diameter; SCDL = Spinal canal lateral diameter. Values with * are moderate and with ** are weak*					

The observer analyses indicated that the vertebral lateral diameter was easier to measure than the AP diameter, and that the anterior vertebral height had a lower repeatability as opposed to the posterior height. Overall, the anterior vertebral height was the least repeatable, as the analysis indicated that almost all the interobserver ICC values were weak. This means that the anterior vertebral body height measurements should be analysed with care due to the low repeatability. Table 4.44 provides the ICC values for all the measurements tested.

Table 4.44: Table showing the interclass correlation coefficients calculated for the various vertebral body measurements (variables)

Variable	IAO	IEO	Variable	IAO	IEO
VDMaxLL1	0.99	0.84	**VDMinAPL1**	0.95	0.84
VDMaxLL2	0.99	0.92	**VDMinAPL2**	0.99	0.72*
VDMaxLL3	0.99	0.91	**VDMinAPL3**	0.99	0.55*
VDMaxLL4	0.96	0.87	**VDMinAPL4**	0.92	0.83
VDMaxLL5	0.96	0.80	**VDMinAPL5**	0.90	0.68*
VDMinLL1	0.98	0.81	**VHaL1**	0.57*	0.40**
VDMinLL2	0.995	0.88	**VHaL2**	0.39**	0.30**
VDMinLL3	0.99	0.74*	**VHaL3**	0.89	0.40**
VDMinLL4	0.99	0.78	**VHaL4**	0.95	0.82
VDMinLL5	0.90	0.85	**VHaL5**	0.85	0.31**
VDMaxAPL1	0.94	0.57*	**VHpL1**	0.94	0.63*
VDMaxAPL2	0.98	0.84	**VHpL2**	0.96	0.85
VDMaxAPL3	0.97	0.87	**VHpL3**	0.92	0.64*
VDMaxAPL4	0.95	0.72*	**VHpL4**	0.92	0.83
VDMaxAPL5	0.97	0.79	**VHpL5**	0.95	0.76

*Key: IAO = Intra-observer ICC results; IEO = Interobserver ICC results; VDMaxL = Maximum vertebral body lateral diameter; VDMinL = Minimum vertebral body lateral diameter; VDMaxAP = Maximum vertebral body anteroposterior diameter; VDMinAP = Minimum vertebral body anteroposterior diameter; VHa = Anterior vertebral height; VHp = Posterior vertebral height. Values with * are moderate and with ** are weak*

4.3 MRI component

The aim was to identify possible population specific trends for the morphological properties considered during lumbar spine procedures. The MRI (Magnetic Resonance Imaging) component

consisted of morphometric measurements taken of the neural foramina and the dorsal nerve root and ganglion for vertebral levels L1 to L5. The sample comprised of black South Africans only. Descriptive statistics were generated for all measurements for the MRI component. Descriptive statistics involved determining the means, standard deviations, and upper and lower limits of the 95% confidence intervals.

Age correlations were not performed for the MRI data, due to the small sample size, and consequently a lack of sufficient number of individuals per age group. Comparisons between males and females were not performed for the coronal or transverse sections, due to the small sample of female measurements. This was due to the difficulty of measuring certain structures on the coronal and transverse images, as well as lack of full lumbar coronal and transverse slices for most of the female sample. The data was first tested for normality using Shapiro-Wilk tests. Values less than 0.05 were considered significant and was evidence for non-normally distributed data. Normally distributed data was compared using two-sided t-tests, and comparisons between non-normal data was tested using Mann-Whitney U tests. These methods were applied when comparing males and females and the different population groups to one another. Paired t-tests were used to compare the left – and right-hand; anterior – and posterior measurements; and superior – and inferior measurements to each other where applicable.

The repeatability and reproducibility of the measurements were evaluated with ICC determination. The raw data used to obtain the results can be accessed in Appendices A.5 to A.7.

4.3.1 MRI descriptive statistics

Sagittal

When looking at the foraminal height depicted in Table 4.45, an increase was seen in the measurements when moving caudally with the vertebral levels. The largest measurement was at: L5 for males (20.8 ± 2.5 mm), L3 for females (20.5 ± 2.6 mm) and L5 for the combined group (20.6 ± 2.4 mm). The smallest measurement was seen at L1 for males, females, and the combined group (16.9 ± 2.4 mm, 17.3 ± 1.9 mm, and 17.0 ± 2.2 mm, respectively).

The nerve root-to-pedicle – and root-to-disc distances are also shown in Table 4.45. The distance from the root to the intervertebral disc (IVD) and the pedicle showed similar trends to the foraminal height, with smaller differences between each level, and an apparent decrease from L3 to L4 for the root-to-pedicle, and from L4 to L5 for the root-to-disc. The nerve root was superior

to the disc at all levels for males and the combined sample, and at L1 to L3 for females. The most superior root was seen at L1 in males and the combined group (-1.3 ± 1.8 mm, and -1.3 ± 1.9 mm, respectively), and at L1 and L3 for females (-1.3 ± 2.0 mm, and -1.3 ± 2.5 mm, respectively). The nerve root was inferior to the disc at L4 and L5 for females, with the most inferior nerve root at L4 (0.9 ± 2.1 mm). The nerve root was closest to the pedicle at L1 for males and the combined sample (10.5 ± 2.0 mm, and 10.4 ± 2.0 mm, respectively), and at L4 for females (9.4 ± 2.2 mm); and furthest at L5 for males (12.4 ± 3.6 mm), and L3 for females and the combined sample (12.2 ± 3.1 mm, and 11.7 ± 2.8 mm, respectively). The descriptive statistics are seen in table 4.45.

Table 4.45: Descriptive statistics of the foraminal height, root-to-disc –, and root-to-pedicle measurements taken on the sagittal images

VL	Sex	FH (mm)			RD (mm)			RP (mm)		
		Mean	SD	95% CI	Mean	SD	95% CI	Mean	SD	95% CI
L1	M	16.9	2.4	15.4 – 18.3	-1.3	1.8	-2.4 – -0.3	10.5	2.0	9.2 – 11.7
	F	17.3	1.9	15.9 – 18.7	-1.3	2.0	-2.9 – 0.4	10.4	2.0	8.8 – 12.0
	C	17.0	2.2	16.0 – 18.0	-1.3	1.9	-2.1 – -0.5	10.4	2.0	9.5 – 11.3
L2	M	19.4	2.5	17.9 – 20.9	-0.8	2.0	-2.0 – 0.4	10.7	2.0	9.5 – 11.9
	F	18.8	2.4	16.7 – 21.0	-1.0	2.1	-2.5 – 0.6	11.4	2.8	9.1 – 13.8
	C	19.2	2.4	18.1 – 20.3	-0.9	2.0	-1.7 – 0.01	11.0	2.3	9.9 – 12.0
L3	M	20.3	2.0	19.1 – 21.6	-0.4	2.4	-1.8 – 1.1	11.4	2.7	9.8 – 13.1
	F	20.5	2.6	18.3 – 22.8	-1.3	2.5	-3.5 – 0.9	12.2	3.1	9.4 – 15.0
	C	20.4	2.1	19.4 – 21.4	-0.7	2.4	-1.8 – 0.4	11.7	2.8	10.4 – 13.0
L4	M	20.7	2.4	19.3 – 22.2	-0.5	3.4	-2.6 – 1.6	12.1	2.7	10.5 – 13.7
	F	20.1	2.2	20.0 – 21.9	0.9	2.1	-0.8 – 2.6	9.4	2.2	7.5 – 11.3
	C	20.5	2.3	19.4 – 21.6	-0.0	3.1	-1.4 – 1.4	11.1	2.8	9.8 – 12.4
L5	M	20.8	2.5	19.3 – 22.3	-1.2	2.9	-2.9 – 0.5	12.4	3.6	10.2 – 14.5
	F	20.2	2.1	18.4 – 21.9	0.6	2.2	-1.3 – 2.4	9.8	2.2	7.9 – 11.6
	C	20.6	2.4	19.5 – 21.6	-0.6	2.7	-1.8 – 0.7	11.4	3.4	10.0 – 12.9

Key: VL = Vertebral level; M = Male; F = Female; C = Combined male and female samples; SD = Standard deviation; CI = Confidence interval; FH = Foraminal height; RD = Root-to-disc distance; RP = Root-to-pedicle distance. Negative values represent measurements taken above the superior border of the IVD

The foraminal sagittal AP diameters (Table 4.46) decreased within each foramen from superior to middle to inferior. The AP diameters of each level also decreased per vertebral level when moving caudally in the spine. The smallest AP diameter was measured at the inferior diameter at L5 for males, females, and the combined sample (4.0 ± 1.6 mm, 3.3 ± 0.8 mm, and 3.8 ± 1.5 mm, respectively); and the largest at the superior diameter of L1 for males, females, and the combined sample (8.1 ± 1.6 mm, 8.6 ± 1.8 mm, and 8.1 ± 1.7 mm, respectively).

Table 4.46: Descriptive statistics of the superior –, middle –, and inferior foraminal diameters measured on sagittal sections

VL	Sex	SFD (mm)			MFD (mm)			IFD (mm)		
		Mean	SD	95% CI	Mean	SD	95% CI	Mean	SD	95% CI
L1	M	8.1	1.6	6.8 – 8.7	7.3	1.5	6.4 – 8.2	6.4	1.5	5.5 – 7.4
	F	8.6	1.8	7.1 – 10.1	7.8	1.2	6.7 – 8.9	7.1	1.3	5.9 – 8.2
	C	8.1	1.7	7.3 – 8.8	7.5	1.5	6.8 – 8.1	6.7	1.5	6.0 – 7.3
L2	M	7.8	1.4	7.2 – 8.6	6.9	1.6	6.1 – 7.8	6.5	1.6	5.6 – 7.4
	F	7.9	1.8	6.3 – 9.4	6.9	2.0	5.2 – 8.5	6.2	1.2	5.1 – 7.2
	C	7.8	1.5	7.2 – 8.5	6.9	1.7	6.2 – 7.6	6.4	1.4	5.7 – 7.0
L3	M	7.3	1.3	6.7 – 7.9	6.1	1.3	5.3 – 6.8	5.5	1.2	4.7 – 6.2
	F	8.1	1.8	6.5 – 9.7	6.9	1.6	5.4 – 8.3	5.7	1.0	4.8 – 6.5
	C	7.6	1.5	6.9 – 8.2	6.3	1.5	5.7 – 7.0	5.5	1.1	5.0 – 6.0
L4	M	6.6	1.3	6.6 – 7.3	5.7	1.4	4.9 – 6.5	5.1	1.0	4.5 – 5.7
	F	7.7	1.6	6.3 – 9.1	6.0	1.4	5.0 – 7.0	4.4	1.1	3.4 – 5.3
	C	7.0	1.5	6.4 – 7.7	5.8	1.4	5.2 – 6.4	4.8	1.0	4.3 – 5.3
L5	M	6.0	1.6	5.0 – 7.0	4.4	1.2	3.7 – 5.1	4.0	1.6	3.0 – 5.0
	F	5.9	1.2	4.9 – 6.9	4.3	1.2	3.2 – 5.3	3.3	0.8	2.7 – 4.0
	C	6.0	1.5	5.3 – 6.6	4.4	1.2	3.8 – 4.9	3.8	1.5	3.1 – 4.4

Key: VL = Vertebral level; M = Male; F = Female; C = Combined male and female samples; SD = Standard deviation; CI = Confidence interval; SFD = Superior foraminal diameter; MFD = Middle foraminal diameter; IFD = Inferior foraminal diameter

Coronal

The left – and right-hand measurements showed clear differences. The middle – and lateral distances from the nerve root to the superior border of the IVD (Table 4.47) were further below

the disc for the right-hand side measurements compared to the left. It was clear that, when moving from medial to lateral, the nerve root was situated further inferiorly when moving laterally. When taking into account the individual levels, the nerve roots appeared to lie more inferiorly when moving caudally in the spine. The most superior root was at the medial border of the pedicles at L5 for left and right (-6.1 ± 1.1 mm, and -6.8 ± 1.6 mm, respectively); and the most inferior at the lateral border of the pedicle at L4 for left and right (6.7 ± 1.8 mm, and 8.3 ± 2.3 mm, respectively). The shortest nerve root-to-disc distance was at the middle of the pedicle of L1 on the right (-0.1 ± 3.1 mm), and L3 on the left (0.1 ± 2.8 mm); and the longest at the lateral border of the pedicle of L4 for left and right (6.7 ± 1.8 mm, and 8.3 ± 2.3 mm, respectively). The descriptive statistics can be found in Tables 4.47 and 4.48

Table 4.47: Descriptive statistics of the coronal measurements in relation to the IVD

VL	Side	MedD (mm)			MidD (mm)			LatD (mm)		
		Mean	SD	95% CI	Mean	SD	95% CI	Mean	SD	95% CI
L1	Left	-5.3	2.0	-9.1 – -1.6	-0.9	3.0	-10.7 – 8.9	4.3	3.0	1.2 – 7.4
	Right	-4.1	1.5	-6.4 – -1.7	-0.1	3.1	-11.9 – 11.6	5.9	3.3	4.9 – 6.9
L2	Left	-5.0	1.5	-8.4 – -1.5	-0.6	1.7	-6.2 – 5.0	2.9	1.9	0.8 – 4.9
	Right	-5.9	2.0	-12.4 – 0.7	1.1	2.8	-1.2 – 3.4	3.8	2.3	-2.0 – 9.5
L3	Left	-5.0	2.3	-9.8 – -0.2	0.1	2.8	-6.4 – 6.6	3.9	2.9	0.2 – 7.5
	Right	-5.3	3.0	-13.3 – 2.7	2.7	2.1	0.4 – 5.0	5.6	1.6	1.4 – 9.8
L4	Left	-5.3	2.1	-8.8 – -1.9	1.1	2.1	-4.6 – 6.8	6.7	1.8	4.4 – 9.0
	Right	-5.1	2.1	-10.6 – 0.4	2.9	2.5	0.3 – 5.5	8.3	2.3	5.8 – 10.8
L5	Left	-6.1	1.1	-8.5 – -3.6	-1.9	0.9	-3.9 – 0.2	5.2	2.3	0.1 – 10.3
	Right	-6.8	1.6	-11.7 – -2.0	1.8	2.9	-0.5 – 4.1	7.1	3.1	-0.8 – 15.0

Key: VL = Vertebral level; SD = Standard deviation; CI = Confidence interval; MedD = Medial root-to-disc distance; MidD = Midline root-to-disc distance; LatD = Lateral root-to-disc distance; Negative values mean that the measurement was taken above the superior border of the IVD

For the distances from the nerve root to the pedicles (Table 4.48), the left – and right-hand sides demonstrated few discrepancies. The medial measurements showed an increase (meaning the nerve root was situated further from or more superiorly in relation to the pedicle) per level when moving caudally until L4, but then a sudden decline was observed from L4 to L5 (meaning the

nerve root was situated closer to the pedicle). The middle measurements showed that the nerve root was situated further away from the pedicle when moving caudally in the spine until L3, with a slight decrease in distance from L3 to L4, before regaining the trend of increasing distance from L4 to L5. The lateral measurement showed an increase in distance (moving further away from the pedicle) from L1 to L3, before decreasing (moving closer to the pedicle) from L3 to L5. The shortest nerve root-to-pedicle distance was at the lateral border of the pedicle at L4 for the left (4.7 ± 1.8 mm), the lateral border of the pedicle at L5 for the right (4.1 ± 3.3 mm), and the lateral border of the pedicle at L4 and L5 for the combined sample (4.7 ± 1.8 mm, and 4.7 ± 2.3 mm, respectively). The longest distance was seen at the medial border of the pedicle at L5 for the left, right and combined sample (15.9 ± 2.0 mm, 15.9 ± 3.1 mm, and 15.9 ± 2.3 mm, respectively).

Table 4.48: Descriptive statistics of the coronal measurements relative to the pedicle

VL	Side	MedP (mm)			MidP (mm)			LatP (mm)		
		Mean	**SD**	**95% CI**	**Mean**	**SD**	**95% CI**	**Mean**	**SD**	**95% CI**
L1	**Left**	11.2	1.7	10.0 – 12.3	6.7	2.3	4.5 – 8.9	6.8	2.3	5.3 – 8.2
	Right	10.6	2.5	8.2 – 13.0	7.0	1.7	4.9 – 9.1	6.8	2.0	5.3 – 8.3
	Combi	10.9	2.0	9.3 – 12.5	6.9	1.7	4.8 – 9.0	6.8	1.9	5.4 – 8.2
L2	**Left**	14.1	2.3	11.4 – 16.8	9.2	1.5	8.0 – 10.4	7.8	2.7	4.4 – 11.1
	Right	13.3	2.9	10.9 – 15.6	8.9	1.5	7.3 – 10.5	7.4	1.6	5.5 – 9.3
	Combi	13.7	2.3	11.9 – 15.4	9.0	1.4	7.9 – 10.2	7.6	2.1	5.0 – 10.2
L3	**Left**	15.7	2.9	13.0 – 18.5	9.1	2.3	6.7 – 11.4	7.4	2.5	4.5 – 10.3
	Right	15.7	3.9	12.6 – 18.8	9.7	2.1	7.8 – 11.7	5.6	2.7	3.2 – 8.0
	Combi	15.7	3.2	13.5 – 17.9	9.4	2.0	7.8 – 11.0	6.5	2.5	3.9 – 9.1
L4	**Left**	15.9	2.0	13.0 – 18.8	9.5	1.3	7.3 – 11.8	4.7	1.8	2.5 – 6.9
	Right	15.9	3.1	12.0 – 19.9	8.3	1.9	5.5 – 11.1	4.6	2.3	1.5 – 7.8
	Combi	15.9	2.3	12.8 – 19.1	8.9	1.5	6.5 – 11.4	4.7	1.8	2.5 – 6.8
L5	**Left**	14.4	1.4	12.5 – 16.3	9.0	2.0	6.2 – 11.8	5.4	1.6	3.4 – 7.4
	Right	14.1	2.6	10.5 – 17.8	9.0	2.2	6.7 – 11.3	4.1	3.3	2.2 – 6.0
	Combi	14.3	1.7	11.7 – 16.8	9.0	2.0	6.5 – 11.5	4.7	2.3	2.8 – 6.7

Key: VL = Vertebral level; SD = Standard deviation; CI = Confidence interval; Combi = Combined left and right measurements; MedP = Medial root-to-pedicle distance; MidP = Midline root-to-pedicle distance; LatP = Lateral root-to-pedicle distance

Transverse

In Table 4.49, the foraminal transverse AP diameter appeared similar for the left – and the right-hand sides for both superior – and inferior measurements. The superior foraminal transverse AP diameter was larger than the inferior at L1 but smaller than the inferior for L2 and L3, before becoming larger again at L4 and L5. The smallest foraminal transverse AP diameter was at the inferior margin of the disc at L1 for the left, right and combined sample (6.6 ± 0.6 mm, 5.9 ± 0.8 mm, and 6.2 ± 0.5 mm, respectively); and the largest at the superior margin of the disc at L4 for the left and the combined sample (8.5 ± 2.0 mm, and 8.1 ± 1.7 mm, respectively), and L5 for the right (8.2 ± 1.6 mm).

Table 4.49: Descriptive statistics of the superior – and inferior foraminal diameters measured transverse images

VL	Side	FDTS (mm)			FDTI (mm)		
		Mean	SD	95% CI	Mean	SD	95% CI
L1	Left	7.8	0.5	6.6 – 8.9	6.6	0.6	5.2 – 7.9
	Right	6.7	0.4	5.6 – 7.7	5.9	0.8	3.9 – 7.8
	Combi	7.2	0.3	6.4 – 8.0	6.2	0.5	4.9 – 7.5
L2	Left	7.4	0.6	6.6 – 8.3	7.4	1.7	4.7 – 10.0
	Right	6.6	0.8	5.4 – 7.9	7.6	1.1	5.8 – 9.4
	Combi	7.0	0.4	6.4 – 7.6	7.5	0.6	6.6 – 8.4
L3	Left	7.7	1.1	6.7 – 8.8	7.8	1.7	6.3 – 9.4
	Right	7.5	0.6	6.9 – 8.0	7.8	1.3	6.6 – 9.0
	Combi	7.6	0.7	6.9 – 8.3	7.8	1.4	6.5 – 9.1
L4	Left	8.5	2.0	6.6 – 10.4	6.9	1.4	5.8 – 8.1
	Right	7.7	1.5	6.3 – 9.1	6.9	1.0	6.1 – 7.8
	Combi	8.1	1.7	6.5 – 9.7	6.9	1.2	6.0 – 7.9
L5	Left	7.9	1.0	7.2 – 8.6	6.9	0.9	6.2 – 7.5
	Right	8.2	1.6	7.0 – 9.3	7.2	1.1	6.5 – 8.0
	Combi	8.0	1.2	7.2 – 8.9	7.0	0.9	6.4 – 7.7

Key: VL = Vertebral level; SD = Standard deviation; CI = Confidence interval; Combi = Combined left and right measurements; FDT = Foraminal transverse anteroposterior diameter; S = Superior to the IVD; I = Inferior to the IVD

Tables 4.50 and 4.51 show that the nerve root was situated more anteriorly (closer to the disc) for the superior measurements for all five levels and the inferior measurement of L2. The root appeared to lie closer to the facet joint for the inferior measurements of L1 and L3 to L5. The shortest distance from the root to the disc was at the inferior border of the disc at L3 for the left and the combined sample (2.0 ± 0.8 mm, and 2.3 ± 0.6 mm, respectively), and at the superior border of the disc at L1 for the right (2.3 ± 0.3 mm). The longest distance was at the inferior border of the disc at L2 for the left (3.5 ± 1.0 mm), at the superior border of the disc at L4 for the right (3.1 ± 0.8 mm), and for the combined sample: at the superior borer of the disc at L4 and the inferior border of the disc at L2 (3.2 ± 0.9 mm, and 3.2 ± 0.6 mm, respectively) (Table 4.50).

Table 4.50: Descriptive statistics of the superior – and inferior root-to-disc distances measured on the transverse images

VL	Side	RDS (mm)			RDI (mm)		
		Mean	SD	95% CI	Mean	SD	95% CI
L1	Left	2.8	0.3	2.0 – 3.5	3.2	0.3	2.5 – 4.0
	Right	2.3	0.3	1.7 – 3.0	2.6	0.9	0.3 – 4.9
	Combi	2.6	0.3	1.9 – 3.2	2.9	0.6	1.5 – 4.4
L2	Left	3.1	1.1	1.3 – 4.9	3.5	1.0	1.9 – 5.1
	Right	2.6	0.6	1.7 – 3.5	2.9	0.6	1.9 – 3.9
	Combi	2.9	0.6	1.8 – 3.9	3.2	0.6	2.2 – 4.2
L3	Left	2.7	0.4	2.3 – 3.1	2.0	0.8	1.2 – 2.7
	Right	2.6	0.9	1.8 – 3.4	2.5	0.5	2.0 – 3.0
	Combi	2.6	0.6	2.1 – 3.2	2.3	0.6	1.7 – 2.8
L4	Left	3.3	1.0	2.4 – 4.2	2.9	1.2	1.9 – 3.9
	Right	3.1	0.8	2.3 – 3.8	2.5	0.8	1.8 – 3.2
	Combi	3.2	0.9	2.4 – 4.0	2.7	1.0	1.9 – 3.5
L5	Left	2.9	0.6	2.4 – 3.3	2.6	0.6	2.2 – 3.0
	Right	2.8	0.9	2.2 – 3.5	2.8	0.6	2.3 – 3.2
	Combi	2.9	0.7	2.4 – 3.3	2.7	0.6	2.3 – 3.0

Key: VL = Vertebral level; SD = Standard deviation; CI = Confidence interval; Combi = Combined left and right measurements; RD = Root-to-disc distance; S = Superior to the IVD; I = Inferior to the IVD

The nerve root-to-facet distance (Table 4.51) was shorter at the superior margin than the inferior margin at all levels. The shortest distance was recorded at the superior border of the disc at L2 for the left and the combined sample (1.9 ± 0.9 mm, and 1.9 ± 0.7 mm, respectively), and at the superior border of the disc at L2 and L3 for the right (2.0 ± 0.6 mm for both levels). The longest distance was seen at the inferior border of the disc at L4 for the left, right and combined sample (4.2 ± 2.3 mm, 4.2 ± 2.1 mm, and 4.2 ± 1.4 mm, respectively).

Table 4.51: Descriptive statistics of the superior – and inferior root-to-facet distances measured on the transverse images

VL	Side	RFS (mm)			RFI (mm)		
		Mean	SD	95% CI	Mean	SD	95% CI
L1	Left	2.7	0.7	1.0 – 4.4	3.7	0.8	1.7 – 5.7
	Right	2.2	0.1	2.0 – 2.4	3.4	1.2	0.4 – 6.3
	Combi	2.5	0.4	1.5 – 3.4	3.5	0.8	1.5 – 5.5
L2	Left	1.9	0.9	0.5 – 3.2	2.5	1.3	0.4 – 4.6
	Right	2.0	0.6	1.1 – 2.9	2.3	1.4	-0.01 – 4.5
	Combi	1.9	0.7	0.9 – 3.0	2.4	1.3	0.3 – 4.5
L3	Left	2.1	0.8	1.3 – 2.9	4.3	1.5	3.0 – 5.7
	Right	2.0	0.6	1.5 – 2.6	3.9	1.7	2.3 – 5.6
	Combi	2.1	0.7	1.5 – 2.7	4.1	1.5	2.7 – 5.6
L4	Left	2.7	1.0	1.8 – 3.6	4.2	2.3	2.2 – 6.1
	Right	2.2	1.1	1.2 – 3.2	4.2	2.1	2.4 – 5.9
	Combi	2.5	1.0	1.5 – 3.4	4.2	1.4	2.3 – 6.0
L5	Left	2.5	1.3	1.6 – 3.4	4.1	1.8	2.8 – 5.4
	Right	2.5	1.2	1.7 – 3.4	4.1	2.0	2.7 – 5.5
	Combi	2.5	1.2	1.7 – 3.4	4.1	1.8	2.8 – 5.4

Key: VL = Vertebral level; SD = Standard deviation; CI = Confidence interval; Combi = Combined left and right measurements; RF = root-to-facet distance; S = Superior to the IVD; I = Inferior to the IVD

The target angle is depicted in Table 4.52. This is the angle at the intersection between the line drawn along the posterior border of the vertebral body where it creates the anterior border of the spinal canal, and the line drawn along the anterior border of the facet joint. The target angle was larger for the superior measurements and showed a clear decrease when moving inferiorly in the

spine. The smallest angle was seen at the inferior margin of the disc at L5 for the left, right and combined sample (12.1 ± 4.5°, 12.6 ± 5.0°, and 12.3 ± 4.5°, respectively). The largest angle was observed at the superior margin of the disc at L2 on the left (26.0 ± 4.1°), and at the superior margin of the disc at L1 on the right and for the combined sample (25.5 ± 6.2°, and 25.6 ± 5.9 °, respectively).

Table 4.52: Descriptive statistics of the superior – and inferior target angles measured on the transverse images

VL	Side	TAS (degrees)			TAI (degrees)		
		Mean	SD	95% CI	Mean	SD	95% CI
L1	Left	25.6	6.2	10.3 – 40.9	23.9	2.9	16.7 – 31.0
	Right	25.5	5.7	11.5 – 39.6	21.2	4.5	10.1 – 32.3
	Combi	25.6	5.9	10.9 – 40.2	22.5	3.6	13.5 – 31.6
L2	Left	26.0	4.1	19.5 – 32.4	22.2	6.6	11.7 – 32.6
	Right	23.6	3.5	17.9 – 29.2	20.7	4.8	13.0 – 28.4
	Combi	24.8	3.8	18.7 – 30.8	21.4	5.6	12.5 – 30.4
L3	Left	19.2	2.9	16.6 – 21.9	17.6	4.3	13.7 – 21.6
	Right	18.6	4.6	14.4 – 22.9	17.9	4.5	13.8 – 22.0
	Combi	18.9	3.7	15.5 – 22.4	17.8	3.9	14.1 – 21.4
L4	Left	18.2	3.4	15.0 – 21.3	14.2	3.9	11.0 – 17.5
	Right	17.6	3.0	14.7 – 20.4	16.7	3.4	12.9 – 18.5
	Combi	17.9	3.2	14.9 – 20.8	15.0	3.4	12.0 – 17.9
L5	Left	14.3	4.0	11.5 – 17.2	12.1	4.5	8.8 – 15.3
	Right	15.3	3.9	12.5 – 18.1	12.6	5.0	9.1 – 16.2
	Combi	14.8	3.8	12.11 – 17.5	12.3	4.5	9.1 – 15.6

Key: VL = Vertebral level; SD = Standard deviation; CI = Confidence interval; Combi = Combined left and right measurements; TA = Target angle (S = Superior to the IVD; I = Inferior to the IVD)

4.3.2 MRI comparative statistics

Sagittal

Independent two-sided t-tests were used to determine if any significant differences exist between the male and female groups. Significant differences between males and females were only found at L4 for the superior foraminal diameter ($p = 0.030$) and the distance from the nerve root to the pedicle ($p = 0.020$), where the males had greater values than females in both cases (Tables 4.45 and 4.46).

Paired t-tests were used to compare the vertebral levels to each other. Due to the fact that males and females differed in only two instances, the males and females were pooled and tested together. The distance between the root and the intervertebral disc showed that L1 and L4 differ ($p = 0.039$), with L4 extending more inferiorly than L1 (Table 4.45). For the root-to-pedicle measurement, L3 extended significantly ($p = 0.024$) more inferiorly than L1. For the foraminal height, L1 and L2 differed from each other as well as the other three levels (Table 4.45). For this measurement, the upper two levels (L1 and L2) had smaller measurements than the middle – (L3) and lower (L4 and L5) levels (Table 4.45). For the superior foraminal diameter, L4 and L5 differed from each other as well as the other three levels, where the lower levels had smaller diameters than the other three levels, and L5 had a smaller diameter than L4. For the middle – and inferior foraminal diameters, all levels differed from each other, except when comparing L1 and L2 to each other, where the diameters decrease as one moves caudally with each level (Table 4.46). These p-values of the foraminal height and the three foraminal diameters are summarised in Table 4.53.

Paired t-tests were used to compare the superior –, middle –, and inferior foraminal diameters to each other. The male and female measurements were pooled, since there were only two measurements where the sexes differed significantly. The tests indicated differences between the middle –, superior –, and inferior diameters for all levels, where the superior diameter was larger than the middle, and the middle larger than the inferior. The only exception was observed when comparing the diameters of L5, where the middle and inferior diameters were larger than the superior diameter (Table 4.54).

Table 4.53: Table indicating the p-values obtained from paired t-tests for comparing the vertebral levels to each other using the sagittal measurements

Variable	Comparison	p-value	Variable	Comparison	p-value
FH	L1 vs L2	0.000	MFD	L1 vs L5	0.000
	L1 vs L3	0.000		L2 vs L3	0.010
	L1 vs L4	0.000		L2 vs L4	0.000
	L1 vs L5	0.000		L2 vs L5	0.000
	L2 vs L3	0.004		L3 vs L4	0.010
	L2 vs L4	0.002		L3 vs L5	0.000
	L2 vs L5	0.020		L4 vs L5	0.000
SFD	L1 vs L4	0.003	IFD	L1 vs L3	0.000
	L1 vs L5	0.000		L1 vs L4	0.000
	L2 vs L4	0.002		L1 vs L5	0.000
	L2 vs L5	0.000		L2 vs L3	0.000
	L3 vs L4	0.010		L2 vs L4	0.000
	L3 vs L5	0.000		L2 vs L5	0.000
	L4 vs L5	0.000		L3 vs L4	0.010
MFD	L1 vs L3	0.002		L3 vs L5	0.000
	L1 vs L4	0.000		L4 vs L5	0.010

Key: vs = Versus; FH = Foraminal height; SFD = Superior foraminal diameter; MFD = Middle foraminal diameter; IFD = Inferior foraminal diameter

Table 4.54: Table indicating the p-values obtained for foraminal diameter comparisons

Comparison	VL	p-value	Comparison	VL	p-value	Comparison	VL	p-value
SFD vs MFD	L1	0.002	SFD vs IFD	L1	0.000	MFD vs IFD	L1	0.000
	L2	0.000		L2	0.000		L2	0.004
	L3	0.000		L3	0.000		L3	0.002
	L4	0.000		L4	0.000		L4	0.003
	L5	0.000		L5	0.000			

Key: VL = Vertebral level; vs = Versus; SFD = Superior foraminal diameter; MFD = Middle foraminal diameter; IFD = Inferior foraminal diameter

Coronal

Paired t-tests were used to compare the left – and right-sided measurements to each other. The results only showed differences at the root-to-disc measurements. The measurements taken at L1 indicated that left was larger than right for the middle measurement, and right larger than left for the lateral measurement (middle: p = 0.040; lateral: p = 0.010). The measurements taken at L5 showed that the right measurement was larger than the left for the medial – and lateral measurements (medial: p = 0.030; lateral: p = 0.040) (Table 4.47).

Paired t-tests were used to compare the vertebral levels to each other (Table 4.55). Left – and right root-to-disc measurements were tested separately. For root-to-disc measurements (Table 4.47), the medial measurements showed differences when comparing L1 and L2 to L4 on the left (with L1 and L2 extending more inferiorly than L4), and L1 to L2, L4, and L5 on the right (with L1 extending more inferiorly than the other three levels). For the middle measurements, L4 and L5 were significantly different on both the left – and right-hand sides, with L4 extending more inferiorly than L5 in both cases. For lateral measurements, the left – and right-hand sides had almost identical results, except at L1. For the left side, L4 extended more inferiorly than L1. For the left – and right-hand sides, L2 lay superior to L3, L4 and L5; and L4 lay inferior to L3.

Table 4.55: Table indicating the p-values from paired t-tests for comparing the vertebral levels to each other using coronal measurements from the root-to-disc distances

Variable	Side	Comparison	p-value	Variable	Side	Comparison	p-value
MedD	**Left**	**L1 vs L4**	0.020	**LatD**	**Left**	**L2 vs L3**	0.020
		L2 vs L4	0.020			**L2 vs L4**	0.000
	Right	**L1 vs L2**	0.055			**L2 vs L5**	0.030
		L1 vs L4	0.020			**L3 vs L4**	0.020
		L1 vs L5	0.030		**Right**	**L2 vs L3**	0.020
MidD	**Left**	**L4 vs L5**	0.010			**L2 vs L4**	0.001
	Right	**L4 vs L5**	0.050			**L2 vs L5**	0.040
LatD	**Left**	**L1 vs L5**	0.002			**L3 vs L4**	0.046

Key: vs = Versus; MedD = Medial root-to-disc distance; MidD = Midline root-to-disc distance; LatD = Lateral root-to-disc distance

Left – and right-hand root-to-pedicle values were pooled due to a lack of differences between the sides. The root-to-pedicle measurements (Table 4.48) showed differences at the medial measurements when comparing L1 to all other levels, and L2 to L3 and L4. In this instance, L1 and L2 were smaller than the other three levels. L1 was smaller than all other levels for the middle measurements as well. The lateral measurements showed between level differences when comparing L1 and L2 to L4 and L5, with the upper levels having larger measurements than the lower levels. P-values for the tests are summarised in Table 4.56.

Table 4.56: Table indicating the p-values from paired t-tests for comparing the vertebral levels to each other using the coronal measurements for the root-to-pedicle measurements

Variable	Comparison	p-value
MedP	**L1 vs L2**	0.010
	L1 vs L3	0.001
	L1 vs L4	0.000
	L1 vs L5	0.004
	L2 vs L3	0.001
	L2 vs L4	0.013
MidP	**L1 vs L2**	0.002
	L1 vs L3	0.010
	L1 vs L4	0.020
	L1 vs L5	0.003
LatP	**L1 vs L4**	0.020
	L1 vs L5	0.003
	L2 vs L4	0.010
	L2 vs L5	0.001
Key: vs = Versus; MedP = Medial root-to-pedicle distance; MidP = Midline root-to-pedicle distance; LatP = Lateral root-to-pedicle distance		

Transverse

Due to the small number of significant comparisons, no tables are provided in the transverse section of MRI comparative statistics. However, reference is made to the descriptive tables to support the few significant results observed.

Paired t-tests were used to compare the left – and right-sided measurements to each other. The results indicated no significant differences between left and right for the inferior measurements. Significant differences were found for the superior measurements, but only in two cases, namely: the distance between the root and the facet at L4 ($p = 0.030$) and the target angle of L2 ($p = 0.010$). In both instances the left measurement was larger than the right (Tables 4.49 and 4.51).

Paired t-tests were used to compare the superior – and inferior measurements and the vertebral levels to each other. The left – and right-hand sides were compared together, as there were only two instances where differences were found between the left – and right-hand sides. For the foraminal transverse AP diameter of L1 (Table 4.49), the superior measurement was larger than the inferior measurement ($p = 0.030$). For the distance between the root and the facet joint (Table 4.51), the inferior measurement was larger than the superior measurement for L3 to L5 ($p = 0.004$ – L3; $p = 0.010$ – L4; $p = 0.020$ – L5). The superior target angle was larger than the inferior angle at L4 ($p = 0.000$) (Table 4.52).

The inferior measurements showed between level differences when comparing the foraminal transverse AP diameters of L1 to L2 ($p = 0.040$), where L2 was larger than L1 (Table 4.49). L4 had a larger distance from the nerve root to the facet on the inferior level than L3 ($p = 0.030$) (Table 4.51). The target angles decreased when moving caudally with the vertebral levels for both the superior – and inferior levels (Table 4.52). This was seen when comparing: for the inferior measurements – L1 to L3 ($p = 0.010$); L3 to L4 and L5 ($p = 0.020$ and 0.002, respectively) and L4 to L5 ($p = 0.000$); for the superior measurements – L5 to L3 and L4 ($p = 0.008$ and 0.020, respectively).

4.3.3 Inter – and intra-observer analysis

The raw data for the inter – and intra-observer analysis for all the MRI measurements can be found in Appendices E.3 to E.5.

For foraminal measurements, the foraminal height and middle foraminal diameter proved to be the least repeatable. The inferior foraminal diameter had the greatest repeatability. When measuring the distance between the nerve root and the disc and the nerve root and the pedicle, it appeared that the nerve root-to-disc measurement was more repeatable than the nerve root-to-pedicle measurement. The weakest ICC values were seen for the interobserver analysis, especially

when considering the levels L2 to L4. The distance from the nerve root to the pedicle should be analysed with the most care due to the large amount of weak correlations seen for this measurement. Table 4.57 provides the ICC values for all the measurements tested.

Table 4.57: Interclass correlation coefficients calculated for the various measurements (variables) taken on the sagittal MRI scans

Variable	IAO	IEO	Variable	IAO	IEO
FHL1	0.89	0.59*	**IFDL1**	0.95	0.92
FHL2	0.62*	0.01**	**IFDL2**	0.88	0.85
FHL3	0.82	0.02**	**IFDL3**	0.93	0.73*
FHL4	0.94	0.81	**IFDL4**	0.86	0.67*
FHL5	0.94	0.95	**IFDL5**	0.94	0.92
SFDL1	0.81	0.50*	**RDL1**	0.99	0.44**
SFDL2	0.97	0.89	**RDL2**	0.96	0.90
SFDL3	0.62*	0.53*	**RDL3**	0.95	0.94
SFDL4	0.33**	0.24**	**RDL4**	0.99	0.85
SFDL5	0.92	0.85	**RDL5**	0.98	0.95
MFDL1	0.87	0.94	**RPL1**	0.39**	0.47**
MFDL2	0.97	0.53*	**RPL2**	0.59*	0.68*
MFDL3	0.94	0.40**	**RPL3**	0.85	0.37**
MFDL4	0.44**	0.36**	**RPL4**	0.97	0.30**
MFDL5	0.95	0.66*	**RPL5**	0.99	0.92

*Key: IAO = Intra-observer ICC results; IEO = Interobserver ICC results; FH = Foraminal height; SFD = Superior foraminal diameter; MFD = Middle foraminal diameter; IFD = Inferior foraminal diameter; RD = Root-to-disc distance; RP = Root-to-pedicle distance. Values with * are moderate, and with ** are weak*

The coronal measurements had greater repeatability as opposed to the sagittal measurements. The intra-observer ICC values were greater than the interobserver ICC values. For the root-to-disc measurements, the left-hand measurements seemed slightly less repeatable compared to the right-hand measurements. For the root-to-pedicle measurements, the right-hand measurements were less repeatable as opposed to the left-hand measurements. The medial and middle measurements showed lower ICC values than the lateral measurements for both the root-to-pedicle and root-to-disc measurements. Table 4.58 provides the ICC values for all the measurements tested.

Table 4.58: Table showing the interclass correlation coefficients calculated for the various measurements (variables) taken on the coronal MRI scans

Left			Right			Left			Right		
Variable	**IAO**	**IEO**	**Variable**	**IAO**	**IEO**	**Variable**	**IAO**	**IEO**	**Variable**	**IAO**	**IEO**
MedD L1	0.88	0.94	**MedD L1**	0.44*	0.94	**MedP L1**	0.84	0.80	**MedP L1**	0.16**	0.37**
MedD L2	0.76	0.44**	**MedD L2**	0.91	0.86	**MedP L2**	0.91	0.84	**MedP L2**	0.90	0.75
MedD L3	0.97	0.94	**MedD L3**	0.92	0.98	**MedP L3**	0.99	0.55*	**MedP L3**	0.98	0.55*
MedD L4	0.98	0.67*	**MedD L4**	0.79	0.82	**MedP L4**	0.97	0.68*	**MedP L4**	0.93	0.07**
MedD L5	0.84	0.96	**MedD L5**	0.90	0.76	**MedP L5**	0.98	0.75	**MedP L5**	0.99	0.87
MidD L1	0.90	0.96	**MidD L1**	0.97	0.97	**MidP L1**	0.90	0.69*	**MidP L1**	0.58*	0.91
MidD L2	0.99	0.88	**MidD L2**	0.98	0.69*	**MidP L2**	0.96	0.82	**MidP L2**	0.81	0.82
MidD L3	0.99	0.98	**MidD L3**	0.99	0.999	**MidP L3**	0.72*	0.71*	**MidP L3**	0.38**	0.70*
MidD L4	0.98	0.73*	**MidD L4**	0.99	0.98	**MidP L4**	0.57*	0.81	**MidP L4**	0.51*	0.44**
MidD L5	0.97	0.12**	**MidD L5**	0.98	0.88	**MidP L5**	0.47*	0.74*	**MidP L5**	0.19**	0.94
LatD L1	0.89	0.92	**LatD L1**	0.98	0.99	**LatP L1**	0.96	0.88	**LatP L1**	0.86	0.81
LatD L2	0.98	0.90	**LatD L2**	0.96	0.81	**LatP L2**	0.95	0.92	**LatP L2**	0.99	0.97
LatD L3	0.99	0.97	**LatD L3**	0.99	0.94	**LatP L3**	0.98	0.97	**LatP L3**	0.94	0.93
LatD L4	0.96	0.88	**LatD L4**	0.88	0.93	**LatP L4**	0.70*	0.25**	**LatP L4**	0.99	0.93
LatD L5	0.96	0.50*	**LatD L5**	0.97	0.93	**LatP L5**	0.96	0.52*	**LatP L5**	0.99	0.97

*Key: IAO = Intra-observer ICC results; IEO = Interobserver ICC results; MedD =Medial root-to-disc distance; MidD = Midline root-to-disc distance; LatD = Lateral root-to-disc distance; MedP = Medial root-to-pedicle distance; MidP = Midline root-to-pedicle distance; LatP = Lateral root-to-pedicle distance. Values with a * are moderate, and with ** are weak*

Levels L1 and L2 were not available on all but two of the transverse MRI scans. ICC tests could therefore not be performed for the measurements for these levels, since the sample size was too small. The transverse measurements showed greater repeatability for the superior measurements in comparison with the inferior measurements. The intra-observer teats showed better results than the interobserver tests. The target angle showed the greatest repeatability, and the root-to-disc distance, the least. Table 4.59 provides the ICC values for all the measurements tested.

Table 4.59: Table showing the interclass correlation coefficients calculated for the various measurements (variables) taken on the transverse MRI scans

Left			Right			Left			Right		
Variable	**IAO**	**IEO**	**Variable**	**IAO**	**IEO**	**Variable**	**IAO**	**IEO**	**Variable**	**IAO**	**IEO**
FDTS L3	0.82	0.79	**FDTS L3**	0.08**	0.73*	**FDTI L3**	0.72*	0.95	**FDTI L3**	0.73*	0.64*
FDTS L4	0.84	0.27**	**FDTS L4**	0.96	0.96	**FDTI L4**	0.97	0.86	**FDTI L4**	0.97	0.76
FDTS L5	0.86	0.69*	**FDTS L5**	0.83	0.28**	**FDTI L5**	0.85	0.001**	**FDTI L5**	0.85	0.17**
RDS L3	0.92	0.94	**RDS L3**	0.97	0.93	**RDI L3**	0.22**	0.75	**RDI L3**	0.96	0.997
RDS L4	0.91	0.82	**RDS L4**	0.97	0.98	**RDI L4**	0.98	0.98	**RDI L4**	0.97	0.34**
RDS L5	0.77	0.33**	**RDS L5**	0.64*	0.87	**RDI L5**	0.29**	0.91	**RDI L5**	0.92	0.34**
RFS L3	0.76	0.78	**RFS L3**	0.97	0.46**	**RFI L3**	0.80	0.53*	**RFI L3**	0.07**	0.85
RFS L4	0.99	0.89	**RFS L4**	0.99	0.89	**RFI L4**	0.39**	0.96	**RFI L4**	0.61*	0.98
RFS L5	0.69*	0.94	**RFS L5**	0.84	0.94	**RFI L5**	0.98	0.67*	**RFI L5**	0.85	0.09**
TAS L3	0.96	0.94	**TAS L3**	0.75	0.92	**TAI L3**	0.90	0.30**	**TAI L3**	0.88	0.99
TAS L4	0.92	0.92	**TAS L4**	0.99	0.95	**TAI L4**	0.97	0.83	**TAI L4**	0.99	0.83
TAS L5	0.96	0.91	**TAS L5**	0.98	0.94	**TAI L5**	0.86	0.97	**TAI L5**	0.90	0.62*

*Key: IAO = Intra-observer ICC results; IEO = Interobserver ICC results; S = Superior to the IVD; I = Inferior to the IVD; FDT = Foraminal transverse anteroposterior diameter. Values with * are moderate, and with ** are weak*

CHAPTER 5: DISCUSSION

The importance of population and sex specific trends and their effect on anatomical considerations prior to surgical procedures cannot be stressed enough. Material and morphometric properties of anatomical structures considered during surgical procedures vary across population groups and between males and females. Therefore, these possible differences should not be disregarded when preparing for interventional treatments such as orthopaedic surgery. Underestimating the variations in anatomy can lead to risk of structural injury and failed surgical outcome. Due to the large number of lumbar spine interventional procedures, the population and sex specific anatomical structures need to be classified and studied in order to prevent poor surgical outcome.

Limited information is available with regard to the differences in anatomy and material properties of the lumbar region of South African population groups (Chantler *et al.*, 2012, Conradie *et al.*, 2014). This study therefore aimed to investigate various morphometric and material properties of the South African lumbar spine using a variety of investigatory methods, namely cadaver dissection, Computed Tomography (CT) – and Magnetic Resonance Imaging (MRI) analysis.

5.1 Cadaver component

When approaching the intervertebral disc space arthroscopically, it is of the utmost importance to understand where critical structures lie in relation to the surgical region. This enables surgeons to avoid injury or damage to important structures, such as the dorsal nerve root and ganglion when performing arthroscopic surgery. The dissection of cadaver material provides a unique environment which enables researchers to explore the relevant anatomical parameters with precision. The use of imaging techniques also provides a view of the structures, however anatomical dissection allows a more tactile approach, and this allows the adjustment of structures which might obscure the view of those under investigation. Anatomical dissection therefore provides an unobscured view of the structures, without the concern of monitoring vital signs or having to retain irrelevant structures (in context of the specific study and study objectives) which, if removed or destroyed, could result in disabling, harming, or endangering a patient's life as would be the case in a surgical setting.

The current study comprised of only cadavers from the white South African population. Therefore, comparisons between population groups could not be performed. However, limited differences were observed between the sexes, where only two instances of significant difference were observed. These differences were seen at the dura mater length (vertical border) measurement for L2 on the right-hand side, where the female group had smaller measurements than the male group (Tables 4.1 and 4.5), and the ganglion position of L4 (Table 4.6). The lack of significant sex differences could be due to the closely related age groups of the males and females and both sexes being from of the same population group.

Most of the ganglia were positioned in the midline (Position B) of the caudal pedicle. This seems to be in contrast to a study done by Silverstein *et al.* (2015), who found the ganglion to lie more laterally for levels L1 through to L5. Left and right, measurements were not extensively variable. The only two levels where variations were seen were at L1 (ganglion position) (Table 4.8) and L4 (diagonal measurement) (Table 4.7). Here the left ganglion was positioned closer to the midline and the right closer to the spinal cord. Furthermore, the left diagonal measurement was smaller than the right at L4. This discrepancy seen at L4 for both the sex- and side comparisons, emphasises its importance in morphological and morphometric studies, as it seems to be the position where most significant differences are encountered between sides and sexes (Hulme *et al.*, 2007). Studies have found symmetry to be dependent on surrounding soft tissue structure and morphology, and the asymmetry of the measurements could be owed to posture and atrophy/hypertrophy of surrounding structures (Hamanishi and Tanaka, 1993, Silverstein *et al.*, 2015).

Table 5.1 compares the results of the current study (males and females pooled) to those from Brazil and Thailand. The South African population groups exhibited results which are similar to those of the Thai population for the vertical measurements and the Brazilian population for the lower level vertical measurements (L1 and L2). Also, similar results were observed for the diagonal measurements in the South African, Brazilian, and Thai population groups.

Table 5.1: Mean and standard deviations of Kambin's triangle measurements for different population groups

Author(s)	Population	DML (vertical) L				DML (vertical) R			
		L1	**L2**	**L3**	**L4**	**L1**	**L2**	**L3**	**L4**
Current study	South African	16.3 ± 2.3	16.9 ± 1.7	16.6 ± 1.5	16.5 ± 1.8	15.7 ± 1.9	16.4 ± 1.7	16.3 ± 2.1	16.3 ± 1.6
a	Brazilian	N/A	N/A	14	17.52	N/A	N/A	16.55	16.4
b	Thai	17.0 ± 5.0	17.2 ± 3.8	18.7 ± 6.0	20.6 ± 3.4	15.2 ± 4.4	15.6 ± 3.8	18.4 ± 5.0	19.8 ± 5.0
		DDMN (horizontal/base) L				**DDMN (horizontal/base) R**			
		L1	**L2**	**L3**	**L4**	**L1**	**L2**	**L3**	**L4**
Current study	South African	14.8 ± 4.0	15.6 ± 2.0	15.7 ± 2.0	17.1 ± 2.2	15.7 ± 2.5	15.3 ± 2.4	15.7 ± 2.0	17.1 ± 2.7
a	Brazilian	N/A	N/A	14.25	14.55	N/A	N/A	13.75	14.17
b	Thai	11.8 ± 2.7	12.1 ± 3.0	13.6 ± 2.0	14.7 ± 2.0	13.1 ± 2.6	12.0 ± 1.8	11.3 ± 1.6	15.6 ± 2.3
		SNL (diagonal) L				**SNL (diagonal) R**			
		L1	**L2**	**L3**	**L4**	**L1**	**L2**	**L3**	**L4**
Current study	South African	21.0 ± 2.1	21.4 ± 1.8	20.4 ± 1.8	22.0 ± 2.7	22.0 ± 2.7	22.0 ± 1.4	21.4 ± 2.2	23.3 ± 2.7
a	Brazilian	N/A	N/A	18.98	23.03	N/A	N/A	21.53	21.72
b	Thai	20.4 ± 4.6	21.4 ± 4.6	23.9 ± 6.2	25.5 ± 3.0	20.1 ± 5.2	19.4 ± 4.2	21.9 ± 4.3	24.9 ± 5.6

Key: L = Left side; R = Right side; DML = Dura mater length (vertical border); DDMN = Distance from dura mater to nerve (horizontal border); SNL = Spinal nerve length (diagonal border); N/A = Not applicable because the values were not recorded in the relevant study; a (Vialle *et al.*, 2015); b - (Lertudomphonwanit *et al.*, 2016)

5.2 CT component

Even though imaging techniques might provide a less tactile approach and a slightly obscured view of the anatomical structures in question, it does have the advantage of providing an observation of the structures in situ. Also, researchers are able to position patients in certain ways which might be relevant to their study. This is especially a more realistic option for studies investigating the position and movement of structures in various postures, as trying to orientate a specimen (especially a formalin-fixed specimen), could prove a greater challenge than asking a patient to stand, sit, lie, or move in a certain manner. The other advantage is that imaging allows researchers to view structures which may be very difficult to reach or may be fragile and prone to damage during dissection procedures. Therefore, the current study used imaging techniques to view certain deep and delicate structures in situ.

CT imaging provides a unique view of the skeletal structures and their internal osteological make-up. It enables a more detailed view of the material properties of bone, and a better in situ approach to the morphometric parameters of the individual bony structures. This is especially important for surgical procedures, as the structural material and morphometric properties could determine the prognosis of a specific individual, especially if the parameters in question are specific to and dependant on various population groups.

5.2.1 Lumbar lordosis angle (LLA)

Lumbar lordosis angle (LLA) values found in this study (Table 4.9) were compared to those of other population groups. The LLA of the white South Africans proved to be more similar to other Middle Eastern, Asian, and European populations, while black South Africans had lower LLA values (Cheng *et al.*, 1998, Vialle *et al.*, 2005, Pinel-Giroux *et al.*, 2006, Been *et al.*, 2010b, Bae *et al.*, 2012, Endo *et al.*, 2012, Bredow *et al.*, 2015, Salem *et al.*, 2015, Le Huec and Hasegawa, 2016). The majority of the samples from other studies did not include individuals of African descent. Other studies with values similar to those of the black South African group exist, however these included samples from older age groups. This indicates that black South Africans seem to have LLA values which are more similar to the older individuals of other population groups (Bergenudd *et al.*, 1989 , Hultman *et al.*, 1991, Waddell *et al.*, 1992, Youdas *et al.*, 1996, Norton *et al.*, 2002). The lower LLA found in the black population group shows that distinct differences exist between black and white population groups. Some studies agree with this assumption that a difference exists between the LLA of black and white population groups; however, they concluded that black individuals have larger LLAs than white individuals (Patrick, 1976, Hanson *et al.*, 1998, Lonner *et al.*, 2010). Conversely, other authors have concluded that no difference exists in the LLA between black and white population groups (Mosner *et al.*, 1989, Goldberg and Chiarello, 2001). These studies have all been conducted on other population groups, and therefore it can be assumed, with caution, that the South African population exhibits unique population trends.

Lumbar lordosis has been shown to affect vertebral body shape (Cheng *et al.*, 1998, Been and Kalichman, 2014). A study done by Cheng *et al.* (1998) found that the LLA had a significant positive correlation with the morphology of the lumbar vertebral body heights in both males and females, especially at the lower vertebral levels. Another study done by Wren *et al.* (2017) found that the LLA has an indirectly proportional relationship to vertebral body cross-sectional area in

female subjects. This means that the AP and lateral vertebral diameters decrease as LLA increases. Similar results were seen in the white male population group of this study, where the maximum and minimum AP diameters of L5 decreased in a quadratic relationship as the LLA increased (Table 4.19).

Even though no correlations were observed between the vertebral heights and LLA, it is important to understand that the LLA itself is created as a result of the changes in the ratio's or differences between the anterior- and posterior vertebral body heights as one moves caudally in the lumbar spine. The lumbar lordosis angle is created by the wedging of the vertebral bodies, meaning that a wedge-like shape is created as a result of the height of one border being greater or smaller than that of the opposite border. This wedging can either be posterior/dorsal (anterior height greater than posterior) or anterior/ventral (posterior height greater than anterior) (Been *et al.*, 2010a). The anterior wedging (greater posterior height) seen for the upper levels (L1 and L2) in the current study (Tables 4.18 and 4.28) was expected due to the transition between the more overall anterior thoracic curvature (kyphosis) and the more overall posterior lumbar curvature (lordosis). L3 is considered to be the pivot point or midpoint in the curvature for the lumbar spine, meaning that the lack of difference between its anterior and posterior vertebral body heights seen in the current study was also expected, as it is the point of transition between the anterior wedging of the upper levels, and the posterior wedging of the lower levels (Table 4.18 and 4.28). As a result of the pelvic tilt and incidence occurring at the sacral spine, L4 and L5 need to have a more posterior wedging in order to compensate for this transition in curvature (Chaleat-Valayer *et al.*, 2011). Therefore, the lack of correlation between the heights and LLA can further be explained by the fact that the total angle of the curvature is not dependant on the magnitude(s) of the vertebral body height(s). The nature of the angle is rather a result of the ratio between the anterior- and posterior vertebral heights, and the relationships between the vertebral heights of the upper, middle, and lower levels. It is important to take into account that soft tissue also influences the change in angle, and therefore, the skeletal measurements should be used in conjunction with soft tissue measurements in order to thoroughly interpret the LLA (Been *et al.*, 2010a). The trend of a larger posterior height for the upper levels, and larger anterior height for lower levels is also seen in other populations (O'Neill *et al.*, 1994, Tan *et al.*, 2004, Gocmen-Mas *et al.*, 2010, Ablyazov, 2012, Atta-Alla *et al.*, 2014), however the exact values of the heights themselves have been proven to vary between sexes and population groups (Ross *et al.*, 1991, O'Neill *et al.*, 1994).

Due to the relevance of the LLA in the clinical setting, the repeatability and reproducibility of the measurements are important. The observer analyses used to test for the repeatability and reproducibility of the measurements indicated excellent correlations for both inter- and intra-observers (Table 4.41). Therefore, this shows high repeatability of the Cobb method used in the current study.

5.2.2 Bone mineral density (BMD)

Bone mineral density (BMD) is important to consider during orthopaedic procedures and is known to be population specific (Schnitzler *et al.*, 1990, McCormick *et al.*, 1991, Russell-Aulet *et al.*, 1991, Patel *et al.*, 1992, Cundy *et al.*, 1995, Bhudhikanok *et al.*, 1996). BMD is also important when considering the strength and structural integrity of any bone. Fracture risk has been speculated to be associated with bone structural integrity. The general conclusion by most authors is that higher bone density results in stronger bone structure and greater bone integrity (Arlot *et al.*, 2008, Fields *et al.*, 2009, Putman *et al.*, 2013, Leslie, 2012).

In the current study, the largest differences between sexes and population groups, especially in the cortical measurements, were observed at L1, L4 and L5 (Tables 4.6, 4.7 and 4.21). This could be a result of the position of these individual vertebrae, as they are known as transitional levels. Transitional vertebrae are areas where morphological changes occur between the thoracic and lumbar; and lumbar and sacral vertebrae (Mahato, 2013).

For the cortical bone mineral density of the entire spine, lower SEP (superior endplate) densities were observed compared to IEP (inferior endplate) (Tables 4.6, 4.7, and 4.22). This was especially evident in the lower vertebral levels. The lower densities in the SEP are likely a result of the load-bearing function of the spine and the axial distribution of that load inferiorly. This would result in higher loads being distributed not only to the lower vertebrae, but to the inferior endplates of each vertebral body, owing to denser material properties of these regions for higher load-bearing capacities (Briggs *et al.*, 2004, Stemper *et al.*, 2018). Other authors have found similar results where the SEP was less dense than the IEP (Nepper-Rasmussen and Mosekilde, 1989, Flynn and Cody, 1993, Silva and Gibson, 1997, Banse *et al.*, 2001, Briggs *et al.*, 2004, Hulme *et al.*, 2007, Jackman *et al.*, 2016). Also, higher densities were observed at the PB (posterior vertebral body border) (Tables 4.6, 4.7 and 4.22), which is possibly due to the attachment of the posterior elements onto the PB. This means that it would require more dense bone to support the posterior bony

elements as opposed to the AB (anterior vertebral body border) which has no bony attachments or projections. These results are also in agreement with studies performed by previous authors (Nepper-Rasmussen and Mosekilde, 1989, Silva and Gibson, 1997, Banse *et al.*, 2001, Hulme *et al.*, 2007).

The location of each of the three medullary ROI's (regions of interest) are key to understanding their BMD trends. As a result of the higher density of cortical bone in comparison to medullary bone, the two regions which border the cortical bone (ROI1 and ROI3), will be denser than the middle region (ROI2), which is not in close proximity to the denser, cortical bone. ROI3 is denser than ROI1, as it borders the IEP which has a higher BMD than the SEP (bordering ROI1) (Table 4.12). The lower vertebral levels proved to be denser than the upper (Tables 4.12 and 4.25), which correlates with the cortical endplate measurements which also showed greater densities at the upper levels. This means that, similar to the cortical endplate BMD, the load distribution is responsible for the change in medullary BMD per level (Briggs *et al.*, 2004, Stemper *et al.*, 2018).

In the black population group, males exhibited greater BMD values than females in all medullary and endplate measurements, as well as greater lower level cortical measurements (Tables 4.10 to 4.12, and 4.20). This is an expected result, as the same trend has been reported by other studies (Nieves *et al.*, 2005, Looker *et al.*, 2009). In contrast, minimal differences between the sexes were observed in the white group (Tables 4.10 to 4.12, and 4.20). However, when differences were apparent, females proved to have higher cortical BMD than males for certain measurements (especially at the anterior border of the vertebral body) (Table 4.11). A possible reason could be due to distinct sexual dimorphism between the two population groups. Overall, white population groups show less sexual-dimorphism in the post-crania than black population groups (Krüger, 2015). However, this is an assumption which will require further investigation in order to resolve or explain the inconsistency with other research.

Even though population differences were more prominent between the male groups, black South Africans had greater bone mineral densities than white South Africans in both sexes for the majority of both cortical and medullary measurements (Tables 4.10 to 4.12, and 4.20). Similar results were reported by Gilsanz *et al.* (1991), Seeman (1997), Hochberg (2007), Cauley (2011) and Zengin *et al.* (2016). This could be due to possible differences in lifestyle, skeletal size, genetic factors, body size and composition and diet between population groups, leading to differences in BMD values and subsequently, variation in bone strength and integrity (Fehily, 1989, Gilsanz *et*

al., 1991, Seeman, 1997, Hill *et al.*, 2008, Leslie, 2012). However, since these factors were not known for the current study, further research needs to be done in order to investigate their role(s).

The significantly higher BMD values found in the black males compared to the three other groups, suggests that they have stronger, more structurally stable bone structure. This is in agreement with studies investigating fracture risk in relation to BMD (Schnitzler *et al.*, 1990, Seeman, 1997, Leslie, 2012), as well as those looking at the variation in BMD between specific population groups (Schnitzler *et al.*, 1990, McCormick *et al.*, 1991, Russell-Aulet *et al.*, 1991, Patel *et al.*, 1992, Cundy *et al.*, 1995, Bhudhikanok *et al.*, 1996). The prevalence of vertebral fractures in the black male population is much lower than the other groups, and this correlates with the higher BMD seen in their vertebral bodies (Schnitzler *et al.*, 1990, Hochberg, 2007). Another study has found similar results when comparing black and white female population groups (Putman *et al.*, 2013).

Research has shown that body mass index (BMI) plays a role in BMD values, specifically when looking at different types of body masses (Morin and Leslie, 2009, Laria *et al.*, 2015, Zhu *et al.*, 2017). It was found that an increased BMI due to increased fat body mass, leads to decreased BMD, however an increased BMI due to lean body mass, resulted in higher BMD values. The BMI values of patients could not be calculated for this study, as the necessary data could not be obtained. This could be incorporated into future studies and might explain some of the discrepancies found within the results.

Age correlations indicated that BMD and age have an inverse relationship (Table 4.21). The BMD of the patients seem to decrease with age, especially in the medullary bone of the female population. The medullary bone is also much more susceptible to age and this is possibly due to its lowered BMD value in relation to the cortical bone. Previous authors have shown that the BMD of the lumbar spine is highly susceptible to degenerative changes (Haderslev *et al.*, 2000, Orstavik *et al.*, 2003, Muraki *et al.*, 2004). This means that the medullary bone would degenerate faster than the cortical bone with age. The reason for the higher incidence of vertebral fractures in the female population is most likely due to the decreased levels in oestrogen after menopause, which has been shown to have a direct effect on bone health (Kanis, 1994, Kanis *et al.*, 1994, Melton *et al.*, 2003, Torstveit and Sundgot-Borgen, 2005, Chain *et al.*, 2017). The white population group seems to be more prone to declining BMD values with age, than the black population, and this can possibly be

an effect of the previously mentioned differences in lifestyle and genetic make-up of the two groups (Fehily, 1989, Gilsanz *et al.*, 1991, Seeman, 1997, Hill *et al.*, 2008, Leslie, 2012).

The observer analyses indicated mostly good to excellent repeatability and reproducibility for the medullary BMD, with only four measurements of the interobserver analysis showing average results (Table 4.41). The strongest correlations were seen at ROI2. This could be a result of the discrepancies of determining the exact locations of ROI1 and ROI3, as the software used was not able to correlate the more precise locations on the sagittal scans onto the transverse slices. The authors therefore had to create certain landmarks and parameters to determine the level of the disc and subsequently the levels of ROI1 and ROI3. These parameters can be subject to observer interpretation. The cortical BMD measurements indicated more discrepancies (more instances of low and average ICC values) compared to the medullary BMD measurements. The majority of these occurring at the endplates and at the anterior border. This can easily be explained by the fact that the software uses a straight line in order to determine the average BMD. However, the endplates and the anterior border are not entirely straight but do exhibit a slight concavity.

5.2.3 Morphometrics

The morphometrics of the spine is important when taking into account the anatomical features that need to be considered during reconstructive techniques. The morphometric analysis of the lumbar spine in the current study produced similar results to previous research, however some unique trends were observed.

Most of the posterior elements seemed to increase in size as one moves caudally with each vertebral level for all individuals. Similar results were observed in population groups from Singapore (Tan *et al.*, 2004), Egypt (Mohamed *et al.*, 2010), and America (Yu *et al.*, 2015). However, the pedicle height decreased per level, and the spinous process length increases from L1 to L3 and then suddenly decreased from L3 to L5. This pattern has also been recorded in other studies (Zindrick *et al.*, 1987, Olsewski *et al.*, 1990, Hou *et al.*, 1993, Kadioglu *et al.*, 2003, Lien *et al.*, 2007, Chanplakorn *et al.*, 2011, Atta-Alla *et al.*, 2014, Gulec *et al.*, 2017). In contrast, many researchers have also observed that the pedicle height either increases or stays uniform when moving caudally in the spine (Amonoo-Kuofi, 1995, Tan *et al.*, 2004, Christodoulou *et al.*, 2005, Sugisaki *et al.*, 2009). Although discrepancies exist for the pedicle height, the pedicle lateral diameter trends seem to prove uniform throughout the studies. This could possibly be indicative

of population specific differences. The gradual incline and subsequent decline in spinous process length is also seen in other studies and could possibly be a result of the LLA and the level of muscle strength in the lumbar region specific to each population group (Ihm *et al.*, 2013, Sun *et al.*, 2014, Shaw *et al.*, 2015).

The increase in size of the spinal canal lateral diameter is related, and proportional to the increase in vertebral body lateral diameter, which has also been seen in other studies (Weisz and Lee, 1983, Amonoo-Kuofi, 1995, Tan *et al.*, 2004, El-Rakhawy *et al.*, 2010). The spinal canal AP diameter of the two male groups decreased in size up until L3 and then gradually increased in size until L5. This trend varied between population groups from previous research, where Hinck *et al.* (1966), Eisenstein (1977), and Tan *et al.* (2004) observed similar patterns to this study, while El-Rakhawy *et al.* (2010) observed a slight increase from L1 to L2, with a subsequent decrease from L2 to L3, followed by another increase from L3 to L5. Again, this is a strong indication of population variation.

Contrary to the sagittal vertebral body measurements, the transverse measurements increased when moving caudally with each level (vertebral lateral and AP diameter). This is a common trend seen across population groups and study samples (Tan *et al.*, 2004, Gocmen-Mas *et al.*, 2010, Wang *et al.*, 2012, Atta-Alla *et al.*, 2014, Azu *et al.*, 2016). L5 exhibited the lowest vertebral body height at its posterior border compared to all other height measurements (anterior and posterior). This phenomenon is reported in other studies, and is very likely the result of the articulation between L5 and the first sacral vertebra (S1), where L5 forms the point of transition between the lumbar and the sacral spine, and needs to match the morphometrics of S1 in order to produce a functional articulation (Zhou *et al.*, 2000, Masharawi *et al.*, 2008)

The male groups displayed larger values than the female groups in both populations for almost all measurements, except for the spinal canal AP diameters in the white group. Many other studies have found that male individuals have larger vertebral morphometrics than females (Olsewski *et al.*, 1990, Hou *et al.*, 1993, Kim *et al.*, 1994, Lotfinia *et al.*, 2010, Alam *et al.*, 2014, Shaw *et al.*, 2015, Yu *et al.*, 2015, Gulec *et al.*, 2017). This is a result of the larger build, greater height and more defined musculature seen in males. Previous authors have found population differences to exist between groups for various spine measurements (Lee *et al.*, 1995, Tan *et al.*, 2004, Shaw *et al.*, 2015), and it was therefore expected that differences would exist between groups in the current study. However, what makes this study unique is the fact that there are measurements in the white

population where females had greater values than males, something which is not seen in other studies. Again, this could be due to the smaller degree of sexual dimorphism in white South African population groups compared to black South African population groups (Krüger, 2015). Similar to the current study, previous comparisons between black and white population groups, exhibited larger measurements in white population groups (Eisenstein, 1977, Shaw *et al.*, 2015). Vertebral body size has been shown to influence biomechanical properties of the lumbar spine, where smaller body size results in higher fracture risk due to an increase in mechanical stress in smaller cross-sectional areas (Gilsanz *et al.*, 1994).

Only the white population group exhibited some correlations between morphometrics and age. The majority of these were for the female group and appeared in the middle and upper levels for the posterior elements, and in the lowest level for the vertebral body measurements. The posterior element size decreased with age for females but increased in males. The vertebral body dimensions showed an overall increase with age for both males and females. Few studies have investigated the morphometric changes occurring with age.

The observer analyses indicated that the posterior element, and spinal canal measurements were more prone to vary between observers, than the vertebral body measurements. The measurements pertaining to the pedicles and the spinal canal were the weakest since the observers possibly had slightly different interpretations of the furthest limits of these structures. The anterior vertebral body height was the weakest of the vertebral body measurements. This could be due to the high incidence of lipping occurring at the anterior portions of the superior and inferior endplates of the vertebral bodies.

5.3 MRI component

MRI (Magnetic Resonance Imaging) is a very effective way of investigating soft-tissue structures on a living or deceased subject. It is therefore an ideal, non-invasive way to determine the position of the dorsal nerve root and neural foramen parameters of the human lumbar spine. This is important, as a background knowledge of the location of the dorsal root and its relations to other structures, will aid in the surgical process and planning in order to avoid damage to this essential structure. It is also essential in the management of lumbar spine stenosis.

Due to the limited sample, only black individuals were investigated, and in some cases analysis of sex differences could not be performed due to the small number of female individuals. The

scans were also not all complete, and full analyses of all sections could not be performed for some individuals. It was also difficult to view skeletal landmarks on some of the MRI images, as the imaging technique mainly focuses on soft-tissue visualisation.

5.3.1 Foramen measurements

The results from the current study showed that the height of the neural foramen increased when moving caudally in the spine (Table 4.45 and 4.53), a finding which could be population specific as discrepancies exist between studies. Some studies show results which align with the current study (Al-Hadidi *et al.*, 2003, Kaneko *et al.*, 2012, Silverstein *et al.*, 2015), whereas others found the foraminal height to decrease when moving caudally (Hurday *et al.*, 2017). Another supporting factor of population variation, is that the foraminal heights measured in the current study mostly lie within the upper ranges of those produced by previous authors (Cinotti *et al.*, 2002, Al-Hadidi *et al.*, 2003, Rao *et al.*, 2015, Hurday *et al.*, 2017), meaning that the average lumbar neural foramen height of the South African population does not correspond with that of other groups. An inverse relationship in terms of change in measurement per level is seen with the foraminal diameters measured sagittally (especially when looking at the superior measurements) (Tables 4.46 and 4.53), where a decrease in magnitude is observed when moving caudally in the spine. As with the foraminal height, a disagreement exists between studies, with some observing a decrease in diameter caudally (Hurday *et al.*, 2017), while others observe an increase (Torun *et al.*, 2006, Arslan *et al.*, 2012). The three different diameters of each foramen (superior, middle, and inferior) differ between themselves. A clear decline in size is seen when moving caudally within the foramen itself on almost all levels, creating a typically inverted teardrop shape of the foramen, with the upper diameters being greater than the lower. This trend is also evident in other studies (van Roy *et al.*, 2001, Hurday *et al.*, 2017).

Previous authors have found that the transverse foraminal measurements taken at the superior border of the intervertebral disc, are greater than those taken at the inferior border or margin of the disc (Cinotti *et al.*, 2002, Hurday *et al.*, 2017). This is in agreement with the current study which indicated larger transverse AP diameter and target angle measurements superiorly (Tables 4.49 and 4.51). Furthermore, the current study as well as other studies (Cinotti *et al.*, 2002, Torun *et al.*, 2006, Arslan *et al.*, 2012, Rao *et al.*, 2015) found that the foraminal transverse AP diameter increases as one moves caudally with the spine, while the opposite is seen in the target angle

measurements (Hurday *et al.*, 2017). Thus, it would appear that there are many variations in the foramen measurements. This variation is not clear but could be a result of population variation or due to alterations with age, however further investigation will be needed in future research.

Due to the importance of the morphometry of the neural foramen, it is essential to maintain repeatability and reproducibility of the measurements taken. The intra-observer repeatability was greater than the interobserver repeatability (Tables 4.57 and 4.59). This is likely due to the difficult methods and the difficulty observing certain skeletal landmarks. The intra-observer had likely established a more accurate measurement technique through repetition of the various measurements during the initial data collection. The interobserver did not have this opportunity, as the number of samples used during the observer analysis was limited.

5.3.2 Nerve root measurements

Most of the nerve root to the pedicle or disc distances measured on the sagittal scans increase as one moves more caudally in the spine (Tables 4.45 and 4.54), especially when comparing the upper (L1 and L2) levels to the lower levels (L4 and L5), and is a common feature in other morphometric studies of the lumbar nerve root (Hasegawa *et al.*, 1996, Gu *et al.*, 1999, Söyüncü *et al.*, 2005, Lien *et al.*, 2007, Arslan *et al.*, 2012, Silav *et al.*, 2016, Hurday *et al.*, 2017). This means that the nerve root lies above the disc when considering the cranial levels, and gradually moves inferior to the disc as one moves caudally in the spine.

The coronal analyses showed that for the medial measurements from the nerve root to the disc and nerve root to pedicle, the nerve root was situated more superiorly in the lower lumbar levels compared to the higher levels (Tables 4.47, 4.48, 4.55 and 4.56). A similar trend has been recorded by other studies (Hasegawa *et al.*, 1996, Jaskwhich *et al.*, 1996, Guvencer *et al.*, 2008, Arslan *et al.*, 2011, Arslan *et al.*, 2012, Gkasdaris *et al.*, 2016, Hurday *et al.*, 2017). This relationship becomes smaller when looking at the midline of the pedicle, where the only difference in distance is seen between L4 and L5 (with the lower level still having a larger distance between the root and the pedicle and/or disc). When moving laterally, an inverse trend is seen, in that the upper levels now show larger distances between the nerve root and pedicle and/or disc than the lower levels. This trend was also observed by other authors (Hamanishi and Tanaka, 1993, Arslan *et al.*, 2012, Gkasdaris *et al.*, 2016, Hurday *et al.*, 2017). As a result of the relatively even inferior angulation of the dorsal nerve root across vertebral levels (Arslan *et al.*, 2011), this appearance makes sense,

as a nerve originating from the dura mater at a more superior position (having a larger measurement above the disc – being further away from the disc), would still remain more superior after crossing the intervertebral disc (having a smaller measurement below the disc – being closer to the disc). When looking at the transverse images, the nerve roots lie more anteriorly at the superior border of the disc, and more posteriorly at the inferior border of the disc (Table 4.51), and is a common trend found in morphometric studies (Spencer *et al.*, 1983, Hurday *et al.*, 2017).

Due to the importance of the location of the spinal nerve within the neural foramen and its relation to the intervertebral disc, it is essential to maintain repeatability and reproducibility of the measurements taken. The intra-observer repeatability was greater than the interobserver repeatability. The coronal measurements seemed to have the best repeatability due to the ease of measurement technique. The intra-observer had likely established a more accurate measurement technique through repetition of the various measurements during the initial data collection. The interobserver did not have this opportunity, as the number of samples used during the observer analysis was limited.

CHAPTER 6: CONCLUSION

In summary, the cadaver analysis showed very little variation between the males and females and between left- and right-hand measurements. However, when variation was present, the most discrepancies between sexes and sides are seen at L4. The ganglia were mostly positioned at the midline of the caudal pedicle for almost all levels. The dimensions of Kambin's triangle in the South African population, were similar to those of other populations.

The CT (Computed Tomography) analysis showed that the lordosis angles (LLAs) of white South Africans are similar to those of other population groups (Cheng *et al.*, 1998, Vialle *et al.*, 2005, Pinel-Giroux *et al.*, 2006, Been *et al.*, 2010b, Bae *et al.*, 2012, Endo *et al.*, 2012, Bredow *et al.*, 2015, Salem *et al.*, 2015, Le Huec and Hasegawa, 2016). The analysis also indicated that black South Africans exhibited lower angles when compared to these same groups, however further investigation showed that the black individuals' LLAs were similar to those of the older individuals from the other population groups. This is a possible indication of population group variation, which is an assumption that is highly debated, as it is supported and observed by some studies (Patrick, 1976, Hanson *et al.*, 1998, Lonner *et al.*, 2010), but not by others (Mosner *et al.*, 1989, Goldberg and Chiarello, 2001). These discrepancies between studies should be further investigated in order to determine whether there are external factors which were not accounted for. Correlations were not seen for vertebral height and LLA, but it is important to understand how the relationships between the anterior- and posterior heights and between the heights of the individual levels, affect the nature of the curvature (Been *et al.*, 2010a, Chaleat-Valayer *et al.*, 2011). Even more importantly, the role of soft tissue should not be disregarded when investigating LLA (Been *et al.*, 2010a). The vertebral body diameters all showed varying degrees of decline in magnitude with an increase in LLA.

The BMD (Bone mineral density) analysis showed a clear difference between the cortical measurements, where the SEP (superior endplate) was denser than the IEP (inferior endplate), and the PB (posterior vertebral bodu border) denser than the AB (anterior vertebral body border). Possible explanations for this is due to the distribution of load within the spine, as well as the attachment of other elements onto the vertebral body. The medullary bone indicated greater densities in regions closer to cortical bone. Also, the more dense the adjacent cortical bone, the higher the density of the medullary region. Both the cortical and medullary BMD increased when

moving caudally in the spine. Males generally exhibited larger densities than females. The exceptions were in the white group only, where females had greater densities than males for some measurements. This was unexpected, and requires further investigation, however sexual-dimorphism is suspected to play a role (Krüger, 2015), especially as it is lower in white population groups.

The morphometric analysis performed on the CT scans showed an increase in size in most of the posterior elements when moving caudally in the spine. The exceptions being at the pedicle heights and spinous process lengths. The lateral diameter of the spinal canal also increased when moving caudally, however the AP diameter decrease in size up until L3 and then gradually increased in size until L5. The sagittal dimensions of the vertebral body (vertebral heights) showed a decrease when moving caudally, however the transverse diameters (AP and lateral) showed an increase when moving caudally. The males had larger measurements as opposed to females for almost all measurements, except at the AP diameter of the spinal canal in the white population group. This could again be a possible result of differences between sexual dimorphism between the two population groups (Krüger, 2015).

Discrepancies exist between studies for various neural foramen parameters investigated using the MRI (Magnetic Resonance Imaging) scans. The current study showed an increase in height for the neural foramen when moving caudally, however there are differences between results from various studies (Al-Hadidi *et al.*, 2003, Kaneko *et al.*, 2012, Silverstein *et al.*, 2015, Hurday *et al.*, 2017). The sagittal diameter of the neural foramen showed a decrease when moving caudally in the spine, and as with the height of the foramen, differences are seen between studies (Torun *et al.*, 2006, Arslan *et al.*, 2012, Hurday *et al.*, 2017). Measurements taken at the superior border of the intervertebral disc were larger than those at the inferior border of the disc. The large discrepancies between studies should be investigated further, as no clear conclusions could be made as to why the studies are not in agreement. The sagittal MRI images indicated that, within the neural foramen, the nerve root was positioned more cranially at the upper levels (L1 and L2), then gradually crosses the disc to lie more caudally at the lower levels (L4 and L5). The coronal images showed that the nerve itself originates more cranially for the lower levels, even though it is positioned more caudally in the foramen itself, when considering the sagittal image. The nerve roots also move from anterior to posterior, as seen on the transverse image.

When considering all three components of the study, a number of different trends can be observed. These trends are possibly due to differences between population groups and might warrant further investigation in order to determine whether the differences are related to population variation, and if so, to what extent.

Future research into all three parts of the study (cadaver, CT, and MRI) should focus on why certain differences exist between population groups, by focusing on lifestyle factors and genetic make-up of the samples from the different population groups. Including larger samples of individuals from various population groups, across more diverse ages, and relatively equal number of males and females, will benefit future research into the differences between groups. Patient history should also be considered in order to eliminate any individuals with underlying pathology affecting the parameters under investigation, which might skew the results. For the cadaver component, an approach should be established which would allow easy access to L5, as Kambin's triangle was inaccessible in the current study. For the LLA studied in the CT component, parameters of the soft tissue elements should be incorporated into future research in order to account for its effects, if any, on the angle. The accuracy of the Cobb method should also be investigated. Looking at the incidence of additional vertebrae can also prove useful for future research in lumbar lordosis angle measurements.

CHAPTER 7: LIMITATIONS

7.1 Cadaver component

This study was limited by the small sample size of cadaveric specimens and by the lack of demographic versatility. Comparisons between population groups could not be performed as a result of the sample comprising of only one population group. Therefore, only partial conclusions could be made for only one population group (white individuals). Also, due to the difficulty dissecting L5, analyses could not be performed on the whole lumbar spine. This could be improved with better equipment or an alternative approach for the dissection. The lack of samples can be solved by extending the data collection period or including more institutions in the study in order to ensure a larger sample size and improve the sample age range for correlation analysis.

7.2 CT component

Limitations for the entire CT component (LLA measurement, BMD and morphometrics) were the difficulty of measuring the transverse sections due to lack of advanced equipment, the lack of population groups other than black and white South Africans and the time it takes to measure each individual scan. A large limitation of the LLA measurement would be the method used to determine the angle (Cobb method), as this method can lead to observer errors, as the correct slice on the sagittal images to see the borders of the vertebrae are subject to interpretation. There are also a wide variety of LLA measurement techniques, and results from different techniques might not be comparable, however the Cobb method remains one of the more frequently used techniques (Cil *et al.*, 2005, Andreasen *et al.*, 2007, Vrtovec *et al.*, 2009, Suzuki *et al.*, 2010, Kalichman *et al.*, 2011, Schuller *et al.*, 2011). Therefore, future research should repeat the measurement by the same author multiple times, and the overall average should be taken. Also, more accurate techniques could be investigated.

7.3 MRI component

The MRI component was limited by the fact that not all the scans were complete in terms of the number of sagittal, coronal, and transverse slices per patient. This was unavoidable, as the full lumbar spine is not routinely scanned during MRI procedures. The sagittal images were the most intact, and could therefore be used fully, however the transverse images were the least available. The demographic spread was therefore also very limited. Future research should obtain complete

sets of transverse and coronal scans for patients and should also try to obtain data with a wider demographic spread in terms of population, sex, and age groups. Obtaining greater samples with complete images of various groups, could increase the repeatability and reproducibility of the measurements.

REFERENCES

Ablyazov, O. 2012. X-ray parameters of lumbar spine. Med Health Sci J. 10:37-40.

Adams, M.A. & Roughley, P.J. 2006. What is intervertebral disc degeneration, and what causes it? Spine (Phila Pa 1976). 31 (18):2151-2161.

Al-Hadidi, M.T., Abu-Ghaida, J.H., Badran, D.H., Al-Hadidi, A.M., Ramadan, H.N. & Massad, D.F. 2003. Magnetic resonance imaging of normal lumbar intervertebral foraminal height. Saudi Med J. 24 (7):736-741.

Alacreu, E., Moratal, D. & Arana, E. 2017. Opportunistic screening for osteoporosis by routine CT in Southern Europe. Osteoporos Int. 28 (3):983-990.

Alam, M.M., Waqas, M., Shallwani, H. & Javed, G. 2014. Lumbar morphometry: a study of lumbar vertebrae from a Pakistani population using computed tomography scans. Asian Spine J. 8 (4):421-426.

Alvarado Hospital Medical Center [Internet]. For treatment of spinal stenosis and sciatica. [updated 2018; cited 2018 Jul 24]. Available from: https://www.alvaradohospital.com/Programs-Services/Advanced-Spine-Joint-Institute/Advanced-Spine-Institute/Lumbar-Laminectomy-and-Laminotomy.aspx

Amonoo-Kuofi, H.S. 1995. Age related variations in the horizontal and vertical diameters of the pedicles of the lumbar spine. J Anat. 186:321-328.

Andreasen, M.L., Langhoff, L., Jensen, T.S. & Albert, H.B. 2007. Reproduction of the lumbar lordosis: a comparison of standing radiographs versus supine magnetic resonance imaging obtained with straightened lower extremities. J Manipulative Physiol Ther 30:26-30.

Ardawi, M.S., Maimany, A.A., Bahksh, T.M., Nasrat, H.A., Milaat, W.A. & Al-Raddadi, R.M. 2005. Bone mineral density of the spine and femur in healthy Saudis. Osteoporos Int. 16 (1):43-55.

Arlot, M.E., Burt-Pichat, B., Roux, J.P., Vashishth, D., Bouxsein, M.L. & Delmas, P.D. 2008. Microarchitecture influences microdamage accumulation in human vertebral trabecular bone. J Bone Miner Res. 23 (10):1613-1618.

Arslan, M., Comert, A., Acar, H.I., Ozdemir, M., Elhan, A., Tekdemir, I., Tubbs, R.S., Attar, A. & Ugur, H.C. 2011. Neurovascular structures adjacent to the lumbar intervertebral discs: an anatomical study of their morphometry and relationships. J Neurosurg Spine. 14 (5):630-638.

Arslan, M., Comert, A., Acar, H.I., Ozdemir, M., Elhan, A., Tekdemir, I., Tubbs, R.S. & Ugur, H.C. 2012. Nerve root to lumbar disc relationships at the intervertebral foramen from a surgical viewpoint: an anatomical study. Clin Anat. 25 (2):218-223.

Atta-Alla, E.S., Saab, I.M., El Shishtawy, M. & Hassan, K.H. 2014. Morphometric study of the lumbosacral spine and some of its related angles in Lebanese adult females. Ital J Anat Embryol. 119 (2):92-105.

Avallone, E.A., Baumeister III, T. & Sadegh, A. Introduction to biomechanics. In*:* Marks' standard handbook for mechanical engineers. 11th edn. McGraw Hill Professional; 2007.

Azu, O.O., Komolafe, O.A., Ofusori, D.A., Ajayi, S.A., Naidu, E.C.S. & Abiodun, A.A. 2016. Morphometric study of lumbar vertebrae in adult South African subjects. Int J Morphol. 34 (4):345-1351.

Bae, J.S., Jang, J.S., Lee, S.H. & Kim, J.U. 2012. A comparison study on the change in lumbar lordosis when standing, sitting on a chair, and sitting on the floor in normal individuals. J Korean Neurosurg Soc. 51 (1):20-23.

Banse, X., Devogelaer, J.P., Munting, E., Delloye, C., Cornu, O. & Grynpas, M. 2001. Inhomogeneity of human vertebral cancellous bone: systematic density and structure patterns inside the vertebral body. Bone. 28 (5):563-571.

Barr, K.P., Concannon, L.G. & Harrast, M.A. Low back pain. In*:* Cifu, D. X. ed. Braddom's physical medicine and rehabilitation. 5th edn. Philadelphia: Elsevier; 2016. p. 711-745.

Becker, S., Chavanne, A., Spitaler, R., Kropik, K., Aigner, N., Ogon, M. & Redl, H. 2008. Assessment of different screw augmentation techniques and screw designs in osteoporotic spines. Eur Spine J. 17 (11):1462-1469.

Been, E., Barash, A., Marom, A. & Kramer, P.A. 2010a. Vertebral bodies or discs: which contributes more to human-like lumbar lordosis? Clin Orthop Relat Res. 468:1822-1829.

Been, E., Barash, A., Pessah, H. & Peleg, S. 2010b. A new look at the geometry of the lumbar spine. Spine (Phila Pa 1976). 35 (20):E1014-E1017.

Been, E. & Kalichman, L. 2014. Lumbar lordosis. Spine J. 14 (1):87-97.

Benglis Jr., D.M., Vanni, S. & Levi, A.D. 2009. An anatomical study of the lumbosacral plexus as related to the minimally invasive transpsoas approach to the lumbar spine. J Neurosurg Spine. 10 (2):139-144.

Bergenudd, H., Nilsson, B., Ude´n, A. & Willmer, S. 1989 Bone mineral content, gender, body posture, and build in relation to back pain in middle age. Spine (Phila Pa 1976). 14:577-579.

Bhudhikanok, G.S., Wang, M.C., Eckert, K., Matkin, C., Marcus, R. & Bachrach, L.K. 1996. Differences in bone mineral in young Asian and Caucasian Americans may reflect differences in bone size. J Bone Miner Res. 11:1545-1556.

Billinghurst, J. & Akbarnia, B.A. 2009. Extreme lateral interbody fusion - XLIF. Curr Orthop Pract. 20 (3):238-251.

Bjorck-van Dijken, C., Fjellman-Wiklund, A. & Hildingsson, C. 2008. Low back pain, lifestyle factors and physical activity: a population based-study. J Rehabil Med. 40 (10):864-869.

Bone and Spine [Internet]. Lumbar spine surgery. [updated 2018; cited 2018 Jul 24]. Available from: https://boneandspine.com/lumbar-spine-surgery/

Bredow, J., Oppermann, J., Scheyerer, M.J., Gundlfinger, K., Neiss, W.F., Budde, S., Floerkemeier, T., Eysel, P. & Beyer, F. 2015. Lumbar lordosis and sacral slope in lumbar spinal stenosis: standard values and measurement accuracy. Arch Orthop Trauma Surg. 135 (5):607-612.

Briggs, A.M., Greig, A.M., Wark, J.D., Fazzalari, N.L. & Bennell, K.L. 2004. A review of anatomical and mechanical factors affecting vertebral body integrity. Int J Med Sci. 1 (3):170-180.

Burval, D.J., McLain, R.F., Milks, R. & Inceoglu, S. 2007. Primary pedicle screw augmentation in osteoporotic lumbar vertebrae: biomechanical analysis of pedicle fixation strength. Spine (Phila Pa 1976). 32 (10):1077-1083.

Cappozzo, A. 1984. Compressive loads in the lumbar vertebral column during normal level walking. J Orthop Res. 1 (3):292-301.

Cauley, J.A. 2011. Defining ethnic and racial differences in osteoporosis and fragility fractures. Clin Orthop Relat Res. 469 (7):1891-1899.

Celenk, C. & Celenk, P. Bone density measurement using computed tomography. In*:* Saba, L. ed. Computed tomography - clinical applications. InTech; 2012. p. 123-136.

Chain, A., Crivelli, M., Faerstein, E. & Bezerra, F.F. 2017. Association between fat mass and bone mineral density among Brazilian women differs by menopausal status: The Pro-Saude Study. Nutrition. 33:14-19.

Chaleat-Valayer, E., Mac-Thiong, J.M., Paquet, J., Berthonnaud, E., Siani, F. & Roussouly, P. 2011. Sagittal spino-pelvic alignment in chronic low back pain. Eur Spine J. 20 (Suppl 5):S634-S640.

Chanplakorn, P., Wongsak, S., Woratanarat, P., Wajanavisit, W. & Laohacharoensombat, W. 2011. Lumbopelvic alignment on standing lateral radiograph of adult volunteers and the classification in the sagittal alignment of lumbar spine. Eur Spine J. 20:706-612.

Chantler, S., Dickie, K., Goedecke, J.H., Levitt, N.S., Lambert, E.V., Evans, J., Joffe, Y. & Micklesfield, L.K. 2012. Site-specific differences in bone mineral density in black and white premenopausal South African women. Osteoporos Int. 23 (2):533-542.

Chen, M.R., Moore, T.A., Cooperman, D.R. & Lee, M.J. 2013. Anatomic variability of 120 L5 spondylolytic defects. Global Spine J. 3 (4):243 - 248.

Chen, P., Miller, P.D., Delmas, P.D., Misurski, D.A. & Krege, J.H. 2006. Change in lumbar spine BMD and vertebral fracture risk reduction in teriparatide-treated postmenopausal women with osteoporosis. J Bone Miner Res. 21 (11):1785-1790.

Cheng, X.G., Sun, Y., Boonen, S., Nicholson, P.H.F., Brys, P., Dequeker, J. & Felsenberg, D. 1998. Measurements of vertebral shape by radiographic morphometry: sex differences and relationships with vertebral level and lumbar lordosis. Skeletal Radiol. 27:380-384.

Cho, W., Cho, S.K. & Wu, C. 2010. The biomechanics of pedicle screw-based instrumentation. J Bone Joint Surg Br. 92 (8):1061-1065.

Choi, C.M., Chung, J.T., Lee, S.J. & Choi, D.J. 2016a. How I do it? Biportal endoscopic spinal surgery (BESS) for treatment of lumbar spinal stenosis. Acta Neurochir (Wien). 158 (3):459-463.

Choi, M.K., Kim, S.M. & Lim, J.K. 2016b. Diagnostic efficacy of Hounsfield units in spine CT for the assessment of real bone mineral density of degenerative spine: correlation study between T-scores determined by DEXA scan and Hounsfield units from CT. Acta Neurochir (Wien). 158 (7):1421-1427.

Christodoulou, A.G., Apostolou, T., Ploumis, A., Terzidis, I., Hantzokos, I. & Pournaras, J. 2005. Pedicle dimensions of the thoracic and lumbar vertebrae in the Greek population. Clin Anat. 18:404-408.

Cil, A., Yazici, M., Uzumcugil, A., Kandemir, U., Alanay, A., Alanay, Y., Acaroglu, R.E. & Surat, A. 2005. The evolution of sagittal segmental alignment of the spine during childhood. Spine (Phila Pa 1976). 30 (1):93-100.

Cinotti, G., De Santis, P., Nofroni, I. & Postacchini, F. 2002. Stenosis of lumbar intervertebral foramen: anatomic study on predisposing factors. Spine (Phila Pa 1976). 27 (3):223-229.

Coe, J.D., Warden, K.E., Herzig, M.A. & McAfee, P.C. 1990. Influence of bone mineral density on the fixation of thoracolumbar implants. A comparative study of transpedicular screws, laminar hooks, and spinous process wires. Spine (Phila Pa 1976). 15 (9):902-907.

Conradie, M., Conradie, M.M., Kidd, M. & Hough, S. 2014. Bone density in black and white South African women: contribution of ethnicity, body weight and lifestyle. Arch Osteoporos. 9:193.

Cook, S.D., Salkeld, S.L., Stanley, T., Faciane, A. & Miller, S.D. 2004. Biomechanical study of pedicle screw fixation in severely osteoporotic bone. Spine J. 4 (4):402-408.

Coric, D., Cahill, K.S. & Kim, P.K. Posterior, transforaminal, lateral, and anterior lumbar interbody fusion: techniques and instrumentation. In*:* Winn, H. R. ed. Youmans and Winn neurological surgery. 7th edn. Philadelphia: Elsevier; 2017. p. 2698-2701.

Cundy, T., Cornish, J., Evans, M.C., Gamble, G., Stapleton, J. & Reid, I.R. 1995. Sources of interracial differences in bone density. J Bone Miner Res 10:368-373.

Cvijetic, S. & Korsic, M. 2004. Apparent bone mineral density estimated from DXA in healthy men and women. Osteoporos Int. 15 (4):295-300.

D'Agostino, R.B., Sullivan, L.M. & Beiser, A.S. Summarizing data. In*:* Introductory applied biostatistics. Australia: Thomson, Brooks/Cole; 2006a. p. 15-85.

D'Agostino, R.B., Sullivan, L.M. & Beiser, A.S. Correlation and regression. In*:* Introductory applied biostatistics. Australia: Thomson, Brooks/Cole; 2006b. p. 465-505.

D'Agostino, R.B., Sullivan, L.M. & Beiser, A.S. Nonparametric tests. In*:* Introductory applied biostatistics. Australia: Thomson, Brooks/Cole; 2006c. p. 545-583.

Deleze, M., Cons-Molina, F., Villa, A.R., Morales-Torres, J., Gonzalez-Gonzalez, J.G., Calva, J.J., Murillo, A., Briceno, A., Orozco, J., Morales-Franco, G., Pena-Rios, H., Guerrero-Yeo, G., Aguirre, E. & Elizondo, J. 2000. Geographic differences in bone mineral density of Mexican women. Osteoporos Int. 11 (7):562-569.

Eisenstein, S. 1977. The morphometry and pathological anatomy of the lumbar spine in South African Negroes and Caucasoids with specific reference to spinal stenosis. J Bone Joint Surg Br. 59 (2):173-180.

El-Rakhawy, M., El-Shahat, A.E., Labib, I. & Abdulaziz, E. 2010. Lumbar vertebral canal stenosis: concept of morphometric and radiometric study of the human lumbar vertebral canal. Anatomy. 4:51-62.

Endo, K., Suzuki, H., Nishimura, H., Tanaka, H., Shishido, T. & Yamamoto, K. 2012. Sagittal lumbar and pelvic alignment in the standing and sitting positions. J Orthop Sci. 17 (6):682-686.

Fehily, A.M. 1989. Dietary determinants of bone mass and fracture risk: a review. J Hum Nutr Diet. 2:299-313.

Fields, A.J., Eswaran, S.K., Jekir, M.G. & Keaveny, T.M. 2009. Role of trabecular microarchitecture in whole-vertebral body biomechanical behavior. J Bone Miner Res. 24 (9):1523-1530.

Flynn, M.J. & Cody, D.D. 1993. The assessment of vertebral bone macroarchitecture with X-ray computed tomography. Calcif Tissue Int. 53 (Suppl 1):S170-S175.

Gardocki, R.J. & Park, A.L. Degenerative disorders of the thoracic and lumbar spine. In*:* Azar, F. M., Beaty, J. H. & Canale, S. T. eds. Campbell's operative orthopaedics. 13th edn. Philadelphia: Elsevier; 2017. p. 1644-1727.

Ghandhari, H., Hesarikia, H., Ameri, E. & Noori, A. 2013. Assessment of normal sagittal alignment of the spine and pelvis in children and adolescents. Biomed Res Int. 2013:1-7.

Gilsanz, V., Boechat, M.I., Gilsanz, R., Loro, M.L., Roe, T.F. & Goodman, W.G. 1994. Gender differences in vertebral sizes in adults: biomechanical implications. Radiology. 190 (3):678-682.

Gilsanz, V., Roe, T.F., Mora, S., Costin, G. & Goodman, W.G. 1991. Changes in vertebral bone density in black girls and white girls during childhood and puberty. N Engl J Med. 325 (23):1597-1600.

Gkasdaris, G., Tripsianis, G., Kotopoulos, K. & Kapetanakis, S. 2016. Clinical anatomy and significance of the thoracic intervertebral foramen: a cadaveric study and review of the literature. J Craniovertebr Junction Spine. 7 (4):228-235.

Go, S. Spine trauma. In*:* Tintinalli, J. E., Stapczynski, J. S., Ma, O. J., Yealy, D. M., Meckler, G. D. & Cline, D. M. eds. Tintinalli's emergency medicine: a comprehensive study guide. 8th edn. New York, NY: McGraw-Hill Education; 2016.

Gocmen-Mas, N., Karabekir, H., Ertekin, T., Edizer, M., Canan, Y. & Izzet Duyar, I. 2010. Evaluation of lumbar vertebral body and disc: a stereological morphometric study. Int. J. Morphol. 28:841-847.

Goldberg, C.A. & Chiarello, C.M. 2001. Lumbar sagittal plane mobility and lordosis in the well elderly as related to gender and activity level. Phys Occup Ther Geriatr. 19 (4):17-34.

Gu, Y., Xu, R., Ebraheim, N.A., Rezcallah, A.T. & Yeasting, R.A. 1999. The quantitative study of the lateral region to the lumbar pedicle. Surg Neurol. 52 (4):353-356.

Gulec, A., Kacira, B.K., Kutahya, H., Ozbiner, H., Ozturk, M., Solbas, C.S. & Gokmen, I.E. 2017. Morphometric analysis of the lumbar vertebrae in the Turkish population using three-dimensional computed tomography: correlation with sex, age, and height. Folia Morphol (Warsz). 76 (3):433-439.

Gupta, M.C., Devlin, V.J. & Gogia, J.S. Procedures for decompression of the spinal cord and nerve roots. In*:* Spine secrets plus. Elsevier; 2012. p. 165-170.

Guvencer, M., Naderi, S., Kiray, A., Yilmaz, H.S. & Tetik, S. 2008. The relation between the lumbar vertebrae and the spinal nerves for far lateral lumbar spinal approaches. J Clin Neurosci. 15 (2):192-197.

Haderslev, K.V., Tjellesen, L., Sorensen, H.A. & Staun, M. 2000. Alendronate increases lumbar spine bone mineral density in patients with Crohn's disease. Gastroenterology. 119 (3):639-646.

Halvorson, T.L., Kelley, L.A., Thomas, K.A., Whitecloud, T.S., 3rd & Cook, S.D. 1994. Effects of bone mineral density on pedicle screw fixation. Spine (Phila Pa 1976). 19 (21):2415-2420.

Hamanishi, C. & Tanaka, S. 1993. Dorsal root ganglia in the lumbosacral region observed from the axial views of MRI. Spine (Phila Pa 1986). 18 (13):1753-1756.

Hanson, P., Magnusson, S.P. & Simonsen, E.B. 1998. Differences in sacral angulation and lumbosacral curvature in black and white young men and women. Cells Tissues Organs. 162 (4):226-231.

Hasegawa, T., Mikawa, Y., Watanabe, R. & An, H.S. 1996. Morphometric analysis of the lumbosacral nerve roots and dorsal root ganglia by magnetic resonance imaging. Spine (Phila Pa 1976). 21 (9):1005-1009.

Hayashi, Y., Kushida, K., Kitazawa, A., Tanizawa, T., Hotokebuchi, T., Hagino, H., Murai, H. & Taneichi, H. 1998. Measurement of vertebral body dimensions of the thoracic and lumbar spines of 242 healthy women. J Bone Miner Metab. 16 (1):27-33.

Hazarika, N. [Internet]. Correlation and data transformations. [updated 2013 Sept 26; cited 2018 Jul 26]. Available from: https://blog.majestic.com/case-studies/correlation-data-transformations/

Hilibrand, A.S. & Robbins, M. 2004. Adjacent segment degeneration and adjacent segment disease: the consequences of spinal fusion? Spine J. 4 (Suppl 6):190S-194S.

Hill, D.D., Cauley, J.A., Sheu, Y., Bunker, C.H., Patrick, A.L., Baker, C.E., Beckles, G.L., Wheeler, V.W. & Zmuda, J.M. 2008. Correlates of bone mineral density in men of African ancestry: the Tobago bone health study. Osteoporos Int. 19 (2):227-234.
Hinck, V.C., Clark, W.M. & Hopkins, C.E. 1966. Normal interpediculate distances (minimum and maximum) in children and adults. AJR Am J Roentgenol. 97 (1):141-153.
Hind, K., Truscott, J.G. & Evans, J.A. 2006. Low lumbar spine bone mineral density in both male and female endurance runners. Bone. 39 (4):880-885.
Hochberg, M.C. 2007. Racial differences in bone strength. Trans Am Clin Climatol Assoc. 118:305-315.
Hogan, Q. 1996. Size of human lower thoracic and lumbosacral nerve roots. Anesthesiology. 85 (1):37-42.
Hohn, E.A., Chu, B., Martin, A., Yu, E., Telles, C., Leasure, J., Lynch, T.L. & Kondrashov, D. 2017. The pedicles are not the densest regions of the lumbar vertebrae: implications for bone quality assessment and surgical treatment strategy. Global Spine J. 7 (6):567-571.
Hou, S., Hu, R. & Shi, Y. 1993. Pedicle morphology of the lower thoracic and lumbar spine in a Chinese population. Spine (Phila Pa 1976). 18 (13):1850-1855.
Houston Methodist [Internet]. Posterior lumbar interbody fusion. [updated 2018; cited 2018 Jul 24]. Available from: https://www.houstonmethodist.org/orthopedics/where-does-it-hurt/lower-back/posterior-lumbar-interbody-fusion/
Hoy, D., Brooks, P., Blyth, F. & Buchbinder, R. 2010. The epidemiology of low back pain. Best Pract Res Clin Rheumatol. 24 (6):769-781.
Hu, Z.J., Fang, X.Q. & Fan, S.W. 2014. Iatrogenic injury to the erector spinae during posterior lumbar spine surgery: underlying anatomical considerations, preventable root causes, and surgical tips and tricks. Eur J Orthop Surg Traumatol. 24 (2):127-135.
Hulme, P.A., Boyd, S.K. & Ferguson, S.J. 2007. Regional variation in vertebral bone morphology and its contribution to vertebral fracture strength. Bone. 41 (6):946-957.
Hultman, G., Sarasfe, H. & Ohlsen, H. 1991. Anthropometry, spinal canal width, and flexibility of the spine and hamstring muscles in 45-55-year-old man with and without low back pain. J Spinal Disord. 5:245-253.
Hurday, Y., Xu, B., Guo, L., Cao, Y., Wan, Y., Jiang, H., Liu, Y., Yang, Q. & Ma, X. 2017. Radiographic measurement for transforaminal percutaneous endoscopic approach (PELD). Eur Spine J. 26 (3):635-645.
Hwang, J.H., Modi, H.N., Suh, S.W., Hong, J.Y., Park, Y.H., Park, J.H. & Yang, J.H. 2010. Reliability of lumbar lordosis measurement in patients with spondylolisthesis: a case-control study comparing the Cobb, centroid, and posterior tangent methods. Spine (Phila Pa 1976). 35 (18):1691-1700.
Ihm, E.H., Han, I.B., Shin, D.A., Kim, T.G., Huh, R. & Chung, S.S. 2013. Spinous process morphometry for interspinous device implantation in Korean patients. World Neurosurg. 79 (1):172-176.
Jackman, T.M., Hussein, A.I., Curtiss, C., Fein, P.M., Camp, A., De Barros, L. & Morgan, E.F. 2016. Quantitative, 3D visualization of the initiation and progression of vertebral fractures under compression and anterior flexion. J Bone Miner Res. 31 (4):777-788.
Jaskwhich, D., Zimlich, R. & Glaser, J. 1996. Anatomy of the posterolateral disc region. Am J Orthop (Belle Mead NJ). 25 (9):628-630.

Jeon, C.H., Lee, H.D., Lee, Y.S., Seo, H.S. & Chung, N.S. 2015. Change in sagittal profiles after decompressive laminectomy in patients with lumbar spinal canal stenosis: a 2-year preliminary report. Spine (Phila Pa 1976). 40 (5):E279-E285.

Jones, G., White, C., Sambrook, P. & Eisman, J. 1998. Allelic variation in the vitamin D receptor, lifestyle factors and lumbar spinal degenerative disease. Ann Rheum Dis. 57 (2):94-99.

Kadioglu, H.H., Takci, E. & Levent, A. 2003. Measurements of the lumbar pedicles in the Eastern Anatolian population. Surg Radiol Anat. 25:120-126.

Kadish, L.J. & Simmons, E.H. 1984. Anomalies of the lumbosacral nerve roots. An anatomical investigation and myelographic study. J Bone Joint Surg Br. 66 (3):411-416.

Kalichman, L., Li, L., Hunter, D.J. & Been, E. 2011. Association between computed tomography–evaluated lumbar lordosis and features of spinal degeneration, evaluated in supine position. Spine J 11:308-315.

Kalra, R.R.S., Schmidt, M.H. & Beisse, R.W. Thorascopic spine surgery. In*:* Winn, H. R. ed. Youmans and Winn neurological surgery. Philadelphia: Elsevier Saunders; 2017. p. 271-279.

Kaneko, Y., Matsumoto, M., Takaishi, H., Nishiwaki, Y., Momoshima, S. & Toyama, Y. 2012. Morphometric analysis of the lumbar intervertebral foramen in patients with degenerative lumbar scoliosis by multidetector-row computed tomography. Eur Spine J. 21 (12):2594-2602.

Kanis, J.A. 1994. Assessment of fracture risk and its application to screening for postmenopausal osteoporosis: synopsis of a WHO report. WHO Study Group. Osteoporos Int. 4 (6):368-381.

Kanis, J.A., Melton, L.J., 3rd, Christiansen, C., Johnston, C.C. & Khaltaev, N. 1994. The diagnosis of osteoporosis. J Bone Miner Res. 9 (8):1137-1141.

Kim, C.W. & Garfin, S.R. Rationale of minimally invasive spine surgery. In*:* Garfin, S. R., Eismont, F. J., Bell, G. R., Fischgrund, J. S. & Bono, C. M. eds. Rothman-Simeone and Herkowitz's the spine. 7th edn. Philadelphia: Elsevier Saunders; 2018. p. 935-943.

Kim, N.H., Lee, H.M., Chung, I.H., Kim, H.J. & Kim, S.J. 1994. Morphometric study of the pedicles of thoracic and lumbar vertebrae in Koreans. Spine (Phila Pa 1976). 19 (12):1390-1394.

Krüger, G.C. Comparison of sexually dimorphic patterns in the postcrania of South Africans and North Americans [dissertation]. South Africa (MSc): University of Pretoria; 2015.

Kumar, M., Baklanov, A. & Chopin, D. 2001. Correlation between sagittal plane changes and adjacent segment degeneration following lumbar spine fusion. Eur Spine J. 10 (4):314-319.

Kurutz, M. Finite element modelling of human lumbar spine. In*:* Moratal, D. ed. Finite element analysis. Sciyo; 2010. p. 209-236.

Laria, A., Lurati, A., Mazzocchi, D., Marrazza, M., Re, K.A. & Scarpellini, M. 2015. FRI0295 Relationship between lumbar bone mineral density (BMD) and body mass index (BMI) in Italian population. Ann Rheum Dis. 74 (Suppl 2):531-532.

Larijani, B., Moayyeri, A., Keshtkar, A.A., Hossein-Nezhad, A., Soltani, A., Bahrami, A., Omrani, G.H., Rajabian, R. & Nabipour, I. 2006. Peak bone mass of Iranian population: the Iranian Multicenter Osteoporosis Study. J Clin Densitom. 9 (3):367-374.

LaVange, L.M. & Koch, G.G. 2006. Rank score tests. Circulation. 114 (23):2528-2533.

Le Huec, J.C. & Hasegawa, K. 2016. Normative values for the spine shape parameters using 3D standing analysis from a database of 268 asymptomatic Caucasian and Japanese subjects. Eur Spine J. 25 (11):3630-3637.

Lee, H.M., Kim, N.H., Kim, H.J. & Chung, I.H. 1995. Morphometric study of the lumbar spinal canal in the Korean population. Spine (Phila Pa 1976). 20 (15):1679-1684.
Lee, P., Wong, A.P. & Ganju, A. Surgical anatomy and operative techniques of lumbar stenosis. In*:* Kim, D. H. ed. Surgical anatomy and techniques to the spine. Philadelphia: Elsevier; 2006. p. 426-431.
Lee, S., Chung, C.K., Oh, S.H. & Park, S.B. 2013. Correlation between bone mineral density measured by Dual-Energy X-Ray Absorptiometry and Hounsfield units measured by diagnostic CT in lumbar spine. J Korean Neurosurg Soc. 54 (5):384-389.
Lehmen, J.A. & Gerber, E.J. 2015. MIS lateral spine surgery: a systematic literature review of complications, outcomes, and economics. Eur Spine J. 24 (Suppl 3):287-313.
Lertudomphonwanit, T., Keorochana, G., Kraiwattanapong, C., Chanplakorn, P., Leelapattana, P. & Wajanavisit, W. 2016. Anatomic considerations of intervertebral disc perspective in lumbar posterolateral approach via Kambin's triangle: cadaveric study. Asian Spine J. 10 (5):821-827.
Leslie, W.D. 2012. Clinical review: ethnic differences in bone mass-clinical implications. J Clin Endocrinol Metab. 97 (12):4329-4340.
Lewis-Beck, M.S., Bryman, A. & Liao, T.F. 2004. Shapiro-Wilk test. *The SAGE Encyclopedia of social science research methods.* Thousand Oaks, California.
Lien, S.B., Liou, N.H. & Wu, S.S. 2007. Analysis of anatomic morphometry of the pedicles and the safe zone for through-pedicle procedures in the thoracic and lumbar spine. Eur Spine J. 16:1215-1222.
Lim, T.-H., Kwon, H., Jeon, C.-H., Kim, J.G., Sokolowski, M., Natarajan, R., An, H.S. & B. J. Andersson, G. 2001. Effect of endplate conditions and bone mineral density on the compressive strength of the graft–endplate interface in anterior cervical spine fusion. Spine (Phila Pa 1976). 26 (8):951-956.
Liuke, M., Solovieva, S., Lamminen, A., Luoma, K., Leino-Arjas, P., Luukkonen, R. & Riihimaki, H. 2005. Disc degeneration of the lumbar spine in relation to overweight. Int J Obes (Lond). 29 (8):903-908.
Lonner, B.S., Auerbach, J.D., Sponseller, P., Rajadhyaksha, A.D. & Newton, P.O. 2010. Variations in pelvic and other sagittal spinal parameters as a function of race in adolescent idiopathic scoliosis. Spine (Phila Pa 1976). 35 (10):E374-E377.
Looker, A.C., Melton, L.J., 3rd, Harris, T., Borrud, L., Shepherd, J. & McGowan, J. 2009. Age, gender, and race/ethnic differences in total body and subregional bone density. Osteoporos Int. 20 (7):1141-1149.
Lotfinia, I., Haddadi, K. & Sayyahmelli, S. 2010. Computed tomographic evaluation of pedicle dimension and lumbar spinal canal Neurosurg Quar. 20 (3):194-198.
Lund, T. & de Moraes, O.J.S. Cervical, thoracic, and lumbar stenosis. In*:* Winn, H. R. ed. Youmans and Winn neurological surgery. Philadelphia: Elsevier Saunders; 2017. p. 2373-2383.
Maalouf, G., Salem, S., Sandid, M., Attallah, P., Eid, J., Saliba, N., Nehme, I. & Johnell, O. 2000. Bone mineral density of the Lebanese reference population. Osteoporos Int. 11 (9):756-764.
Magee, D.J. Lumbar spine. In*:* Magee, D. J. ed. Orthopedic physical assessment. 6th edn. Elsevier; 2014. p. 550-648.
Mahato, N.K. 2013. Trabecular bone structure in lumbosacral transitional vertebrae: distribution and densities across sagittal vertebral body segments. Spine J. 13 (8):932-937.

Mai, H.T., Mitchell, S.M., Hashmi, S.Z., Jenkins, T.J., Patel, A.A. & Hsu, W.K. 2016. Differences in bone mineral density of fixation points between lumbar cortical and traditional pedicle screws. Spine J. 16 (7):835-841.

Manchikanti, L. 2000. Epidemiology of low back pain. Pain Physician. 3 (2):167-192.

Manchikanti, L., Singh, V., Falco, F.J., Benyamin, R.M. & Hirsch, J.A. 2014. Epidemiology of low back pain in adults. Neuromodulation. 17 (Suppl 2):3-10.

Manisali, M., Ozaksoy, D., Yilmaz, E., Senocak, O., Tatari, H., Baran, O. & Havitcioglu, H. 2003. Bone mineral density reference values in the normal female and male population of Izmir, Turkey. Eur Radiol. 13 (1):157-162.

Martin, B.I., Mirza, S.K., Comstock, B.A., Gray, D.T., Kreuter, W. & Deyo, R.A. 2007. Reoperation rates following lumbar spine surgery and the influence of spinal fusion procedures. Spine (Phila Pa 1976). 32 (3):382-387.

Masharawi, Y., Salame, K., Mirovsky, Y., Peleg, S., Dar, G., Steinberg, N. & Hershkovitz, I. 2008. Vertebral body shape variation in the thoracic and lumbar spine: characterization of its asymmetry and wedging. Clin Anat. 21 (1):46-54.

Matuoka, C.M. & Basile Júnior, R. 2002. Anatomical study of lumbar vertebral pedicle and adjacent neural structures. Acta Ortop Bras. 10 (3):25-34.

Mayfield Clinic [Internet]. Spinal stenosis. [updated 2016 Apr; cited 2018 Jul 24]. Available from: https://www.mayfieldclinic.com/PE-STEN.htm

Mazess, R.B. & Barden, H. 1999. Bone density of the spine and femur in adult white females. Calcif Tissue Int. 65 (2):91-99.

McCormick, D.P., Ponder, S.W., Fawcett, H.D. & Palmer, J.L. 1991. Spinal bone mineral density in 355 normal and obese children and adolescents: evidence for ethnic and sex differences. J Bone Miner Res 6:507-513.

Melton, L.J., 3rd, Crowson, C.S., O'Fallon, W.M., Wahner, H.W. & Riggs, B.L. 2003. Relative contributions of bone density, bone turnover, and clinical risk factors to long-term fracture prediction. J Bone Miner Res. 18 (2):312-318.

Merloz, P., Tonetti, J., Pittet, L., Coulomb, M., Lavallee, S., Troccaz, J., Cinquin, P. & Sautot, P. 1998. Computer-assisted spine surgery. Comput Aided Surg. 3 (6):297-305.

Mirkovic, S.R., Schwartz, D.G. & Glazier, K.D. 1995. Anatomic considerations in lumbar posterolateral percutaneous procedures. Spine (Phila Pa 1976). 20 (18):1965-1971.

Mohamed, A.M., Adel Saad, B. & Mohey, E.E. 2010. Morphological measurements of lumbar pedicles in Egyptian population using computerized tomography and cadaver direct caliber measurements. Egypt J Radiol Nucl Med. 41 (4):475-481.

Montgomery, D.C. & Runger, G.C. Simple linear regression and correlation. In*:* Applied statistics and probability for engineers. 4th edn. Hoboken, NJ: Wiley; 2007. p. 391-434.

Montgomery, S. [Internet]. Transforaminal lumbar interbody fusion (TLIF). The Back Center; [updated 2018; cited 2018 Jul 24]. Available from: http://www.thebackcenter.net/transforaminal-lumbar-interbody-fusion.html

Morin, S. & Leslie, W.D. 2009. High bone mineral density is associated with high body mass index. Osteoporos Int. 20 (7):1267-1271.

Mosner, E.A., Bryan, J.M., Stull, M.A. & Shippee, R. 1989. A comparison of actual and apparent lumbar lordosis in black and white adult females. Spine (Phila Pa 1976). 14 (3):310-314.

Muraki, S., Yamamoto, S., Ishibashi, H., Horiuchi, T., Hosoi, T., Orimo, H. & Nakamura, K. 2004. Impact of degenerative spinal diseases on bone mineral density of the lumbar spine in elderly women. Osteoporos Int. 15 (9):724-728.

Nepper-Rasmussen, J. & Mosekilde, L. 1989. Local differences in mineral content in vertebral trabecular bone measured by dual-energy computed tomography. Acta Radiol. 30 (4):369-371.

Nieves, J.W., Formica, C., Ruffing, J., Zion, M., Garrett, P., Lindsay, R. & Cosman, F. 2005. Males have larger skeletal size and bone mass than females, despite comparable body size. J Bone Miner Res. 20 (3):529-535.

Norton, B.J., Hensler, K. & Zou, D. 2002. Comparisons among noninvasive methods for measuring lumbar curvature in standing. J Orthop Sports Phys Ther. 32 (8):405-414.

Nuket, G.-M., Hamit, K., Tolga, E., Edize, M., Yazici, C. & Izzet, D. 2010. Evaluation of lumbar vertebral body and disc: a stereological morphometric study. Int J Morphol. 28 (3):841-847.

O'Neill, T.W., Varlow, J., Felsenberg, D., Johnell, O., Weber, K., Marchant, F., Delmas, P.D., Cooper, C., Kanis, J. & Silman, A.J. 1994. Variation in vertebral height ratios in population studies. J Bone Miner Res. 9 (12):1895-1907.

O'Sullivan, P.B., Grahamslaw, K.M., Kendell, M., Lapenskie, S.C., Möller, N.E. & Richards, K.V. 2002. The effect of different standing and sitting postures on trunk muscle activity in a pain-free population. Spine (Phila Pa 1976). 27 (11):1238-1244.

Olsewski, J.M., Simmons, E.H., Kallen, F.C., Mendel, F.C., Severin, C.M. & Berens, D.L. 1990. Morphometry of the lumbar spine: anatomical perspectives related to transpedicular fixation. J Bone Joint Surg Am. 72 (4):541-549.

Orstavik, R.E., Haugeberg, G., Uhlig, T., Falch, J.A., Halse, J.I., Hoiseth, A., Lilleas, F. & Kvien, T.K. 2003. Vertebral deformities in 229 female patients with rheumatoid arthritis: associations with clinical variables and bone mineral density. Arthritis Rheum. 49 (3):355-360.

Park, P., Garton, H.J., Gala, V.C., Hoff, J.T. & McGillicuddy, J.E. 2004. Adjacent segment disease after lumbar or lumbosacral fusion: review of the literature. Spine (Phila Pa 1976). 29 (17):1938-1944.

Parke, W.W., Bono, C.M. & Garfin, S.R. Applied anatomy of the spine. In*:* Herkowitz, H. N., Garfin, S. R., Eismont, F. J., Bell, G. R. & Balderston, R. A. eds. Rothman-Simeone the spine. 6th edn. Philadelphia: Elsevier; 2011. p. 15-53.

Patel, D.N., Pettifor, J.M., Becker, P.J., Grieve, C. & Leschner, K. 1992. The effect of ethnic group on appendicular bone mass in children J Bone Miner Res 7:263-272.

Patrick, J.M. 1976. Thoracic and lumbar spinal curvatures in Nigerian adults. Ann Hum Biol. 3 (4):383-386.

Pedrazzoni, M., Girasole, G., Bertoldo, F., Bianchi, G., Cepollaro, C., Del Puente, A., Giannini, S., Gonnelli, S., Maggio, D., Marcocci, C., Minisola, S., Palummeri, E., Rossini, M., Sartori, L. & Sinigaglia, L. 2003. Definition of a population-specific DXA reference standard in Italian women: the Densitometric Italian Normative Study (DINS). Osteoporos Int. 14 (12):978-982.

Perese, D.M. & Fracasso, J.E. 1959. Anatomical considerations in surgery of the spinal cord: a study of vessels and measurements of the cord. J Neurosurg. 16 (3):314-325.

Phillips, B.B. General principles of arthroscopy. In*:* Azar, F. M., Beaty, J. H. & Canale, S. T. eds. Campbell's operative orthopaedics. Philadelphia: Elsevier; 2017. p. 2457-2470.

Pinel-Giroux, F.-M., Mac-Thiong, J.-M., de Guise, J.A., Berthonnaud, E. & Labelle, H. 2006. Computerized sssessment of sagittal curvatures of the spine

comparison between Cobb and tangent circles techniques. J Spinal Disord Tech. 19:507-512.

Ponnusamy, K.E., Iyer, S., Gupta, G. & Khanna, A.J. 2011. Instrumentation of the osteoporotic spine: biomechanical and clinical considerations. Spine J. 11 (1):54-63.

Pope, M.H., Goh, K.L. & Magnusson, M.L. 2002. Spine ergonomics. Annu Rev Biomed Eng. 4:49-68.

Prakash, Prabhu, L.V., Saralaya, V.V., Pai, M.M., Ranade, A.V., Singh, G. & Madhyastha, S. 2007. Vertebral body integrity: a review of various anatomical factors involved in the lumbar region. Osteoporosis International. 18 (7):891-903.

Putman, M.S., Yu, E.W., Lee, H., Neer, R.M., Schindler, E., Taylor, A.P., Cheston, E., Bouxsein, M.L. & Finkelstein, J.S. 2013. Differences in skeletal microarchitecture and strength in African-American and white women. J Bone Miner Res. 28 (10):2177-2185.

Radcliff, K.E., Kepler, C.K., Jakoi, A., Sidhu, G.S., Rihn, J., Vaccaro, A.R., Albert, T.J. & Hilibrand, A.S. 2013. Adjacent segment disease in the lumbar spine following different treatment interventions. Spine J. 13 (10):1339-1349.

Rampersaud, Y.R., Moro, E.R., Neary, M.A., White, K., Lewis, S.J., Massicotte, E.M. & Fehlings, M.G. 2006. Intraoperative adverse events and related postoperative complications in spine surgery: implications for enhancing patient safety founded on evidence-based protocols. Spine (Phila Pa 1976). 31 (13):1503-1510.

Rao, P.J., Maharaj, M.M., Phan, K., Lakshan Abeygunasekara, M. & Mobbs, R.J. 2015. Indirect foraminal decompression after anterior lumbar interbody fusion: a prospective radiographic study using a new pedicle-to-pedicle technique. Spine J. 15 (5):817-824.

Ratish, S., Gao, Z.-X., Prasad, H.M., Pei, Z. & Bijendra, D. 2018. Percutaneous endoscopic lumbar spine surgery for lumbar disc herniation and lumbar spine stenosis: emphasizing on clinical outcomes of transforaminal technique. Surgical Science. 9 (2):63-84.

Reina, M.A., Andrés, J.A.D., Hernández, J.M., Prats-Galino, A., Machés, F. & Peláez, J. 2010. Transforaminal or translaminar approach for dorsal root ganglion and dorsal nerve root. Anatomical reason for technique decision. Eur J Pain Suppl. 4 (4):287-297.

Ross, P.D., Wasnich, R.D., Davis, J.W. & Vogel, J.M. 1991. Vertebral dimension differences between Caucasian populations, and between Caucasians and Japanese. Bone. 12 (2):107-112.

Routledge, R. Fisher's Exact test. In*:* Armitage, P. & Colton, T. eds. Encyclopedia of biostatistics. 2005.

Roux, J.P., Belghali, S., Wegrzyn, J., Rendu, E.S. & Chapurlat, R. 2016. Vertebral body morphology is associated with incident lumbar vertebral fracture in postmenopausal women. The OFELY study. Osteoporosis International. 27 (8):2507-2513.

Russell-Aulet, M., Wang, J., Thornton, J., Colt, E.W.D. & Pierson, R.N. 1991. Bone mineral density and mass by total body dual photon absorptiometry in normal white and Asian men. J Bone Miner Res. 10:1109-1113.

Salem, W., Coomans, Y., Brismee, J.M., Klein, P., Sobczak, S. & Dugailly, P.M. 2015. Sagittal thoracic and lumbar spine profiles in upright standing and lying prone positions among healthy subjects: influence of various biometric features. Spine (Phila Pa 1976). 40 (15):E900-E908.

Salkind, N.J. 2010a. Mann-Whitney U test. *Encyclopedia of research design.* Thousand Oaks, California: SAGE.

Salkind, N.J. 2010b. McNemar's test. *Encyclopedia of research design.* Thousand Oaks, California: SAGE.

Santoni, B.G., Hynes, R.A., McGilvray, K.C., Rodriguez-Canessa, G., Lyons, A.S., Henson, M.A., Womack, W.J. & Puttlitz, C.M. 2009. Cortical bone trajectory for lumbar pedicle screws. Spine J. 9 (5):366-373.

Schnake, K.J., Schroeder, G.D., Vaccaro, A.R. & Oner, C. 2017. AOSpine classification systems (subaxial, thoracolumbar). J Orthop Trauma. 31 (Suppl 4):S14-S23.

Schnitzler, C.M., Pettifor, J.M., Mesquita, J.M., Bird, M.D.T., Schnaid, E. & Smith, A.E. 1990. Histomorphometry of iliac creast bone in 346 normal black and white South African adults. Bone Miner. 10:183-199.

Schreiber, J.J., Anderson, P.A., Rosas, H.G., Buchholz, A.L. & Au, A.G. 2011. Hounsfield units for assessing bone mineral density and strength: a tool for osteoporosis management. J Bone Joint Surg Am. 93 (11):1057-1063.

Schuller, S., Charles, Y.P. & Steib, J.P. 2011. Sagittal spinopelvic alignment and body mass index in patients with degenerative spondylolisthesis. Eur Spine J 20:713-719.

Schumann, B., Bolm-Audorff, U., Bergmann, A., Ellegast, R., Elsner, G., Grifka, J., Haerting, J., Jager, M., Michaelis, M. & Seidler, A. 2010. Lifestyle factors and lumbar disc disease: results of a German multi-center case-control study (EPILIFT). Arthritis Res Ther. 12 (5):R193.

Schwaiger, B.J., Gersing, A.S., Baum, T., Noel, P.B., Zimmer, C. & Bauer, J.S. 2014. Bone mineral density values derived from routine lumbar spine multidetector row CT predict osteoporotic vertebral fractures and screw loosening. AJNR Am J Neuroradiol. 35 (8):1628-1633.

Seeman, E. 1997. From density to structure: growing up and growing old on the surfaces of bone. J Bone Miner Res. 12 (4):509-521.

Shaw, J.D., Shaw, D.L., Cooperman, D.R., Eubanks, J.D., Li, L. & Kim, D.H. 2015. Characterization of lumbar spinous process morphology: a cadaveric study of 2,955 human lumbar vertebrae. Spine J. 15 (7):1645-1652.

Silav, G., Arslan, M., Cömert, A., Açar, H.I., Kahiloğullari, G., Dolgun, H., Tubbs, R.S. & Tekdemir, I. 2016. Relationship of dorsal root ganglion to intervertebral foramen in lumbar region: an anatomical study and review of literature. J Neurosurg Sci 60 (3):339-344.

Silva, M.J. & Gibson, L.J. 1997. Modeling the mechanical behavior of vertebral trabecular bone: effects of age-related changes in microstructure. Bone. 21 (2):191-199.

Silverstein, M.P., Romrell, L.J., Benzel, E.C., Thompson, N., Griffith, S. & Lieberman, I.H. 2015. Lumbar dorsal root ganglia location: an anatomic and MRI assessment. Int J Spine Surg. 9 (3).

Singh, H., Ghobrial, G.M., Hann, S.W. & Harrop, J.S. Fundamentals of spine surgery. In*:* Steinmetz, M. P. & Benzel, E. C. eds. Benzel's spine surgery. Philadelphia: Elsevier Saunders; 2017. p. 206-209.

Söyüncü, Y., Yldrm, F.B., Sekban, H., Özdemir, H., Akyldz, F. & Sindel, M. 2005. Anatomic evaluation and relationship between the lumbar pedicle and adjacent neural structures: an anatomic study. J Spinal Disord Tech. 18 (3):243-246.

Spencer, D.L., Irwin, G.S. & Miller, J.A. 1983. Anatomy and significance of fixation of the lumbosacral nerve roots in sciatica. Spine (Phila Pa 1976). 8 (6):672-679.

Spine Center Atlanta [Internet]. Anterior lumbar interbody fusion surgery in Atlanta. [updated 2017; cited 2018 Jul 24]. Available from: http://spinecenteratlanta.com/surgical-treatment/anterior-lumbar-interbody-fusion-surgery/

Standring, S. Back. In*:* Standring, S. ed. Gray's anatomy. The anatomical basis of clinical Practice. 41st edn. Elsevier; 2016. p. 709-750.

Stemper, B.D., Chirvi, S., Doan, N., Baisden, J.L., Maiman, D.J., Curry, W.H., Yoganandan, N., Pintar, F.A., Paskoff, G. & Shender, B.S. 2018. Biomechanical tolerance of whole lumbar spines in straightened posture subjected to axial acceleration. J Orthop Res. 36 (6):1747-1756.

Sugisaki, K., Howard, S., Espinozaorias, A.A., Rim, R., Andersson, G.B.J. & Inoue, N. 2009. In-vivo three dimentional morphometric analysis of the lumbar pedicle isthmus. Spine (Phila Pa 1976). 34:2599-2604.

Sun, X., Murgatroyd, A.A., Mullinix, K.P., Cunningham, B.W., Ma, X. & McAfee, P.C. 2014. Biomechanical and anatomical considerations in lumbar spinous process fixation-an in vitro human cadaveric model. Spine J. 14 (9):2208-2215.

Suzuki, H., Endo, K., Kobayashi, H., Tanaka, H. & Yamamoto, K. 2010. Total sagittal spinal alignment in patients with lumbar canal stenosis accompanied by intermittent claudication. Spine (Phila Pa 1976). 35 (9):E344-E346.

Tan, S.H., Teo, E.C. & Chua, H.C. 2004. Quantitative three-dimensional anatomy of cervical, thoracic and lumbar vertebrae of Chinese Singaporeans. Eur Spine J. 13 (2):137-146.

Taylor, B.A., Vaccaro, A.R., Hilibrand, A.S., Zlotolow, D.A. & Albert, T.J. 2001. The risk of foraminal violation and nerve root impingement after anterior placement of lumbar interbody fusion cages. Spine (Phila Pa 1976). 26 (1):100-104.

Torstveit, M.K. & Sundgot-Borgen, J. 2005. Low bone mineral density is two to three times more prevalent in non-athletic premenopausal women than in elite athletes: a comprehensive controlled study. Br J Sports Med. 39 (5):282-287.

Torun, F., Dolgun, H., Tuna, H., Attar, A., Uz, A. & Erdem, A. 2006. Morphometric analysis of the roots and neural foramina of the lumbar vertebrae. Surg Neurol. 66 (2):148-151.

Uribe, J.S., Vale, F.L. & Dakwar, E. 2010. Electromyographic monitoring and its anatomical implications in minimally invasive spine surgery. Spine (Phila Pa 1976). 35 (Suppl 26):S368-S374.

van Roy, P., Barbaix, E., Clarijs, J.P. & Mense, S. 2001. Anatomical background of low back pain: variability and degeneration of the lumbar spinal canal and intervertebral disc. Schmerz. 15 (6):418-424.

Vialle, E., Vialle, L.R., Contreras, W. & Jacob, C.J. 2015. Anatomical study on the relationship between the dorsal root ganglion and the intervertebral disc in the lumbar spine. Rev Bras Ortop. 50 (4):450-454.

Vialle, R., Levassor, N., Rillardon, L., Templier, A., Skalli, W. & Guigui, P. 2005. Radiographic analysis of the sagittal alignment and balance of the spine in asymptomatic subjects. J Bone Joint Surg Am. 87 (2):260-267.

Vrtovec, T., Pernus, F. & Likar, B. 2009. A review of methods for quantitative evaluation of spinal curvature. Eur Spine J. 18:593-607.

Waddell, G., Somerville, D., Henderson, I. & Newton, M. 1992. Objective clinical evaluation of physical impairment in chronic low back pain. Spine (Phila Pa 1976). 17 (6):617-628.

Waldman, S.D. & Campbell, R.S.D. Anatomy: special imaging considerations of the lumbar spine. In*:* Waldman, S. D. & Campbell, R. S. D. eds. Imaging of pain. Philadelphia: Elsevier Saunders; 2011. p. 109-110.

Wang, Y., Battie, M.C. & Videman, T. 2012. A morphological study of lumbar vertebral endplates: radiographic, visual and digital measurements. Eur Spine J. 21 (11):2316-2323.

Warner, W.C. & Sawyer, J.R. Scoliosis and kyphosis. In*:* Azar, F. M., Beaty, J. H. & Canale, S. T. eds. Campbell's operative orthopaedics. Philadelphia: Elsevier; 2017. p. 1897-2120.
Warren, C.Y., Richard, G.B. & Ali, M.S. Solid biomechanics. In*:* Roark's formulas for stress and strain. 8th edn. McGraw Hill Professional; 2012.
Wei, R.L., Jung, B.C., Manzano, W., Sehgal, V., Klempner, S.J., Lee, S.P., Ramsinghani, N.S. & Lall, C. 2016. Bone mineral density loss in thoracic and lumbar vertebrae following radiation for abdominal cancers. Radiother Oncol. 118 (3):430-436.
Weir, J.P. 2005. Quantifying test-retest reliability using the intraclass correlation coefficient and the SEM. J Strength Cond Res. 19 (1):231-240.
Weisz, G.M. & Lee, P. 1983. Spinal canal stenosis. Concept of spinal reserve capacity: radiologic measurements and clinical applications. . Clinic Orthop Relat Res. 179:134 -140.
Wilcox, R.R. Hypothesis testing. In*:* Applying contemporary statistical techniques. Amsterdam: Academic Press; 2003a. p. 141-172.
Wilcox, R.R. Regression and correlation. In*:* Applying contemporary statistical techniques. Amsterdam: Academic Press; 2003b. p. 173-206.
Wilcox, R.R. Rank-based and nonparametric methods. In*:* Applying contemporary statistical techniques. Amsterdam: Academic Press; 2003c. p. 557-608.
Williams, S.K. Thoracic and lumbar spinal injuries. In*:* Herkowitz, H. N., Garfin, S. R., Eismont, F. J., Bell, G. R. & Balderston, R. A. eds. Rothman-Simeone the spine. Philadelphia: Elsevier; 2011. p. 1363-1389.
Woodward, H.R., Abdelgany, M.F. & Faizan, A. 2011. *Interspinous fusion device and method*. US 12/766,864.
Wren, T.A.L., Aggabao, P.C., Poorghasamians, E., Chavez, T.A., Ponrartana, S. & Gilsanz, V. 2017. Association between vertebral cross-sectional area and lumbar lordosis angle in adolescents. PLoS ONE. 12 (2):1-9.
Yagi, M., Akilah, K.B. & Boachie-Adjei, O. 2011. Incidence, risk factors and classification of proximal junctional kyphosis: surgical outcomes review of adult idiopathic scoliosis. Spine (Phila Pa 1976). 36 (1):E60-E68.
Yoganandan, N., Arun, M.W.J., Dickman, C.A. & Benzel, E.C. Practical anatomy and fundamental biomechanics. In*:* Steinmetz, M. P. & Benzel, E. C. eds. Benzel's spine surgery: techniques, complication avoidance, and management Philadelphia: Elsevier Saunders; 2017. p. 58-82.
Youdas, J.W., Garrett, T.R., Harmsen, S., Suman, V.J. & Carey, J.R. 1996. Lumbar lordosis and pelvic inclination of asymptomatic adults. Phys Ther. 76 (10):1066-1081.
Yu, C.C., Yuh, R.T., Bajwa, N.S., Toy, J.O., Ahn, U.M. & Ahn, N.U. 2015. Pedicle morphometry of lumbar vertebrae: male, taller, and heavier specimens have bigger pedicles. Spine (Phila Pa 1976). 40 (21):1639-1646.
Zampolin, R., Erdfarb, A. & Miller, T. 2014. Imaging of lumbar spine fusion. Neuroimaging Clin N Am. 24 (2):268-286.
Zengin, A., Pye, S.R., Cook, M.J., Adams, J.E., Wu, F.C., O'Neill, T.W. & Ward, K.A. 2016. Ethnic differences in bone geometry between white, black and South Asian men in the UK. Bone. 91:180-185.
Zhou, S.H., McCarthy, I.D., McGregor, A.H., Coombs, R.R.H. & Hughes, S.P.F. 2000. Geometrical dimensions of the lower lumbar vertebrae – analysis of data from digitised CT images. Eur Spine J. 9 (3):242-248.

Zhu, K., Hunter, M., James, A., Lim, E.M., Cooke, B.R. & Walsh, J.P. 2017. Discordance between fat mass index and body mass index is associated with reduced bone mineral density in women but not in men: the Busselton Healthy Ageing Study. Osteoporos Int. 28 (1):259-268.

Zhu, L. & Yin, J. 2016. Interspinous fusion device: a systematic review of clinical and biomechanical evidence. Adv Mech Eng. 8 (11):1-12.

Zindrick, M.R., Wiltse, L.L., Doornick, A., Widell, E.H., Knight, G.W. & Patwardhan, A.G. 1987. Analysis of the morphometric characteristics of the thoracic and lumbar pedicles. Spine (Phila Pa 1976). 12:160-166.

APPENDICES

Appendix A.1 – Raw cadaver data

Table A.1.2: Table indicating the measurements (in millimetres) for the spinal nerve length (SNL)

Cadaver number	Sex	Age	L1		L2		L3		L4	
			Left	Right	Left	Right	Left	Right	Left	Right
7326	**M**	**83**	N/A	26.62	19.79	22.56	21.58	20.30	18.68	20.49
7332	**M**	**75**	21.34	18.22	20.03	23.93	20.11	21.43	22.20	26.16
7336	**M**	**66**	24.98	27.88	24.84	23.58	20.63	24.05	27.15	29.50
7389	**M**	**78**	22.45	22.29	21.69	21.71	21.40	20.91	22.43	20.41
7379	**M**	**79**	18.05	17.72	21.33	21.25	21.84	23.90	24.65	24.92
9411W	**M**	**100**	22.10	24.79	23.41	24.40	23.74	26.52	25.07	27.50
9408W	**M**	**78**	22.03	21.93	21.84	21.8	20.55	21.32	22.28	22.28
9428W	**M**	**75**	21.72	21.61	20.94	21.44	20.40	20.94	22.82	21.91
7338	**F**	**67**	19.59	20.26	21.10	22.10	17.38	21.18	20.58	23.93
7343	**F**	**82**	17.32	20.19	17.76	19.92	16.20	18.05	17.12	21.16
7344	**F**	**90**	24.48	24.65	17.97	20.59	17.18	16.24	17.56	19.78
7398	**F**	**64**	18.10	22.09	21.10	21.20	19.59	22.71	23.72	24.32
7399	**F**	**80**	20.97	20.40	22.15	21.34	21.80	23.15	21.78	20.09
9393W	**F**	**29**	21.42	22.92	22.05	23.47	22.12	21.26	23.10	24.74
9389W	**F**	**81**	20.70	21.84	21.09	20.97	20.60	21.00	21.37	22.32
9367W	**F**	**76**	21.03	20.56	21.38	21.78	21.64	21.07	N/A	N/A
9462W	**F**	**51**	21.37	21.22	22.69	21.90	21.22	22.82	23.32	22.30
9455W	**F**	**82**	22.30	23.94	24.41	23.57	20.72	22.04	23.13	25.23
7374	**M**	**74**	18.20	18.19	20.92	19.42	19.79	19.78	17.78	20.32
7381	**F**	**79**	20.02	20.89	22.18	23.38	20.16	20.03	23.80	24.99

Key: M = Male; F = Female; N/A = Not applicable – these are instances where the measurement was not possible to perform. All measurements are in millimetres. The cadaver numbers ending in 'W', are those obtained from the University of Witwatersrand

Table A.1.3: Table indicating the measurements (in millimetres) for the dura mater length (DML)

Cadaver number	Sex	Age	L1		L2		L3		L4	
			Left	Right	Left	Right	Left	Right	Left	Right
7326	**M**	**83**	N/A	15.77	15.49	17.49	16.67	15.14	14.70	15.42
7332	**M**	**75**	16.32	13.00	15.26	17.15	17.40	17.97	16.83	15.18
7336	**M**	**66**	18.18	17.72	18.97	16.42	17.82	17.15	16.12	17.51
7389	**M**	**78**	16.19	13.73	16.10	17.94	15.92	16.62	17.51	16.93
7379	**M**	**79**	15.81	13.80	17.88	16.56	15.62	15.66	15.52	17.60
9411W	**M**	**100**	18.26	17.26	18.86	18.25	17.52	18.06	17.14	17.05
9408W	**M**	**78**	18.41	16.45	18.31	18.01	17.92	18.55	17.22	17.07
9428W	**M**	**75**	16.56	17.32	16.47	17.73	16.30	16.15	17.59	16.22
7338	**F**	**67**	11.67	11.41	17.93	13.12	17.46	16.96	17.78	16.22
7343	**F**	**82**	11.85	12.46	14.29	13.30	12.32	9.56	12.04	12.20
7344	**F**	**90**	20.84	16.84	13.80	14.42	14.86	12.50	13.80	14.60
7398	**F**	**64**	14.83	16.49	14.82	13.09	15.23	16.20	16.80	13.79
7399	**F**	**80**	12.81	14.25	18.02	17.93	19.35	18.82	18.98	18.84
9393W	**F**	**29**	16.74	17.63	16.38	16.20	16.59	16.50	16.15	16.24
9389W	**F**	**81**	17.26	16.65	16.34	15.46	17.94	16.27	16.66	17.74
9367W	**F**	**76**	16.65	17.52	17.32	17.49	16.52	16.10	N/A	N/A
9462W	**F**	**51**	16.88	17.42	17.39	16.50	16.85	17.10	16.21	16.82
9455W	**F**	**82**	16.12	16.22	16.97	17.70	16.37	17.15	16.05	17.42
7374	**M**	**74**	17.32	15.22	20.54	17.21	17.74	18.24	19.92	18.05
7381	**F**	**79**	17.24	17.07	17.01	15.82	15.22	15.25	17.12	14.58

Key: M = Male; F = Female; N/A = Not applicable – these are instances where the measurement was not possible to perform. All measurements are in millimetres. The cadaver numbers ending in 'W', are those obtained from the University of Witwatersrand

Table A.1.4: Table indicating the measurements (in millimetres) for the distance from the dura mater to the nerve (DDMN)

Cadaver number	Sex	Age	L1		L2		L3		L4	
			Left	Right	Left	Right	Left	Right	Left	Right
7326	**M**	**83**	N/A	18.10	14.81	13.14	13.13	13.76	12.92	13.87
7332	**M**	**75**	14.94	14.12	12.53	12.56	13.88	14.24	15.18	17.00
7336	**M**	**66**	15.38	18.18	20.22	19.91	16.33	20.00	22.88	24.55
7389	**M**	**78**	19.82	19.48	16.64	16.69	16.87	18.12	18.33	17.59
7379	**M**	**79**	12.81	12.12	12.62	12.20	20.54	17.46	18.98	12.39
9411W	**M**	**100**	13.02	13.96	14.12	13.74	16.41	15.89	18.10	19.45
9408W	**M**	**78**	16.58	16.39	17.11	17.42	16.92	17.50	16.81	16.52
9428W	**M**	**75**	15.14	15.94	14.90	15.81	14.82	15.15	16.56	14.89
7338	**F**	**67**	15.69	14.26	15.87	12.44	16.94	14.23	18.14	19.25
7343	**F**	**82**	10.47	11.39	12.47	11.29	11.60	13.40	16.00	16.39
7344	**F**	**90**	17.14	12.57	12.84	13.87	12.44	11.00	14.20	13.76
7398	**F**	**64**	19.94	19.72	15.9	16.72	18.00	17.28	18.88	19.50
7399	**F**	**80**	15.08	13.14	17.44	18.86	15.33	17.24	15.92	16.25
9393W	**F**	**29**	15.67	16.02	17.61	17.10	16.52	15.90	18.00	18.84
9389W	**F**	**81**	15.62	15.69	14.82	14.31	15.54	15.38	16.13	17.15
9367W	**F**	**76**	15.54	16.79	16.20	16.24	15.36	16.10	N/A	N/A
9462W	**F**	**51**	15.40	15.00	15.67	15.25	15.60	15.00	14.62	15.02
9455W	**F**	**82**	17.34	17.38	17.30	18.35	15.75	15.52	18.02	17.88
7374	**M**	**74**	14.70	17.94	15.93	14.81	17.11	16.08	16.73	17.48
7381	**F**	**79**	13.35	13.01	16.67	14.29	14.51	14.18	17.85	17.88

Key: M = Male; F = Female; N/A = Not applicable – these are instances where the measurement was not possible to perform. All measurements are in millimetres. The cadaver numbers ending in 'W', are those obtained from the University of Witwatersrand

Table A.1.5: Table indicating the position of the dorsal root ganglion

Cadaver number	Sex	Age	L1		L2		L3		L4	
			Left	Right	Left	Right	Left	Right	Left	Right
7326	**M**	**83**	N/A	A	B	B	B	C	B	B
7332	**M**	**75**	C	C	B	B	B	B	B	B
7336	**M**	**66**	A	A	B	B	A	B	B	B
7389	**M**	**78**	B	A	B	B	B	A	B	B
7379	**M**	**79**	B	B	B	B	C	C	A	A
9411W	**M**	**100**	C	C	A	B	B	B	B	C
9408W	**M**	**78**	B	A	B	A	B	B	B	B
9428W	**M**	**75**	B	A	B	B	B	B	C	C
7338	**F**	**67**	B	B	B	B	A	A	B	B
7343	**F**	**82**	B	B	B	B	C	B	B	B
7344	**F**	**90**	B	B	B	B	B	B	C	C
7398	**F**	**64**	B	B	B	B	B	A	C	C
7399	**F**	**80**	C	A	B	A	B	B	C	C
9393W	**F**	**29**	B	A	B	B	B	B	C	C
9389W	**F**	**81**	B	A	B	B	B	B	C	C
9367W	**F**	**76**	B	A	A	B	B	B	N/A	N/A
9462W	**F**	**51**	B	B	B	B	B	B	C	C
9455W	**F**	**82**	B	A	B	B	B	B	C	C
7374	**M**	**74**	A	B	B	A	B	B	B	B
7381	**F**	**79**	B	B	A	B	B	B	C	C

Key: M = Male; F = Female; A = Position A (medial foraminal); B = Position B (middle foraminal); C = Position C (extra-foraminal); N/A = Not applicable – these are instances where the measurement was not possible to perform. The cadaver numbers ending in 'W', are those obtained from the University of Witwatersrand

Appendix A.2 – Raw CT data: LLA and BMD

Table A.2.6: Table indicating the raw data for the LLA using the CT scans

Case ID	P	Age	LLA
175281	**BF**	**28**	32.9
376411	**BF**	**41**	22
696271	**BF**	**27**	13.2
940381	**BF**	**38**	24.6
1188251	**BF**	**25**	22.7
1689331	**BF**	**33**	22.4
1983451	**BF**	**45**	33.8
2286451	**BF**	**45**	33.3
2622521	**BF**	**52**	42.9
3313231	**BF**	**23**	34.5
4006211	**BF**	**21**	33.5
4811371	**BF**	**37**	19.6
4921271	**BF**	**27**	27.9
5378491	**BF**	**49**	41.9
5642231	**BF**	**23**	26.2
6309241	**BF**	**24**	50.4
7346221	**BF**	**22**	32.1
7479241	**BF**	**24**	44.5
7591291	**BF**	**29**	12.3
7963301	**BF**	**30**	20.6
8677261	**BF**	**26**	24.1
10277341	**BF**	**34**	27.8
745400	**BM**	**40**	31.8
1224630	**BM**	**63**	42.2
1751390	**BM**	**39**	26.7
1837250	**BM**	**25**	39.3
2139430	**BM**	**43**	30.4
2336320	**BM**	**32**	42.9
2583380	**BM**	**38**	34.3
2838310	**BM**	**31**	24.8
2975380	**BM**	**38**	33.5
3591250	**BM**	**25**	20.2
3796340	**BM**	**34**	24.9
3819360	**BM**	**36**	8.3
4274270	**BM**	**27**	36.6
4421330	**BM**	**33**	25.3

Case ID	P	Age	LLA
4518330	**BM**	**33**	44.5
4759360	**BM**	**36**	16.3
5114370	**BM**	**37**	39.4
5989270	**BM**	**27**	25.6
6105390	**BM**	**39**	32.7
6426270	**BM**	**27**	25.3
6771200	**BM**	**20**	19.1
7172230	**BM**	**23**	27.3
8199370	**BM**	**37**	26.7
8213390	**BM**	**39**	18.9
8313270	**BM**	**27**	30.1
8720220	**BM**	**22**	23.2
8887370	**BM**	**37**	30.6
9053260	**BM**	**26**	22.1
9519250	**BM**	**25**	25.1
9895210	**BM**	**21**	40.5
10037320	**BM**	**32**	30.8
10318380	**BM**	**38**	47
543250	**BM**	**25**	24.4
228651	**WF**	**65**	28.4
1041321	**WF**	**32**	45.8
1391501	**WF**	**50**	46.1
1505241	**WF**	**24**	42.2
3080371	**WF**	**37**	48.5
4697341	**WF**	**34**	33.6
5049551	**WF**	**55**	35.1
5219261	**WF**	**26**	38.6
6672461	**WF**	**46**	48.9
7010401	**WF**	**40**	31.4
8517231	**WF**	**23**	34.9
8968431	**WF**	**43**	22.7
9444231	**WF**	**23**	32.7
9766331	**WF**	**33**	29.7
474590	**WM**	**59**	21.8
844300	**WM**	**30**	37
2446350	**WM**	**35**	37

Case ID	P	Age	LLA
2796360	**WM**	**36**	32.4
3406620	**WM**	**62**	43.2
3996360	**WM**	**36**	31.9
4337270	**WM**	**27**	28
5431250	**WM**	**25**	28.7
5816390	**WM**	**39**	45.3
8064380	**WM**	**38**	24.6
9672360	**WM**	**36**	31.6
10153260	**WM**	**26**	24.2
10412510	**WM**	**51**	32.9

Key: P = Population group; BM = Black males; BF = Black females; WM = White males; WF = White females; LLA = Lumbar lordosis angle measurement. All measurements are in degrees

Table A.2.7: Table indicating the BMD measurements taken at the region of interest 1 (ROI1) on the CT scans

Case ID	P	Age	ROI1				
			L1	L2	L3	L4	L5
175281	**BF**	**28**	233	226	239	254	265
376411	**BF**	**41**	213	233	220	225	218
696271	**BF**	**27**	198	166	188	216	250
940381	**BF**	**38**	190	205	218	247	102
1188251	**BF**	**25**	261	267	299	335	248
1689331	**BF**	**33**	194	194	184	205	169
1983451	**BF**	**45**	172	200	231	171	203
2286451	**BF**	**45**	200	213	195	221	179
2622521	**BF**	**52**	171	166	189	189	154
3313231	**BF**	**23**	229	225	191	189	196
4006211	**BF**	**21**	236	234	285	261	279
4811371	**BF**	**37**	236	218	235	222	219
4921271	**BF**	**27**	197	178	217	180	208
5378491	**BF**	**49**	170	191	227	223	208
5642231	**BF**	**23**			359	356	368
6309241	**BF**	**24**	243	236	248	199	237
7346221	**BF**	**22**	254	255	203	238	229

Case ID	P	Age	ROI1				
			L1	L2	L3	L4	L5
7479241	**BF**	**24**	265	237	253	267	249
7591291	**BF**	**29**	261	260	246	259	274
7963301	**BF**	**30**	226	235	243	202	250
8677261	**BF**	**26**	222	222	223	215	238
10277341	**BF**	**34**	215	218	217	211	224
745400	**BM**	**40**	211	222	231	238	211
1224630	**BM**	**63**		145		134	107
1751390	**BM**	**39**	222	215	216	213	219
1837250	**BM**	**25**	208	204	220	215	210
2139430	**BM**	**43**	222	236	227	236	219
2336320	**BM**	**32**	235	266	257	253	257
2583380	**BM**	**38**	229	229	231	228	243
2838310	**BM**	**31**	275	255	279	259	307
2975380	**BM**	**38**	229	222	217	224	236
3591250	**BM**	**25**	237	236	234	255	278
3796340	**BM**	**34**	228	222	242	220	218
3819360	**BM**	**36**	226	229	250	268	255
4274270	**BM**	**27**	227	231	255	264	234
4421330	**BM**	**33**	243	219	213	238	
4518330	**BM**	**33**	247	232	227	263	262
4759360	**BM**	**36**	244	258	270	264	254
5114370	**BM**	**37**	209	214	247	252	240
5989270	**BM**	**27**	240	218	238	254	215
6105390	**BM**	**39**	245	234	240	232	
6426270	**BM**	**27**	240	233	249	264	242
6771200	**BM**	**20**	246	265	256	240	242
7172230	**BM**	**23**	204	201	204	257	225
8199370	**BM**	**37**	252	235	268	251	207
8213390	**BM**	**39**	250	257	262	253	250
8313270	**BM**	**27**	263	240	234	258	238
8720220	**BM**	**22**	236	246	220	254	219
8887370	**BM**	**37**	274	269	266	256	253
9053260	**BM**	**26**	259	285	267	294	285
9519250	**BM**	**25**	270	289	231	227	249
9895210	**BM**	**21**	289	297	312	293	

Case ID	P	Age	ROI1				
			L1	L2	L3	L4	L5
10037320	**BM**	**32**	273	276	280	271	288
10318380	**BM**	**38**	213	215	214	222	224
543250	**BM**	**25**	185	212	175	212	213
228651	**WF**	**65**	99.2	70.1	70.5	97	119.2
1041321	**WF**	**32**	233	220	270	257	295
1391501	**WF**	**50**	155	178	168	184	151
1505241	**WF**	**24**	146	151	170	164	200
3080371	**WF**	**37**	243	243	242	203	225
4697341	**WF**	**34**	227	225	207	202	219
5049551	**WF**	**55**	129	121	128	110	109
5219261	**WF**	**26**	231	239	241	238	246
6672461	**WF**	**46**	178	172	175	187	192
7010401	**WF**	**40**	209	213	200	214	217
8517231	**WF**	**23**	221	214	218	215	218
8968431	**WF**	**43**	215	231	263	230	265
9444231	**WF**	**23**	243	266	249	251	243
9766331	**WF**	**33**	239	245	230	269	242
474590	**WM**	**59**		160	158	143	231
844300	**WM**	**30**	208	218	245	299	261
2446350	**WM**	**35**	186	197	220	230	186
2796360	**WM**	**36**	213	221	214	207	193
3406620	**WM**	**62**	208	203	239	235	205
3996360	**WM**	**36**	226	222	257	281	281
4337270	**WM**	**27**	219	255	292	247	272
5431250	**WM**	**25**	214	217	222	213	216
5816390	**WM**	**39**	211	204	209	205	228
8064380	**WM**	**38**	221	226	243	235	228
9672360	**WM**	**36**		278	258	277	238
10153260	**WM**	**26**	213	214	213	208	228
10412510	**WM**	**51**	191	180	198	187	181

Key: P = Population group; BM = Black males; BF = Black females; WM = White males; WF = White females. All measurements are in Hounsfield units. Blank cells are those where measurements could not be performed

Table A.2.8: Table indicating the BMD measurements taken at the region of interest 2 (ROI2) on the CT scans

Case ID	P	Age	ROI2				
			L1	L2	L3	L4	L5
175281	**BF**	**28**	217	240	215	230	216
376411	**BF**	**41**	240.5	253	232	219	213
696271	**BF**	**27**	174	193	177	190	205
940381	**BF**	**38**	210	213	215	191.5	201
1188251	**BF**	**25**	257	270	245	275	246
1689331	**BF**	**33**	173	182	172	163	174
1983451	**BF**	**45**	153	180	170	178	153
2286451	**BF**	**45**	167	158	179	134	169
2622521	**BF**	**52**	126	120	113	109	112
3313231	**BF**	**23**	183	181	162	163	178
4006211	**BF**	**21**	191	177	184	190	
4811371	**BF**	**37**	205	204	191	193	181
4921271	**BF**	**27**	151	156	144	122	156
5378491	**BF**	**49**	138	127	100	106	102
5642231	**BF**	**23**	356	349	335	310	335
6309241	**BF**	**24**	179	167	169	163	197
7346221	**BF**	**22**	200	197	196	188	194
7479241	**BF**	**24**	226	222	235	233	243
7591291	**BF**	**29**	226	221	219	234	260
7963301	**BF**	**30**	127	127	107	103	124
8677261	**BF**	**26**	203	174	177	169	180
10277341	**BF**	**34**	196	189	194	194	205
745400	**BM**	**40**	232	239	220	208	284
1224630	**BM**	**63**	142	157	146	144	193
1751390	**BM**	**39**	230	239	228	221	200
1837250	**BM**	**25**	198	194	177	181	175
2139430	**BM**	**43**	232	232	195	199	222
2336320	**BM**	**32**	219	213	216	208	243
2583380	**BM**	**38**	217	214	218	221	214
2838310	**BM**	**31**	240	236	230	232	258
2975380	**BM**	**38**	219	220	210	210	211

Case ID	P	Age	ROI2				
			L1	L2	L3	L4	L5
3591250	**BM**	**25**	198	197	191	208	287
3796340	**BM**	**34**	203	205	212	215	204
3819360	**BM**	**36**	246	240	233	240	239
4274270	**BM**	**27**	196	179	175	190	177
4421330	**BM**	**33**	191	194	181	187	
4518330	**BM**	**33**	232	216	220	228	228
4759360	**BM**	**36**	239	239	225	248	237
5114370	**BM**	**37**	186	194	198	197	227
5989270	**BM**	**27**	210	191	179	187	185
6105390	**BM**	**39**	209	198	218	216	
6426270	**BM**	**27**	221	216	201	199	209
6771200	**BM**	**20**	246	236	229	218	226
7172230	**BM**	**23**	154	140	135	148	155
8199370	**BM**	**37**	209	188	184	188	192
8213390	**BM**	**39**	234	247	238	243	242
8313270	**BM**	**27**	215	218	216	226	223
8720220	**BM**	**22**	175	170	171	166	173
8887370	**BM**	**37**	257	227	218	222	244
9053260	**BM**	**26**	240	237	226	238	276
9519250	**BM**	**25**	238	242	221	229	243
9895210	**BM**	**21**	279	262	249	247	
10037320	**BM**	**32**	263	262	251	260	250
10318380	**BM**	**38**	207	203	203	193	199
543250	**BM**	**25**	191	164	184	158	170
228651	**WF**	**65**	158	79.4	79.5	71.7	66.8
1041321	**WF**	**32**	243	236	249	255	232
1391501	**WF**	**50**	190	197	146	178	148
1505241	**WF**	**24**	157	144	141	135	173
3080371	**WF**	**37**	167	170	154	162	176
4697341	**WF**	**34**	210	199	197	199	206
5049551	**WF**	**55**	97.2	99.3	96.4	99.5	97.6
5219261	**WF**	**26**	217	220	221	227	233
6672461	**WF**	**46**	170	174	168	181	188
7010401	**WF**	**40**	196	196	191	183	179
8517231	**WF**	**23**	212	214	216	218	224

Case ID	P	Age	ROI2				
			L1	L2	L3	L4	L5
8968431	**WF**	**43**	163	162	166	183	219
9444231	**WF**	**23**	236	239	229	242	241
9766331	**WF**	**33**	222	227	210	223	217
474590	**WM**	**59**	168	152	163	154	159
844300	**WM**	**30**	248	209	170	196	187
2446350	**WM**	**35**	133	138	136	138	139
2796360	**WM**	**36**	185	173	166	183	173
3406620	**WM**	**62**	145	144	137	154	159
3996360	**WM**	**36**	194	198	197	196	199
4337270	**WM**	**27**	198	199	183	187	191
5431250	**WM**	**25**	155	168	145	179	197
5816390	**WM**	**39**	215	207	195	189	206
8064380	**WM**	**38**	180	171	162	177	164
9672360	**WM**	**36**	214	204	197	196	192
10153260	**WM**	**26**	186	186	181	179	192
10412510	**WM**	**51**	149	145	156	155	165

Key: P = Population group BM = Black males; BF = Black females; WM = White males; WF = White females. All measurements are in Hounsfield units. Blank cells are those where measurements could not be performed

Table A.2.9: Table indicating the BMD measurements taken at the region of interest 3 (ROI3) on the CT scans

Case ID	P	Age	ROI3				
			L1	L2	L3	L4	L5
175281	**BF**	**28**	213.5	216	247	240	241
376411	**BF**	**41**	264	281	227.5	252	231
696271	**BF**	**27**	267	257	276	234	196
940381	**BF**	**38**	248	254	233	213	191
1188251	**BF**	**25**	338	376	365	301	288
1689331	**BF**	**33**	192	189	195	175	180
1983451	**BF**	**45**	164	163	171	177	180
2286451	**BF**	**45**	201	198	183	171	188
2622521	**BF**	**52**	163	136	135	119	111

Case ID	P	Age	ROI3				
			L1	L2	L3	L4	L5
3313231	**BF**	**23**	229	259	178	188	206
4006211	**BF**	**21**	224	271	204	228	
4811371	**BF**	**37**	232	228	227	227	225
4921271	**BF**	**27**	195	218	178	196	183
5378491	**BF**	**49**	243	153	245	186	155
5642231	**BF**	**23**	417	383	385	376	356
6309241	**BF**	**24**	269	248	277	218	214
7346221	**BF**	**22**	246	239	241	217	221
7479241	**BF**	**24**	294	291	289	269	267
7591291	**BF**	**29**	251	285	265	275	285
7963301	**BF**	**30**	272	206	204	294	235
8677261	**BF**	**26**	224	243	239	266	237
10277341	**BF**	**34**	207	214	227	231	229
745400	**BM**	**40**	231	249	228	214	253
1224630	**BM**	**63**	132	178	138	137	151
1751390	**BM**	**39**	266	281	247	231	208
1837250	**BM**	**25**	204	206	216	201	190
2139430	**BM**	**43**	256	241	243	221	243
2336320	**BM**	**32**	233	230	247	233	256
2583380	**BM**	**38**	234	238	241	238	250
2838310	**BM**	**31**	296	291	254	291	264
2975380	**BM**	**38**	247	238	244	249	243
3591250	**BM**	**25**	241	247	257	215	239
3796340	**BM**	**34**	238	227	226	242	243
3819360	**BM**	**36**	262	263	260	259	274
4274270	**BM**	**27**	238	231	221	240	227
4421330	**BM**	**33**	216	206	208	217	
4518330	**BM**	**33**	263	246	240	248	246
4759360	**BM**	**36**	238	251	242	264	276
5114370	**BM**	**37**	247	214	253	228	270
5989270	**BM**	**27**	260	227	277	289	318
6105390	**BM**	**39**	236	246	247	239	
6426270	**BM**	**27**	247	264	239	296	255
6771200	**BM**	**20**	269	284	283	288	289
7172230	**BM**	**23**	216	220	223	210	214

Case ID	P	Age	ROI3				
			L1	L2	L3	L4	L5
8199370	**BM**	**37**	265	254	295	207	286
8213390	**BM**	**39**	274	266	260	265	268
8313270	**BM**	**27**	277	260	273	250	260
8720220	**BM**	**22**	269	232	279	270	232
8887370	**BM**	**37**	282	273	277	286	266
9053260	**BM**	**26**	290	293	294	300	300
9519250	**BM**	**25**	258	268	249	249	270
9895210	**BM**	**21**	294	302	296	294	
10037320	**BM**	**32**	316	303	294	294	292
10318380	**BM**	**38**	229	224	213	212	228
543250	**BM**	**25**	186.5	171	249	210	272
228651	**WF**	**65**	140			151.5	187
1041321	**WF**	**32**	277	261		274	258
1391501	**WF**	**50**	232	232	215	197	181
1505241	**WF**	**24**	195	157	168	157	164
3080371	**WF**	**37**	225	207	234	233	197
4697341	**WF**	**34**	231	223	219	227	238
5049551	**WF**	**55**	121			103	114
5219261	**WF**	**26**	243	237	232	232	252
6672461	**WF**	**46**	204	213	232	246	255
7010401	**WF**	**40**	207	212	218	225	232
8517231	**WF**	**23**	224	228	227	230	235
8968431	**WF**	**43**	251	223	242	274	292
9444231	**WF**	**23**	245	245	252	268	264
9766331	**WF**	**33**	247	264	259	260	251
474590	**WM**	**59**	168	199	219	177	175
844300	**WM**	**30**	270	239	241	219	202
2446350	**WM**	**35**	182	208	235	194	197
2796360	**WM**	**36**	244	237	244	208	209
3406620	**WM**	**62**	212	159	200	232	203
3996360	**WM**	**36**	239	262	246	238	243
4337270	**WM**	**27**	213	217	222	211	235
5431250	**WM**	**25**	230	247	207	239	207
5816390	**WM**	**39**	247	226	227	218	237
8064380	**WM**	**38**	198	195	205	215	223

Case ID	P	Age	ROI3				
			L1	L2	L3	L4	L5
9672360	**WM**	**36**	264	250	232	255	250
10153260	**WM**	**26**	213	210	223	220	282
10412510	**WM**	**51**	192	187	209	224	190

Key: P = Population group; BM = Black males; BF = Black females; WM = White males; WF = White females. All measurements are in Hounsfield units. Blank cells are those where measurements could not be performed

Table A.2.10: Table indicating the BMD measurements taken at the superior endplate (SEP) on the CT scans

Case ID	P	Age	SEP				
			L1	L2	L3	L4	L5
175281	**BF**	**28**	315	325	330	356	309
376411	**BF**	**41**	296	275	416	317	411
696271	**BF**	**27**	366	394	327	350	311
940381	**BF**	**38**	475	412	353	384	323
1188251	**BF**	**25**	444	423	406	505	384
1689331	**BF**	**33**	428	395	404	422	334
1983451	**BF**	**45**	428	454	443	427	448
2286451	**BF**	**45**	360	340	382	384	323
2622521	**BF**	**52**	467	452	415	493	389
3313231	**BF**	**23**	583	563	576	555	540
4006211	**BF**	**21**	477	549	552	635	
4811371	**BF**	**37**	526	484	424	403	394
4921271	**BF**	**27**	533	441	470	510	387
5378491	**BF**	**49**	377	445	403	408	396
5642231	**BF**	**23**	573	538	551	584	601
6309241	**BF**	**24**	436	440	468	441	463
7346221	**BF**	**22**	422	431	401	414	360
7479241	**BF**	**24**	511	569	505	570	582
7591291	**BF**	**29**	518	565	560	526	564
7963301	**BF**	**30**	438	487	535	520	535
8677261	**BF**	**26**	472	483	495	522	526
10277341	**BF**	**34**	532	560	589	576	655

Case ID	P	Age	SEP				
			L1	L2	L3	L4	L5
745400	**BM**	**40**	485	494	427	458	373
1224630	**BM**	**63**	661	411	338	325	449
1751390	**BM**	**39**	417	431	425	547	462
1837250	**BM**	**25**	327	365	357	388	308
2139430	**BM**	**43**	379	442	479	441	440
2336320	**BM**	**32**	433	481	429	506	491
2583380	**BM**	**38**	410	414	462	502	457
2838310	**BM**	**31**	455	541	551	458	496
2975380	**BM**	**38**	420	424	478	539	495
3591250	**BM**	**25**	405	424	386	497	404
3796340	**BM**	**34**	462	498	483	561	569
3819360	**BM**	**36**	443	462	420	475	446
4274270	**BM**	**27**	475	491	520	572	452
4421330	**BM**	**33**	344	416	438	411	
4518330	**BM**	**33**	557	569	657	533	562
4759360	**BM**	**36**	448	493	477	525	452
5114370	**BM**	**37**	523	526	575	549	562
5989270	**BM**	**27**	377	483	466	517	444
6105390	**BM**	**39**	416	383	487	501	470
6426270	**BM**	**27**	463	465	470	472	426
6771200	**BM**	**20**	450	484	615	559	560
7172230	**BM**	**23**	379	348	405	441	342
8199370	**BM**	**37**	443	518	541	524	594
8213390	**BM**	**39**	534	590	609	528	586
8313270	**BM**	**27**	437	508	648	684	617
8720220	**BM**	**22**	479	484	453	518	543
8887370	**BM**	**37**	559	532	577	493	545
9053260	**BM**	**26**	514	568	535	541	493
9519250	**BM**	**25**	495	479	514	543	502
9895210	**BM**	**21**	586	548	584	635	640
10037320	**BM**	**32**	535	588	545	550	486
10318380	**BM**	**38**	383	399	437	456	382
543250	**BM**	**25**	283	287	287	314	378
228651	**WF**	**65**	255	352	338	262	318
1041321	**WF**	**32**	533	434	520	539	486

Case ID	P	Age	SEP				
			L1	L2	L3	L4	L5
1391501	**WF**	**50**	360	261	288	264	331
1505241	**WF**	**24**	283	253	285	312	279
3080371	**WF**	**37**	421	532	424	378	443
4697341	**WF**	**34**	434	435	462	377	375
5049551	**WF**	**55**	463	349	386	349	350
5219261	**WF**	**26**	439	436	450	441	432
6672461	**WF**	**46**	419	401	501	520	443
7010401	**WF**	**40**	460	431	460	497	429
8517231	**WF**	**23**	590	581	537	615	615
8968431	**WF**	**43**	497	519	521	540	563
9444231	**WF**	**23**	546	579	559	556	565
9766331	**WF**	**33**	448	512	558	586	567
474590	**WM**	**59**	360	375	385	424	371
844300	**WM**	**30**	439	469	619	547	481
2446350	**WM**	**35**	342	295	294	368	287
2796360	**WM**	**36**	421	501	521	440	427
3406620	**WM**	**62**	411	476	438	562	426
3996360	**WM**	**36**	449	477	489	494	359
4337270	**WM**	**27**	475	562	593	535	517
5431250	**WM**	**25**	358	480	414	434	335
5816390	**WM**	**39**	418	423	424	525	469
8064380	**WM**	**38**	494	482	470	478	460
9672360	**WM**	**36**		577	608	570	513
10153260	**WM**	**26**	442	443	490	461	496
10412510	**WM**	**51**	443	405	411	420	379

Key: P = Population group; BM = Black males; BF = Black females; WM = White males; WF = White females. All measurements are in Hounsfield units. Blank cells are those where measurements could not be performed

Table A.2.11: Table indicating the BMD measurements taken at the inferior endplate (IEP) on the CT scans

Case ID	P	Age	IEP				
			L1	L2	L3	L4	L5
175281	**BF**	**28**	402	468	524	579	327
376411	**BF**	**41**	380	496	461	385	440
696271	**BF**	**27**	303	444	452	380	390
940381	**BF**	**38**	368	426	356	418	385
1188251	**BF**	**25**	577	549	613	579	664
1689331	**BF**	**33**	378	440	416	488	446
1983451	**BF**	**45**	446	430	437	502	498
2286451	**BF**	**45**	436	375	334	363	487
2622521	**BF**	**52**	464	648	589	554	439
3313231	**BF**	**23**	539	544	576	601	632
4006211	**BF**	**21**	601	730	671	543	
4811371	**BF**	**37**	494	456	557	538	444
4921271	**BF**	**27**	424	478	454	518	434
5378491	**BF**	**49**	419	574	441	557	436
5642231	**BF**	**23**	582	608	682	627	638
6309241	**BF**	**24**	426	462	468	472	412
7346221	**BF**	**22**	477	464	485	499	505
7479241	**BF**	**24**	556	550	596	623	616
7591291	**BF**	**29**	594	622	663	755	585
7963301	**BF**	**30**	546	504	564	626	601
8677261	**BF**	**26**	487	515	531	617	611
10277341	**BF**	**34**	629	572	640	704	710
745400	**BM**	**40**	639	453	524	436	447
1224630	**BM**	**63**	438	323	402	504	495
1751390	**BM**	**39**	409	510	556	625	465
1837250	**BM**	**25**	360	351	344	356	425
2139430	**BM**	**43**	496	481	483	616	496
2336320	**BM**	**32**	596	555	662	601	565
2583380	**BM**	**38**	370	361	496	646	517
2838310	**BM**	**31**	415	414	575	541	633
2975380	**BM**	**38**	443	513	564	513	652
3591250	**BM**	**25**	455	490	522	653	565
3796340	**BM**	**34**	526	567	591	568	586
3819360	**BM**	**36**	574	579	531	592	669
4274270	**BM**	**27**	452	517	431	692	631

Case ID	P	Age	IEP				
			L1	L2	L3	L4	L5
4421330	**BM**	**33**	457	530	519	551	
4518330	**BM**	**33**	547	541	578	676	623
4759360	**BM**	**36**	629	567	642	665	486
5114370	**BM**	**37**	513	514	574	513	556
5989270	**BM**	**27**	460	604	597	708	638
6105390	**BM**	**39**	469	430	468	443	494
6426270	**BM**	**27**	502	520	586	574	554
6771200	**BM**	**20**	564	600	768	679	554
7172230	**BM**	**23**	403	372	412	628	360
8199370	**BM**	**37**	563	532	521	587	553
8213390	**BM**	**39**	572	534	607	551	633
8313270	**BM**	**27**	564	606	703	684	722
8720220	**BM**	**22**	577	546	596	609	608
8887370	**BM**	**37**	518	610	507	563	631
9053260	**BM**	**26**	492	535	526	535	546
9519250	**BM**	**25**	443	404	571	588	627
9895210	**BM**	**21**	522	595	566	750	640
10037320	**BM**	**32**	565	627	672	667	618
10318380	**BM**	**38**	442	493	510	538	560
543250	**BM**	**25**	293	299		331	501
228651	**WF**	**65**	267	286	296	488	386
1041321	**WF**	**32**	667	493	601	543	543
1391501	**WF**	**50**	275	356	417	445	400
1505241	**WF**	**24**	315	287	373	319	378
3080371	**WF**	**37**	437	614	520	467	422
4697341	**WF**	**34**	421	421	482	466	433
5049551	**WF**	**55**	484	344	439	373	413
5219261	**WF**	**26**	451	445	429	423	450
6672461	**WF**	**46**	540	547	554	480	626
7010401	**WF**	**40**	493	458	449	509	582
8517231	**WF**	**23**	562	567	602	523	564
8968431	**WF**	**43**	543	525	569	619	520
9444231	**WF**	**23**	617	592	614	617	653
9766331	**WF**	**33**	586	535	603	653	684
474590	**WM**	**59**	373	468	580	544	347

Case ID	P	Age	IEP				
			L1	L2	L3	L4	L5
844300	**WM**	**30**	471	563	625	718	577
2446350	**WM**	**35**	352	371	328	364	299
2796360	**WM**	**36**	582	566	513	587	511
3406620	**WM**	**62**	430	483	424	512	462
3996360	**WM**	**36**	425	492	520	589	653
4337270	**WM**	**27**	471	443	505	533	507
5431250	**WM**	**25**	319	396	413	465	525
5816390	**WM**	**39**	416	454	585	503	532
8064380	**WM**	**38**	563	535	554	517	513
9672360	**WM**	**36**	516	552	572	668	690
10153260	**WM**	**26**	451	490	466	550	556
10412510	**WM**	**51**	356	379	397	408	400

Key: P = Population group; BM = Black males; BF = Black females; WM = White males; WF = White females. All measurements are in Hounsfield units. Blank cells are those where measurements could not be performed

Table A.2.12: Table indicating the BMD measurements taken at the anterior border (AB) on the CT scans

Case ID	P	Age	AB				
			L1	L2	L3	L4	L5
175281	**BF**	**28**	439	377	441	332	478
376411	**BF**	**41**	483	402	411	340	426
696271	**BF**	**27**	421	445	447	467	440
940381	**BF**	**38**	531	474	514	492	432
1188251	**BF**	**25**	516	597	549	585	550
1689331	**BF**	**33**	384	470	447	424	495
1983451	**BF**	**45**	335	447	418	423	427
2286451	**BF**	**45**	461	412	427	440	356
2622521	**BF**	**52**	331	350	395	316	374
3313231	**BF**	**23**	498	539	491	526	492
4006211	**BF**	**21**	486	442	479	543	
4811371	**BF**	**37**	395	424	482	419	402
4921271	**BF**	**27**	415	412	404	458	423

Case ID	P	Age	AB				
			L1	L2	L3	L4	L5
5378491	**BF**	**49**	412	375	319	343	310
5642231	**BF**	**23**	563	571	535	543	546
6309241	**BF**	**24**	501	520	526	462	504
7346221	**BF**	**22**	394	406	385	401	495
7479241	**BF**	**24**	476	540	483	504	613
7591291	**BF**	**29**	659	575	533	560	611
7963301	**BF**	**30**	420	438	447	419	555
8677261	**BF**	**26**	483	547	465	450	476
10277341	**BF**	**34**	364	368	422	430	481
745400	**BM**	**40**	366	421	407	445	466
1224630	**BM**	**63**	383	320	350	317	320
1751390	**BM**	**39**	500	420	437	407	508
1837250	**BM**	**25**	347	357	452	575	406
2139430	**BM**	**43**	445	472	438	561	557
2336320	**BM**	**32**	461	465	425	461	514
2583380	**BM**	**38**	439	423	390	411	463
2838310	**BM**	**31**	473	508	511	470	584
2975380	**BM**	**38**	462	517	485	421	426
3591250	**BM**	**25**	413	403	433	463	507
3796340	**BM**	**34**	407	450	415	531	543
3819360	**BM**	**36**	452	417	449	482	517
4274270	**BM**	**27**	452	403	472	414	584
4421330	**BM**	**33**	371	368	407	452	
4518330	**BM**	**33**	391	373	388	450	463
4759360	**BM**	**36**	456	494	489	469	543
5114370	**BM**	**37**	451	442	471	406	549
5989270	**BM**	**27**	425	449	448	451	505
6105390	**BM**	**39**	448	465	501	508	495
6426270	**BM**	**27**	488	481	469	479	559
6771200	**BM**	**20**	443	456	457	471	517
7172230	**BM**	**23**	413	433	448	428	433
8199370	**BM**	**37**	419	414	479	436	561
8213390	**BM**	**39**	514	563	484	486	650
8313270	**BM**	**27**	479	479	476	460	602
8720220	**BM**	**22**	382	382	326	335	466

Case ID	P	Age	AB				
			L1	L2	L3	L4	L5
8887370	**BM**	**37**	514	541	499	489	572
9053260	**BM**	**26**	566	572	548	560	590
9519250	**BM**	**25**	436	454	476	484	573
9895210	**BM**	**21**	521	507	555	507	603
10037320	**BM**	**32**	436	430	410	446	512
10318380	**BM**	**38**	436	414	388	388	492
543250	**BM**	**25**	339	367	393	392	524
228651	**WF**	**65**	297	507	437	264	419
1041321	**WF**	**32**	472	394	376	487	474
1391501	**WF**	**50**	373	437	401	390	416
1505241	**WF**	**24**	373	476	455	417	457
3080371	**WF**	**37**	390	400	387	502	497
4697341	**WF**	**34**	471	446	494	527	577
5049551	**WF**	**55**	297	339	321	343	372
5219261	**WF**	**26**	428	437	414	417	466
6672461	**WF**	**46**	479	463	446	472	478
7010401	**WF**	**40**	431	501	491	456	552
8517231	**WF**	**23**	484	507	469	555	520
8968431	**WF**	**43**	433	509	456	580	613
9444231	**WF**	**23**	626	611	562	586	651
9766331	**WF**	**33**	503	543	605	567	630
474590	**WM**	**59**	282	378	372	367	510
844300	**WM**	**30**	396	341	404	346	402
2446350	**WM**	**35**	388	419	367	334	407
2796360	**WM**	**36**	423	438	562	567	466
3406620	**WM**	**62**	364	348	338	342	439
3996360	**WM**	**36**	406	414	495	473	459
4337270	**WM**	**27**	483	463	475	441	465
5431250	**WM**	**25**	445	416	416	421	499
5816390	**WM**	**39**	460	371	458	476	515
8064380	**WM**	**38**	464	364	368	387	414
9672360	**WM**	**36**	439	413	512	504	646
10153260	**WM**	**26**	428	426	393	403	488
10412510	**WM**	**51**	392	511	442	497	462

Case ID	P	Age	AB				
			L1	L2	L3	L4	L5
Key: P = Population group; BM = Black males; BF = Black females; WM = White males; WF = White females. All measurements are in Hounsfield units. Blank cells are those where measurements could not be performed							

Table A.2.13: Table indicating the BMD measurements taken at the posterior border (PB) on the CT scans

Case ID	P	Age	PB				
			L1	L2	L3	L4	L5
175281	**BF**	**28**	298	366	300	341	375
376411	**BF**	**41**	396	302	286	333	405
696271	**BF**	**27**	414	375	382	459	558
940381	**BF**	**38**	376	632	457	558	354
1188251	**BF**	**25**	472	654	576	736	703
1689331	**BF**	**33**	442	526	543	461	467
1983451	**BF**	**45**	571	585	556	612	425
2286451	**BF**	**45**	528	553	563	647	623
2622521	**BF**	**52**	496	486	643	555	447
3313231	**BF**	**23**	702	803	622	681	648
4006211	**BF**	**21**	832	798	834	902	
4811371	**BF**	**37**	569	679	715	715	705
4921271	**BF**	**27**	436	495	542	637	492
5378491	**BF**	**49**	670	679	681	684	563
5642231	**BF**	**23**	665	720	892	930	959
6309241	**BF**	**24**	779	759	704	774	689
7346221	**BF**	**22**	743	720	729	798	556
7479241	**BF**	**24**	607	649	740	786	730
7591291	**BF**	**29**	628	693	678	676	733
7963301	**BF**	**30**	733	656	823	575	553
8677261	**BF**	**26**	592	839	742	709	656
10277341	**BF**	**34**	476	521	735	765	615
745400	**BM**	**40**	402	524	375	569	683
1224630	**BM**	**63**	327	465	435	571	586
1751390	**BM**	**39**	441	532	654	677	576

Case ID	P	Age	PB				
			L1	L2	L3	L4	L5
1837250	**BM**	**25**	408	593	502	514	471
2139430	**BM**	**43**	566	761	654	721	517
2336320	**BM**	**32**	491	450	485	517	431
2583380	**BM**	**38**	602	671	680	624	719
2838310	**BM**	**31**	590	678	662	645	729
2975380	**BM**	**38**	550	688	668	648	653
3591250	**BM**	**25**	633	564	668	631	577
3796340	**BM**	**34**	798	767	710	772	797
3819360	**BM**	**36**	584	610	600	633	615
4274270	**BM**	**27**	550	617	775	850	807
4421330	**BM**	**33**	564	554	606	690	
4518330	**BM**	**33**	698	708	807	826	840
4759360	**BM**	**36**	553	644	655	643	702
5114370	**BM**	**37**	641	787	786	774	746
5989270	**BM**	**27**	502	692	717	764	600
6105390	**BM**	**39**	536	787	766	756	856
6426270	**BM**	**27**	558	727	720	785	791
6771200	**BM**	**20**	503	649	791	755	680
7172230	**BM**	**23**	415	621	695	685	695
8199370	**BM**	**37**	456	473	727	800	671
8213390	**BM**	**39**	707	857	812	823	842
8313270	**BM**	**27**	691	826	881	827	639
8720220	**BM**	**22**	504	514	632	682	658
8887370	**BM**	**37**	864	926	772	976	760
9053260	**BM**	**26**	513	797	830	814	682
9519250	**BM**	**25**	519	718	529	685	584
9895210	**BM**	**21**	682	853	816	911	565
10037320	**BM**	**32**	588	653	641	659	660
10318380	**BM**	**38**	529	584	618	631	519
543250	**BM**	**25**	300	268	426	483	593
228651	**WF**	**65**	192	151	181	275	221
1041321	**WF**	**32**	409	531	627	792	382
1391501	**WF**	**50**	606	440	419	566	328
1505241	**WF**	**24**	315	432	724	695	416
3080371	**WF**	**37**	677	690	519	467	421

Case ID	P	Age	PB				
			L1	L2	L3	L4	L5
4697341	**WF**	**34**	493	555	780	774	775
5049551	**WF**	**55**	643	599	652	648	573
5219261	**WF**	**26**	556	536	689	658	544
6672461	**WF**	**46**	556	691	635	739	460
7010401	**WF**	**40**	536	672	629	762	737
8517231	**WF**	**23**	584	867	850	835	854
8968431	**WF**	**43**	572	862	853	949	697
9444231	**WF**	**23**	670	686	739	740	796
9766331	**WF**	**33**	622	720	805	778	750
474590	**WM**	**59**	239	317	417	337	350
844300	**WM**	**30**	434	584	632	570	439
2446350	**WM**	**35**	518	663	454	425	557
2796360	**WM**	**36**	429	537	777	598	566
3406620	**WM**	**62**	523	597	756	718	695
3996360	**WM**	**36**	457	483	507	488	643
4337270	**WM**	**27**	606	704	581	659	758
5431250	**WM**	**25**	403	680	658	736	514
5816390	**WM**	**39**	758	829	736	723	553
8064380	**WM**	**38**	623	675	787	690	653
9672360	**WM**	**36**	627	798	892	734	662
10153260	**WM**	**26**	449	551	629	600	693
10412510	**WM**	**51**	469	707	793	733	612

Key: P = Population group; BM = Black males; BF = Black females; WM = White males; WF = White females. All measurements are in Hounsfield units. Blank cells are those where measurements could not be performed

Appendix A.3 – Raw CT data: Posterior elements and spinal canal

Table A.3.14: Table indicating the transverse process length (TPL) measurements taken on the CT scans

Case ID	P	Age	TPL				
			L1	L2	L3	L4	L5
175281	**BF**	**28**	75.3	91.2	94.6	89.6	102
376411	**BF**	**41**	62.1	78.6	103	92.1	98.4
696271	**BF**	**27**	67.2	77.3	84.5	89.9	89
940381	**BF**	**38**	60.5	69.4	75.8	85.6	75.8
1188251	**BF**	**25**	58.7	73	81.2	77.6	77.6
1689331	**BF**	**33**	57.6	73.1	77.1	79.1	87.1
1983451	**BF**	**45**	56.3	66.1	78.7	77.9	73.3
2286451	**BF**	**45**	70.9	85	93.1	89.6	89.8
2622521	**BF**	**52**	68.1	87.3	96.2	86.7	93.3
3313231	**BF**	**23**	67.7	71.2	76.1	79.5	79.5
4006211	**BF**	**21**	61.4	70	77.9	78.9	
4811371	**BF**	**37**	58.4	74.7	82.6	89.2	93.1
4921271	**BF**	**27**	64.3	83	96	90.7	96.5
5378491	**BF**	**49**	65.8	75.9	86.4	73	80.2
5642231	**BF**	**23**	65.9	72.5	81.7	77.3	82.7
6309241	**BF**	**24**	71.4	83.5	92.6	58.5	86.2
7346221	**BF**	**22**	58.9	69.5	73.9	77.1	74
7479241	**BF**	**24**	72.6	77.8	92.5	81.3	89.2
7591291	**BF**	**29**	63.4	74.7	78.8	83.5	94.6
7963301	**BF**	**30**	69.8	76.2	97.2	87.5	88.2
8677261	**BF**	**26**	65.8	68.8	80.9	76.5	71.5
10277341	**BF**	**34**	71.9	81.8	93.8	82.8	83.4
745400	**BM**	**40**	79.3	89.1	101	81.6	93.9
1224630	**BM**	**63**	65.2	67.8	89.6	91.6	88.4
1751390	**BM**	**39**	74.6	80.3	92.2	88.3	92.5
1837250	**BM**	**25**	84.6	75.4	81.9	90.4	88.7
2139430	**BM**	**43**	75.5	84.1	97	86.7	90
2336320	**BM**	**32**	79.5	93.3	94.9	94.5	95
2583380	**BM**	**38**	75.7	89.3	98.4	97.1	89.8
2838310	**BM**	**31**	82.4	97.2	106	101	96.6
2975380	**BM**	**38**	70.8	82.7	96.8	92.9	97.6
3591250	**BM**	**25**	94.1	102	104	107	106
3796340	**BM**	**34**	78.9	85.8	95.5	89.4	93.5
3819360	**BM**	**36**	76.9	83.4	94	85.4	92.2
4274270	**BM**	**27**	75	89.3	99.4	93.3	95.2

Case ID	P	Age	TPL				
			L1	L2	L3	L4	L5
4421330	**BM**	**33**	89.3	103	110	89.8	
4518330	**BM**	**33**	73.2	92.3	103	88.5	93.5
4759360	**BM**	**36**	73.4	83.4	97.9	99.2	93.3
5114370	**BM**	**37**	83.1	92.9	101	93.3	89.8
5989270	**BM**	**27**	70.9	87.9	94.8	88.9	93
6105390	**BM**	**39**	83.5	95.3	110	96.7	102
6426270	**BM**	**27**	77.3	83.8	92.6	81.5	87
6771200	**BM**	**20**	59.6	77.3	88.8	79.9	82.7
7172230	**BM**	**23**	70.4	88.1	103	89.8	92
8199370	**BM**	**37**	70.3	84.7	101	90.8	94.2
8213390	**BM**	**39**	81.7	92.1	113	102	98.1
8313270	**BM**	**27**	77.2	87	95.5	93.9	101
8720220	**BM**	**22**	77.1	84.4	91.7	84.7	101
8887370	**BM**	**37**	64.7	75.5	77.1	77.9	83.6
9053260	**BM**	**26**	78.5	79.2	91.8	89.2	83.7
9519250	**BM**	**25**	70.4	84.2	102	93.1	92.8
9895210	**BM**	**21**	71.8	85.7	93.1	88.1	87
10037320	**BM**	**32**	79.4	80.1	94	91.1	94.3
10318380	**BM**	**38**	69	85.8	88.9	82.5	88.8
543250	**BM**	**25**	73.3	91	101	89.3	88.1
228651	**WF**	**65**	64.9	77.6	87.7	83.8	94
1041321	**WF**	**32**	66.4	74.5	71.1	65.6	81.2
1391501	**WF**	**50**	65.3	77.3	83.9	84.2	75
1505241	**WF**	**24**	77.4	90.1	87.3	93.2	105
3080371	**WF**	**37**	72.7	80.7	91.3	84.8	97.9
4697341	**WF**	**34**	74.7	79.6	85.4	88.3	93.6
5049551	**WF**	**55**	84.2	89.6	96.8	90.1	96.1
5219261	**WF**	**26**	63.8	72.4	72.4	67.4	74.2
6672461	**WF**	**46**	68.3	76.2	76.5	82.1	89.8
7010401	**WF**	**40**	64.5	73.9	85.5	81.9	82
8517231	**WF**	**23**	74.7	86.6	92.3	88.8	94.8
8968431	**WF**	**43**	77.4	77.1	84.2	82.1	98.4
9444231	**WF**	**23**	72.3	83.3	92.4	91.5	91.3
9766331	**WF**	**33**	70.3	79.1	99.5	89.8	89.8
474590	**WM**	**59**	79.1	86.5	96.5	91.4	94.7

Case ID	P	Age	TPL				
			L1	L2	L3	L4	L5
844300	**WM**	**30**	75.4	80.9	96.5	83.9	95.4
2446350	**WM**	**35**	90.1	94	115	99.4	106
2796360	**WM**	**36**	70.7	73.4	83.4	86.7	
3406620	**WM**	**62**	75.7	92.8	105	101	102
3996360	**WM**	**36**	68.5	71.3	83.9	85.3	
4337270	**WM**	**27**	70.2	80.5	96.5	87.4	95.6
5431250	**WM**	**25**	83	91.3	109	97.7	106
5816390	**WM**	**39**	79.9	87.9	98.1	84.3	95.3
8064380	**WM**	**38**	77.9	79.7	92.4	101	95.9
9672360	**WM**	**36**	75.8	89.1	93.2	86.6	88.6
10153260	**WM**	**26**	75	84.8	106	94	92.1
10412510	**WM**	**51**	81.8	99.1	108	90.8	94

Key: P = Population group; BM = Black males; BF = Black females; WM = White males; WF = White females. All measurements are in millimetres. Blank cells are those where measurements could not be performed

Table A.3.15: Table indicating the spinous process length (SPL) measurement taken on the CT scans

Case ID	P	Age	SPL				
			L1	L2	L3	L4	L5
175281	**BF**	**28**	28.3	29.9	32.5	33.9	29.9
376411	**BF**	**41**	32	34.2	37.9	36.1	28.1
696271	**BF**	**27**	30.2	31	30.1	25.4	24.5
940381	**BF**	**38**	32.1	34.7	38.1	40.4	33.3
1188251	**BF**	**25**	25.2	27.4	29.5	27	24.5
1689331	**BF**	**33**	33	36.8	34.2	38.2	28
1983451	**BF**	**45**	27.5	34.6	35.9	36.3	33.5
2286451	**BF**	**45**	31.9	34.5	38.3	36.2	36.3
2622521	**BF**	**52**	30.9	33.5	31	25	24.2
3313231	**BF**	**23**	34	36.8	38.5	39.6	33.9
4006211	**BF**	**21**	31.1	32.5	32.9	28.2	
4811371	**BF**	**37**	31.2	33.4	35.6	32.9	30.3
4921271	**BF**	**27**	31.7	36.1	36.2	33.7	29.8

Case ID	P	Age	SPL				
			L1	L2	L3	L4	L5
5378491	**BF**	**49**	33.5	37.9	41	38.3	32.9
5642231	**BF**	**23**	28	30.1	32.3	29.4	21
6309241	**BF**	**24**	37.2	38.5	36.5	37.4	34.3
7346221	**BF**	**22**	37.2	36.8	34	30	23.5
7479241	**BF**	**24**	34.3	38.8	39.9	33.6	28.6
7591291	**BF**	**29**	35.2	38.4	40.5	36.1	30.9
7963301	**BF**	**30**	32	37.4	38.2	39.7	34.8
8677261	**BF**	**26**	24.1	28	31.2	30	26.7
10277341	**BF**	**34**	30.1	35	34.5	31.2	24.6
745400	**BM**	**40**	30.8	35.3	37.5	35.6	33.4
1224630	**BM**	**63**	29.7	33.9	35	33.9	27.5
1751390	**BM**	**39**	29.1	37.6	39.5	40.7	31.4
1837250	**BM**	**25**	35.8	39.4	34.3	34.8	24.4
2139430	**BM**	**43**	31.9	38.2	42.8	42.7	34.7
2336320	**BM**	**32**	25.1	27.8	37.9	38.9	33
2583380	**BM**	**38**	39	39.2	42.4	34.3	31.8
2838310	**BM**	**31**	31.1	35.9	40.6	39.9	31.4
2975380	**BM**	**38**	38.8	42.1	43.5	43	37.4
3591250	**BM**	**25**	25.6	34.3	37.8	32.3	33.2
3796340	**BM**	**34**	35.3	35.7	34.5	31.1	28.2
3819360	**BM**	**36**	33.2	34.1	38.6	38.2	36
4274270	**BM**	**27**	33.7	39.2	44.3	44.6	36
4421330	**BM**	**33**	33.5	35	35.2	31	
4518330	**BM**	**33**	34.8	38.2	38.1	36	31.1
4759360	**BM**	**36**	33.1	35.7	41.2	38.9	31.5
5114370	**BM**	**37**	37.6	40.8	39.8	32.6	26.4
5989270	**BM**	**27**	32.2	37.9	40.4	38.5	28.9
6105390	**BM**	**39**	40.5	49.3	50.6	47.3	39.6
6426270	**BM**	**27**	30.6	34.5	39.7	39.4	33.1
6771200	**BM**	**20**	28.9	34.5	35.7	38.9	32
7172230	**BM**	**23**	34	38.8	37.6	41.6	33.3
8199370	**BM**	**37**	37	38.3	36.9	34.8	29.7
8213390	**BM**	**39**	38.5	43.5	40.8	38.3	32.1
8313270	**BM**	**27**	38.3	43.9	44.6	44.1	36.9
8720220	**BM**	**22**	36.5	39.5	43.1	41.8	37.3

Case ID	P	Age	SPL				
			L1	L2	L3	L4	L5
8887370	**BM**	**37**	31.1	34.8	37.9	33.5	28.6
9053260	**BM**	**26**	31.8	35.7	37.3	35.6	31.3
9519250	**BM**	**25**	29.9	34.3	33.8	30.9	23.5
9895210	**BM**	**21**	32.6	35.4	34.3	35.3	24.8
10037320	**BM**	**32**	31.4	35.7	39.7	35.1	31.1
10318380	**BM**	**38**	36.7	40.9	42.2	37.5	34
543250	**BM**	**25**	30.7	35.6	36.3	33.7	29.3
228651	**WF**	**65**	26.9	33.1	32.4	31.8	32.2
1041321	**WF**	**32**	35.7	36.6	39.3	38.3	31.8
1391501	**WF**	**50**	34.6	39.9	39.4	40.2	34.4
1505241	**WF**	**24**	31.7	37.9	40.3	30.6	22.8
3080371	**WF**	**37**	34.3	32.5	34.8	30.3	23.2
4697341	**WF**	**34**	31.7	33.4	35.6	32.3	24.6
5049551	**WF**	**55**	34.7	40	41	37.3	34.6
5219261	**WF**	**26**	31.2	34.7	36.1	36.1	27.7
6672461	**WF**	**46**	35.8	39.5	35.8	31.4	26.8
7010401	**WF**	**40**	30.9	36.6	38.2	36.4	30.2
8517231	**WF**	**23**	30.8	34.7	38.3	38.1	35.5
8968431	**WF**	**43**	37	41.4	44.4	39.3	34.2
9444231	**WF**	**23**	29.5	34.9	35.6	34.8	34.7
9766331	**WF**	**33**	32.3	33.8	35.6	34.2	28.4
474590	**WM**	**59**	35.6	42	44.1	42.5	35.4
844300	**WM**	**30**	30.7	35.2	31.7	32.8	26.5
2446350	**WM**	**35**	35.8	46.6	42.9	45.7	34.7
2796360	**WM**	**36**	36	41.7	41.9	39.9	33.3
3406620	**WM**	**62**	38	44.7	48.5	41.2	36.1
3996360	**WM**	**36**	37.4	40.4	43.7	42.9	35.5
4337270	**WM**	**27**	33.1	37.8	38.2	34.4	32.5
5431250	**WM**	**25**	38.4	41.4	37.5	34.7	30.9
5816390	**WM**	**39**	35.3	38.6	38.9	36.6	23
8064380	**WM**	**38**	35	38.7	41.2	33.3	28.7
9672360	**WM**	**36**	35.2	38.9	41.2	37.4	30.8
10153260	**WM**	**26**	32.5	36	39.1	42.3	34.5
10412510	**WM**	**51**	41.2	45.9	47.9	45.7	41.3

Case ID	P	Age	SPL				
			L1	L2	L3	L4	L5
Key: P = Population group; BM = Black males; BF = Black females; WM = White males; WF = White females. All measurements are in millimetres. Blank cells are those where measurements could not be performed							

Table A.3.16: Table indicating the pedicle height (PDH) measurement taken on the CT scans

Case ID	P	Age	PDH				
			L1	L2	L3	L4	L5
175281	**BF**	**28**	16.1	16.6	16.2	15.3	12.6
376411	**BF**	**41**	18	15.4	17.6	15.9	15.5
696271	**BF**	**27**	17.9	16.7	16.3	15.7	14
940381	**BF**	**38**	16.9	16.2	15	15.1	15.9
1188251	**BF**	**25**	15	14.6	15.4	14.4	13
1689331	**BF**	**33**	16.6	17.1	15.1	14.5	13.7
1983451	**BF**	**45**	15.3	13.5	13.6	13.5	12.9
2286451	**BF**	**45**	15	14.7	15.8	13.3	12.3
2622521	**BF**	**52**	16.9	16.9	15.8	14.6	12.6
3313231	**BF**	**23**	15.4	14	14.5	13.2	11.3
4006211	**BF**	**21**	14.8	13.5	14.1	13.1	
4811371	**BF**	**37**	15.6	16.2	16.1	15.2	14.6
4921271	**BF**	**27**	16.5	14.9	15	14.3	12.6
5378491	**BF**	**49**	16.4	15.6	15.3	14.5	14.7
5642231	**BF**	**23**	14.5	14.1	14.8	13.8	12.8
6309241	**BF**	**24**	18.3	17.4	19.3	17.8	15.4
7346221	**BF**	**22**	15.7	16.8	15.2	16.4	14.9
7479241	**BF**	**24**	17.6	18.9	16.9	15.3	12.3
7591291	**BF**	**29**	16.6	15	16.6	15.1	13.7
7963301	**BF**	**30**	18	17.7	17.7	15	13
8677261	**BF**	**26**	14.7	15.3	14.6	15.2	12.7
10277341	**BF**	**34**	17.6	17.8	18.3	16.5	13.6
745400	**BM**	**40**	17.7	18.9	16.9	15.3	15.9
1224630	**BM**	**63**	16.1	14.1	15.2	14.1	14.3
1751390	**BM**	**39**	16.2	18.5	17.9	14.3	14.2
1837250	**BM**	**25**	18	18.4	13.9	16.2	14.8

Case ID	P	Age	PDH				
			L1	L2	L3	L4	L5
2139430	**BM**	**43**	16.8	15.2	16.6	17.5	12.8
2336320	**BM**	**32**	14.8	17.5	17.1	19	19.8
2583380	**BM**	**38**	19.2	17.9	16.3	16.8	12.7
2838310	**BM**	**31**	18	18.2	18.4	18.1	14.8
2975380	**BM**	**38**	18.8	18.7	18.1	19	16.8
3591250	**BM**	**25**	16.3	18.9	19	19	16.7
3796340	**BM**	**34**	17.6	17.5	17.9	17.1	15.7
3819360	**BM**	**36**	18.2	16.2	17.1	14.1	12
4274270	**BM**	**27**	18.4	17.6	19.3	18.6	16.2
4421330	**BM**	**33**	18.2	17.6	16.1	14	
4518330	**BM**	**33**	16.1	16.1	17.2	15.7	13.5
4759360	**BM**	**36**	18.7	18.9	18.7	17.3	14.3
5114370	**BM**	**37**	16.1	16.9	17.7	16.5	15.1
5989270	**BM**	**27**	17.6	17.4	17.7	15.8	14.9
6105390	**BM**	**39**	17	19.3	16.1	19.6	18.3
6426270	**BM**	**27**	17.8	17.9	17.7	17.5	13.8
6771200	**BM**	**20**	18.4	18.2	17.1	14.9	15.7
7172230	**BM**	**23**	18.4	18.4	17.1	15.4	12.8
8199370	**BM**	**37**	19.2	20.8	18.4	17.2	16.6
8213390	**BM**	**39**	18.9	19.4	20.2	17.7	15.1
8313270	**BM**	**27**	19.7	19.5	20.5	19.4	18.2
8720220	**BM**	**22**	17.6	17.2	18.2	17.2	14.8
8887370	**BM**	**37**	18.6	17.1	17.7	17.7	15
9053260	**BM**	**26**	19.1	17.7	18	16.9	15.8
9519250	**BM**	**25**	16.7	16.9	18.7	16.3	14.3
9895210	**BM**	**21**	19.5	18.8	17.7	17.5	15.1
10037320	**BM**	**32**	20.2	20.2	19.7	18.8	18.7
10318380	**BM**	**38**	21.7	20.6	20.9	19.5	17.3
543250	**BM**	**25**	16.2	18.6	18.6	17.7	14.5
228651	**WF**	**65**	17.6	15.2	16.7	14.8	13.5
1041321	**WF**	**32**	14.7	16.5	16.8	15.8	13.1
1391501	**WF**	**50**	16.1	17.9	16	15.5	11
1505241	**WF**	**24**	15.2	14.3	13.5	12	14.4
3080371	**WF**	**37**	15.6	15.4	13.4	12.9	11.1
4697341	**WF**	**34**	16	15.2	16.9	14.6	14.7

Case ID	P	Age	PDH				
			L1	L2	L3	L4	L5
5049551	**WF**	**55**	19.5	18.7	21.1	19	16.7
5219261	**WF**	**26**	17.5	17.3	17.9	15.3	14.2
6672461	**WF**	**46**	13.5	14.3	14.9	14.4	14.3
7010401	**WF**	**40**	16.5	15	14.1	13.8	14
8517231	**WF**	**23**	17.9	16.2	16.2	18	15.2
8968431	**WF**	**43**	16.3	16.9	16.3	16.6	15.5
9444231	**WF**	**23**	14.4	13.9	14.4	13.7	13
9766331	**WF**	**33**	17.3	16.8	16.7	16.9	14.7
474590	**WM**	**59**	15.9	16.3	16.2	13.8	14.6
844300	**WM**	**30**	17	16.9	18	16.3	14.6
2446350	**WM**	**35**	15.7	12.3	14.7	16.2	15.7
2796360	**WM**	**36**	17.8	17.2	17.1	17	13.8
3406620	**WM**	**62**	16.5	17.5	16	14.9	14.2
3996360	**WM**	**36**	17.5	18.6	17.8	17.9	13.7
4337270	**WM**	**27**	18.6	18	16	17.5	14.2
5431250	**WM**	**25**	20.3	19.6	17.8	17	15.4
5816390	**WM**	**39**	19.2	18	18.8	17.1	16.1
8064380	**WM**	**38**	18.7	21.3	20.3	19.3	17.6
9672360	**WM**	**36**	16	16.6	17.3	17.3	15.4
10153260	**WM**	**26**	17.9	17.8	18.5	17.2	12.5
10412510	**WM**	**51**	20.6	20.1	22.5	17.7	14.6

Key: P = Population group; BM = Black males; BF = Black females; WM = White males; WF = White females. All measurements are in millimetres. Blank cells are those where measurements could not be performed

Table A.3.17: Table indicating the lateral pedicle diameter (PDDL) measured on the CT scans

Case ID	P	Age	PDDL				
			L1	L2	L3	L4	L5
175281	**BF**	**28**	10.45	9.8	9.65	12.25	13.1
376411	**BF**	**41**	7.8	8.05	10.6	12.85	16.1
696271	**BF**	**27**	9.35	9.75	10.2	12.35	15.15
940381	**BF**	**38**	8.5	10.2	12.4	14.05	16.05

Case ID	P	Age	PDDL				
			L1	L2	L3	L4	L5
1188251	**BF**	**25**	8.85	11.2	12.25	13.85	17.5
1689331	**BF**	**33**	9.45	8.85	10	11.05	14.35
1983451	**BF**	**45**	7.5	6.85	7.75	10.25	13.2
2286451	**BF**	**45**	10.1	11.05	11.95	11.5	12.15
2622521	**BF**	**52**	10.55	11.9	11.15	11.25	16.45
3313231	**BF**	**23**	7.5	7.75	10.1	10.65	14.1
4006211	**BF**	**21**	8.3	9.25	10.65	14.6	
4811371	**BF**	**37**	9.75	11.1	13.2	16.05	19.15
4921271	**BF**	**27**	8.15	9.85	10.6	11.7	15
5378491	**BF**	**49**	10.3	10.8	12.6	14.7	17.85
5642231	**BF**	**23**	9.5	10.05	11.1	13.2	15.7
6309241	**BF**	**24**	10.85	10.45	11.15	12.25	18.8
7346221	**BF**	**22**	10.7	10.1	10.2	12.1	13.2
7479241	**BF**	**24**	8.65	9.8	11.85	12.5	15.85
7591291	**BF**	**29**	10	8.85	11.35	13.8	17.9
7963301	**BF**	**30**	5.05	5.75	8.1	9.55	16.6
8677261	**BF**	**26**	6.45	7.1	9.05	11.05	12.55
10277341	**BF**	**34**	13.25	11.9	13.3	15	18.4
745400	**BM**	**40**	8.35	9.05	10.9	12.85	17.6
1224630	**BM**	**63**	8.3	9.45	11.1	13.3	15.2
1751390	**BM**	**39**	10.1	10.1	11.05	15	16.45
1837250	**BM**	**25**	6.85	7.5	9.3	9.65	10.65
2139430	**BM**	**43**	9.3	10.8	12.55	14.4	17.45
2336320	**BM**	**32**	11.15	11.15	11.75	14.45	17.45
2583380	**BM**	**38**	10.25	11.7	12.35	13.3	15.85
2838310	**BM**	**31**	13.4	11.35	13.05	15.1	16.65
2975380	**BM**	**38**	12.15	12.75	14.2	16.55	19.8
3591250	**BM**	**25**	12.55	14.15	14.4	17.25	22.45
3796340	**BM**	**34**	13.9	12.55	13.7	14.35	21.75
3819360	**BM**	**36**	10.95	10.65	10.9	12.95	16.5
4274270	**BM**	**27**	10.4	9.75	11.15	17.35	19.7
4421330	**BM**	**33**	11.45	11.95	15.5	18.1	
4518330	**BM**	**33**	10.65	10.7	12.35	14.6	16.2
4759360	**BM**	**36**	11.45	10.05	12.25	14.35	16.55
5114370	**BM**	**37**	10.3	10.7	12.2	13.3	17.55

Case ID	P	Age	PDDL				
			L1	L2	L3	L4	L5
5989270	**BM**	**27**	8.9	7.35	9.85	11.7	14.5
6105390	**BM**	**39**	12.5	13.8	14.3	15	16.45
6426270	**BM**	**27**	9.1	9	12	14.25	18.15
6771200	**BM**	**20**	9.9	10.2	11.7	14.05	17.45
7172230	**BM**	**23**	12.45	11.85	12.05	13.5	15.5
8199370	**BM**	**37**	10.5	12.45	12.95	16.3	19.5
8213390	**BM**	**39**	11.6	10.6	13.85	13.95	15.8
8313270	**BM**	**27**	11.65	11.95	13.05	14.8	17.4
8720220	**BM**	**22**	10	10.05	11.4	12.75	18.9
8887370	**BM**	**37**	11	11.05	12.6	13.2	19.6
9053260	**BM**	**26**	9.3	9.55	10.6	11.75	14.2
9519250	**BM**	**25**	11.85	11.9	13.8	16	17.3
9895210	**BM**	**21**	10.25	10.35	12.35	13.5	17.25
10037320	**BM**	**32**	12.45	11.85	13.25	15.6	21.7
10318380	**BM**	**38**	11.7	12.3	14.35	15.45	17.35
543250	**BM**	**25**	10.15	9.9	11.15	13.7	18.5
228651	**WF**	**65**	6.1	7.4	6.8	8	14.35
1041321	**WF**	**32**	8.5	9.85	10.6	13.55	14.85
1391501	**WF**	**50**	6.55	7.05	8.45	10.2	10.25
1505241	**WF**	**24**	7.5	9.4	11.7	13.65	16.35
3080371	**WF**	**37**	8.35	9.55	12.3	13.25	16.85
4697341	**WF**	**34**	5.2	5.65	7.2	9.95	13.45
5049551	**WF**	**55**	9.25	10.1	13.05	15.05	20.2
5219261	**WF**	**26**	5.7	7.45	8.8	10.15	13.7
6672461	**WF**	**46**	7.45	7.1	8.75	10.9	15.35
7010401	**WF**	**40**	6.4	7	7.55	9.85	13.65
8517231	**WF**	**23**	9.5	10.05	11.35	13.2	16.8
8968431	**WF**	**43**	8.55	8	10.95	12.2	17.8
9444231	**WF**	**23**	7.75	6.45	9.25	11.4	14.45
9766331	**WF**	**33**	8.35	9.15	12	13.55	18.3
474590	**WM**	**59**	7.85	9.5	10.1	13.5	17.85
844300	**WM**	**30**	7.85	9.1	11.4	13.25	16.7
2446350	**WM**	**35**	11.3	13	14.8	17.35	20
2796360	**WM**	**36**	7.7	8.6	11.25	13.8	16.6
3406620	**WM**	**62**	8.9	9.3	10.7	14.45	18.05

Case ID	P	Age	PDDL				
			L1	L2	L3	L4	L5
3996360	**WM**	**36**	7.65	8.85	10.95	13.2	17
4337270	**WM**	**27**	9.15	10.1	12.65	13.6	17.2
5431250	**WM**	**25**	9.85	12.25	13.55	13.8	19.9
5816390	**WM**	**39**	10.2	11.65	13.15	15.5	19.1
8064380	**WM**	**38**	7.9	8.5	10.35	13.55	14.7
9672360	**WM**	**36**	9.35	10.55	12.25	13.7	18.4
10153260	**WM**	**26**	9.35	9.55	9.9		14.5
10412510	**WM**	**51**	12.3	13.15	13.9	15.4	21.75

Key: P = Population group; BM = Black males; BF = Black females; WM = White males; WF = White females. All measurements are in millimetres. Blank cells are those where measurements could not be performed

Table A.3.18: Table indicating the AP diameter of the spinal canal (SCDAP) measured on the CT scans

Case ID	P	Age	SCDAP				
			L1	L2	L3	L4	L5
175281	**BF**	**28**	16	14.2	13.6	15.1	14.8
376411	**BF**	**41**	16.7	15.6	15.2	13.6	15.7
696271	**BF**	**27**	21.7		19.7	22.9	20
940381	**BF**	**38**	16.2	16.5	13.1	15.7	16.5
1188251	**BF**	**25**	16.6	15.5	15	13.8	14.8
1689331	**BF**	**33**	17.1	14.8	15.7	14.1	16.4
1983451	**BF**	**45**	15.9	14.4	13.1	12.1	11.7
2286451	**BF**	**45**	15.6	14.8	14.6	14.8	16
2622521	**BF**	**52**	16.8	16.6	18.2	18.2	16.5
3313231	**BF**	**23**	14.7	14.3	13.1	12.4	12.4
4006211	**BF**	**21**	13.5	12.9	12.9	14.6	
4811371	**BF**	**37**	13.7	13.1	12.5	11.6	11.9
4921271	**BF**	**27**	17.4	15.4	16.4	15.9	16.3
5378491	**BF**	**49**	12.7	13	12.7	12.9	13.6
5642231	**BF**	**23**	12.8	13.1	12.1	14.7	16.3
6309241	**BF**	**24**	15.6	14.8	15.9	16.2	18.9
7346221	**BF**	**22**	13.5	12.2	13	13.3	14.4

Case ID	P	Age	SCDAP				
			L1	L2	L3	L4	L5
7479241	**BF**	**24**	16.5	16.2	16	17.2	20.5
7591291	**BF**	**29**	13.9	11.8	13.6	12.6	12.4
7963301	**BF**	**30**	15.9	14.3	13.3	13.7	15.3
8677261	**BF**	**26**	14.6	13.8	13.3	12.5	13.6
10277341	**BF**	**34**	12.9	12.1	12.4	14.6	15.4
745400	**BM**	**40**	17.9	15.2	15.5	12.7	14
1224630	**BM**	**63**	16	17.3	16.1	16.6	17.3
1751390	**BM**	**39**	19.1	19	16.2	16.2	18.7
1837250	**BM**	**25**	13.1	13.1	13.6	11.5	12.3
2139430	**BM**	**43**	15.6	14.2	12.8	13.1	17.2
2336320	**BM**	**32**	16.4	15.2	14.8	15.4	16.2
2583380	**BM**	**38**	14.8	16.8	14.1	14.1	18.6
2838310	**BM**	**31**	14.2	15.6	14.2	14.3	17.5
2975380	**BM**	**38**	14	15.7	16.7	16.1	16.6
3591250	**BM**	**25**	17.3	16.8	17	18.3	18.5
3796340	**BM**	**34**	13.8	14.2	13.1	13	12.3
3819360	**BM**	**36**	15.5	15.2	14.2	13.1	14.5
4274270	**BM**	**27**	16.3	16.1	14	14.5	14.7
4421330	**BM**	**33**	15.9	15.8	18.3	21	
4518330	**BM**	**33**	12.9	13.3	12.7	14.9	15.2
4759360	**BM**	**36**	19.2	18.2	17.5	16.3	18.3
5114370	**BM**	**37**	15.7	16.2	16.2	17.3	19.5
5989270	**BM**	**27**	16.8	15.6	13.9	13.8	14.2
6105390	**BM**	**39**	13.2	15.1	14.3	17.8	18.6
6426270	**BM**	**27**	16.3	14.7	13.9	13.7	14.4
6771200	**BM**	**20**	13.2	12.3	11.6	13.5	13.6
7172230	**BM**	**23**	17.1	15.4	15.1	17.1	19.7
8199370	**BM**	**37**	13.9	13.9	16.5	20.2	20.5
8213390	**BM**	**39**	13.2	11.6	11.9	11.9	15.8
8313270	**BM**	**27**	14.8	13.8	14.3	15	16.4
8720220	**BM**	**22**	17.6	15.2	14.4	15.7	17.6
8887370	**BM**	**37**	14	12.6	11	12.4	13.7
9053260	**BM**	**26**	13.4	13	11.7	13.2	13.1
9519250	**BM**	**25**	16	16.1	15.8	14.9	17.9
9895210	**BM**	**21**	16.3	15.7	16.5	16.2	17

Case ID	P	Age	SCDAP				
			L1	L2	L3	L4	L5
10037320	**BM**	**32**	15.5	15.8	14.8	14.8	15.5
10318380	**BM**	**38**	15.5	15.5	14.4	15.5	16.6
543250	**BM**	**25**	18.5		20.2	21.9	17.9
228651	**WF**	**65**	19.2	19.3	22	19.9	20
1041321	**WF**	**32**	16.2	13.9	13	12.2	12.5
1391501	**WF**	**50**	17.1	17.8	15.8	14.9	15
1505241	**WF**	**24**	17.7	16.3	19.2	19	18.4
3080371	**WF**	**37**	13	12.9	14.3	14.7	16.1
4697341	**WF**	**34**	15.9	16.8	14.5	17.6	17.1
5049551	**WF**	**55**	19.2	17.5	18.8	16.8	19.4
5219261	**WF**	**26**	17.8	15.9	15.2	14.9	15.2
6672461	**WF**	**46**	16.4	17.9	17.2	18.5	19.9
7010401	**WF**	**40**	16	14.7	15.2	13.9	13.5
8517231	**WF**	**23**	18.4	18.3	16.6	16.6	17.3
8968431	**WF**	**43**	16.2	12.8	13.1	13.1	12
9444231	**WF**	**23**	18.4	18.9	18.4	16.7	17.3
9766331	**WF**	**33**	17.4	17	18.1	20.9	18.1
474590	**WM**	**59**	15.7	14.4	12	13.5	13.7
844300	**WM**	**30**	14.1	14.5	15.6	13	15.3
2446350	**WM**	**35**	15	14.1	14.4	13.7	17.7
2796360	**WM**	**36**	14.8	13.5	13.9	11.1	14.4
3406620	**WM**	**62**	15.4		16.1	17.9	18.3
3996360	**WM**	**36**	16	14	12	11.8	15.5
4337270	**WM**	**27**	15.4	13.9	14.5	16.7	19.7
5431250	**WM**	**25**	14.9	14.9	17.4	19.5	18.5
5816390	**WM**	**39**	15.3	13.6	12.4	13.1	15.6
8064380	**WM**	**38**	14.9	14.3	14.1	15.7	16.8
9672360	**WM**	**36**	16.7	14.5	13.6	15.8	19.2
10153260	**WM**	**26**	16	14.4	13.1	12.6	14.4
10412510	**WM**	**51**	14.8	14.6	12.2	12.4	14.8

Key: P = Population group; BM = Black males; BF = Black females; WM = White males; WF = White females. All measurements are in millimetres. Blank cells are those where measurements could not be performed

Table A.3.19: Table indicating the lateral spinal canal diameter (SCDL) measured on the CT scans

Case ID	P	Age	SCDL				
			L1	L2	L3	L4	L5
175281	**BF**	**28**	20.5	20.2	22.4	21.7	26.8
376411	**BF**	**41**	19.3	19.7	20.2	25.8	26.1
696271	**BF**	**27**	19.7	20.1	23.9	26.4	27.9
940381	**BF**	**38**	18.7	21.2	19.8	21.5	22
1188251	**BF**	**25**	18.5	19.4	22.4	24.3	25.6
1689331	**BF**	**33**	21.6	20.4	23.4	25.7	31.2
1983451	**BF**	**45**	19.2	17.8	18.2	20.1	21.6
2286451	**BF**	**45**	20.6	20.1	20.3	24.1	31.1
2622521	**BF**	**52**	24.6	25.2	26	29.6	31.1
3313231	**BF**	**23**	21.4	21.1	22.1	22.5	25.1
4006211	**BF**	**21**	21.7	21.2	21.1	24.3	
4811371	**BF**	**37**	21	20.6	21	21.8	29.4
4921271	**BF**	**27**	22.2	21.4	23.1	22.6	27
5378491	**BF**	**49**	19.8	19.6	22.2	22.2	22.7
5642231	**BF**	**23**	18.2	16.8	20	21.2	26.3
6309241	**BF**	**24**	21.8	22.4	24.5	22.9	24
7346221	**BF**	**22**	18.7	17.5	17.6	17.8	19.8
7479241	**BF**	**24**	22.9	21.9	22.2	20.6	23.9
7591291	**BF**	**29**	18	19	19.2	21.4	27
7963301	**BF**	**30**	21.3	21.7	21.9	21.7	24.9
8677261	**BF**	**26**	21.4	20.6	19.7	23.8	24.9
10277341	**BF**	**34**	16.8	19	22.8	22.8	27.3
745400	**BM**	**40**	20.4	20.4	24.5	25.4	27.2
1224630	**BM**	**63**	20.6	19.5	22.1	23.4	25.9
1751390	**BM**	**39**	24.6	24.6	25.3	27.1	33.8
1837250	**BM**	**25**	22.9	20.7	20.7	22.7	22.7
2139430	**BM**	**43**	22.8	22.5	21.3	22.6	25.2
2336320	**BM**	**32**	21.7	24.5	25.6	29	33.2
2583380	**BM**	**38**	21.7	23.3	25.5	26.8	33.8
2838310	**BM**	**31**	20.2	21.4	21.5	21.1	24.9
2975380	**BM**	**38**	23.4	19.8	20.6	24.4	24.2

Case ID	P	Age	SCDL				
			L1	L2	L3	L4	L5
3591250	**BM**	**25**	21.3	22.6	26.4	25.9	31.1
3796340	**BM**	**34**	20.3	20.7	20.7	23.2	25.6
3819360	**BM**	**36**	24.8	23.1	24.7	26.4	30.9
4274270	**BM**	**27**	21.6	21.8	22.8	22.8	22.1
4421330	**BM**	**33**	27.3	26.7	27.2	32.3	
4518330	**BM**	**33**	21.1	19.7	22.6	22.8	26.8
4759360	**BM**	**36**	22.2	23.8	23.4	24.6	24.2
5114370	**BM**	**37**	20.5	22	24.3	26.8	27.1
5989270	**BM**	**27**	22.3	21.3	22.3	28.3	29.6
6105390	**BM**	**39**	21.4	24.8	23.3	30	31
6426270	**BM**	**27**	25.6	24.2	24.5	27.3	25.7
6771200	**BM**	**20**	19.7	21.6	22.2	21.5	22.1
7172230	**BM**	**23**	25.5	23.6	28.2	29.6	33.7
8199370	**BM**	**37**	23.1	24.7	28.6	28.6	29.2
8213390	**BM**	**39**	21.9	20.9	26.1	26.4	29.9
8313270	**BM**	**27**	22.3	21.2	20.6	22.6	25.7
8720220	**BM**	**22**	24.8	25	26.5	30.4	28.5
8887370	**BM**	**37**	19.1	20.4	19.9	20.1	24.7
9053260	**BM**	**26**	19	20.7	21.4	25.4	28
9519250	**BM**	**25**	19.1	19.3	22.4	23.3	26.6
9895210	**BM**	**21**	20.4	21.5	23.1	23.5	25.9
10037320	**BM**	**32**	21.1	20.7	22.8	28.7	28.4
10318380	**BM**	**38**	21.8	23.2	23.1	26.5	29.8
543250	**BM**	**25**	25.6	24.8	25.7	32.5	34.2
228651	**WF**	**65**	24.1	24.8	30.1	29.3	34.4
1041321	**WF**	**32**	19.7	20.8	21.8	19.1	20.7
1391501	**WF**	**50**	21.9	21.6	21.6	21.9	24
1505241	**WF**	**24**	22.1	22.1	24	32.8	32.9
3080371	**WF**	**37**	20.8	23	22.6	24.4	29
4697341	**WF**	**34**	22.3	22	22.8	28	28.5
5049551	**WF**	**55**	21.5	22.4	22.4	25.5	27.4
5219261	**WF**	**26**	22.7	22	22	25.4	25.1
6672461	**WF**	**46**	21.3	21.4	24.7	25.8	32
7010401	**WF**	**40**	22.9	22.2	21.2	22.2	24.9
8517231	**WF**	**23**	23.7	23.9	25.2	26.6	26.9

Case ID	P	Age	SCDL				
			L1	L2	L3	L4	L5
8968431	**WF**	**43**	21.5	20.4	22.6	22.9	24.9
9444231	**WF**	**23**	22.5	23.8	22.5	23.3	25
9766331	**WF**	**33**	23.5	23.1	24.4	23.3	26.4
474590	**WM**	**59**	24.3	23.8	24.7	26.1	25.2
844300	**WM**	**30**	20.8	21.5	24.5	22.6	26.8
2446350	**WM**	**35**	26.2	25.2	24.5	27.4	28.5
2796360	**WM**	**36**	21.8	21.3	23.5	24	25.4
3406620	**WM**	**62**	24.5	24.1	25.2	26.3	29.6
3996360	**WM**	**36**	23.1	24.3	22.8	25.2	27.2
4337270	**WM**	**27**	23	22.4	23.9	24.5	26.3
5431250	**WM**	**25**	24.2	22.6	26.3	27.8	31.5
5816390	**WM**	**39**	23.5	23.7	25.3	24.1	26.6
8064380	**WM**	**38**	22.7	22.3	23.4	25	32.9
9672360	**WM**	**36**	21.5	19.5	19.4	21.9	27.1
10153260	**WM**	**26**	22.6	22.3	24.8	24.6	27
10412510	**WM**	**51**	22.6	21.6	20.5	21.8	26.1

Key: P = Population group; BM = Black males; BF = Black females; WM = White males; WF = White females. All measurements are in millimetres. Blank cells are those where measurements could not be performed

Appendix A.4 – Raw CT data: Vertebral body measurements

Table A.4.20: Table indicating the maximum lateral vertebral body diameter (VDMaxL) measurements taken on the CT scans

Case ID	P	Age	VDMaxL				
			L1	L2	L3	L4	L5
175281	**BF**	**28**	35.9	38.4	41.3	43.3	44.9
376411	**BF**	**41**	38.5	39.2	40.3	44.1	46.4
696271	**BF**	**27**	36.5	40.3	44.3	44.6	46.2
940381	**BF**	**38**	38.2	42.3	45	49	53.4
1188251	**BF**	**25**	40.7	42.4	45	47.7	50.6

Case ID	P	Age	VDMaxL				
			L1	L2	L3	L4	L5
1689331	**BF**	**33**	39.6	43.2	45.3	46.9	50.4
1983451	**BF**	**45**	36	40.5	42.2	44.4	46.1
2286451	**BF**	**45**	40.5	43.6	45.9	49.4	48.2
2622521	**BF**	**52**	46.2	46.6	46.9	51.6	57.3
3313231	**BF**	**23**	39.4	40.6	40.5	42.7	46.1
4006211	**BF**	**21**	38.5	42.4	43.7	45.4	
4811371	**BF**	**37**	42.7	45.6	49.8	51.7	53.5
4921271	**BF**	**27**	38.6	42.8	45	45.7	46.9
5378491	**BF**	**49**	45.4	48.4	51.4	55.9	55.5
5642231	**BF**	**23**	35.4	36.5	38.9	41.7	42.2
6309241	**BF**	**24**	44.4	47.4	50.6	50.1	50.4
7346221	**BF**	**22**	36	39.6	41.6	42.9	44
7479241	**BF**	**24**	38.6	41.7	42.7	44.2	47.2
7591291	**BF**	**29**	40.1	42.2	42.6	45.8	47.4
7963301	**BF**	**30**	39.4	40.3	41.2	45	44.9
8677261	**BF**	**26**	35.3	37.4	38.2	43.3	43.3
10277341	**BF**	**34**	48.3	48.6	51.4	53.6	56
745400	**BM**	**40**	44	45.8	49.4	51.2	51.9
1224630	**BM**	**63**	39.6	44.2	46.3	47.8	53.1
1751390	**BM**	**39**	47.7	50.9	51.8	55.2	57.2
1837250	**BM**	**25**	41.9	44.8	44.8	46.6	47.8
2139430	**BM**	**43**	45.6	46.7	49.4	50.2	52.8
2336320	**BM**	**32**	44.5	46.9	49.7	51.7	49.9
2583380	**BM**	**38**	50.9	54	57.5	57.8	57.9
2838310	**BM**	**31**	47.1	49	53.5	52.6	58.4
2975380	**BM**	**38**	44.8	48.2	53	51.6	54.8
3591250	**BM**	**25**	53.5	54.8	56.3	58.9	61.4
3796340	**BM**	**34**	48.9	50.8	52.8	55.3	63.4
3819360	**BM**	**36**	47.9	50.3	53.2	52.5	59
4274270	**BM**	**27**	46.7	47.4	50	51.3	56.3
4421330	**BM**	**33**	49.1	51.4	53.1	55.9	
4518330	**BM**	**33**	43.4	47.8	49.9	53	55.2
4759360	**BM**	**36**	44.9	47.5	48.7	50.5	53.6
5114370	**BM**	**37**	45.4	47.8	47.6	48.9	53.2
5989270	**BM**	**27**	40.5	43.4	45.1	47.3	46.3

Case ID	P	Age	VDMaxL				
			L1	L2	L3	L4	L5
6105390	**BM**	**39**	49.2	53.1	50.3	52.1	56.3
6426270	**BM**	**27**	47	47.6	50.2	53	53
6771200	**BM**	**20**	41	43.3	45.6	47.7	48.7
7172230	**BM**	**23**	44.7	46.6	49.4	51.6	53.4
8199370	**BM**	**37**	48	51.7	53.8	55.6	57.8
8213390	**BM**	**39**	46.7	46.6	51.1	52.1	56
8313270	**BM**	**27**	49	50.7	52.2	52.8	52.7
8720220	**BM**	**22**	46.4	48.3	49.4	52.1	55.4
8887370	**BM**	**37**	43.8	46.5	49.2	51.3	53.4
9053260	**BM**	**26**	44.7	47	47.7	49.2	51.4
9519250	**BM**	**25**	42.6	46.2	48.1	48.8	52.8
9895210	**BM**	**21**	45.7	48.1	48.1	51.6	48.5
10037320	**BM**	**32**	47.8	46.8	49.8	55.1	57.3
10318380	**BM**	**38**	45.1	49.7	52.7	57	56.6
543250	**BM**	**25**	44.8	47.5	52.2	53.1	53.5
228651	**WF**	**65**	42.4	46	48.1	49.6	55.6
1041321	**WF**	**32**	40.6	44.1	44.4	46.8	48
1391501	**WF**	**50**	40.3	45	46	52.7	55.9
1505241	**WF**	**24**	40.5	41.9	41.2	46.2	45.1
3080371	**WF**	**37**	37.2	38.7	42.8	44.7	46
4697341	**WF**	**34**	37.4	40.4	41.7	45	45.9
5049551	**WF**	**55**	43.3	46.5	47.2	49.5	56.2
5219261	**WF**	**26**	37.4	39.9	43.4	45.5	46
6672461	**WF**	**46**	36.7	43.6	43	42.4	44.7
7010401	**WF**	**40**	38.5	39.3	40	44	45.9
8517231	**WF**	**23**	40.8	44.3	46.6	48.2	49.1
8968431	**WF**	**43**	40.8	44.4	46.7	49.2	49.7
9444231	**WF**	**23**	39.5	39.2	40.6	43.3	46.6
9766331	**WF**	**33**	40.1	42.4	44.3	45.9	50.2
474590	**WM**	**59**	46.1	46.1	51.1	52.7	56.9
844300	**WM**	**30**	44.3	46.2	48.7	49	52.2
2446350	**WM**	**35**	50.5	54.7	56.2	59.4	59.1
2796360	**WM**	**36**	45.7	47.6	51.8	52.1	51.7
3406620	**WM**	**62**	51.5	54.1	54.8	53.7	59.2
3996360	**WM**	**36**	45.4	47.9	48	52.2	52.7

Case ID	P	Age	VDMaxL				
			L1	L2	L3	L4	L5
4337270	**WM**	**27**	40.2	42.6	46.3	46	50.2
5431250	**WM**	**25**	47.3	49.1	50.2	51.8	58.5
5816390	**WM**	**39**	47.3	49.1	53.4	53.4	53.9
8064380	**WM**	**38**	43.6	44.7	47	49.7	50.4
9672360	**WM**	**36**	45.9	44.8	47.9	51.5	53.8
10153260	**WM**	**26**	44.1	47.1	46.9	48.7	51.8
10412510	**WM**	**51**	52.3	55.8	57	58.9	61.7

Key: P = Population group; BM = Black males; BF = Black females; WM = White males; WF = White females. All measurements are in millimetres. Blank cells are those where measurements could not be performed

Table A.4.21: Table indicating the minimum lateral vertebral body diameter (VDMinL) measurement taken on the CT scans

Case ID	P	Age	VDMinL				
			L1	L2	L3	L4	L5
175281	**BF**	**28**	34.5	34.7	38.6	40.2	42
376411	**BF**	**41**	33.9	35.7	36.3	40.4	40.1
696271	**BF**	**27**	33.2	35.1	38.7	42.5	41.8
940381	**BF**	**38**	36.5	38.2	40.3	43.8	47.6
1188251	**BF**	**25**	36	37.2	41.9	45	43.8
1689331	**BF**	**33**	36	39	41.7	45.5	46.2
1983451	**BF**	**45**	33.3	35.5	36.7	37.5	36.5
2286451	**BF**	**45**	37.4	38.6	40.9	43.9	40.9
2622521	**BF**	**52**	41.3	41.5	44.2	45.9	49.1
3313231	**BF**	**23**	34.2	34.9	36.4	36.1	36
4006211	**BF**	**21**	36.4	38	39.2	37.3	
4811371	**BF**	**37**	40.1	42.1	43.9	47.1	46.8
4921271	**BF**	**27**	34.6	36.9	37.4	38.6	33.8
5378491	**BF**	**49**	41	43.7	45.3	49.8	45.2
5642231	**BF**	**23**	33.7	33.3	33.4	35.4	33.8
6309241	**BF**	**24**	41.7	42	43.9	45.2	38.8

Case ID	P	Age	VDMinL				
			L1	L2	L3	L4	L5
7346221	**BF**	**22**	33.1	35.7	37.3	38.7	38.8
7479241	**BF**	**24**	34.6	36.7	37.7	40.6	38.1
7591291	**BF**	**29**	36	35.7	38.3	41.6	40.8
7963301	**BF**	**30**	34.5	35	36.5	39.4	39.4
8677261	**BF**	**26**	33.8	34.6	36.9	37.8	36.4
10277341	**BF**	**34**	44.3	45.9	46.7	47.6	49.7
745400	**BM**	**40**	37.9	37.6	40.9	44.1	40.7
1224630	**BM**	**63**	35.8	36.8	40.8	40.4	43.6
1751390	**BM**	**39**	43.1	45	46	47.2	48.1
1837250	**BM**	**25**	35.7	34	37.4	38.2	40.2
2139430	**BM**	**43**	39.9	40.9	42.8	41.9	45
2336320	**BM**	**32**	41.8	42	45.3	48.4	44.6
2583380	**BM**	**38**	44.4	49.2	50.6	50.2	47.6
2838310	**BM**	**31**	42.3	44	46.2	48.8	47.5
2975380	**BM**	**38**	40.8	42.8	46.8	48.6	48.8
3591250	**BM**	**25**	48.2	49.7	50.8	52.3	49.7
3796340	**BM**	**34**	44.7	44.2	46.8	49.2	52.9
3819360	**BM**	**36**	45.7	46.7	46.9	50.5	47.7
4274270	**BM**	**27**	40	40.7	43.1	47.6	50.3
4421330	**BM**	**33**	47.9	48.3	49.6	47.1	
4518330	**BM**	**33**	39.7	39.7	41.9	44.2	45.3
4759360	**BM**	**36**	40.6	41	42.5	44.2	43.7
5114370	**BM**	**37**	42.4	42.1	41.9	44.1	46.1
5989270	**BM**	**27**	37.9	39.3	42.3	41.6	40.5
6105390	**BM**	**39**	46	48.3	44.7	45.1	51.8
6426270	**BM**	**27**	40.1	42.2	44.4	46.3	43.4
6771200	**BM**	**20**	39	39.1	41.2	43.8	42.7
7172230	**BM**	**23**	42.4	44.8	45.4	45.6	45.4
8199370	**BM**	**37**	45.1	47.2	49	52.2	49.1
8213390	**BM**	**39**	40.2	42.8	43.7	46.6	43.8
8313270	**BM**	**27**	41.9	44.7	45.1	46.7	44.2
8720220	**BM**	**22**	41.1	43.7	45.7	47.9	49.9
8887370	**BM**	**37**	39.5	43	45.4	47	43.5
9053260	**BM**	**26**	41.4	41.9	42.4	43.4	44.4
9519250	**BM**	**25**	40.5	41.7	44.6	45.7	46.6

Case ID	P	Age	VDMinL				
			L1	L2	L3	L4	L5
9895210	**BM**	**21**	41.8	42.9	42.5	44.4	40.9
10037320	**BM**	**32**	43.4	43	43.7	48.6	47.6
10318380	**BM**	**38**	42.3	44.2	46.4	47.3	42.9
543250	**BM**	**25**	42.5	43.2	46.3	47.1	47.6
228651	**WF**	**65**	38.4	40.9	44.2	47.2	47.2
1041321	**WF**	**32**	36.3	39	39.9	39.8	38.4
1391501	**WF**	**50**	33.4	35.5	37.3	37.6	41.1
1505241	**WF**	**24**	36.7	35.3	37.4	41.6	39.5
3080371	**WF**	**37**	33.3	35	37.8	39.6	36.9
4697341	**WF**	**34**	34.1	34	36	37.9	38.7
5049551	**WF**	**55**	41	42.8	45.7	46.9	43.2
5219261	**WF**	**26**	33.8	35.4	37.6	36.5	36.6
6672461	**WF**	**46**	32.8	35.9	36	37	38.6
7010401	**WF**	**40**	33.8	33.2	35.8	38.5	37.3
8517231	**WF**	**23**	37.1	39.8	41	42.2	41.7
8968431	**WF**	**43**	36.9	38.3	42.2	45.5	43
9444231	**WF**	**23**	33.7	31	35.4	35.4	36.7
9766331	**WF**	**33**	34.4	37.6	40.3	41.4	43
474590	**WM**	**59**	40.5	41.4	43.8	46.7	45.3
844300	**WM**	**30**	40	40.9	42.5	43.7	41.5
2446350	**WM**	**35**	42.6	43.2	44.7	49.7	48.3
2796360	**WM**	**36**	40.2	43.7	45.3	45.3	44.3
3406620	**WM**	**62**	42.8	43.5	46.8	48.6	49.7
3996360	**WM**	**36**	39.7	42.2	44.1	44.6	43.5
4337270	**WM**	**27**	35.1	36	40.6	41.7	40.2
5431250	**WM**	**25**	44	44.2	45.2	47.5	46.5
5816390	**WM**	**39**	39.6	43	44.2	43.7	40.6
8064380	**WM**	**38**	36.5	38.2	41	42.2	44.1
9672360	**WM**	**36**	39.1	39.6	41.6	43.2	42.7
10153260	**WM**	**26**	39.6	40.3	39.2	42.3	42.3
10412510	**WM**	**51**	49.7	49.8	51.3	50.2	47.8

Key: P = Population group; BM = Black males; BF = Black females; WM = White males; WF = White females. All measurements are in millimetres. Blank cells are those where measurements could not be performed

Table A.4.22: Table indicating the maximum AP vertebral body diameter (VDMaxAP) measurement taken on the CT scans

Case ID	P	Age	VDMaxAP				
			L1	L2	L3	L4	L5
175281	**BF**	**28**	26.6	29.1	30.9	31.4	33.2
376411	**BF**	**41**	26.3	28.3	29.2	32.4	34.3
696271	**BF**	**27**	29.1	31.9	33.5	32.9	32.2
940381	**BF**	**38**	27.7	30.4	30.7	33.5	32.7
1188251	**BF**	**25**	25.4	27.1	28.5	31	31.5
1689331	**BF**	**33**	26.6	29.2	31.4	32.2	33.5
1983451	**BF**	**45**	27.1	27.6	29.7	31.1	32.6
2286451	**BF**	**45**	29.6	32.4	34.1	35.2	35.9
2622521	**BF**	**52**	30.4	31.1	33.5	35.8	39.7
3313231	**BF**	**23**	28.1	31.1	31.1	34.1	34.8
4006211	**BF**	**21**	26.2	28.9	29.2	30.2	
4811371	**BF**	**37**	30.2	32	34.4	37	37.5
4921271	**BF**	**27**	28.6	33.1	34	34.3	34.7
5378491	**BF**	**49**	28.3	30.7	33.4	33.2	36
5642231	**BF**	**23**	26.5	27.3	29.6	29.6	30
6309241	**BF**	**24**	30.7	29.7	31	32.3	37.9
7346221	**BF**	**22**	24.2	23.5	25.8	28.2	29.4
7479241	**BF**	**24**	26.5	28.4	29.6	28.8	29.6
7591291	**BF**	**29**	28.4	27.9	29.3	29.6	30.2
7963301	**BF**	**30**	27.8	28.7	31.6	32.9	33.4
8677261	**BF**	**26**	29.6	28.5	32.6	30.3	30.9
10277341	**BF**	**34**	30.5	32.4	33.5	34.2	35.2
745400	**BM**	**40**	31.5	34	35.1	36.5	38.2
1224630	**BM**	**63**	28.1	31.3	31	31.9	37.3
1751390	**BM**	**39**	38.1	37.2	37.2	35.9	36.4
1837250	**BM**	**25**	30.1	33.3	43.6	34.3	35.2
2139430	**BM**	**43**	35.7	38.6	38.4	39.6	36.7
2336320	**BM**	**32**	32.1	31.2	33.4	35.3	37.5
2583380	**BM**	**38**	33.7	35	33.8	34.9	38
2838310	**BM**	**31**	31.4	33.3	33	36	36.5
2975380	**BM**	**38**	32.8	35.7	34.5	35.9	39.6

Case ID	P	Age	VDMaxAP				
			L1	L2	L3	L4	L5
3591250	**BM**	**25**	34.5	35.5	36.1	37.8	42.9
3796340	**BM**	**34**	34.6	35.4	35.8	37.8	38.2
3819360	**BM**	**36**	32.4	34.1	37.2	38	38.9
4274270	**BM**	**27**	37.2	37	36	35.2	35.6
4421330	**BM**	**33**	32.4	33.1	32.8	34.7	
4518330	**BM**	**33**	29.1	30.7	33.2	34.9	36.9
4759360	**BM**	**36**	29.5	30.1	32.4	34.3	34.6
5114370	**BM**	**37**	32.5	33.1	34.2	33.7	34.8
5989270	**BM**	**27**	30	31.7	34.8	35.7	37.7
6105390	**BM**	**39**	33.7	35.7	35.9	38.1	
6426270	**BM**	**27**	32	35.3	36.2	36.7	38.4
6771200	**BM**	**20**	28.7	30.4	32.9	32.4	35
7172230	**BM**	**23**	32.1	33.9	34.3	33.4	35.6
8199370	**BM**	**37**	32.9	36.2	37.8	36.2	37.5
8213390	**BM**	**39**	30.9	32.8	36.3	36.7	36.8
8313270	**BM**	**27**	32.5	32.6	34.3	35.6	36.6
8720220	**BM**	**22**	36.1	38.5	38.8	40.8	37.7
8887370	**BM**	**37**	29.6	32.6	35.2	37.1	37.9
9053260	**BM**	**26**	30.7	32.4	34.6	34.6	37.3
9519250	**BM**	**25**	32	35.1	34.4	37	36.3
9895210	**BM**	**21**	29.1	31.4	32.8	34	38.5
10037320	**BM**	**32**	30.1	30.3	32	34	35.2
10318380	**BM**	**38**	33	34.4	34.8	34.6	37.8
543250	**BM**	**25**	29.9	32	32.8	33.7	35
228651	**WF**	**65**	36.3	37.9	33.7	33.3	32.8
1041321	**WF**	**32**	31.9	33.1	33.5	34.3	39.6
1391501	**WF**	**50**	33.4	35.2	37.1	37.3	33.5
1505241	**WF**	**24**	30.4	31.8	31.1	31.4	36
3080371	**WF**	**37**	32.3	32.7	32.3	33.6	37.7
4697341	**WF**	**34**	26.6	28.5	30.5	29.9	31.1
5049551	**WF**	**55**	30	30.2	31.4	30.4	31.8
5219261	**WF**	**26**	30.9	33	31.7	30.5	32.5
6672461	**WF**	**46**	27.4	30.5	30.1	30.1	33.6
7010401	**WF**	**40**	28	29.2	31.2	30.6	32
8517231	**WF**	**23**	30.6	32.7	33.9	33.7	34.9

Case ID	P	Age	VDMaxAP				
			L1	L2	L3	L4	L5
8968431	**WF**	**43**	33	35.5	36.6	37.2	38.9
9444231	**WF**	**23**	33.7	31.8	31.8	33.2	34.8
9766331	**WF**	**33**	30	29.4	32.1	33.1	34.4
474590	**WM**	**59**	34.7	37.9	37.9	36.9	39.1
844300	**WM**	**30**	36.2	36.8	36.3	37.5	39.7
2446350	**WM**	**35**	41.5	43.9	42.5	40.3	40.7
2796360	**WM**	**36**	33.4	34.2	34.9	37.3	34.7
3406620	**WM**	**62**	38.1	37.6	39.1	38.4	43.6
3996360	**WM**	**36**	32.4	32.5	32.5	34.4	35.1
4337270	**WM**	**27**	31.8	33.3	33.3	33	33.9
5431250	**WM**	**25**	33.2	35.8	35.9	35.3	36.3
5816390	**WM**	**39**	32.1	32.1	35.4	35.4	40.9
8064380	**WM**	**38**	35.5	36.9	35.9	36.9	39.4
9672360	**WM**	**36**	33.9	34.4	35	34.6	35.3
10153260	**WM**	**26**	32.5	34.5	35.8	37	35.2
10412510	**WM**	**51**	37.7	40.8	39.9	40.1	39.2

Key: P = Population group; BM = Black males; BF = Black females; WM = White males; WF = White females. All measurements are in millimetres. Blank cells are those where measurements could not be performed

Table A.4.23: Table indicating the minimum AP vertebral body diameter (VDMinAP) measured on the CT scans

Case ID	P	Age	VDMinAP				
			L1	L2	L3	L4	L5
175281	**BF**	**28**	25.7	27.1	28.9	29.8	31.8
376411	**BF**	**41**	22.3	24.1	26.1	29	31.5
696271	**BF**	**27**	26.2	28.9	31.8	31.6	31.8
940381	**BF**	**38**	24.5	28.3	28.9	29.5	29.8
1188251	**BF**	**25**	22.6	24.5	25.4	28	30.7
1689331	**BF**	**33**	24.7	26.2	29.1	31	32
1983451	**BF**	**45**	24.4	25.2	27.3	28.5	30.7
2286451	**BF**	**45**	26.3	29.4	30.6	32.1	34.6
2622521	**BF**	**52**	26.5	29.4	31.1	34.2	35.2

Case ID	P	Age	VDMinAP				
			L1	L2	L3	L4	L5
3313231	**BF**	**23**	26.2	28.5	29.2	30.7	33.7
4006211	**BF**	**21**	24.8	26.7	28.1	29.5	
4811371	**BF**	**37**	28.2	30.3	32.1	35.5	35.7
4921271	**BF**	**27**	24.2	29.5	30.6	32.1	31.4
5378491	**BF**	**49**	26.7	28.9	31.9	31.7	33
5642231	**BF**	**23**	25.9	26.6	27.9	28.2	29.6
6309241	**BF**	**24**	29.2	29.1	29.1	31	36.6
7346221	**BF**	**22**	22.6	22.2	25	26.7	28.2
7479241	**BF**	**24**	24.6	27.4	27.9	28.1	27.7
7591291	**BF**	**29**	24.8	26.5	27.3	28.2	29.4
7963301	**BF**	**30**	26.4	26.4	29.4	31.1	32.4
8677261	**BF**	**26**	26.3	28.2	30.1	29	29.5
10277341	**BF**	**34**	29.4	31.3	32.1	33.8	33.8
745400	**BM**	**40**	27.2	30.4	33.4	35.1	35.1
1224630	**BM**	**63**	25.3	26.9	27.7	29.3	34.1
1751390	**BM**	**39**	34.5	35.9	34	33.1	33.7
1837250	**BM**	**25**	26.1	28.3	37	33	33.3
2139430	**BM**	**43**	32.3	35.9	35.9	37.1	35.7
2336320	**BM**	**32**	27.8	29	32.3	32.2	36.2
2583380	**BM**	**38**	29.9	32.1	31.7	33.8	36.9
2838310	**BM**	**31**	28.1	30.4	31.7	34.3	34.4
2975380	**BM**	**38**	31.7	32.6	31.7	34.2	38.6
3591250	**BM**	**25**	32.5	32.2	33.5	35.8	40.3
3796340	**BM**	**34**	31.3	33.8	34.2	34.1	34.1
3819360	**BM**	**36**	29.2	32.4	35.5	35.5	36.3
4274270	**BM**	**27**	36	35.3	34.6	32.6	33.4
4421330	**BM**	**33**	29.3	30.2	31	32.9	
4518330	**BM**	**33**	27	29.3	29.8	33.2	34.6
4759360	**BM**	**36**	27.1	28.3	30.2	32	33.5
5114370	**BM**	**37**	29.3	32.4	33.7	32.2	32.2
5989270	**BM**	**27**	27.6	30	32	34	36.4
6105390	**BM**	**39**	31.2	33.5	34.7	37.5	42.3
6426270	**BM**	**27**	31.4	33.6	34.3	34.8	36
6771200	**BM**	**20**	26.2	29.4	31.5	31.5	33.8
7172230	**BM**	**23**	30.8	32.8	32.8	33.2	32.6

Case ID	P	Age	VDMinAP				
			L1	L2	L3	L4	L5
8199370	**BM**	**37**	31.6	35.9	37.5	35.4	36.7
8213390	**BM**	**39**	28	30.2	33.8	34.7	33.5
8313270	**BM**	**27**	30.6	32.3	33.3	33.5	36
8720220	**BM**	**22**	34.8	35.9	37.7	36.9	35.5
8887370	**BM**	**37**	29.1	31.7	33.4	35.7	37.4
9053260	**BM**	**26**	28.3	31.2	33.9	33.1	35.9
9519250	**BM**	**25**	31.1	32.8	31.6	35.1	34.2
9895210	**BM**	**21**	27.8	29.1	31.3	32.3	38.1
10037320	**BM**	**32**	29.1	29.4	30.6	32.5	34
10318380	**BM**	**38**	31.6	32.3	33.5	33	37.4
543250	**BM**	**25**	26.9	30.4	31.7	32.8	34.2
228651	**WF**	**65**	31.8	32.2	33.4	31.6	30.7
1041321	**WF**	**32**	28.5	31.2	31.3	31.2	36.8
1391501	**WF**	**50**	29.5	32.5	34.2	33.4	32.1
1505241	**WF**	**24**	27.6	28.3	29	30.4	34.8
3080371	**WF**	**37**	29.5	29.9	30.8	30.4	36.4
4697341	**WF**	**34**	23.6	27.4	28.6	28	28.6
5049551	**WF**	**55**	27.9	29.3	27.8	28.8	30.1
5219261	**WF**	**26**	29.2	30.5	29	29	31.5
6672461	**WF**	**46**	26	28.2	28.9	29.5	32.2
7010401	**WF**	**40**	25.2	27.5	29.2	29.3	29.5
8517231	**WF**	**23**	29.3	31.8	31.7	31.8	32
8968431	**WF**	**43**	30.7	34.1	34.4	34.1	36
9444231	**WF**	**23**	27.7	29.9	29.9	31	32.3
9766331	**WF**	**33**	28.8	28.5	29.2	32	32.8
474590	**WM**	**59**	30.7	32.7	35.1	34.6	34.9
844300	**WM**	**30**	33.1	33.4	34	35.9	37.8
2446350	**WM**	**35**	36.9		39.3	38.9	39.6
2796360	**WM**	**36**	31	32.9	32.2	34.4	32.7
3406620	**WM**	**62**	34.8	35.4	35.4	36.2	41.3
3996360	**WM**	**36**	28.6	30.3	31.1	31.7	31.1
4337270	**WM**	**27**	28.7	29.7	30.5	30.6	32.1
5431250	**WM**	**25**	31.3	33.8	33.2	32.1	34.8
5816390	**WM**	**39**	29.4	30.4	32	33	39.9
8064380	**WM**	**38**	33.2	34.4	34.2	34.6	35.9

Case ID	P	Age	VDMinAP				
			L1	L2	L3	L4	L5
9672360	**WM**	**36**	32.6	32.1	32.3	32.3	31.7
10153260	**WM**	**26**	31.7	33.6	34.1	35.2	33.2
10412510	**WM**	**51**	37.2	39.1	36.7	37.3	38.9

Key: P = Population group; BM = Black males; BF = Black females; WM = White males; WF = White females. All measurements are in millimetres. Blank cells are those where measurements could not be performed

Table A.4.24: Table indicating the anterior vertebral height (VHa) measured on the CT scans

Case ID	P	Age	VHa				
			L1	L2	L3	L4	L5
175281	**BF**	**28**	26.5	27.2	29.5	30.3	26.9
376411	**BF**	**41**	27.6	28.4	30.7	28.9	30.9
696271	**BF**	**27**	25.9	27.4	31.1	29.4	32.1
940381	**BF**	**38**	28	28.1	29.4	27.6	30.2
1188251	**BF**	**25**	28.6	29.3	29	28.5	29.2
1689331	**BF**	**33**	26.8	27.6	28.3	29.5	28.6
1983451	**BF**	**45**	24.8	26.1	25.2	27.8	26.6
2286451	**BF**	**45**	26.9	27.7	28.8	28.1	30.5
2622521	**BF**	**52**	27.5	29	29.3	27.3	27
3313231	**BF**	**23**	27.9	29.5	29.9	30.3	31.4
4006211	**BF**	**21**	23.6	25.2	26.7	26.1	
4811371	**BF**	**37**	27.7	26.9	27.2	27	26.6
4921271	**BF**	**27**	29.3	28.1	30.1	30.7	32.9
5378491	**BF**	**49**	25.8	26.4	26.1	26.1	27.7
5642231	**BF**	**23**	25.5	25.9	29.2	27.9	27.8
6309241	**BF**	**24**	27.3	28.1	27.7	30.1	31.9
7346221	**BF**	**22**	25.9	27.3	28	26.2	27
7479241	**BF**	**24**	29.7	31.6	32.5	33.6	34.2
7591291	**BF**	**29**	27	26.3	29.2	28.2	29.1
7963301	**BF**	**30**	29.4	30.9	30.6	32	31.8
8677261	**BF**	**26**	24.1	26.1	28.2	28	28.1
10277341	**BF**	**34**	28.1	30.4	29.9	31.3	30.7
745400	**BM**	**40**	27.3	29.4	30.9	30.6	29.9

Case ID	P	Age	VHa				
			L1	L2	L3	L4	L5
1224630	**BM**	**63**	26.7	27.4	27.6	26.7	28.6
1751390	**BM**	**39**	26.2	29.5	31.7	31.1	32.8
1837250	**BM**	**25**	30.2	32.1	32	31.9	32.6
2139430	**BM**	**43**	28.6	31.6	30.4	30.1	25.7
2336320	**BM**	**32**	35.5	34.6	31.9	33	33.3
2583380	**BM**	**38**	28.4	28.7	28.8	30.8	31.8
2838310	**BM**	**31**	31.1	32.2	31.4	30.4	32.4
2975380	**BM**	**38**	28.7	30.3	30.4	32.7	29.1
3591250	**BM**	**25**	28.8	29	31.7	31.4	32.9
3796340	**BM**	**34**	27.9	29.3	30.3	29	30.1
3819360	**BM**	**36**	29.8	30.5	32.2	29.8	31.1
4274270	**BM**	**27**	33.8	34.9	36.7	34	36.4
4421330	**BM**	**33**	27.8	28.5	28.1	28.2	
4518330	**BM**	**33**	27.6	28.7	30.4	29.3	30.8
4759360	**BM**	**36**	28.8	30	29.8	29.1	31.8
5114370	**BM**	**37**	28.7	29.8	28.3	33.1	31.3
5989270	**BM**	**27**	29.6	30.5	30.6	31.9	32.4
6105390	**BM**	**39**	30.4	32.7	34.9	34.4	34.9
6426270	**BM**	**27**	28.2	29.1	33.5	31.6	31.8
6771200	**BM**	**20**	26.4	29.2	30.1	28.1	30.8
7172230	**BM**	**23**	28.9	29.5	32.8	32.3	34.4
8199370	**BM**	**37**	28.3	29.1	31.6	32.8	33
8213390	**BM**	**39**	28.9	29.4	31.8	30.3	32.4
8313270	**BM**	**27**	30.2	30.1	32.2	33.6	32.1
8720220	**BM**	**22**	32.9	33.2	36.2	35.1	36
8887370	**BM**	**37**	29.9	32.1	31.8	31.1	31.2
9053260	**BM**	**26**	27.8	27.5	29.1	29.5	29.4
9519250	**BM**	**25**	29	29.8	27.6	29.8	28.8
9895210	**BM**	**21**	31	31.2	30.5	31.8	32.8
10037320	**BM**	**32**	32.1	33	34.6	33.8	34.6
10318380	**BM**	**38**	32.4	34.8	35.9	34.5	34.2
543250	**BM**	**25**	32.7	31.4	30.6	29.3	31.3
228651	**WF**	**65**	25.1	28.3	29.8	28.7	28
1041321	**WF**	**32**	29.1	30.1	30.7	29.4	29
1391501	**WF**	**50**	28.8	29.6	28.6	28.8	29.7

Case ID	P	Age	VHa				
			L1	L2	L3	L4	L5
1505241	**WF**	**24**	27.4	29	29.7	30.3	30.9
3080371	**WF**	**37**	28.4	26.9	26.9	26.9	28.3
4697341	**WF**	**34**	27.5	29.1	30.4	29.8	31.9
5049551	**WF**	**55**	25.1	27.1	29.9	30.1	29.9
5219261	**WF**	**26**	29.7	30.1	31.6	31.6	32.5
6672461	**WF**	**46**	29.6	33	32.2	33.7	32.2
7010401	**WF**	**40**	25.2	27.5	28.7	29.1	30.3
8517231	**WF**	**23**	29.7	30.8	31.5	32	33.3
8968431	**WF**	**43**	30.3	31.7	32.3	33.6	33.7
9444231	**WF**	**23**	25.3	28.9	29	30.2	30.2
9766331	**WF**	**33**	28.1	31.1	31.9	31.3	31.1
474590	**WM**	**59**	25.5	27.8	28.6	27.5	28.9
844300	**WM**	**30**	27.2	29.9	31.2	31.3	30.9
2446350	**WM**	**35**	29.3	30.8	31.5	32.9	32.5
2796360	**WM**	**36**	26	29	30.4	28.3	30.2
3406620	**WM**	**62**	28.6	28.4	32.2	33.8	33.8
3996360	**WM**	**36**	27.4	28.8	31.5	28.4	32.5
4337270	**WM**	**27**	26	28.3	28.6	29	30.3
5431250	**WM**	**25**	30.6	31.1	32.7	31.2	28.7
5816390	**WM**	**39**	31.3	33.9	34	30.8	33.5
8064380	**WM**	**38**	30	32.5	31.9	30.7	32.3
9672360	**WM**	**36**	29.1	30.8	31.6	31.8	32.4
10153260	**WM**	**26**	30.5	31.6	31.4	32.3	31.9
10412510	**WM**	**51**	32.5	34.6		35	35.8

Key: P = Population group; BM = Black males; BF = Black females; WM = White males; WF = White females. All measurements are in millimetres. Blank cells are those where measurements could not be performed

Table A.4.25: Table indicating the posterior vertebral height (VHp) measured on the CT scans

Case ID	P	Age	VHp				
			L1	L2	L3	L4	L5
175281	**BF**	**28**	26.7	28.6	28.3	27.9	27.4
376411	**BF**	**41**	30.2	29.9	31.2	30.7	26
696271	**BF**	**27**	28.3	30.2	32.4	30.8	27.9
940381	**BF**	**38**	28.1	28.9	27.9	27.7	26.2
1188251	**BF**	**25**	29.6	31.4	29.9	28.9	26.9
1689331	**BF**	**33**	28.4	29	28.9	28.5	27.4
1983451	**BF**	**45**	22.3	26.7	26.3	27	24.3
2286451	**BF**	**45**	27.7	29	28.5	28.1	26.5
2622521	**BF**	**52**	29.5	30.8	29	27.9	24.7
3313231	**BF**	**23**	29.8	30.1	29.9	29.3	27.7
4006211	**BF**	**21**	25.1	24.2	22.6	23.3	
4811371	**BF**	**37**	27.4	28.8	26.3	26	25.5
4921271	**BF**	**27**	31	29.7	31.1	31.1	29.3
5378491	**BF**	**49**	25.7	26.9	27.3	26.4	23.7
5642231	**BF**	**23**	26.2	27.5	26.4	26	23.8
6309241	**BF**	**24**	28	28.1	27.8	26.3	24.6
7346221	**BF**	**22**	27.2	28.2	29.9	28.8	25.3
7479241	**BF**	**24**	29.7	32.1	32.2	31.4	27.5
7591291	**BF**	**29**	27.3	26.8	28.4	27.8	25.7
7963301	**BF**	**30**	31.7	31.8	31.8	30.5	26.8
8677261	**BF**	**26**	27.3	28.2	27.3	27.2	26
10277341	**BF**	**34**	28.5	30.2	31.5	29	27.2
745400	**BM**	**40**	29.8	31.4	32.3	31.1	30.6
1224630	**BM**	**63**	29.7	26.5	26.8	26.7	26
1751390	**BM**	**39**	30.9	30.6	31	30.5	28.5
1837250	**BM**	**25**	31.7	32.5	31.5	30.5	29.1
2139430	**BM**	**43**	29.4	33.4	31.3	30.6	30.4
2336320	**BM**	**32**	29.6	31.5	30.9	33.1	33.4
2583380	**BM**	**38**	28.7	29.5	28.1	28.9	26.7
2838310	**BM**	**31**	32.8	32.3	32.4	30.9	28.5
2975380	**BM**	**38**	31.1	32.6	29.1	28	27.5
3591250	**BM**	**25**	31.5	32.6	33.9	31.6	30.5
3796340	**BM**	**34**	28.8	29	29.4	28.9	27.8
3819360	**BM**	**36**	31.7	32.1	32.9	31.4	29.4
4274270	**BM**	**27**	35.6	36.1	37.4	35.6	31.5

Case ID	P	Age	VHp				
			L1	L2	L3	L4	L5
4421330	**BM**	**33**	29.5	27	27.7	26.9	
4518330	**BM**	**33**	29.9	29.5	28.2	27	25.6
4759360	**BM**	**36**	31.6	32.6	31	31.3	30.2
5114370	**BM**	**37**	29.8	29.6	29.2	30.7	26.3
5989270	**BM**	**27**	32.4	32	30.5	29	30.2
6105390	**BM**	**39**	32.7	34.5	32.7	31	32.1
6426270	**BM**	**27**	32.5	32.9	33.1	30.5	28.8
6771200	**BM**	**20**	29.5	29	28.4	27.3	28.3
7172230	**BM**	**23**	30.6	32.8	32.1	31.4	28.5
8199370	**BM**	**37**	31.7	32.6	30.8	31.8	27
8213390	**BM**	**39**	32	34.2	33	31.3	27.8
8313270	**BM**	**27**	34.3	32.5	34.1	34.4	31.3
8720220	**BM**	**22**	33	34.5	36.2	34.8	31.7
8887370	**BM**	**37**	31.2	30.5	29.5	28.2	27
9053260	**BM**	**26**	29.1	29.3	28.1	29.1	26
9519250	**BM**	**25**	27.9	30.6	29.9	28.7	25.1
9895210	**BM**	**21**	31.4	31.1	29.7	29.8	28.1
10037320	**BM**	**32**	32.4	33.8	34.5	33.7	30
10318380	**BM**	**38**	34.1	36.2	35.1	32.7	30.8
543250	**BM**	**25**	35	34.1	32.3	31	28.3
228651	**WF**	**65**	28.8	30.9	28.8	27.3	22.1
1041321	**WF**	**32**	30.5	29.4	29.7	29	24.9
1391501	**WF**	**50**	32.2	32.4	30.6	26.6	24.7
1505241	**WF**	**24**	28.3	29	27	27.3	27.4
3080371	**WF**	**37**	27.4	25.9	27.2	25.1	24.5
4697341	**WF**	**34**	29	30	29.8	27.8	25.7
5049551	**WF**	**55**	29.8	28.9	31.2	29.8	27.2
5219261	**WF**	**26**	30.5	30.3	30.6	30.4	26.1
6672461	**WF**	**46**	30	29.5	29.7	28.8	27.6
7010401	**WF**	**40**	27	28.5	27.4	26.7	25.1
8517231	**WF**	**23**	31.5	31.9	32.7	30.1	27
8968431	**WF**	**43**	33.4	32.4	32.1	28.7	28.4
9444231	**WF**	**23**	29.6	30.9	31.4	28.6	26.1
9766331	**WF**	**33**	30.2	30.9	30.5	30.6	28.1
474590	**WM**	**59**	28.9	30.4	30.1	26.4	25.7

Case ID	P	Age	VHp				
			L1	L2	L3	L4	L5
844300	**WM**	**30**	29.4	30.1	30.5	30.9	24.6
2446350	**WM**	**35**	28.1	31	29.9	30.1	32
2796360	**WM**	**36**	27.3	29.4	33.7	29.4	27.5
3406620	**WM**	**62**	30.6	32.4	31.3	30.4	30.5
3996360	**WM**	**36**	31.7	31.5	31.2	28.6	26.9
4337270	**WM**	**27**	31.6	30	28.2	28.2	27.3
5431250	**WM**	**25**	36.3	33.3	31.9	27.5	25.4
5816390	**WM**	**39**	30.6	31.4	31.4	29.7	29.5
8064380	**WM**	**38**	32.9	32.7	33.2	32.3	29.1
9672360	**WM**	**36**	31.6	31	31.6	30.6	27.3
10153260	**WM**	**26**	32.5	32.4	31.2	33.3	28.7
10412510	**WM**	**51**	34.9	35.4		34.7	30.4

Key: P = Population group; BM = Black males; BF = Black females; WM = White males; WF = White females. All measurements are in millimetres. Blank cells are those where measurements could not be performed

Appendix A.5 – Raw MRI data: Sagittal

Table A.5.26: Table indicating the foraminal height (FH) measurements taken on the MRI scans

Case ID	P	Age	FH				
			L1	L2	L3	L4	L5
183380	**BM**	**38**	18.9	20.2	20.1	21.3	19.7
314460	**BM**	**46**	17.4	22	21	25	20
408471	**BF**	**47**	19.9	20	22.4	22.2	21.9
530410	**BM**	**41**	15.5	15.7	18	19.7	22.4
659360	**BM**	**36**	17.4	18.6	23.3	23	24.9
726421	**BF**	**42**	17.1	19	24.3	24.1	21.9
818341	**BF**	**34**	19.4	21.1	19.6	19.4	22.7
1178240	**BM**	**24**	15.9	17.5	18.4	17.4	17.4
1268220	**BM**	**22**	18.3	22.4	22.4	23.4	24.8
1496550	**BM**	**55**	17.4	17.9	18.2	19.3	18.8

Case ID	P	Age	FH				
			L1	L2	L3	L4	L5
1523431	**BF**	**43**	14.4	18.3	18.5	18.7	
1750490	**BM**	**49**	18.6	19.8	19.5	23.3	
1858360	**BM**	**36**	16.2	16.5	18.3	18.3	18.7
1939260	**BM**	**26**	19.6	20.2	20.3	20.3	21.7
2019270	**BM**	**27**	18	20.4	21.1	18.7	18.1
2183330	**BM**	**33**	18.4	21.1	19.6	22.3	19.1
2253281	**BF**	**28**	16.2	15	15.9	17.8	17.6
2324340	**BM**	**34**	11.1	14.8	17.5	17.4	20.4
2411580	**BM**	**58**	14.5	17.1	19	20	23.4
2585450	**BM**	**45**	12.7	19.2	20.1	18.6	24.4
2667260	**BM**	**26**	18.4	22.7	23.8	23.6	19.7
2824511	**BF**	**51**	14.7	15.3	18	17.7	19.5
2942340	**BM**	**34**	20.3	22.5	22.9	22.1	22.7
3021501	**BF**	**50**	17.4	21.8	20.5	19	18.3
3103241	**BF**	**24**	17.5	18	21.2	21.2	21.6
3772341	**BF**	**34**	16.2	20.4	22.3	19.1	17.7

Key: P = Population group; B = Black; W= White; M = Male; F = Female. All measurements are in millimetres. Blank cells are those where measurements could not be performed

Table A.5.27: Table indicating the superior foraminal diameter (SFD) measurement taken on the MRI scans

Case ID	P	Age	SFD				
			L1	L2	L3	L4	L5
183380	**BM**	**38**	9.6	7.6	7	6.6	4.1
314460	**BM**	**46**	9.1	8	8.3	7.5	7.3
408471	**BF**	**47**	6.6	6.1	7.6	6.7	5.6
530410	**BM**	**41**	9.2	11	9.1	6	3.5
659360	**BM**	**36**	8.8	7.5	5.5	6.3	4.7
726421	**BF**	**42**	7.2	10.3	9.5	7.8	5.2
818341	**BF**	**34**	9.6	6.7	6.7	6.3	5.7
1178240	**BM**	**24**	4.5	6	5.7	5.2	5.4
1268220	**BM**	**22**	6.5	5.5	6.5	5	5.3
1496550	**BM**	**55**	7	9.2	8.7	8.5	8

Case ID	P	Age	SFD				
			L1	L2	L3	L4	L5
1523431	**BF**	**43**	7.1	9.2	7.6	7.5	
1750490	**BM**	**49**	6.3	6	3.8	3.5	
1858360	**BM**	**36**	8.1	7.6	7.7	5.9	4.9
1939260	**BM**	**26**	6.3	5.9	6.1	5.9	5.9
2019270	**BM**	**27**	7.7	6.7	7.9	6.4	6.1
2183330	**BM**	**33**	8.6	8.8	7.4	7.7	7.5
2253281	**BF**	**28**	7.7	6.5	7.5	7.9	5.5
2324340	**BM**	**34**	7.5	8.2	7.4	5.6	5.4
2411580	**BM**	**58**	8.7	8.2	7.6	6.2	
2585450	**BM**	**45**	6.9	8	7.8	8	7.1
2667260	**BM**	**26**	5.3	7.5	6	5.5	5
2824511	**BF**	**51**	11.6	8	7.6	6.6	6.2
2942340	**BM**	**34**	10.2	7.6	6.9	8.5	9.7
3021501	**BF**	**50**	7.6	8.6	8.5	9.7	7.2
3103241	**BF**	**24**	10.8	10.5	11.8	10.7	7.8
3772341	**BF**	**34**	7.6	6.1	5.5	6	4.1

Key: P = Population group; B = Black; W= White; M = Male; F = Female. All measurements are in millimetres. Blank cells are those where measurements could not be performed

Table A.5.28: Table indicating the middle foraminal diameter (MFD) measurement taken on the MRI scans

Case ID	P	Age	MFD				
			L1	L2	L3	L4	L5
183380	**BM**	**38**	8.4	6.6	4.1	5	3.5
314460	**BM**	**46**	9.2	8.4	7.8	5.3	5.5
408471	**BF**	**47**	6.1	5.3	5.5	5.6	3.8
530410	**BM**	**41**	10.1	9.7	8.2	6.9	3.1
659360	**BM**	**36**	7.6	7.2	5.7	6	4.7
726421	**BF**	**42**	6.9	9.6	9	6.7	4.6
818341	**BF**	**34**	9.8	5.3	5.8	5.2	3.1
1178240	**BM**	**24**	5.3	5.1	3.4	4.1	4.3
1268220	**BM**	**22**	7	4.5	5.8	3.7	4.1
1496550	**BM**	**55**	5.9	9	6.6	7.1	6.9

Case ID	P	Age	MFD				
			L1	L2	L3	L4	L5
1523431	**BF**	**43**	7.6	8.9	6.5	3.5	
1750490	**BM**	**49**	5.8	4.5	4.2	4.1	
1858360	**BM**	**36**	7.7	6.2	5.2	3.8	2.9
1939260	**BM**	**26**	5.3	4.2	4.9	4.5	4.9
2019270	**BM**	**27**	7	6.4	6.7	6.1	4.3
2183330	**BM**	**33**	6.6	6.7	7.1	7.4	5.3
2253281	**BF**	**28**	7.9	6.4	6.3	5.8	3
2324340	**BM**	**34**	7	7.3	5.4	4.6	3.4
2411580	**BM**	**58**	7.7	8	6.3	4.1	
2585450	**BM**	**45**	7.1	8	6.9	5.8	4.5
2667260	**BM**	**26**	4.2	5.4	5.5	5.3	3.4
2824511	**BF**	**51**	8.8	6.6	5.4	5.3	5.8
2942340	**BM**	**34**	9.1	6.2	6.3	8.2	6.2
3021501	**BF**	**50**	7	7.9	9.1	6.5	6.2
3103241	**BF**	**24**	9	9.6	8.6	8.3	4.2
3772341	**BF**	**34**	6.7	4.1	5.1	4.6	3.3

Key: P = Population group; B = Black; W= White; M = Male; F = Female. All measurements are in millimetres. Blank cells are those where measurements could not be performed

Table A.5.29: Table indicating the inferior foraminal diameter (IFD) measured on the MRI scans

Case ID	P	Age	IFD				
			L1	L2	L3	L4	L5
183380	**BM**	**38**	8.3	7.9	6.6	5.3	4.8
314460	**BM**	**46**	8.7	7.7	5.1	5.9	0
408471	**BF**	**47**	5.8	4.4	5	4.2	4.6
530410	**BM**	**41**	8.4	9.2	7.2	6.3	2
659360	**BM**	**36**	5	4.4	5.6	5.4	3.2
726421	**BF**	**42**	5.6	7.6	7.4	4.4	3.1
818341	**BF**	**34**	8.9	5.2	5.2	4.2	3.1
1178240	**BM**	**24**	3.9	5.5	2.8	3.4	5
1268220	**BM**	**22**	8	5	4.5	4.3	4.2
1496550	**BM**	**55**	6.3	9	6.8	6.6	7.6

Case ID	P	Age	IFD				
			L1	L2	L3	L4	L5
1523431	**BF**	**43**	7	6.5	4.9	4.6	
1750490	**BM**	**49**	5.7	4.8	4.4	4.8	
1858360	**BM**	**36**	6.4	6	6.2	4.3	3.5
1939260	**BM**	**26**	4.8	3.4	4	4.3	4.5
2019270	**BM**	**27**	5.1	5.8	4.7	6	5.1
2183330	**BM**	**33**	5.2	6.2	6.6	6.1	4.7
2253281	**BF**	**28**	7	6.4	5.5	5	3.2
2324340	**BM**	**34**	5.9	6.8	5.9	4.7	3.3
2411580	**BM**	**58**	7.3	6.5	5	4.4	
2585450	**BM**	**45**	6.9	7	5.8	3.7	3.8
2667260	**BM**	**26**	4.1	5.1	3.5	3.6	3.7
2824511	**BF**	**51**	8	6.6	5.3	3.7	3.4
2942340	**BM**	**34**	7.7	5.1	5.1	5.4	5.2
3021501	**BF**	**50**	5.4	6.9	5.7	3.1	1.8
3103241	**BF**	**24**	8.4	7.4	6.8	6.8	3.8
3772341	**BF**	**34**	7.3	4.7	4.3	3.6	3.5

Key: P = Population group; B = Black; W= White; M = Male; F = Female. All measurements are in millimetres. Blank cells are those where measurements could not be performed

Table A.5.30: Table indicating the root to disc length (RD) measured on the MRI scans

Case ID	P	Age	RD				
			L1	L2	L3	L4	L5
183380	**BM**	**38**	-1.7	2	2.4	3.8	3.7
314460	**BM**	**46**	0	1.7	1.8	3.5	-1.2
408471	**BF**	**47**	-4	-4.1	-1.9	1.7	4.1
530410	**BM**	**41**	-3.7	-1.9	-2.7	-3.8	2.4
659360	**BM**	**36**	-2.5	-3.5	-5.5	-5.2	-8.5
726421	**BF**	**42**	-2.1	-1.6	-1.5	-1.2	0.8
818341	**BF**	**34**	1.8	-1.9	-3.7	0	0
1178240	**BM**	**24**	-3	1.8	-2.5	4.1	1.4
1268220	**BM**	**22**	-1.8	-0.7	-2	-5.5	-4.3
1496550	**BM**	**55**	-2.5	-2	2.4	1.7	-1.8
1523431	**BF**	**43**	1.3	2.7	0.2	3.7	

Case ID	P	Age	RD				
			L1	L2	L3	L4	L5
1750490	**BM**	**49**	-2.6	-2.5	-2.1	-0.9	
1858360	**BM**	**36**	1.3	-1.3	1.7	-3.4	1
2019270	**BM**	**27**	-2.1	-0.9	-2.3	-4.1	-1.5
2183330	**BM**	**33**	-2.5	-3.3	-2.4	-2	-0.7
2253281	**BF**	**28**	1	1.4	-1	2.6	-2
2324340	**BM**	**34**	2	1.6	0	2.2	-1.9
2411580	**BM**	**58**	-3.7	-1.9	-0.2	-0.2	-1.3
2585450	**BM**	**45**	1.2	1.2	1.9	-2.6	-2.7
2667260	**BM**	**26**	-0.8	-3.1	-0.5	0	-1.3
2824511	**BF**	**51**	-2.7	0	-2.4	-2.7	-2.6
2942340	**BM**	**34**	-2.5	-2.8	2.6	3.8	-1.3
3021501	**BF**	**50**	-0.6	-0.9	0	2.9	0.5
3103241	**BF**	**24**	-0.8	1.4	4.4	2.9	2.8
3772341	**BF**	**34**	-2.6	-2	-4.2	1.2	0.9

Key: P = Population group; B = Black; W= White; M = Male; F = Female. All measurements are in millimetres. Blank cells are those where measurements could not be performed. Negative values are the measurements taken above the superior border of the disc

Table A.5.31: Table indicating the root to pedicle distance (RP) measured on the MRI scans

Case ID	P	Age	RP				
			L1	L2	L3	L4	L5
183380	**BM**	**38**	11.1	8.1	9.7	9	8.5
314460	**BM**	**46**	11.4	11.7	13.2	12.4	7.8
408471	**BF**	**47**	14	14	13.8	11.1	11.6
530410	**BM**	**41**	12.8	8	11.2	14.8	14.9
659360	**BM**	**36**	11.5	12.6	17.7	16.7	20.1
726421	**BF**	**42**	9.5	13.2	14.9	13.7	9.8
818341	**BF**	**34**	9.2	12	12.6	8.7	13.3
1178240	**BM**	**24**	11.3	9	9.5	7.4	9.6
1268220	**BM**	**22**	13.8	13.7	16.3	16.5	16.3
1496550	**BM**	**55**	9	8.4	8.5	8.7	8.7
1523431	**BF**	**43**	7.7	8.5	11.7	8.5	
1750490	**BM**	**49**	9.4	13.2	13.3	14.1	

Case ID	P	Age	RP				
			L1	L2	L3	L4	L5
1858360	**BM**	**36**	9.2	10.3	9.6	11.5	13.9
2019270	**BM**	**27**	9.4	10.5	8.4	12.1	10
2183330	**BM**	**33**	9	12.2	12.8	13.7	10.8
2253281	**BF**	**28**	7.8	10.6	8.6	8.3	11.3
2324340	**BM**	**34**	5.4	8.4	9.6	10.6	12.1
2411580	**BM**	**58**	11.5	9.9	9.7	9.4	13.3
2585450	**BM**	**45**	9.1	10.5	11.3	12.1	17.4
2667260	**BM**	**26**	10.3	13.2	12.9	13.2	11.5
2824511	**BF**	**51**	9.3	6.7	10.1	9.5	8.6
2942340	**BM**	**34**	13	13.2	9.3	10.3	11.4
3021501	**BF**	**50**	10.7	13.2	13	7.2	6.5
3103241	**BF**	**24**	10.8	7.8	7.2	6.5	7.9
3772341	**BF**	**34**	12.1	13.9	17.2	10.2	9

Key: P = Population group; B = Black; W= White; M = Male; F = Female. All measurements are in millimetres. Blank cells are those where measurements could not be performed

Appendix A.6 – Raw MRI data: Coronal

Table A.6.32: Table indicating the distance from the intervertebral disc to where the vertical line drawn from the medial border of the pedicle intersects the nerve root (MedD) taken on the MRI scans

Case ID	P	Age	MedD									
			L1		L2		L3		L4		L5	
			Left	Right	Left	Right	Left	Right	Left	Right	Left	Right
183380	**BM**	**38**	-1.9	-4.1	-2.5	-4.5	-5.8	-4.3	-7.2	-5.8	-6.3	-2.8
408471	**BF**	**47**	-3.6	-2.8	-4.8	-3.2		-2.9	-4	-7.8	-7.5	-8.5
530410	**BM**	**41**	-4.1	-3.1	-3.4	-2.9	-6.5	-2.5	-3.9	-7.2	-7.2	-9.1
659360	**BM**	**36**	-6.3	-4.6	-5.9	-7.2	-9.6	-7.7	-8.3	-8	-9.8	-7.5
1178240	**BM**	**24**	-7	-5	-6.1	-7.9	-2.8	-4.6	-6.7	-5.3	-5.6	-5.6
1268220	**BM**	**22**	-2.8	-3.8	-5.3		-4.6	-3	-6.6	-4.1	-5.8	-8.4
1496550	**BM**	**55**	-5.9	-2.3	-5.1	-4.8	-6.8	-6.3	-6.5	-7.3	-4.5	-6
2183330	**BM**	**33**	-8	-7.7	-8.1	-7	-8.2	-10.6	-9.6	-10.1		

Case ID	P	Age	MedD									
			L1		L2		L3		L4		L5	
			Left	Right	Left	Right	Left	Right	Left	Right	Left	Right
2411580	**BM**	**58**	-4.9	-4.1	-5.4	-6.8	-5.7	-8.8	-5.4	-2.8	-5.4	-5.8
2585450	**BM**	**45**	-5.8	-5.8	-7.3	-7.5	-9.7	-10	-10	-7.2		

Key: P = Population group; BM = Black male; BF = Black female; WM = White male. All measurements are in millimetres. Blank cells are those where measurements could not be performed. Measurements with a negative value are those which lie above the superior border of the intervertebral disc

Table A.6.33: Table indicating the distance from the intervertebral disc to where the vertical line drawn from the midline of the pedicle intersects the nerve root (MidD) taken on the MRI scans

Case ID	P	Age	MidD									
			L1		L2		L3		L4		L5	
			Left	Right	Left	Right	Left	Right	Left	Right	Left	Right
183380	**BM**	**38**	1.9	0.4	0	0	0.8	1.9	0.6	1.8	-2.8	2.4
408471	**BF**	**47**	-2.1	0.6	0	2.9		-1.9	-1.9	-1.6	-3.8	-4.3
530410	**BM**	**41**	-2.6	-1.2	-1.7	-2.2	-2.9	-1	-1.3	-1.9	-2.7	-1.5
659360	**BM**	**36**	0.8	4.3	1.3	1.5	2.3	3.7	3.6	3.9	-1.6	2.2
1178240	**BM**	**24**	-3.6	-2	-2.8	-4.5	4	3.2	-1.7	2.7	3.4	3.4
1268220	**BM**	**22**	2.7	3.3	2		2.6	2.8	0.6	2.3	-2.5	-4.1
1496550	**BM**	**55**	-5.4	-5.1	-3.1	1.7	-2.8	2.4	-0.9	3	-1.2	0.7
2183330	**BM**	**33**	-5.6	-4.1	-3.6	-5.1	-2.2	-1.9	2.4	1.9		
2411580	**BM**	**58**	1.4	2.2	-2	-1.7	-2	-2.3	2.8	5.4	-2	1.7
2585450	**BM**	**45**	-1.8	-1.8	-3.3	-1.6	-1.8	0	-1.8	-2.7		

Key: P = Population group; BM = Black male; BF = Black female; WM = White male. All measurements are in millimetres. Blank cells are those where measurements could not be performed. Measurements with a negative value are those which lie above the superior border of the intervertebral disc

Table A.6.34: Table indicating the distance from the intervertebral disc to where the vertical line drawn from the lateral border of the pedicle intersects the nerve root (LatD) taken on the MRI scans

Case ID	P	Age	LatD									
			L1		L2		L3		L4		L5	
			Left	Right	Left	Right	Left	Right	Left	Right	Left	Right
183380	**BM**	**38**	3.6	6.4	2.2	1.2	2.5	5.2	6.5	7.2	7.5	10.5
408471	**BF**	**47**	4.6	5.4	2.9	3.2		3.4	3.5	2.7	3	2.7
530410	**BM**	**41**	-1	0.4	-1	0.7	-1.6	2.5	4.9	5.9	4.2	8.9
659360	**BM**	**36**	3.5	5.7	3.8	4.4	5.4	7.5	7.7	8.5	3.6	4.2
1178240	**BM**	**24**	1.9	3.1	3.1	3.6	8.7	5.3	7.5	9.3	9.8	10.8
1268220	**BM**	**22**	4.8	5.4	4		6.1	7.2	8.3	3.8	4.1	3.6
1496550	**BM**	**55**	5.7	5.7	2.6	5.7	3.7	4.2	5.9	9.2	4.5	6.6
2183330	**BM**	**33**	-3.6	-3.3	-1.5	-1.9	5.8	4.4	5.5	7.4		
2411580	**BM**	**58**	2.7	6.3	3.1	2.3	5.7	4.3	9.6	8.8	4.6	6.3
2585450	**BM**	**45**	1.8	2.4	2.7	3.5	4	6.1	5.4	6.5		

Key: P = Population group; BM = Black male; BF = Black female; WM = White male. All measurements are in millimetres. Blank cells are those where measurements could not be performed. Measurements with a negative value are those which lie above the superior border of the intervertebral disc

Table A.6.35: Table indicating the distance from the pedicle to where the vertical line drawn from the medial border of the pedicle intersects the nerve root (MedP) taken on the MRI scans

Case ID	P	Age	MedP									
			L1		L2		L3		L4		L5	
			Left	Right	Left	Right	Left	Right	Left	Right	Left	Right
183380	**BM**	**38**	10.8	10.6	14.7	12.8	17.9	12.8	15.4	16.2	16.1	14.3
408471	**BF**	**47**	12.8	12.5	13.1	11.5		13.6	15.2	16	15.5	13.9
530410	**BM**	**41**	10.3	11.2	12.2	10.8	15.3	14.4	13.3	15.9	12.1	10.6
659360	**BM**	**36**	14.4	14.9	17.2	17.5	20.3	21.6	18.5	23	21.3	22.1
1178240	**BM**	**24**	11.8	12.8	13.9	13.4	12.3	14.6	14.2	11.8	15.1	13.7
1268220	**BM**	**22**	14.2	12.5	13.2		14.8	14.5	16.3	16.3	13.7	17
1496550	**BM**	**55**	10.4	7.5	17.5	13.2	17.5	18.7	17.5	15.1	13.7	13.4
2183330	**BM**	**33**	15	16.8	15.1	17.8	20.2	21.9	18.5	17.3		
2411580	**BM**	**58**	12.5	11.1	12.2	16.1	15.6	17.9	19	20.7	15.1	18.7
2585450	**BM**	**45**	12.8	13.7	18.1	18.4	20.4	23.2	17.3	18.6		

Case ID	P	Age	MedP									
			L1		L2		L3		L4		L5	
			Left	Right	Left	Right	Left	Right	Left	Right	Left	Right
Key: P = Population group; BM = Black male; BF = Black female; WM = White male. All measurements are in millimetres. Blank cells are those where measurements could not be performed												

Table A.6.36: Table indicating the distance from the pedicle to where the vertical line drawn from the midline of the pedicle intersects the nerve root (MidP) taken on the MRI scans

Case ID	P	Age	MidP									
			L1		L2		L3		L4		L5	
			Left	Right	Left	Right	Left	Right	Left	Right	Left	Right
183380	**BM**	**38**	8.1	8.9	8.3	8.9	8.5	8.7	8	7.5	8	8.3
408471	**BF**	**47**	11.9	5.6	13.1	10.9		9.9	9.9	9.9	10.6	11.4
530410	**BM**	**41**	7.8	8.4	8.4	8.7	10.6	12.1	9.7	9.6	12.4	11.8
659360	**BM**	**36**	6.4	6.4	9.5	8.5	10	11	10.3	10	11.3	12.9
1178240	**BM**	**24**	7.5	7.3	10.3	11	6.7	9	9.5	5.9	10	8.5
1268220	**BM**	**22**	8.4	8.4	9.7		7.4	6.8	9.7	9.4	10.6	12.4
1496550	**BM**	**55**	3.7	5.1	10.1	7.6	11.3	8.3	8	6.9	6.5	6.8
2183330	**BM**	**33**	10.7	10.2	11.3	10.8	12.7	13	10.3	10.1		
2411580	**BM**	**58**	6.5	5.5	8.8	8.2	8.2	10.6	12.5	11.6	8.2	9.6
2585450	**BM**	**45**	8.2	7.1	10.4	11.7	12.9	12.4	9.3	11.7		
Key: P = Population group; BM = Black male; BF = Black female; WM = White male. All measurements are in millimetres. Blank cells are those where measurements could not be performed												

Table A.6.37: Table indicating the distance from pedicle to where the vertical line drawn from the lateral border of the pedicle intersects the nerve root (LatP) taken on the MRI scans

Case ID	P	Age	LatP									
			L1		L2		L3		L4		L5	
			Left	Right	Left	Right	Left	Right	Left	Right	Left	Right
183380	**BM**	**38**	6.5	7.1	3.9	5.4	4.7	3.6	3.6	1.8	4.3	2.8
408471	**BF**	**47**	12.8	10.3	13.4	10.9		9.9	5.3	6.1	7.7	12.1
530410	**BM**	**41**	8.6	8.6	10.9	9.2	10.6	8.6	6.2	7.9	7.8	6.4

Case ID	P	Age	LatP									
			L1		L2		L3		L4		L5	
			Left	Right	Left	Right	Left	Right	Left	Right	Left	Right
659360	**BM**	**36**	10.8	7.7	7.7	6.9	7.5	8.5	6.9	7.7	8.2	10.8
1178240	**BM**	**24**	5.8	6.7	9.3	8.6	7	4.2	5.9	5.6	6.4	4.7
1268220	**BM**	**22**	9.2	5	8.9		3.6	3.9	7.1	6.4	5.5	6.4
1496550	**BM**	**55**	5.8	5.4	8.2	7.3	8.9	6.2	2.1	5.6	4.5	3.9
2183330	**BM**	**33**	8.8	8.5	7.7	8.9	10.3	11.8	8.6	8.7		
2411580	**BM**	**58**	7.1	6.2	6.5	6.5	6	5.4	5.7	2.3	4	2.6
2585450	**BM**	**45**	7.3	3.4	8.9	7.8	9.5	8	5.8	6.9		

Key: P = Population group; BM = Black male; BF = Black female; WM = White male. All measurements are in millimetres. Blank cells are those where measurements could not be performed

Appendix A.7 – Raw MRI data: Transverse

Table A.7.38: Table indicating the inferior transverse foraminal depth (FDT) taken on the MRI scans

Case ID	P	Age	FDT									
			L1		L2		L3		L4		L5	
			Left	Right	Left	Right	Left	Right	Left	Right	Left	Right
408471	**BF**	**47**			5.1	9.2						
530410	**BM**	**41**									5.6	7.6
726421	**BF**	**42**							6.7	6.1	7.7	6.6
1178240	**BM**	**24**					9.1	8.4	7.6	7.5	6.7	6.7
1268220	**BM**	**22**					6.7	5.7	6.8	6.9	8.3	8.6
1496550	**BM**	**55**			8.9	7.6	10.7	9.9	9.8	8.9	6.1	7.4
1523431	**BF**	**43**							6.4	6.2	7.1	7
1750490	**BM**	**49**	6.2	6.5	8.2	6.9	8.2	7.4	6.8	7.5	6.4	6.6
1858360	**BM**	**36**					7.4	7.9	6.4	6.3	8.2	9.5
1939260	**BM**	**26**	7.2	6.1								
2183330	**BM**	**33**									6.6	6
2411580	**BM**	**58**					7.4	8	5	5.9	5.9	6.3
2667260	**BM**	**26**	6.3	5	7.3	6.7	5.4	7.1				

Case ID	P	Age	FDT									
			L1		L2		L3		L4		L5	
			Left	Right	Left	Right	Left	Right	Left	Right	Left	Right

Key: P = Population group; BM = Black male; BF = Black female; WM = White male. All measurements are in millimetres. Blank cells are those where measurements could not be performed

Table A.7.39: Table indicating the inferior root to disc distance (RD) taken on the MRI scans

Case ID	P	Age	RD									
			L1		L2		L3		L4		L5	
			Left	Right	Left	Right	Left	Right	Left	Right	Left	Right
408471	**BF**	**47**			2.9	3.4						
530410	**BM**	**41**									1.7	2.1
726421	**BF**	**42**							2	2.1	3.5	3.5
1178240	**BM**	**24**					2.1	2.8	3.6	2.7	2.9	3.4
1268220	**BM**	**22**					0.5	1.6	2.1	2.1	2.7	2.5
1496550	**BM**	**55**			5	3	2.9	2.6	5.4	4.2	2.6	3.2
1523431	**BF**	**43**							3.1	3.1	2.5	1.8
1750490	**BM**	**49**	3.5	3.7	3	3.3	2.3	3.3	2.5	2.6	2.1	2.5
1858360	**BM**	**36**					2.4	2.7	1.9	1.9	3	3.5
1939260	**BM**	**26**	3.3	2.2								
2183330	**BM**	**33**									2.8	2.4
2411580	**BM**	**58**					2.2	2.1	2.5	1.6	1.8	2.9
2667260	**BM**	**26**	2.9	2	3	2	1.4	2.6				

Key: P = Population group; BM = Black male; BF = Black female; WM = White male. All measurements are in millimetres. Blank cells are those where measurements could not be performed

Table A.7.40: Table indicating the inferior root to facet distance (RF) taken on the MRI scans

Case ID	P	Age	RF									
			L1		L2		L3		L4		L5	
			Left	Right	Left	Right	Left	Right	Left	Right	Left	Right
408471	**BF**	**47**			4.2	3.6						
530410	**BM**	**41**									4.2	6.1
726421	**BF**	**42**							8.7	8.4	3.7	3.3

Case ID	P	Age	RF									
			L1		L2		L3		L4		L5	
			Left	Right	Left	Right	Left	Right	Left	Right	Left	Right
1178240	**BM**	**24**					4.2	6.1	4.5	5.4	6	7.4
1268220	**BM**	**22**					5.5	4.8	5.5	4.4	6.3	5.4
1496550	**BM**	**55**			1	0.4	3	2.6	2	2.4	3.6	4.2
1523431	**BF**	**43**							2.9	3.6	1.8	3.2
1750490	**BM**	**49**	3	4	2.6	1.9	2.9	1.5	1.1	1.5	2.1	1.1
1858360	**BM**	**36**					6.6	5.3	4.3	3.8	6.6	5.2
1939260	**BM**	**26**	4.6	4.1								
2183330	**BM**	**33**									2	1.7
2411580	**BM**	**58**					5.3	4.9	4.3	3.8	4.8	3.3
2667260	**BM**	**26**	3.5	2	2.1	3.1	2.9	2.4				

Key: P = Population group; BM = Black male; BF = Black female; WM = White male. All measurements are in millimetres. Blank cells are those where measurements could not be performed

Table A.7.41: Table indicating the inferior target angle (TA) taken on the MRI scans

Case ID	P	Age	TA									
			L1		L2		L3		L4		L5	
			Left	Right	Left	Right	Left	Right	Left	Right	Left	Right
408471	**BF**	**47**			16.1	15.6						
530410	**BM**	**41**									8.3	8.5
726421	**BF**	**42**							18.3	19.6	16.1	18.6
1178240	**BM**	**24**					13.1	19.3	11.2	15.3	8.1	11.2
1268220	**BM**	**22**					17.2	14.3	8.2	10.8	5.6	4.3
1496550	**BM**	**55**			25.8	21.1	21.8	26.2	19.8	18.5	18.4	17.8
1523431	**BF**	**43**							15.6	16.2	10.1	17.1
1750490	**BM**	**49**	24.6	23.8	29.6	27.1	24.6	20.4	15.9	18.7	14.7	13.8
1858360	**BM**	**36**					13.3	13.5	13.2	15.4	12.3	9.9
1939260	**BM**	**26**	26.3	23.7								
2183330	**BM**	**33**									18.1	17.2
2411580	**BM**	**58**					15.6	15.9	11.6	11	9	7.8
2667260	**BM**	**26**	20.7	16	17.2	18.9	17.9	15.5				

Key: P = Population group; BM = Black male; BF = Black female; WM = White male. All measurements are in degrees. Blank cells are those where measurements could not be performed

Table A.7.42: Table indicating the superior transverse foraminal diameter (FDT) taken on the MRI scans

Case ID	P	Age	FDT									
			L1		L2		L3		L4		L5	
			Left	Right	Left	Right	Left	Right	Left	Right	Left	Right
408471	**BF**	**47**			6.6	7.1						
530410	**BM**	**41**									7.9	7.5
726421	**BF**	**42**									8.5	7.6
1178240	**BM**	**24**					9.4	8.2	11	9	7.2	8
1268220	**BM**	**22**					6.3	7.8	6.7	6.2	7.8	7.2
1496550	**BM**	**55**			7.7	5.5	8.9	7.9	11.5	9.2	10	11.9
1523431	**BF**	**43**							8.6	8.8	7.9	10
1750490	**BM**	**49**	7.3	6.8	7.7	6.7	7	7.4	7.4	7	6.8	7.2
1858360	**BM**	**36**					6.9	6.8	8.1	8.1	7.1	8.2
1939260	**BM**	**26**	8.2	7								
2183330	**BM**	**33**									8.5	7.3
2411580	**BM**	**58**					8.2	6.6	6.2	5.3	7	6.6
2667260	**BM**	**26**	7.8	6.2	7.7	7.2	7.4	7.7				

Key: P = Population group; BM = Black male; BF = Black female; WM = White male. All measurements are in millimetres. Blank cells are those where measurements could not be performed

Table A.7.43: Table indicating the superior root to disc distance (RD) taken on the MRI scans

Case ID	P	Age	RD									
			L1		L2		L3		L4		L5	
			Left	Right	Left	Right	Left	Right	Left	Right	Left	Right
408471	**BF**	**47**			2.5	3.2						
530410	**BM**	**41**									2.7	2.2
726421	**BF**	**42**									2.2	3
1178240	**BM**	**24**					2.8	2.7	2.4	3	3.6	2.2
1268220	**BM**	**22**					2.7	1.9	2.9	2.1	3.4	2.7
1496550	**BM**	**55**			2.5	1.8	3.5	3.5	4.7	4	3.2	4.8

Case ID	P	Age	RD									
			L1		L2		L3		L4		L5	
			Left	Right	Left	Right	Left	Right	Left	Right	Left	Right
1523431	**BF**	**43**							3.7	3.7	2.6	3.1
1750490	**BM**	**49**	2.7	2.1	2.7	2.8	2.2	2.4	2.3	2.5	1.9	1.4
1858360	**BM**	**36**					2.5	2.5	4.4	4	2.8	3.2
1939260	**BM**	**26**	3.1	2.6								
2183330	**BM**	**33**									3.8	3.6
2411580	**BM**	**58**					2.4	1.3	2.7	2.2	2.5	2.2
2667260	**BM**	**26**	2.5	2.3	4.8	2.6	2.6	3.8				

Key: P = Population group; BM = Black male; BF = Black female; WM = White male. All measurements are in millimetres. Blank cells are those where measurements could not be performed

Table A.7.44: Table indicating the superior root to facet distance (RF) taken on the MRI scans

Case ID	P	Age	RF									
			L1		L2		L3		L4		L5	
			Left	Right	Left	Right	Left	Right	Left	Right	Left	Right
408471	**BF**	**47**			1.9	2.5						
530410	**BM**	**41**									4.2	3.5
726421	**BF**	**42**									2.7	3.1
1178240	**BM**	**24**					1.6	2.6	4.1	3.5	3.9	2.4
1268220	**BM**	**22**					2.2	1.9	3.9	3.9	3.3	4.4
1496550	**BM**	**55**			2.2	2.2	1.5	1	2.4	1.9	3.3	4.1
1523431	**BF**	**43**							1.8	2	0.7	0.9
1750490	**BM**	**49**	3.5	2.3	2.7	2.1	2.1	2.5	1.7	0.9	1.3	1.8
1858360	**BM**	**36**					3.7	2.6	2	1.5	1.4	1.5
1939260	**BM**	**26**	2.4	2.1								
2183330	**BM**	**33**									3.3	2.3
2411580	**BM**	**58**					2.4	2.3	2.9	1.8	1	1.3
2667260	**BM**	**26**	2.2	2.2	0.7	1.2	1.1	1.4				

Key: P = Population group; BM = Black male; BF = Black female; WM = White male. All measurements are in millimetres. Blank cells are those where measurements could not be performed

Table A.7.45: Table indicating the superior target angle (TA) taken on the MRI scans

Case ID	P	Age	TA									
			L1		L2		L3		L4		L5	
			Left	Right	Left	Right	Left	Right	Left	Right	Left	Right
408471	**BF**	**47**			25.9	22.6						
530410	**BM**	**41**									13.3	14.8
726421	**BF**	**42**									20.2	20.4
1178240	**BM**	**24**					17.7	15.1	15.9	15.4	10.2	10.5
1268220	**BM**	**22**					15.6	12.3	13.7	14.2	9.4	9.1
1496550	**BM**	**55**			22.9	21.6	22.2	23.8	22.2	22.6	13.8	13.5
1523431	**BF**	**43**							20.8	18.2	11	17.1
1750490	**BM**	**49**	27.7	28.2	31.7	28.8	23.2	25.3	20.1	18.9	16.4	19.3
1858360	**BM**	**36**					19.6	19.3	19.9	19.1	11.5	12.8
1939260	**BM**	**26**	30.5	29.3								
2183330	**BM**	**33**									20.2	19.8
2411580	**BM**	**58**					16.4	16.5	14.5	14.5	17.2	16.1
2667260	**BM**	**26**	18.7	19	23.3	21.2	20	18.2				

Key: P = Population group; BM = Black male; BF = Black female; WM = White male. All measurements are in degrees. Blank cells are those where measurements could not be performed

Appendix B.1 – Scatterplots of LLA and age correlations

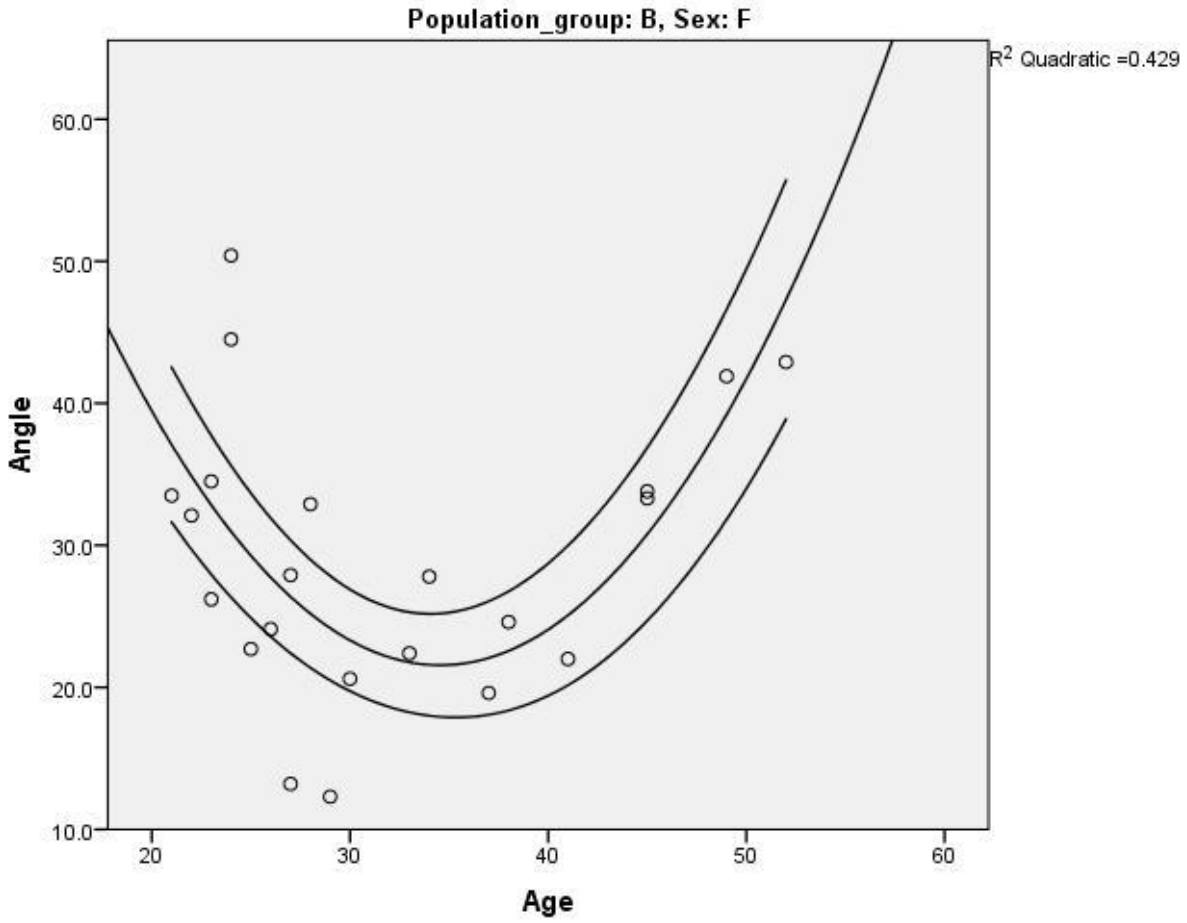

Figure B.1.13: Figure showing the quadratic regression line between Age and LLA for black females drawn from the scatterplot along with the 95% Confidence interval (lines running parallel to the midline)

Appendix B.2 – Scatterplots of LLA and morphometric correlations

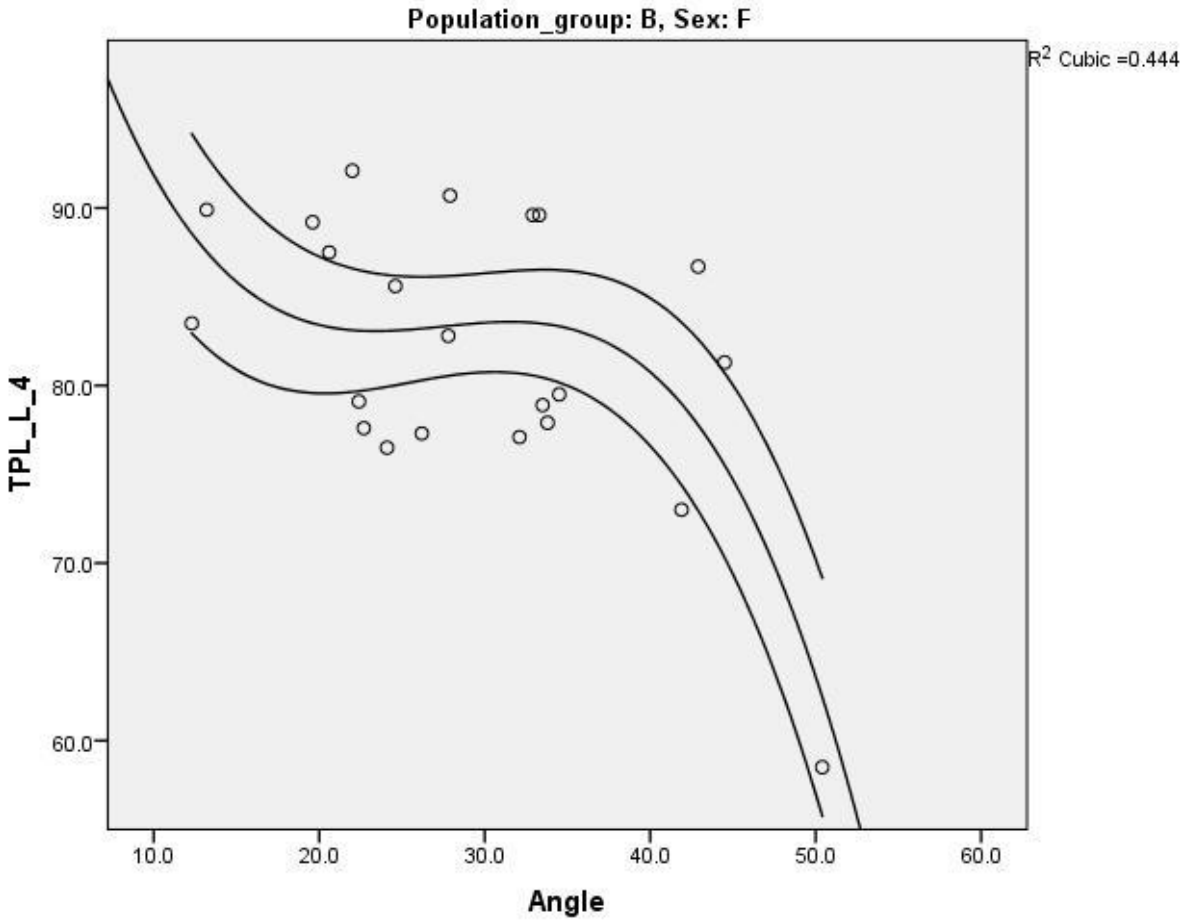

Figure B.2.14: Figure showing the cubic regression line between the transverse process length (TPL) of L4 and LLA for black females drawn from the scatterplot along with the 95% Confidence interval (lines running parallel to the midline)

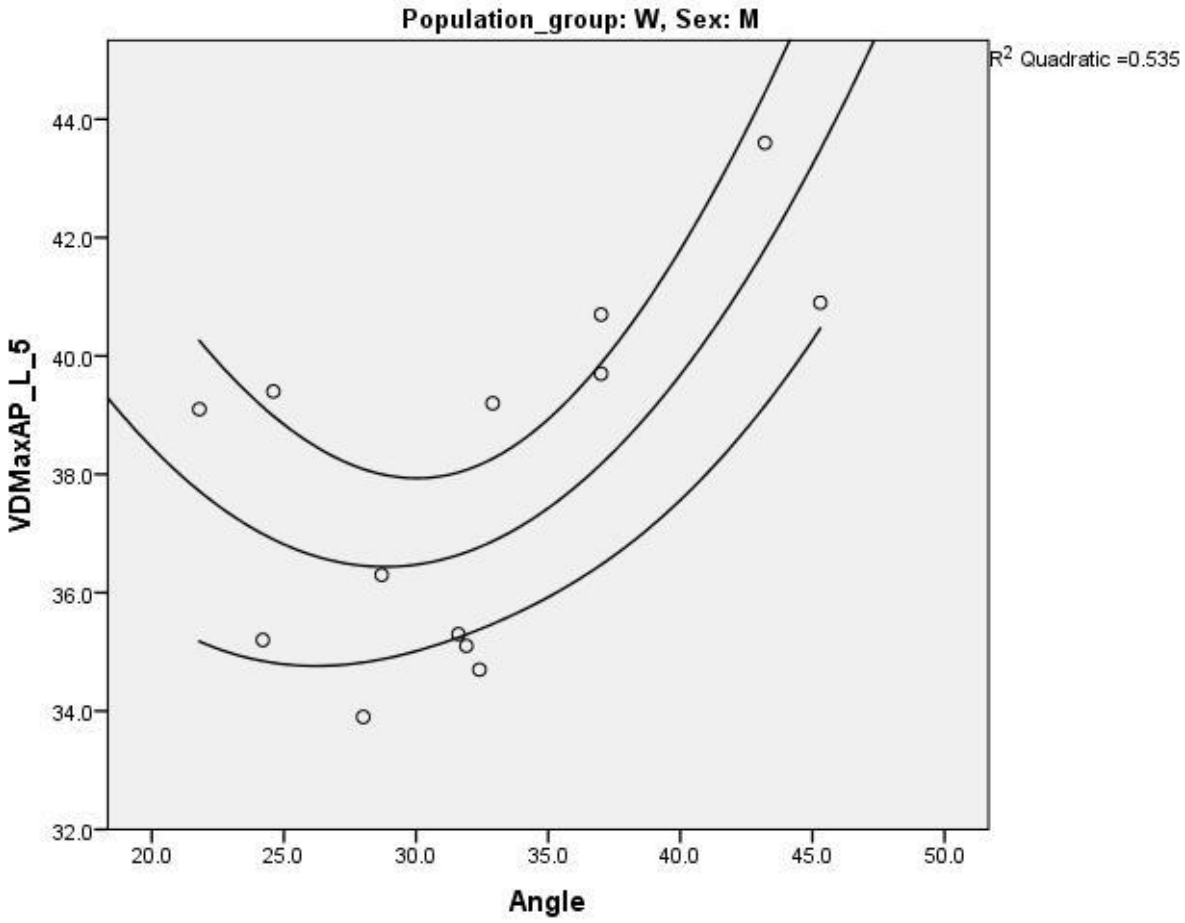

Figure B.2.15: Figure showing the quadratic regression line between the maximum AP vertebral body diameter (VDMaxAP) of L5 and LLA for white males drawn from the scatterplot along with the 95% Confidence interval (lines running parallel to the midline)

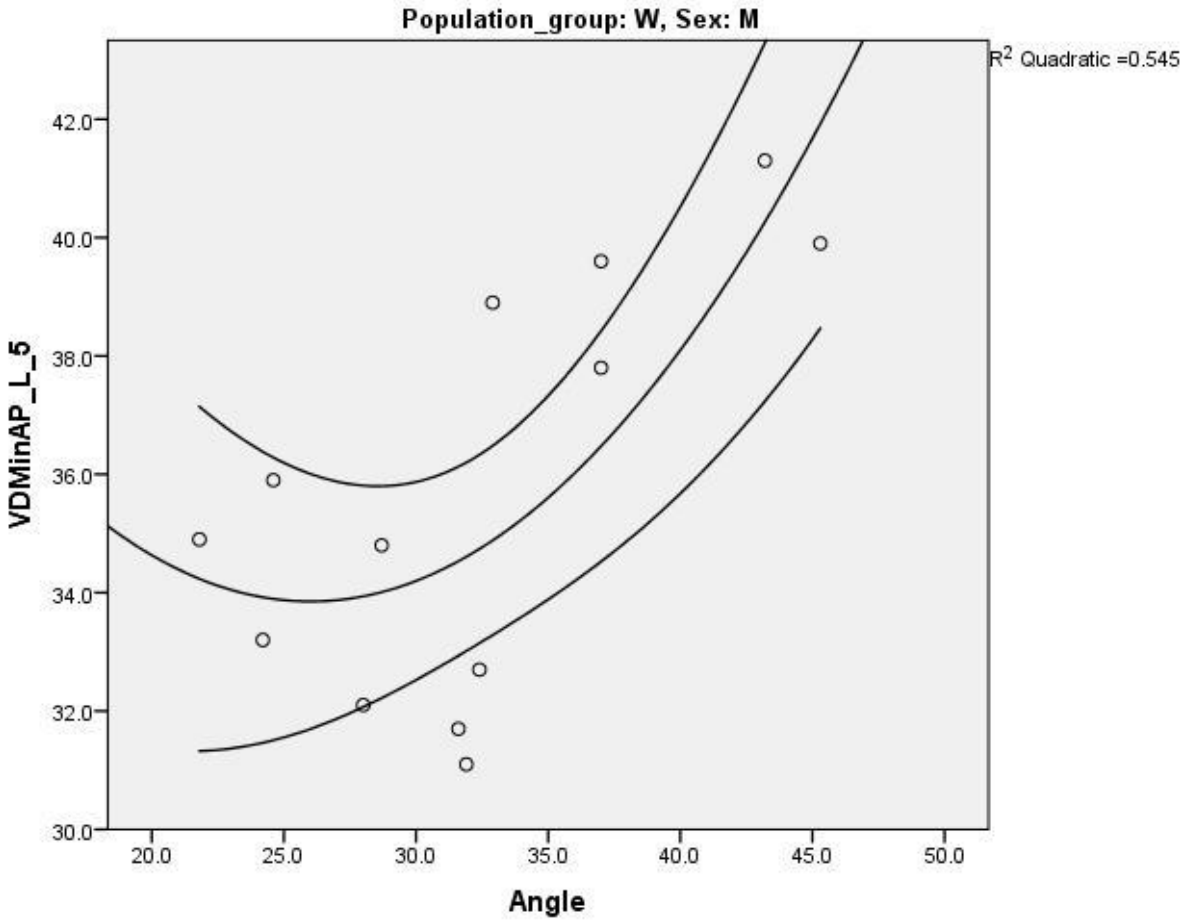

Figure B.2.16: Figure showing the quadratic regression line between the minimum AP vertebral diameter (VDMinAP) of L5 and LLA for white males drawn from the scatterplot along with the 95% Confidence interval (lines running parallel to the midline)

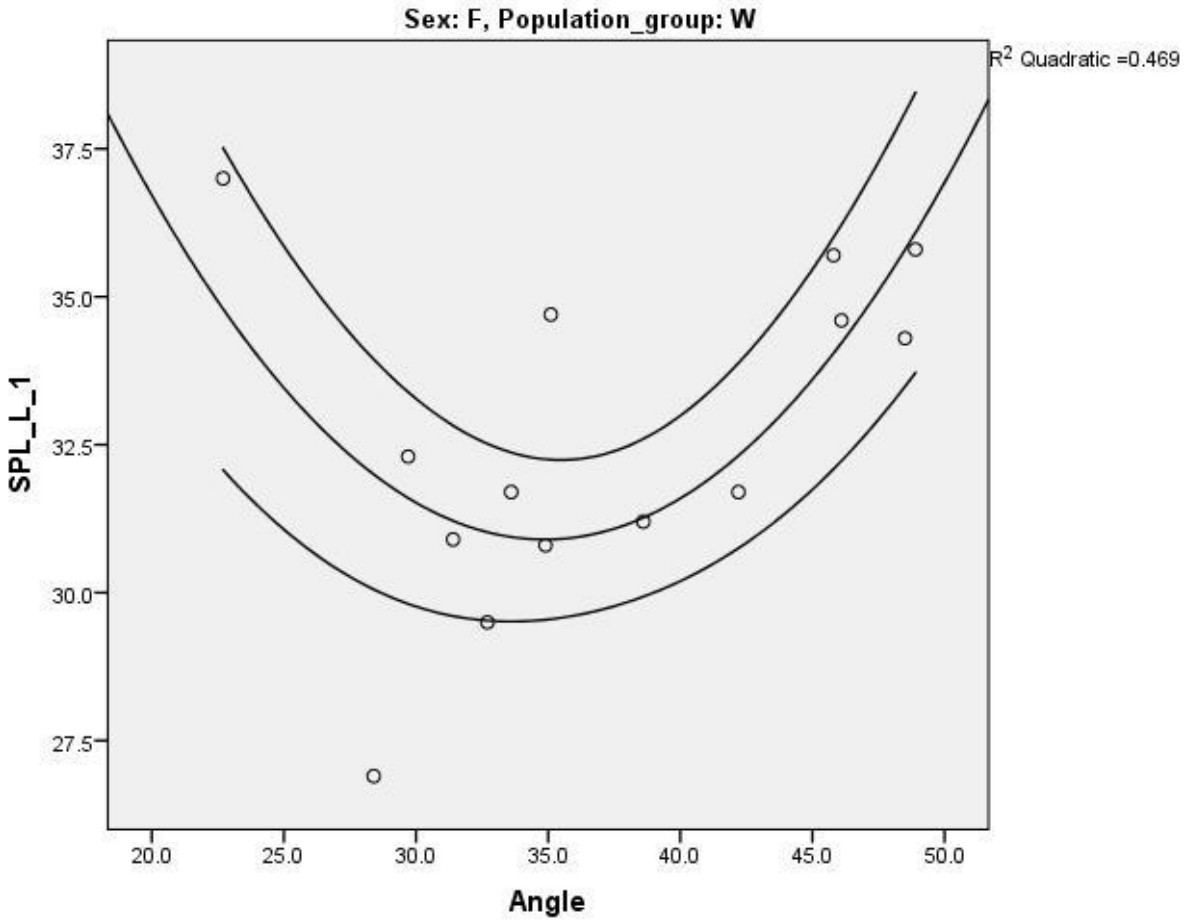

Figure B.2.17: Figure showing the quadratic regression line between spinous process length (SPL) of L1 and LLA for white females drawn from the scatterplot along with the 95% Confidence interval (lines running parallel to the midline)

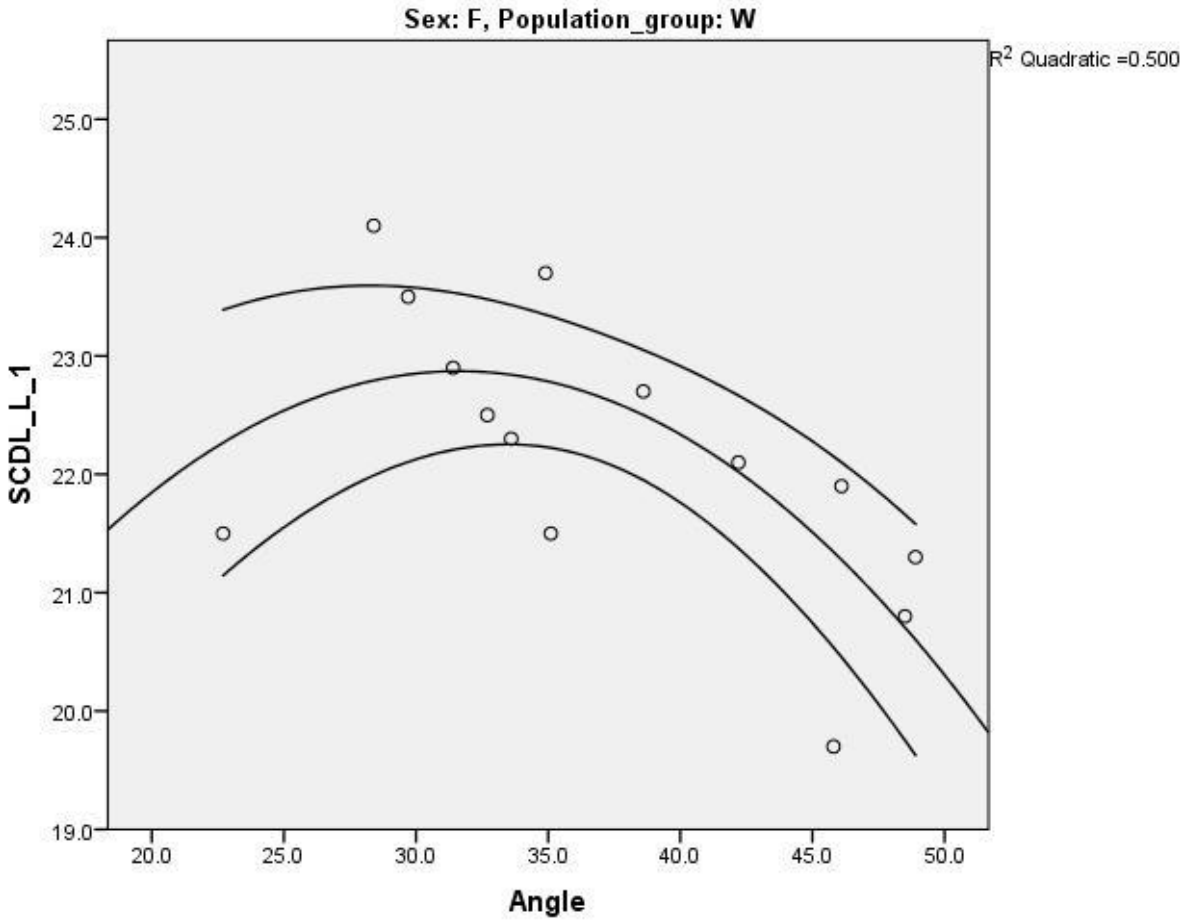

Figure B.2.18: Figure showing the quadratic regression line between the lateral spinal canal diameter (SCDL) of L1 and LLA for white females drawn from the scatterplot along with the 95% Confidence interval (lines running parallel to the midline)

Appendix B.3 – Scatterplots of age and BMD correlations

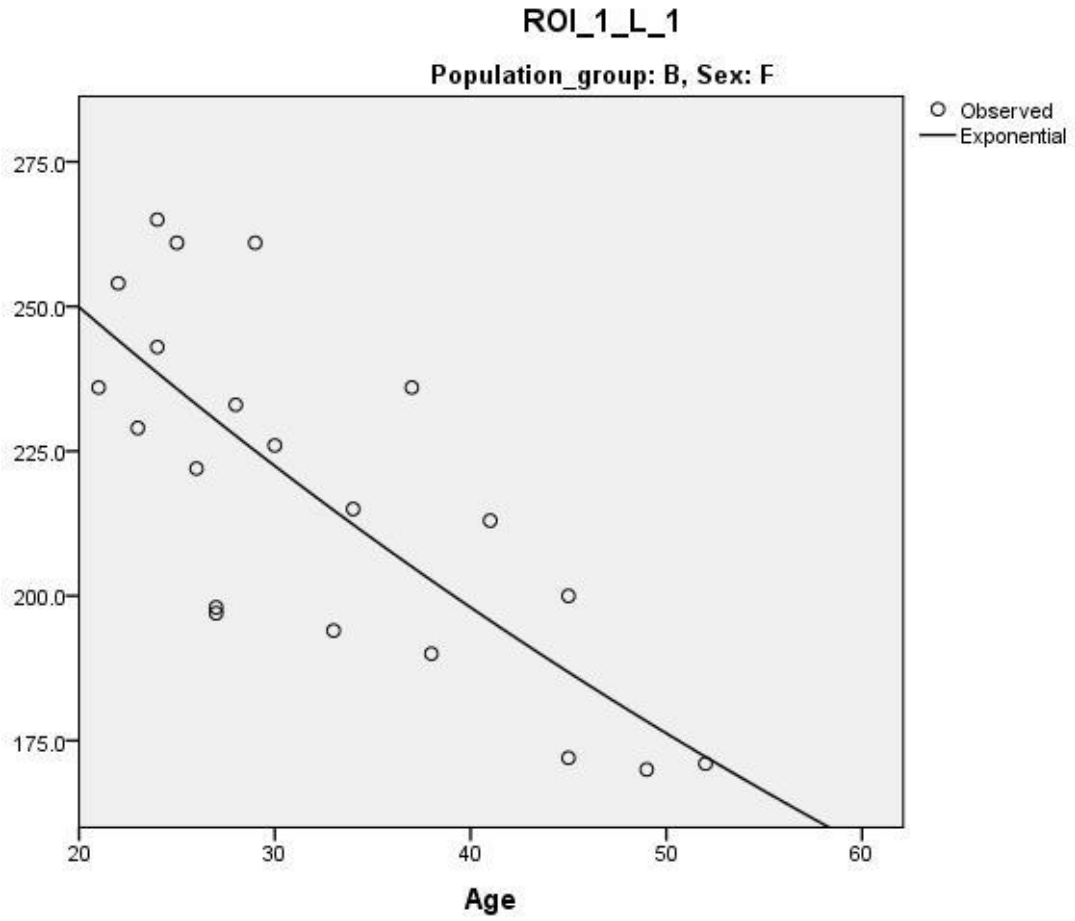

Figure B.3.19: Figure showing the exponential regression line between the ROI1 of L1 and age for black females drawn from the scatterplot. The r^2 value is 0.61

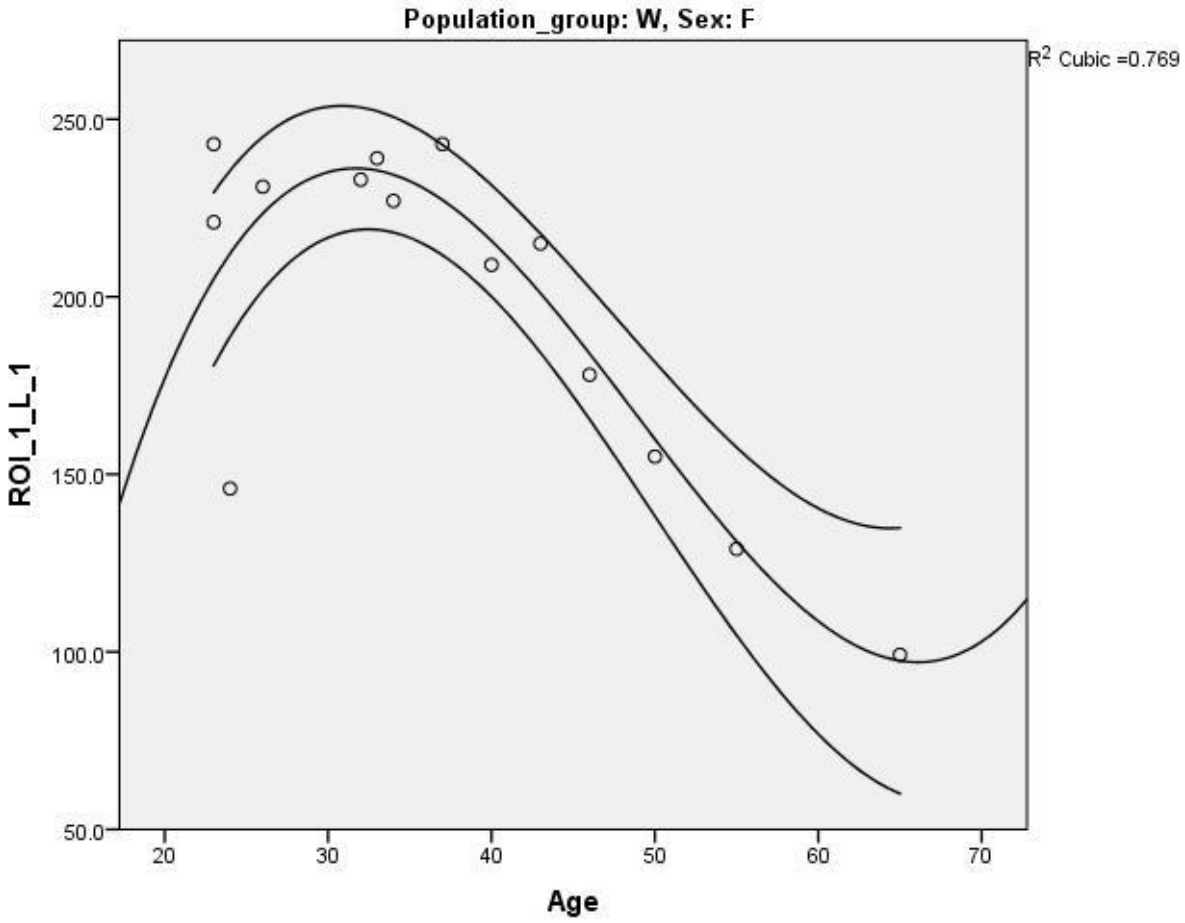

Figure B.3.20: Figure showing the cubic regression line between the ROI1 of L1 and age for white females drawn from the scatterplot along with the 95% Confidence interval (lines running parallel to the midline)

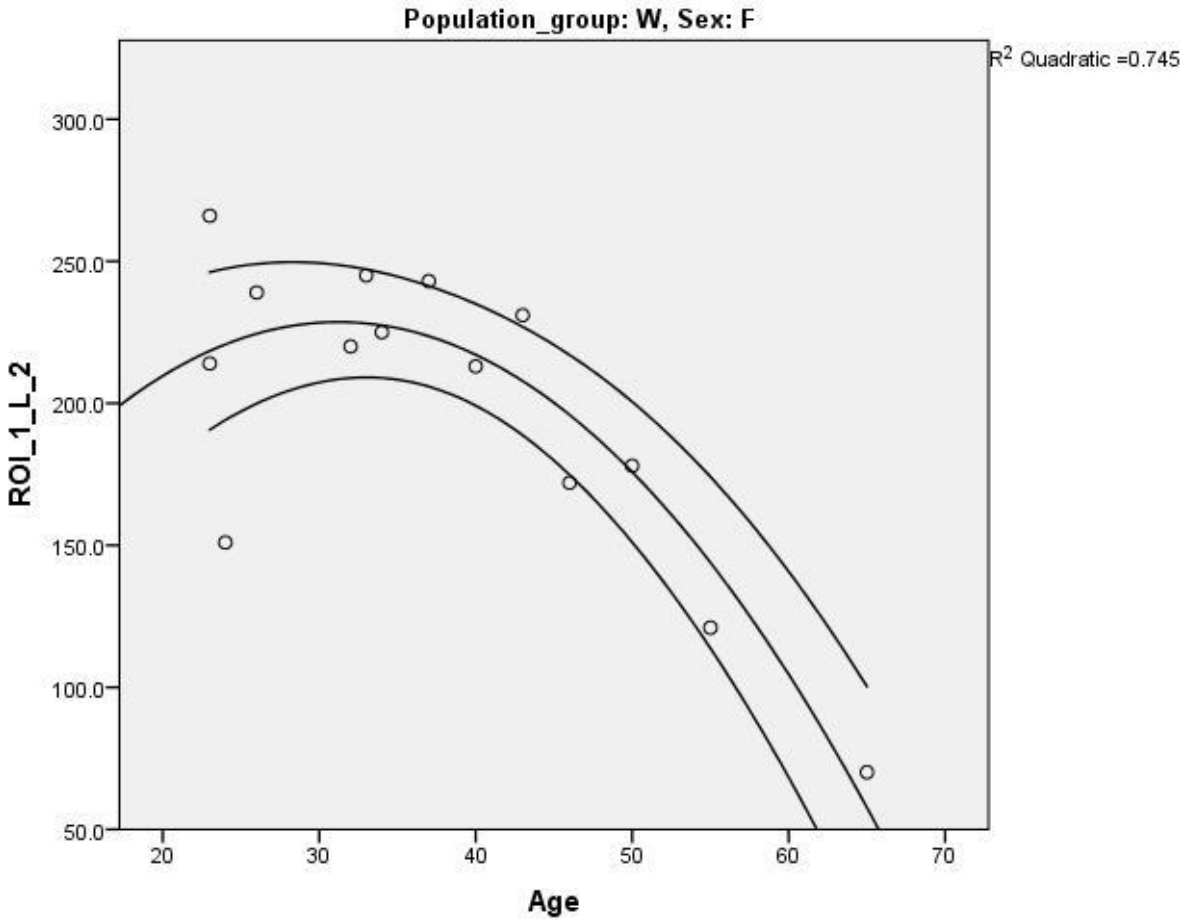

Figure B.3.21: Figure showing the quadratic regression line between ROI1 of L2 and age for white females drawn from the scatterplot along with the 95% Confidence interval (lines running parallel to the midline)

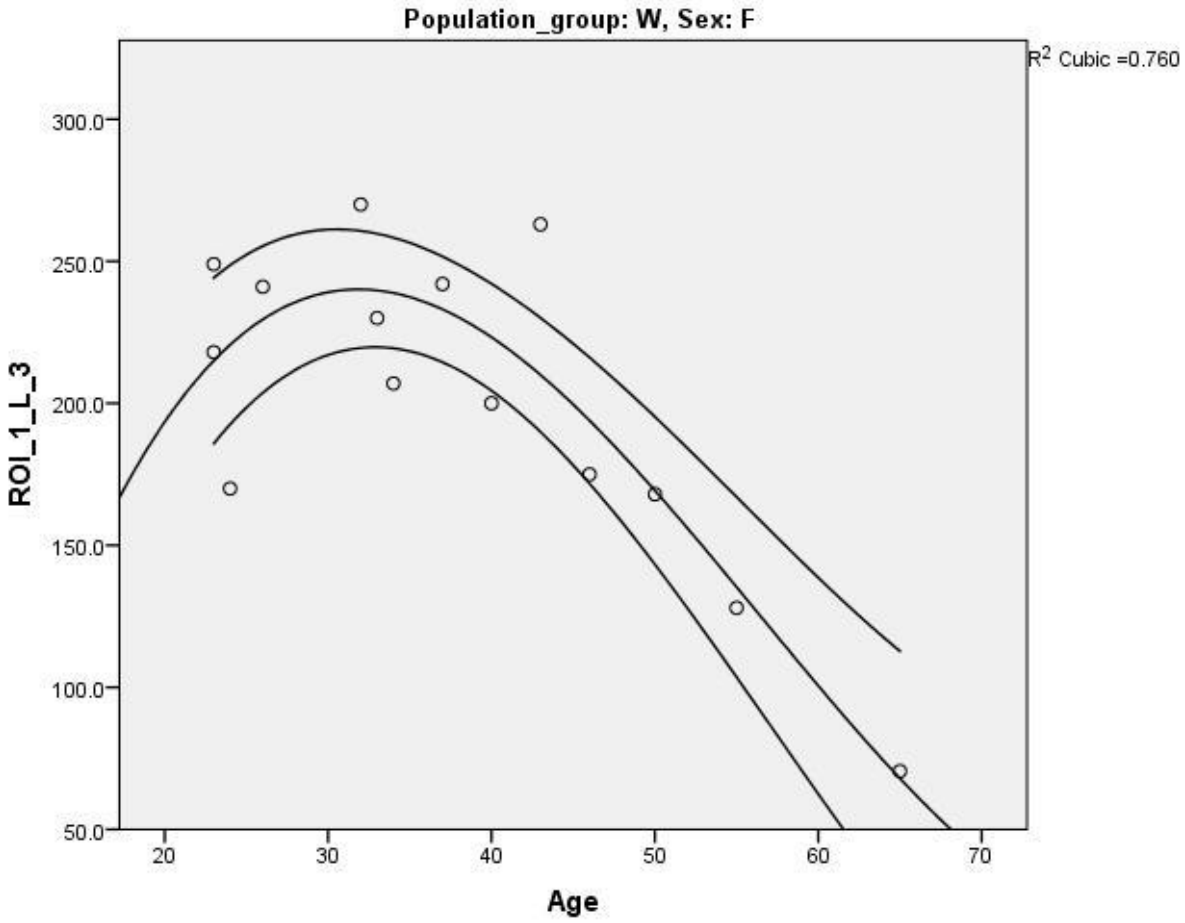

Figure B.3.22: Figure showing the cubic regression line between ROI1 of L3 and age for white females drawn from the scatterplot along with the 95% Confidence interval (lines running parallel to the midline)

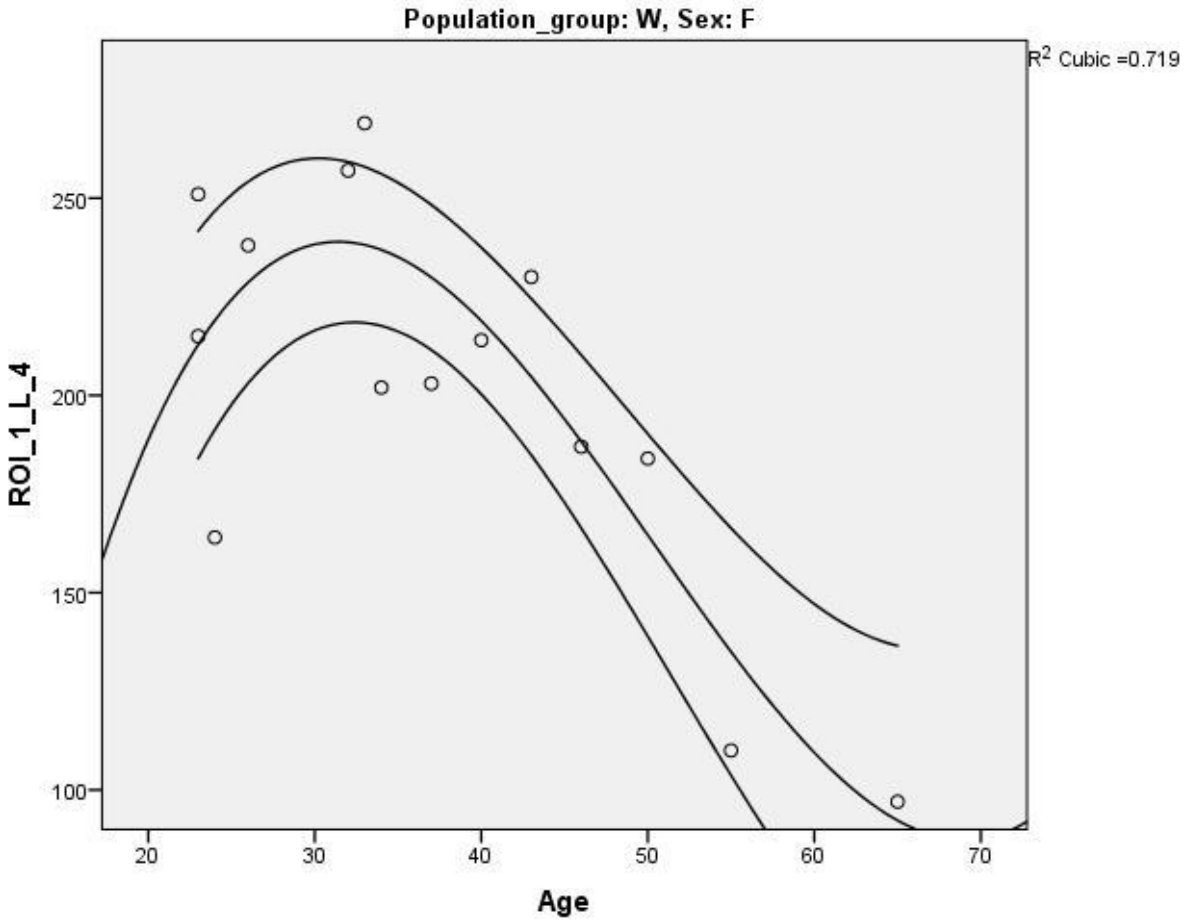

Figure B.3.23: Figure showing the cubic regression line between ROI1 of L4 and age for white females drawn from the scatterplot along with the 95% Confidence interval (lines running parallel to the midline)

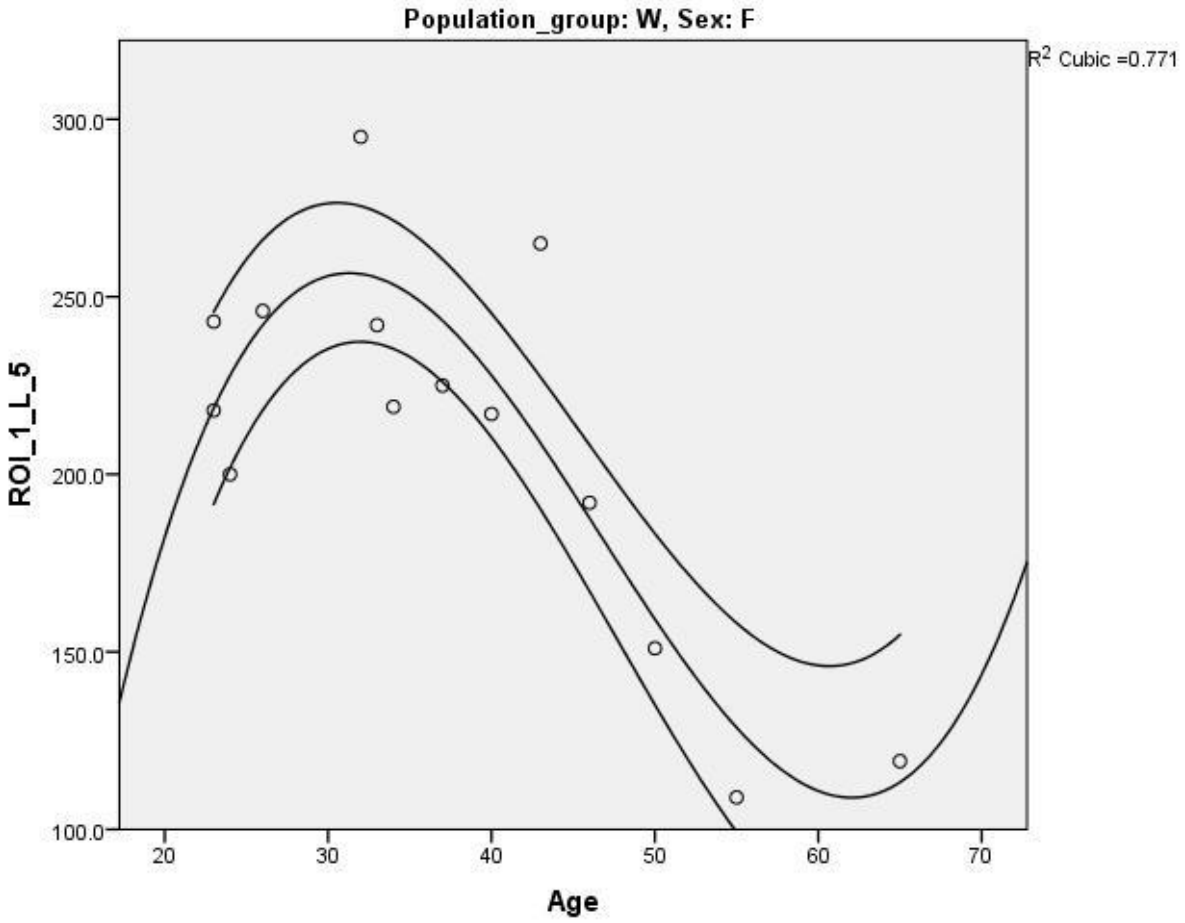

Figure B.3.24: Figure showing the cubic regression line between ROI1 of L5 and age for white females drawn from the scatterplot along with the 95% Confidence interval (lines running parallel to the midline)

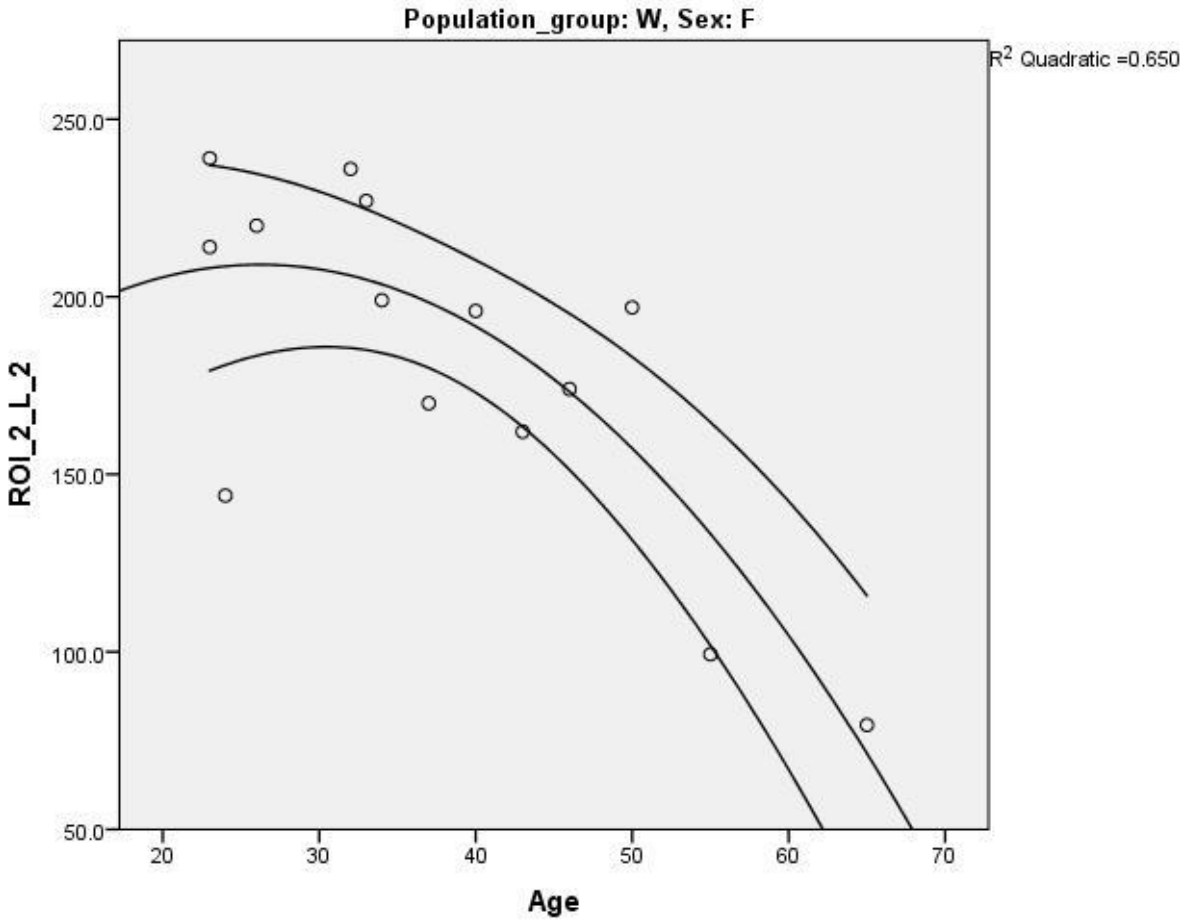

Figure B.3.25: Figure showing the quadratic regression line between ROI2 of L2 and age for white females drawn from the scatterplot along with the 95% Confidence interval (lines running parallel to the midline)

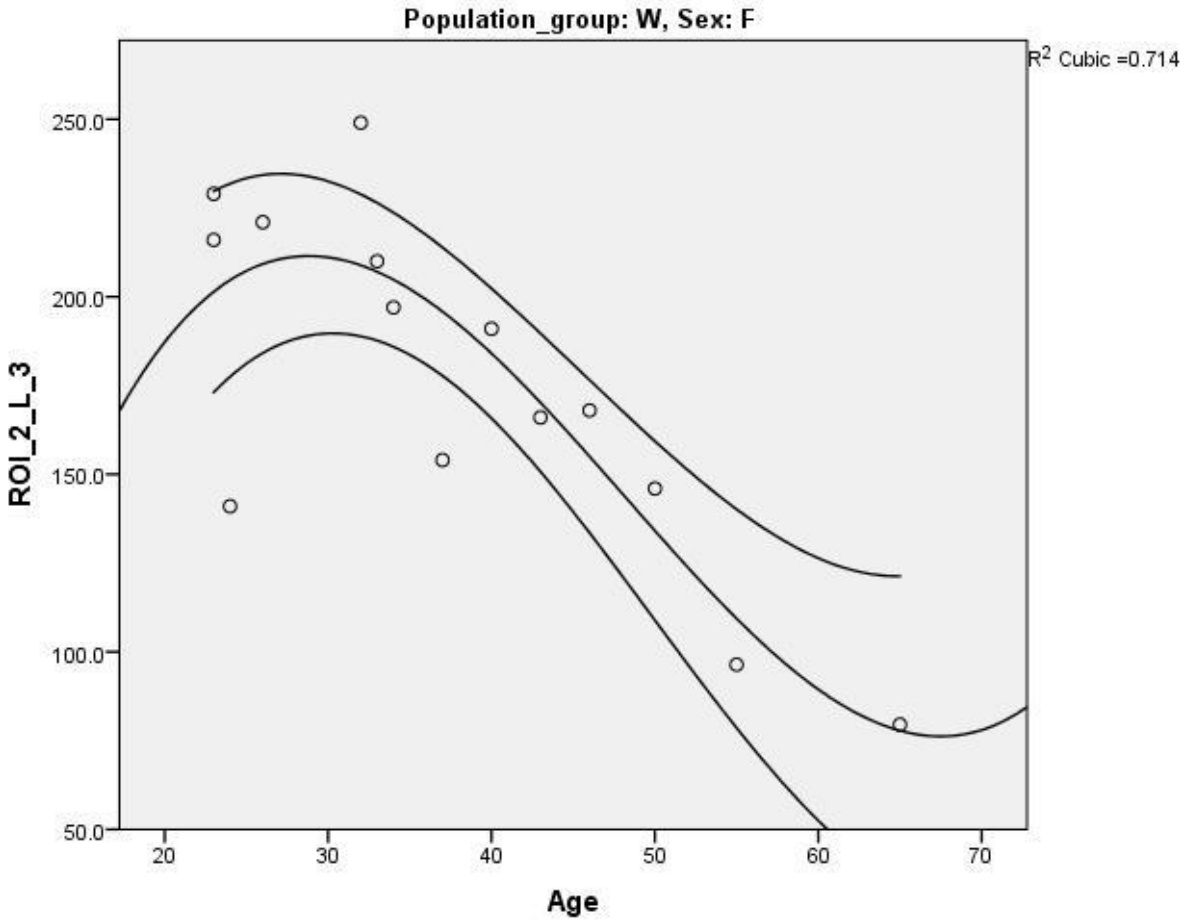

Figure B.3.26: Figure showing the cubic regression line between ROI2 of L3 and age for white females drawn from the scatterplot along with the 95% Confidence interval (lines running parallel to the midline)

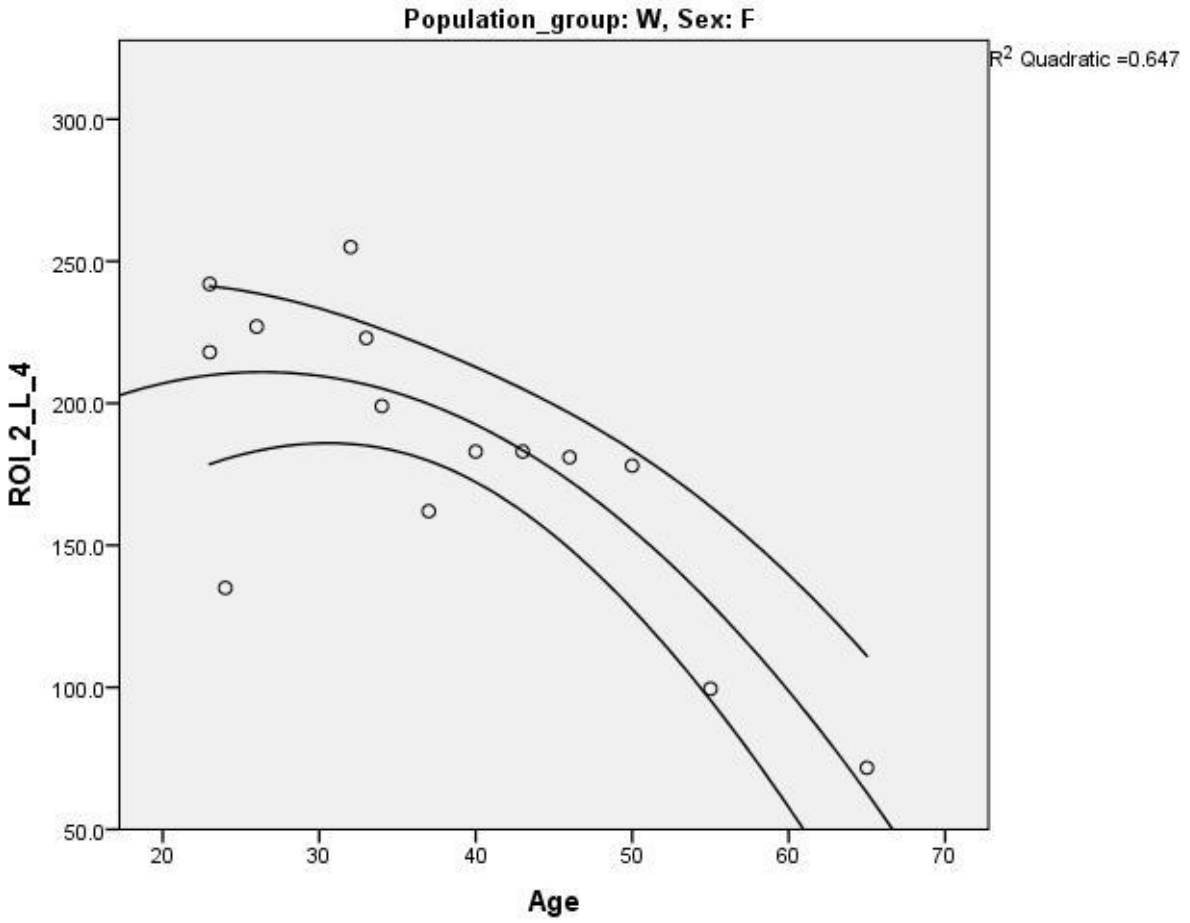

Figure B.3.27: Figure showing the quadratic regression line between ROI2 of L4 and age for white females drawn from the scatterplot along with the 95% Confidence interval (lines running parallel to the midline)

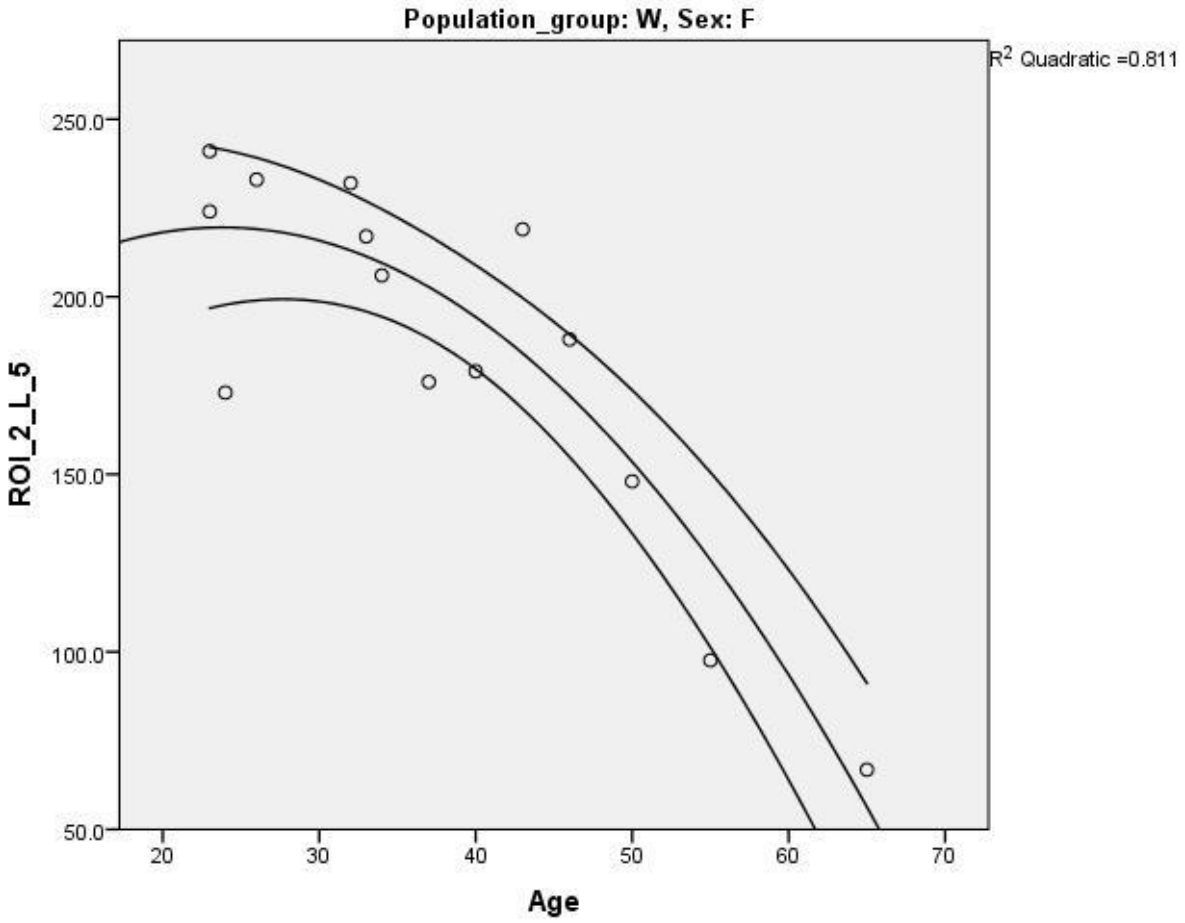

Figure B.3.28: Figure showing the quadratic regression line between ROI2 of L5 and age for white females drawn from the scatterplot along with the 95% Confidence interval (lines running parallel to the midline)

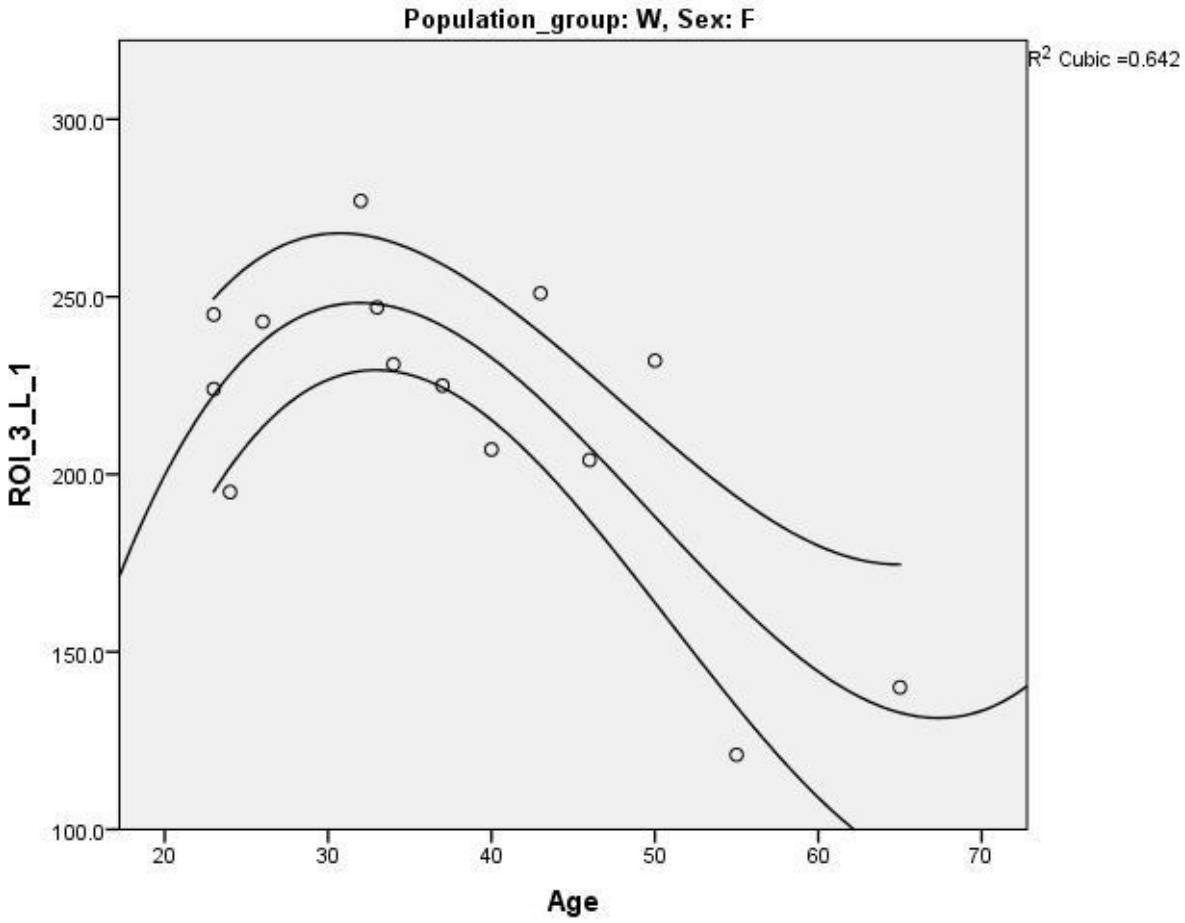

Figure B.3.29: Figure showing the cubic regression line between ROI3 of L1 and age for white females drawn from the scatterplot along with the 95% Confidence interval (lines running parallel to the midline)

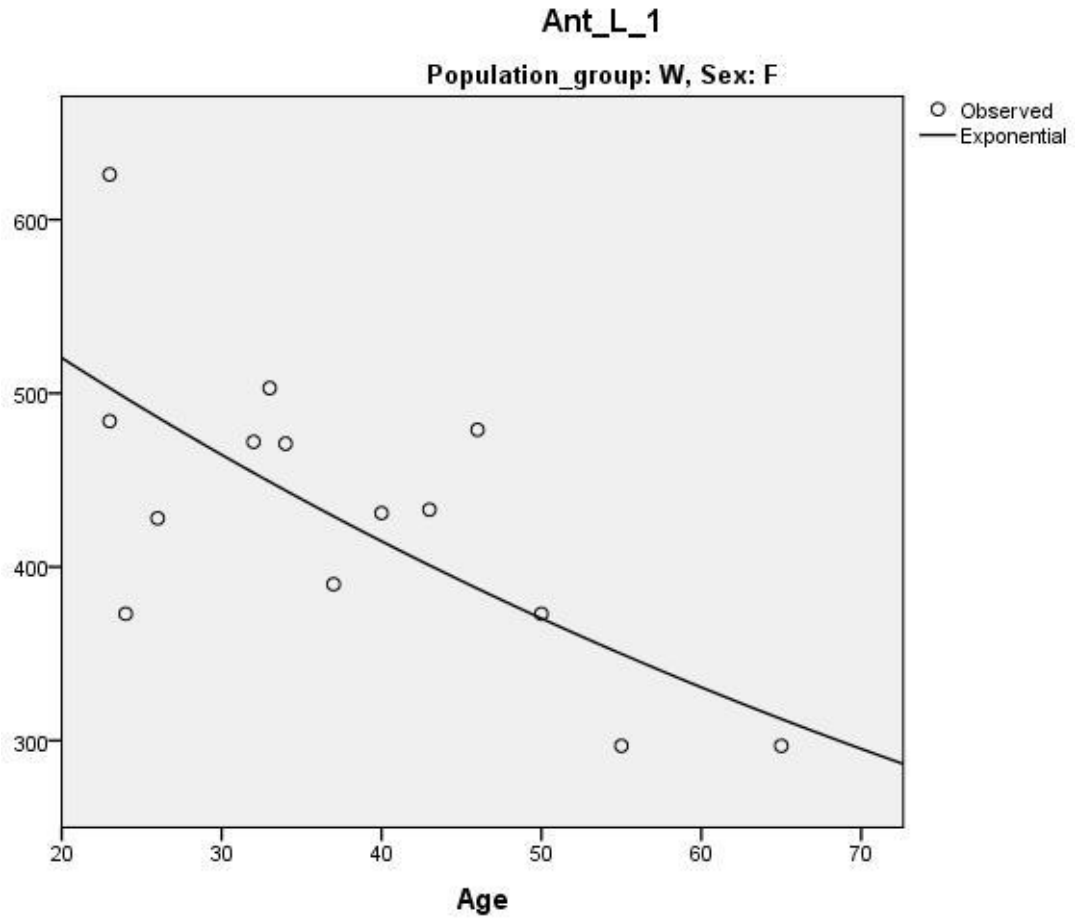

Figure B.3.30: Figure showing the exponential regression line between the anterior border (Ant) of L1 and age for white females drawn from the scatterplot. The r^2 value is 0.52

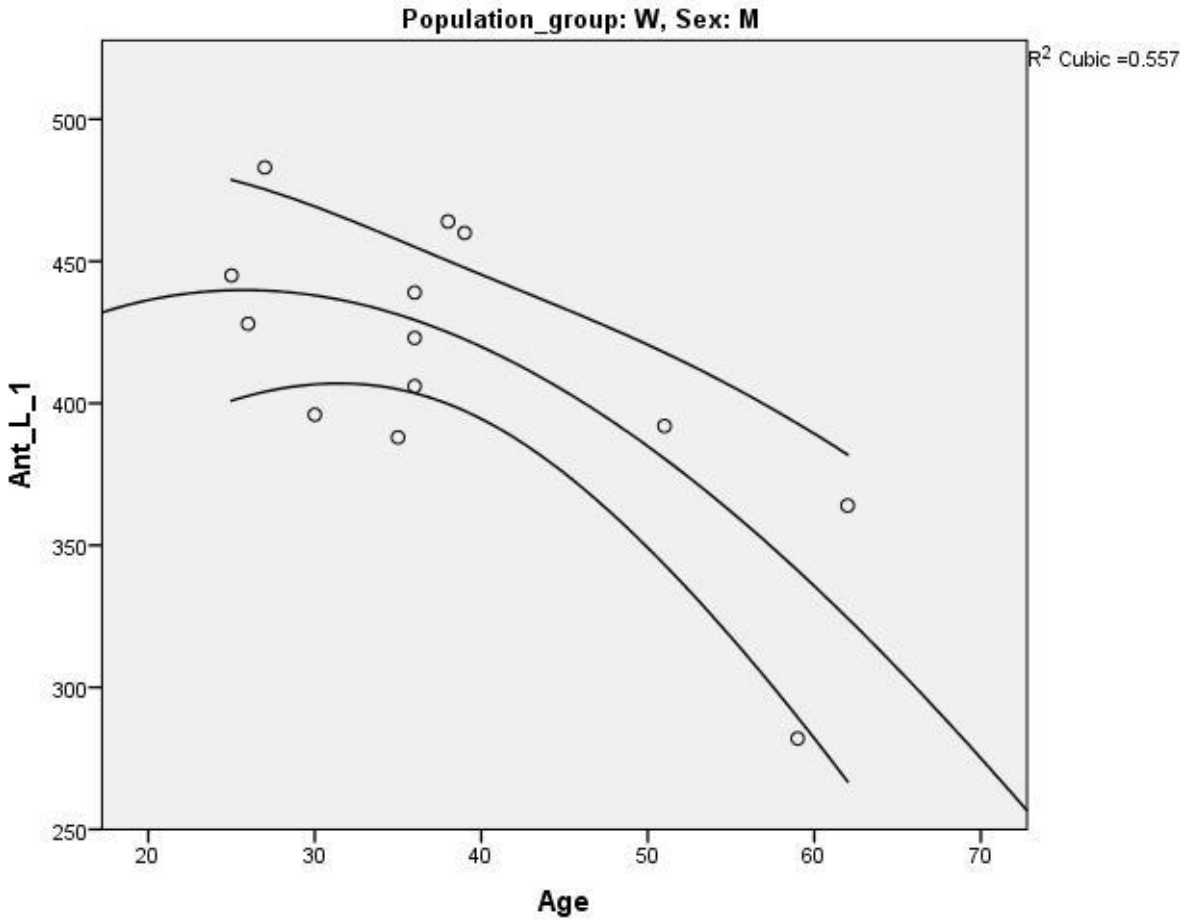

Figure B.3.31: Figure showing the cubic regression line between the anterior border (Ant) of L1 and age for white males drawn from the scatterplot along with the 95% Confidence interval (lines running parallel to the midline)

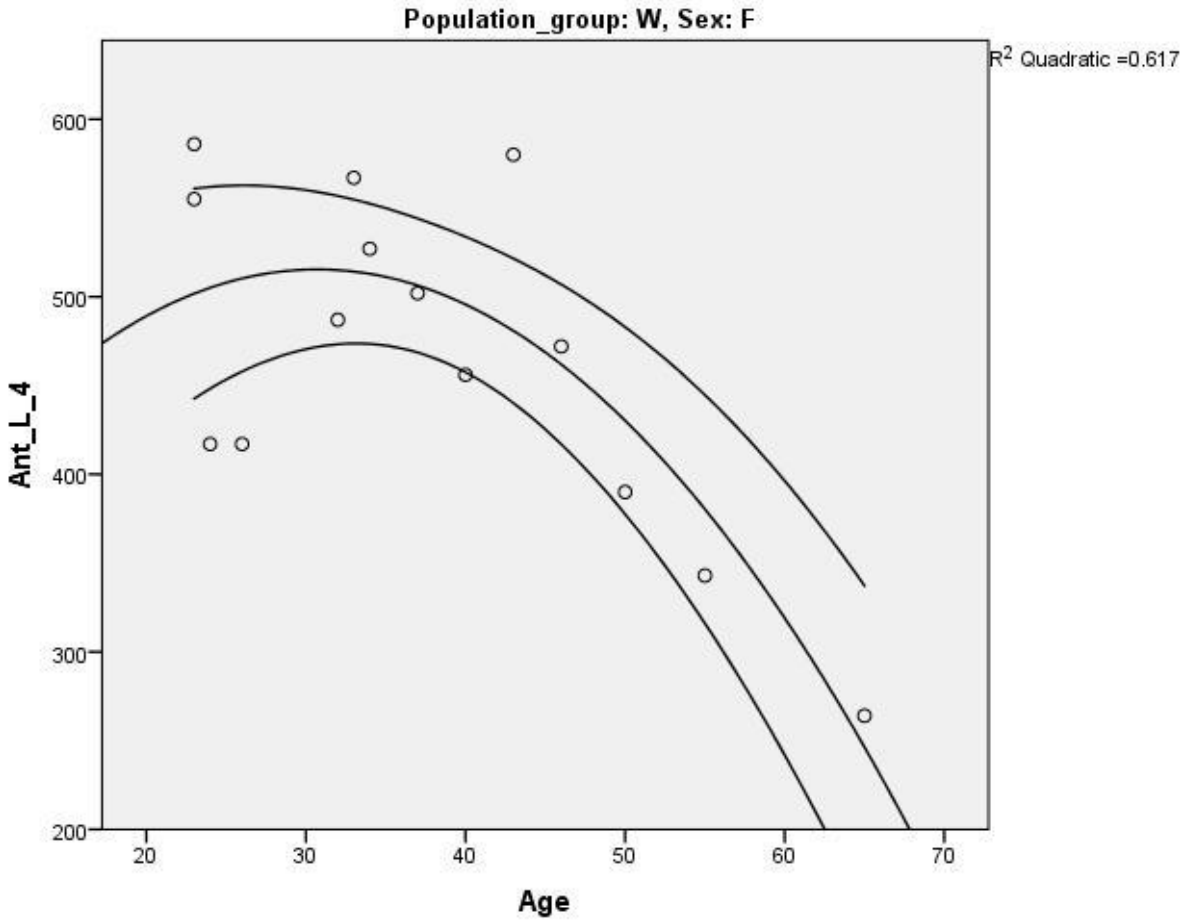

Figure B.3.32: Figure showing the quadratic regression line between the anterior border (Ant) of L4 and age for white females drawn from the scatterplot along with the 95% Confidence interval (lines running parallel to the midline)

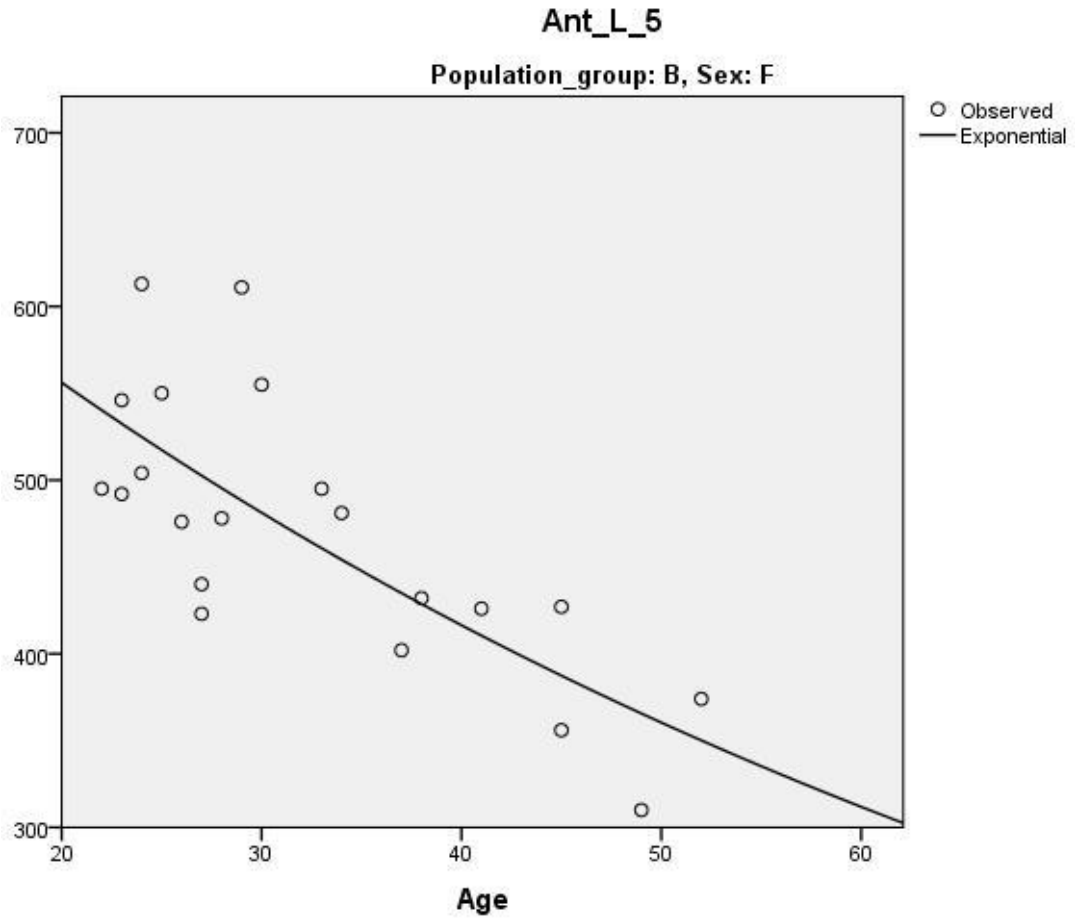

Figure B.3.33: Figure showing the exponential regression line between the anterior border (Ant) of L5 and age for black females drawn from the scatterplot. The r^2 value is 0.61

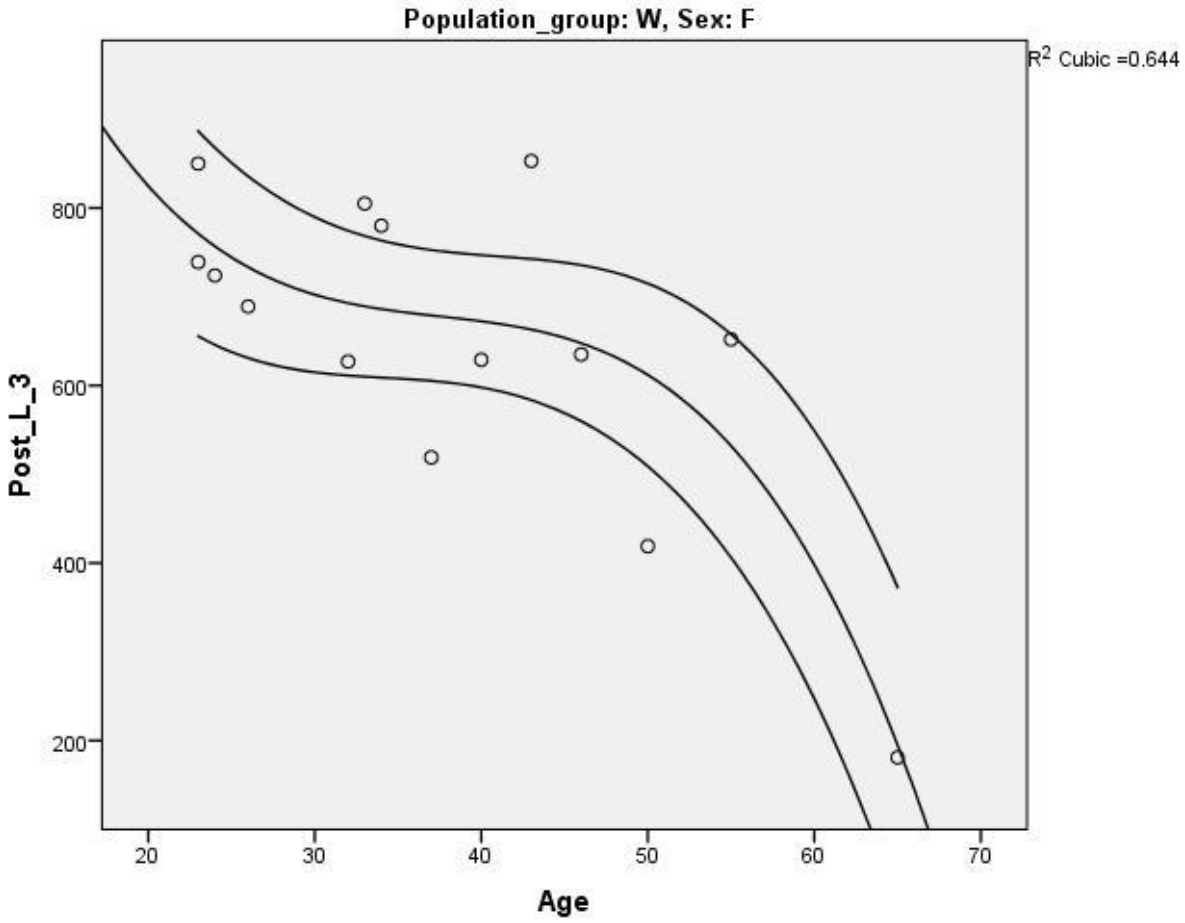

Figure B.3.34: Figure showing the cubic regression line between the posterior border (Post) of L3 and age for white females drawn from the scatterplot along with the 95% Confidence interval (lines running parallel to the midline)

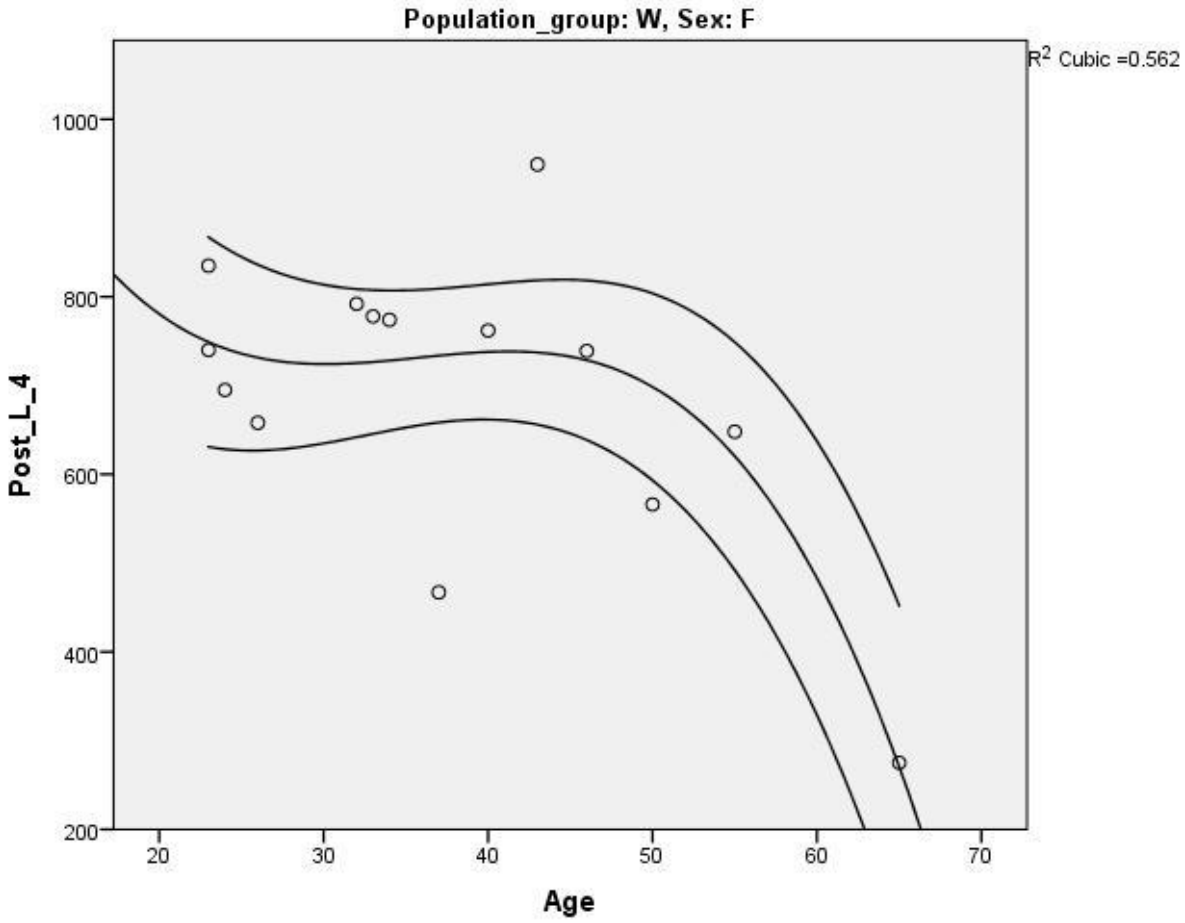

Figure B.3.35: Figure showing the cubic regression line between the posterior border (Post) of L4 and age for white females drawn from the scatterplot along with the 95% Confidence interval (lines running parallel to the midline)

Appendix B.4 – Scatterplot of age and morphometrics correlations

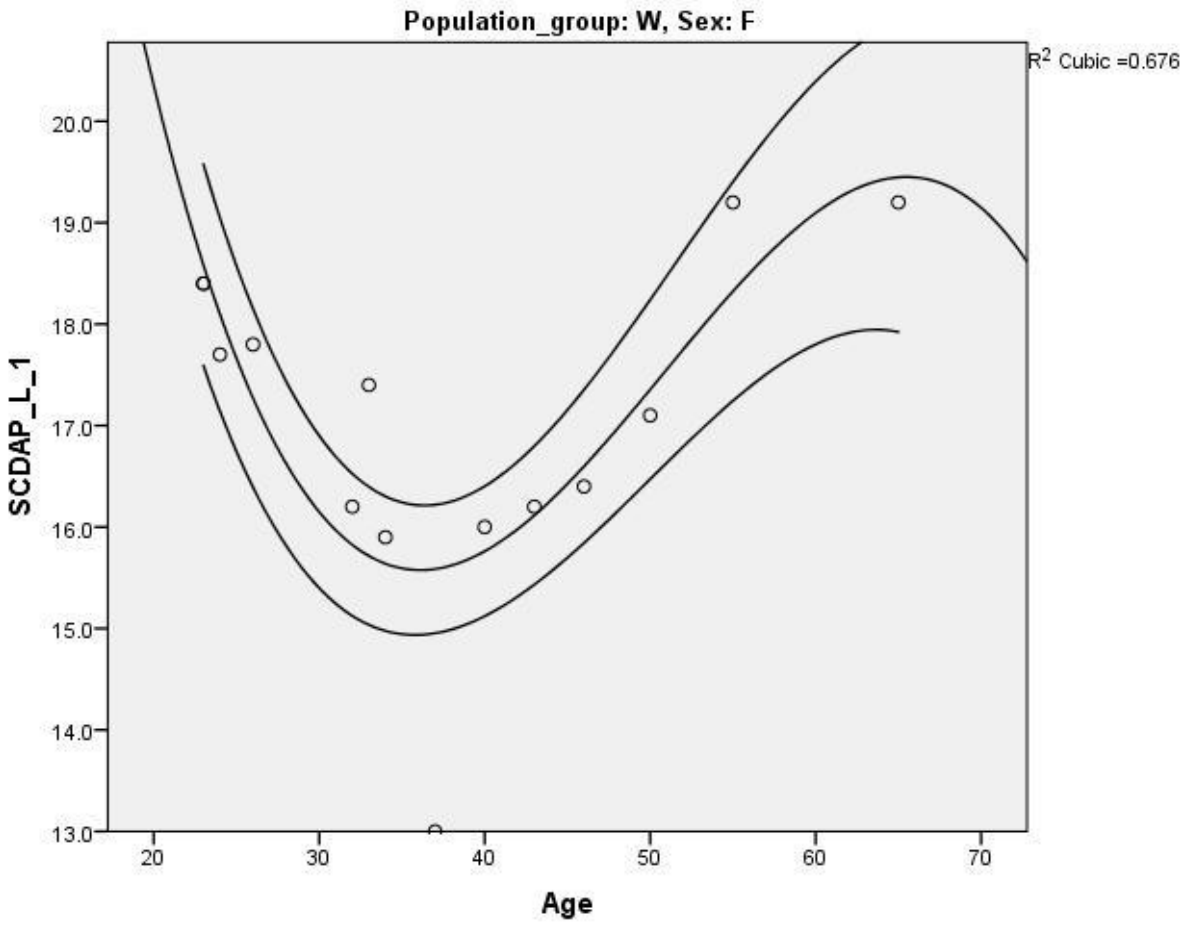

Figure B.4.36: Figure showing the cubic regression line between the AP spinal canal diameter (SCDAP) of L1 and age for white females drawn from the scatterplot along with the 95% Confidence interval (lines running parallel to the midline)

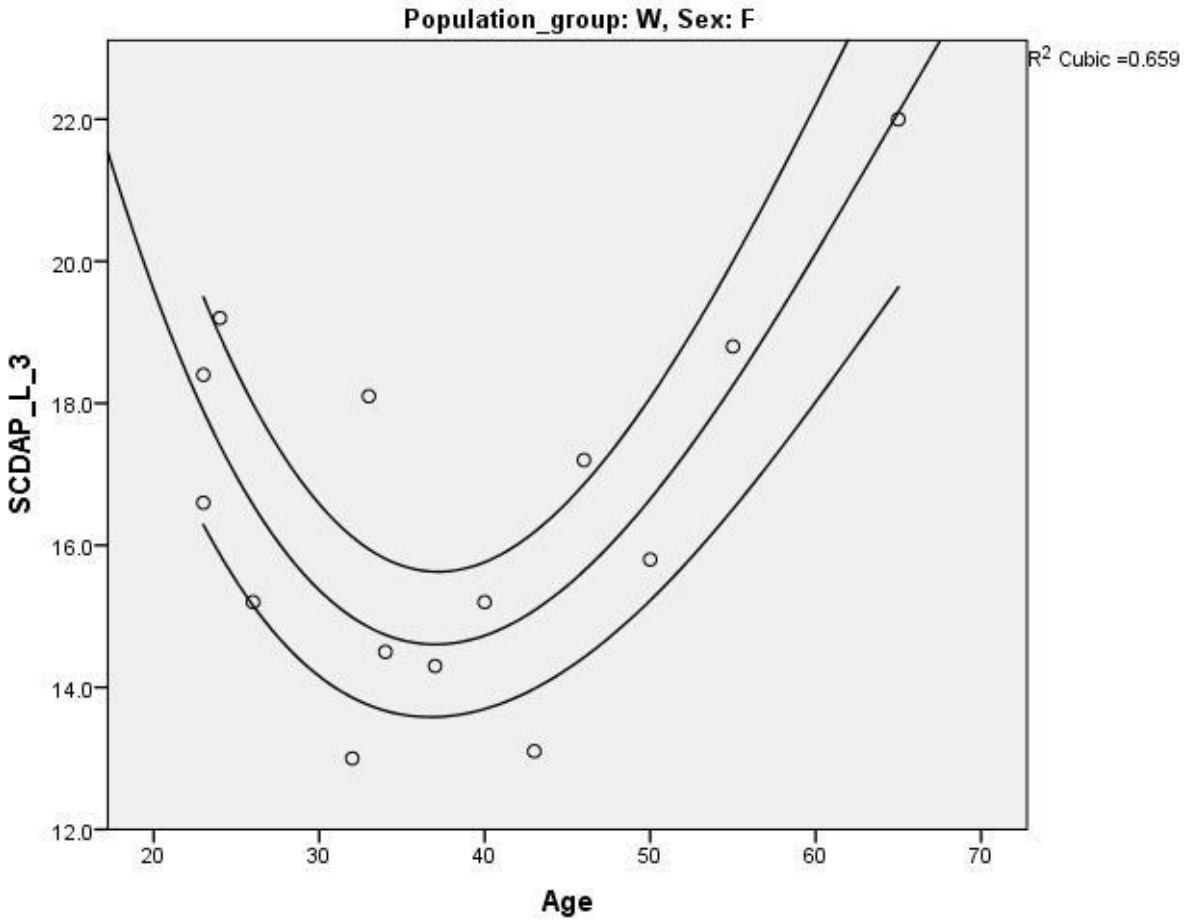

Figure B.4.37: Figure showing the cubic regression line between the AP spinal canal diameter (SCDAP) of L3 and age for white females drawn from the scatterplot along with the 95% Confidence interval (lines running parallel to the midline)

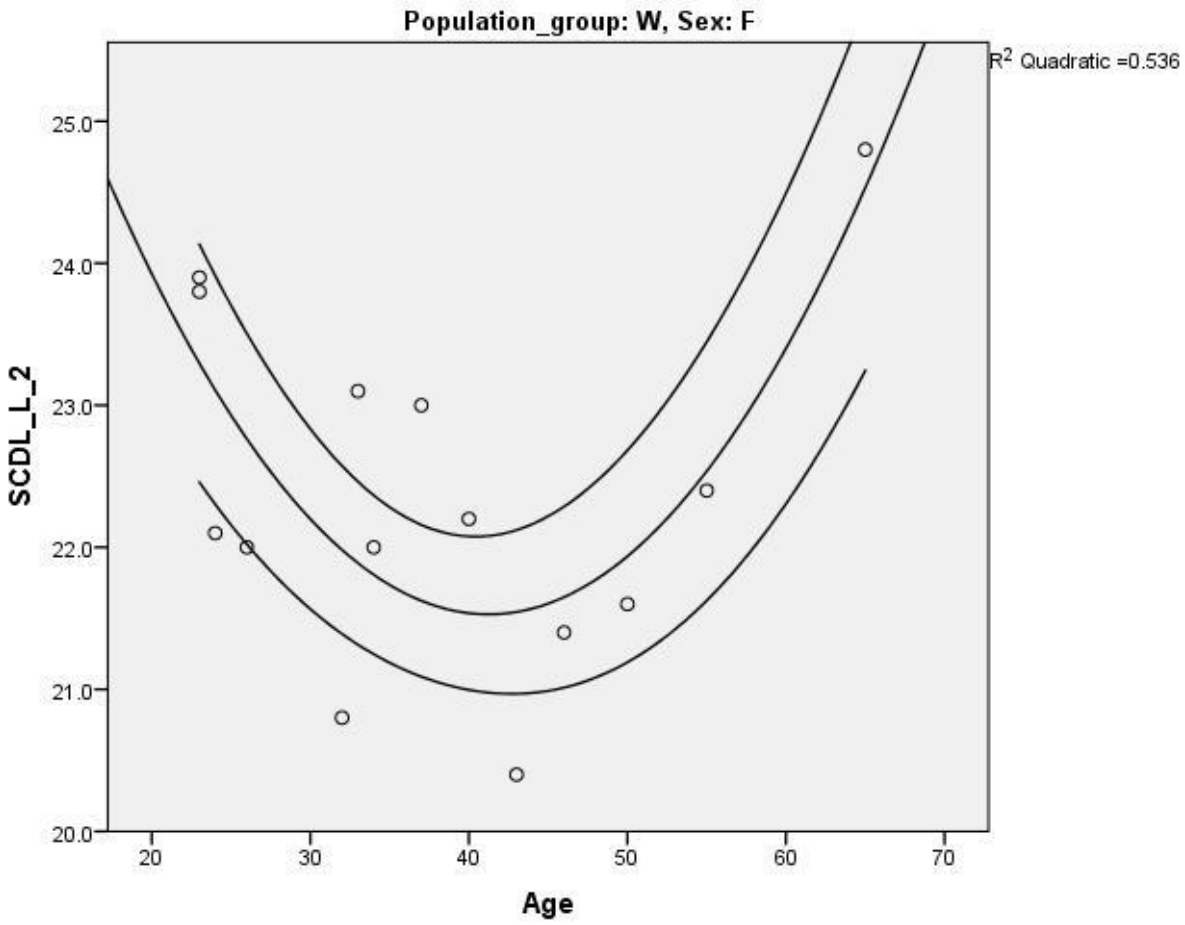

Figure B.4.38: Figure showing the quadratic regression line between the lateral spinal canal diameter (SCDL) of L2 and age for white females drawn from the scatterplot along with the 95% Confidence interval (lines running parallel to the midline)

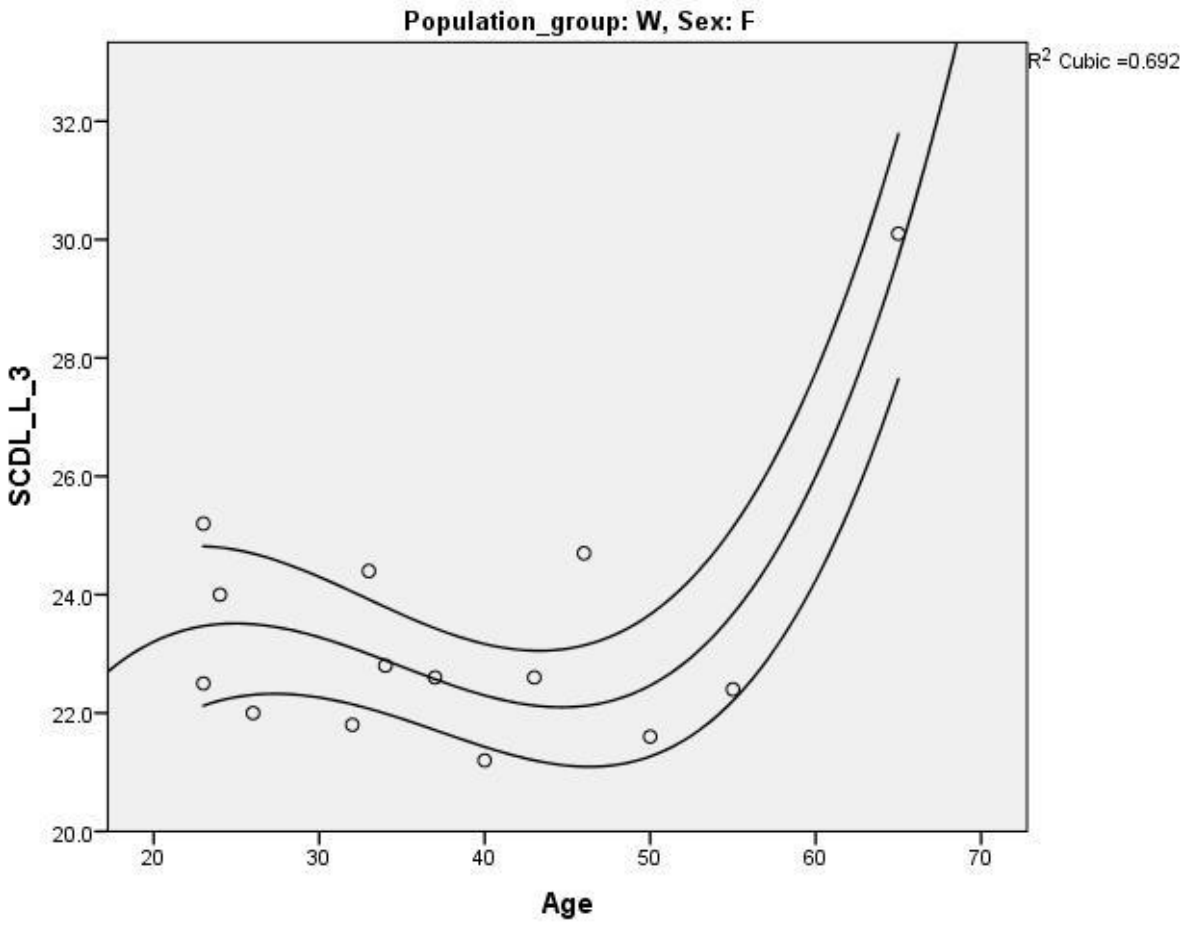

Figure B.4.39: Figure showing the cubic regression line between the lateral spinal canal diameter (SCDL) of L3 and age for white females drawn from the scatterplot along with the 95% Confidence interval (lines running parallel to the midline)

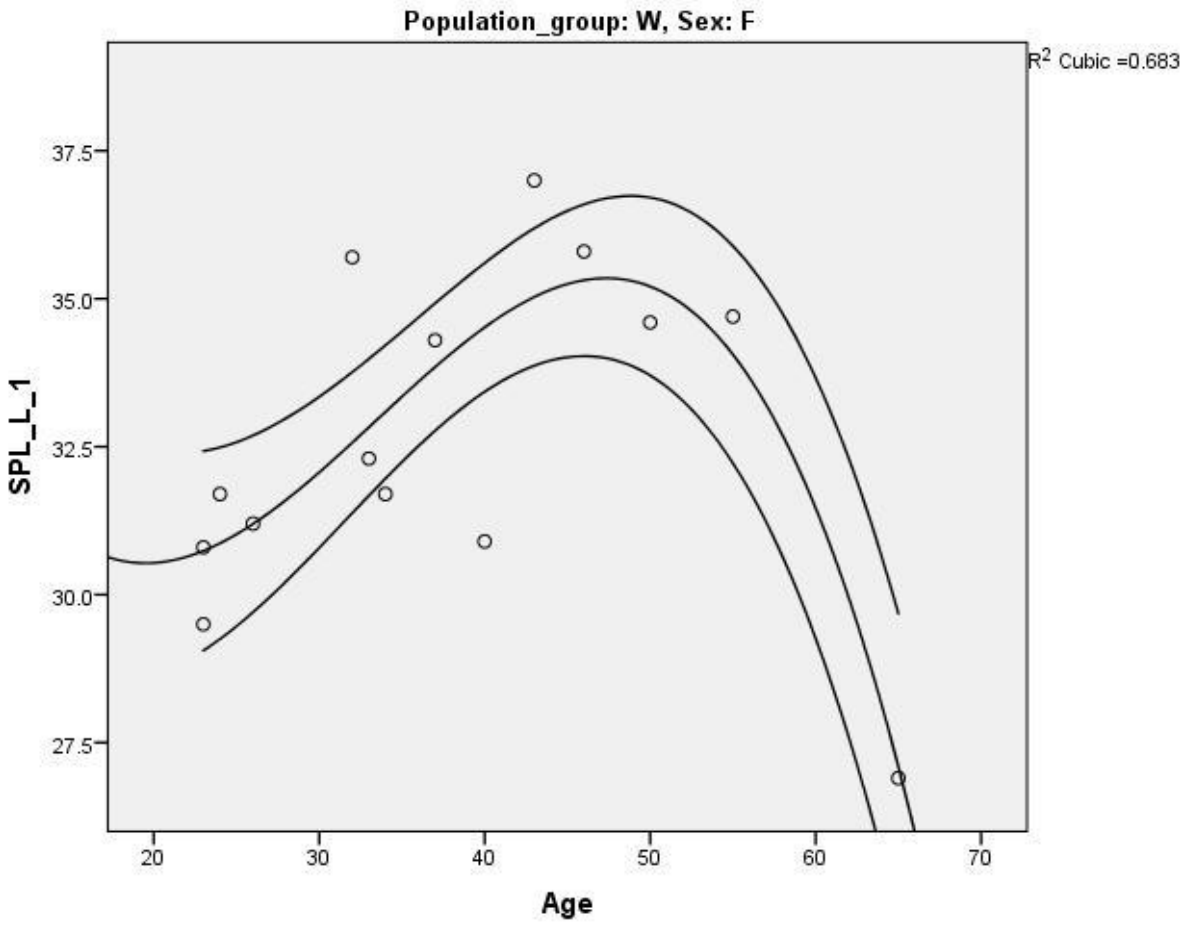

Figure B.4.40: Figure showing the cubic regression line between the spinous process length (SPL) of L1 and age for white females drawn from the scatterplot along with the 95% Confidence interval (lines running parallel to the midline)

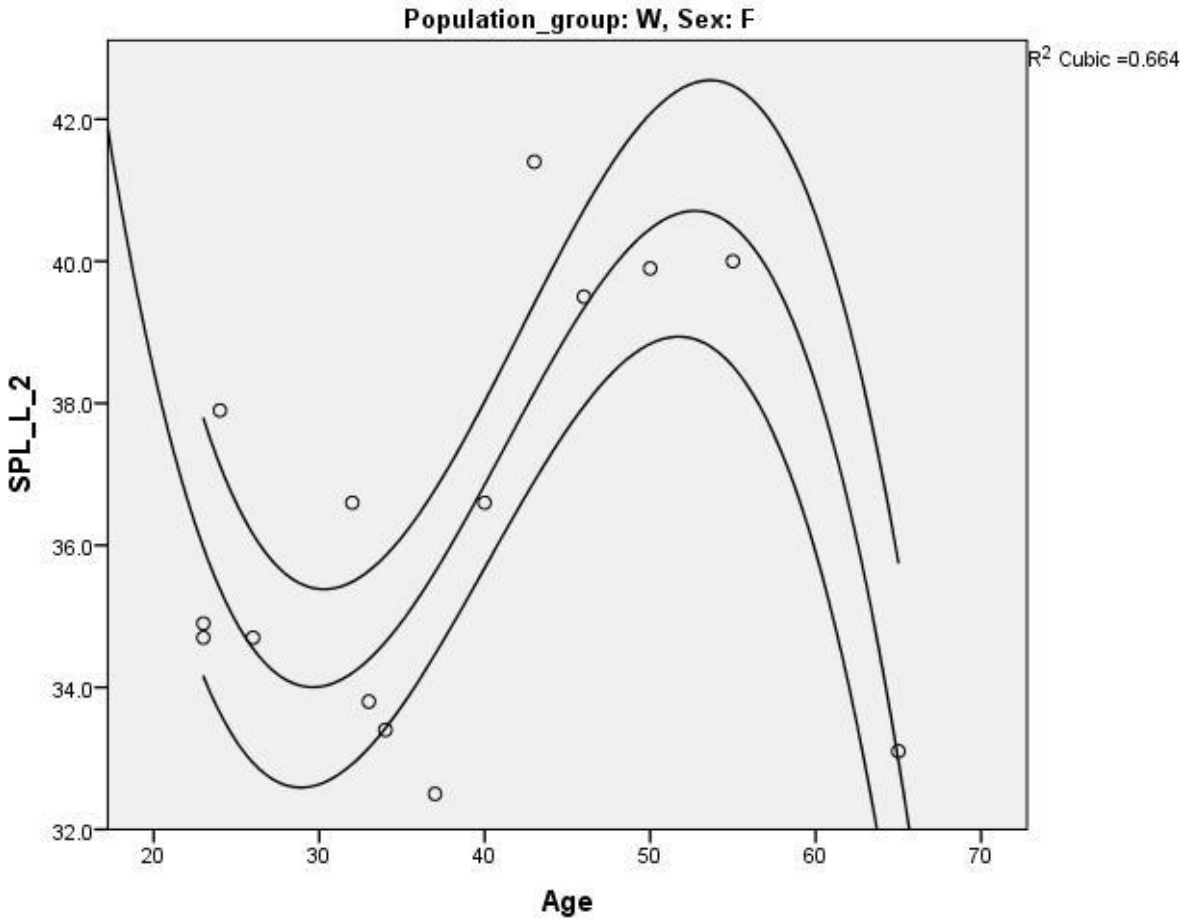

Figure B.4.41: Figure showing the cubic regression line between the spinous process length (SPL) of L2 and age for white females drawn from the scatterplot along with the 95% Confidence interval (lines running parallel to the midline)

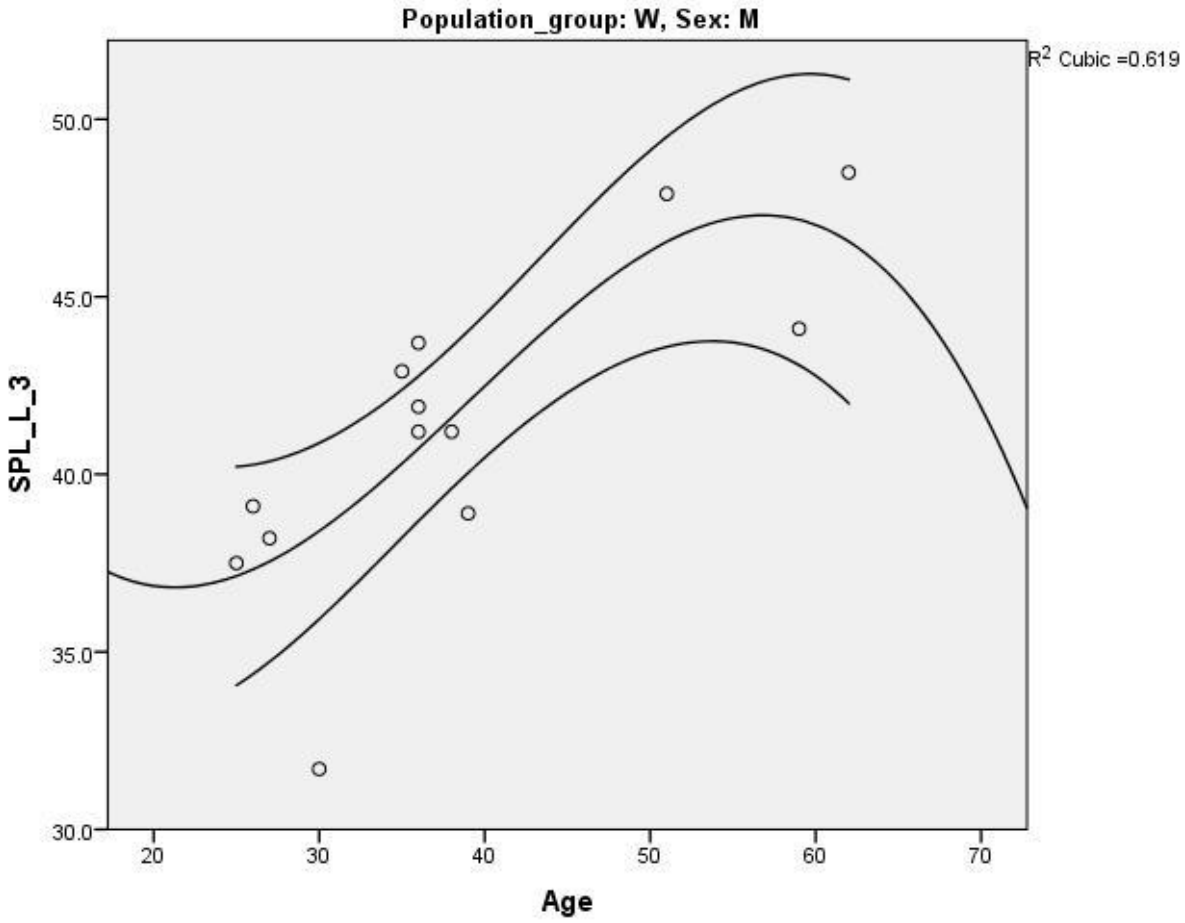

Figure B.4.42: Figure showing the cubic regression line between the spinous process length (SPL) of L3 and age for white males drawn from the scatterplot along with the 95% Confidence interval (lines running parallel to the midline)

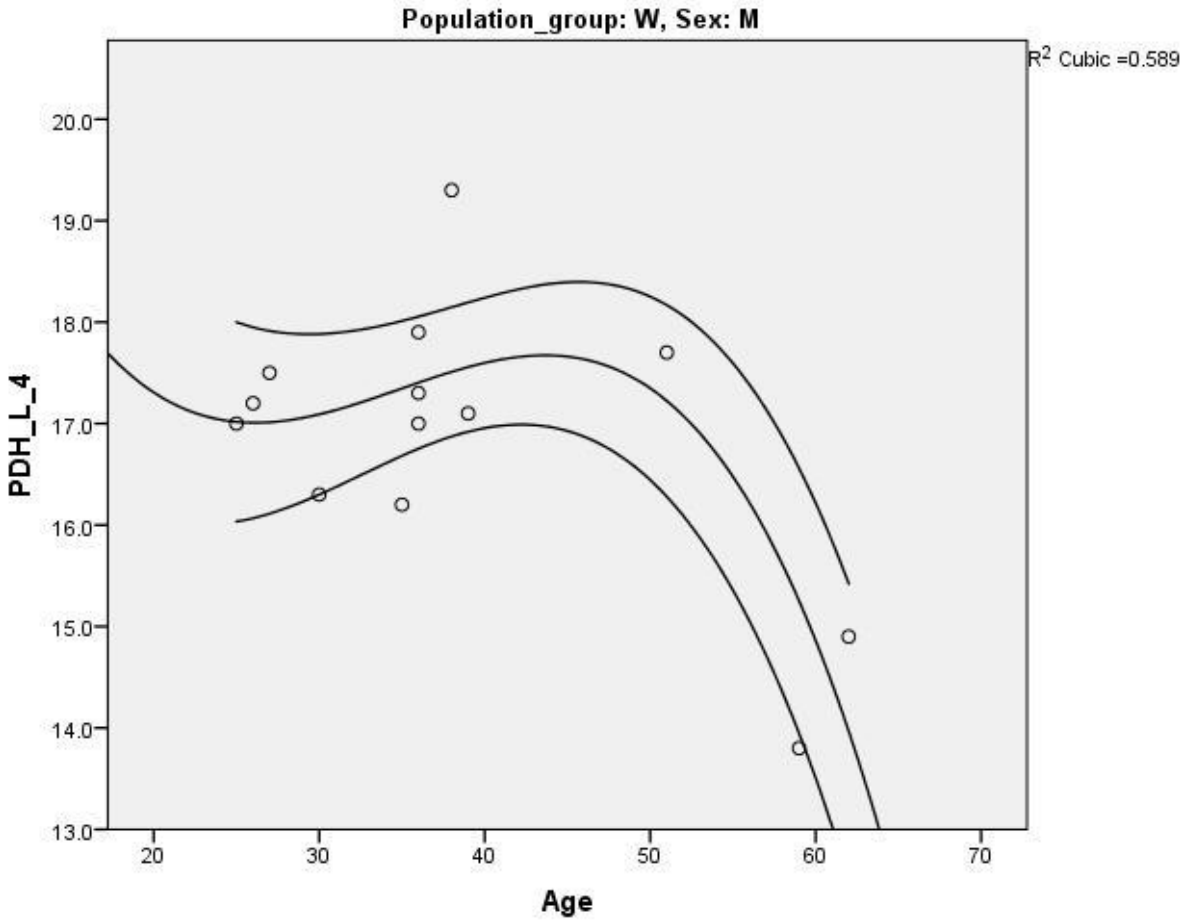

Figure B.4.43: Figure showing the cubic regression line between the pedicle height (PDH) of L4 and age for white males drawn from the scatterplot along with the 95% Confidence interval (lines running parallel to the midline)

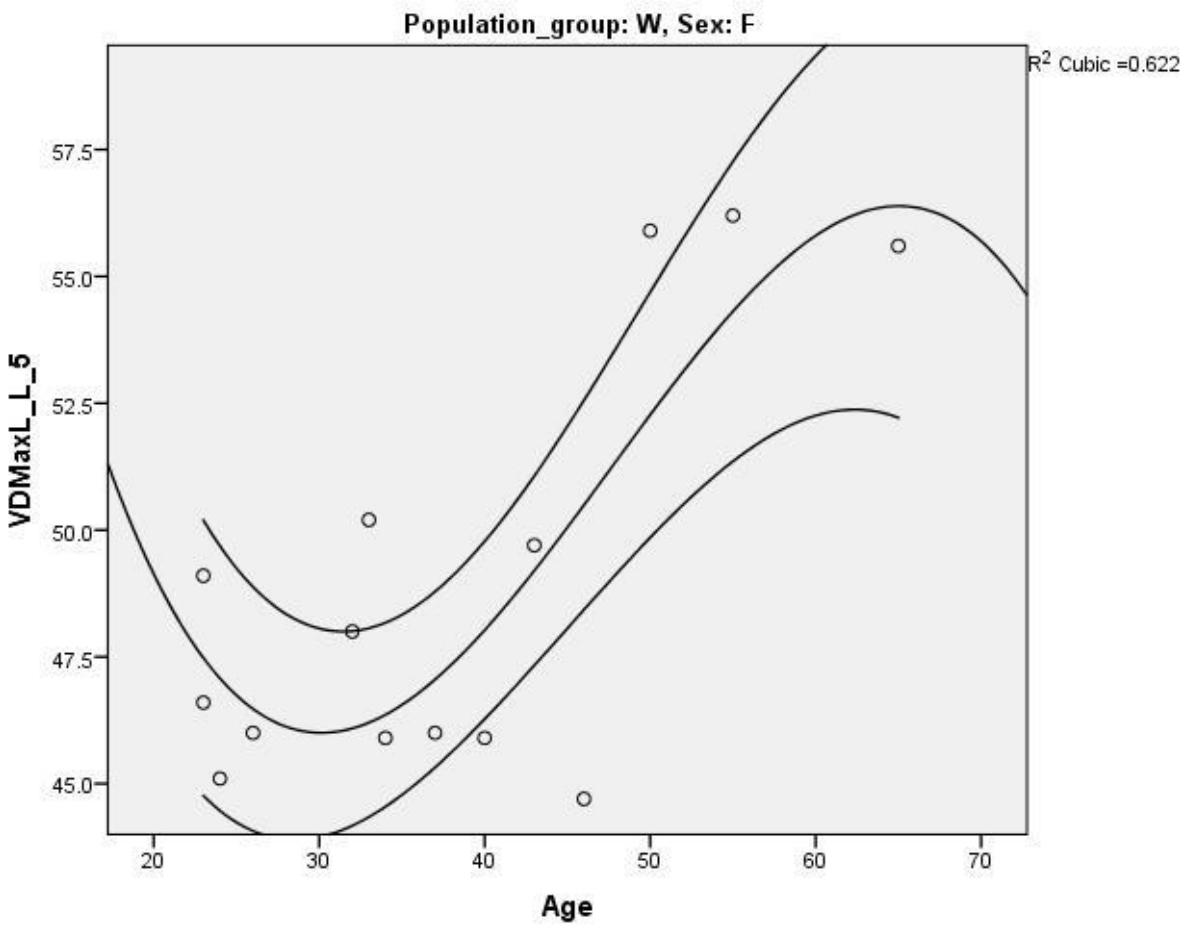

Figure B.4.44: Figure showing the cubic regression line between the maximum lateral vertebral body diameter (VDMaxL) of L5 and age for white females drawn from the scatterplot along with the 95% Confidence interval (lines running parallel to the midline)

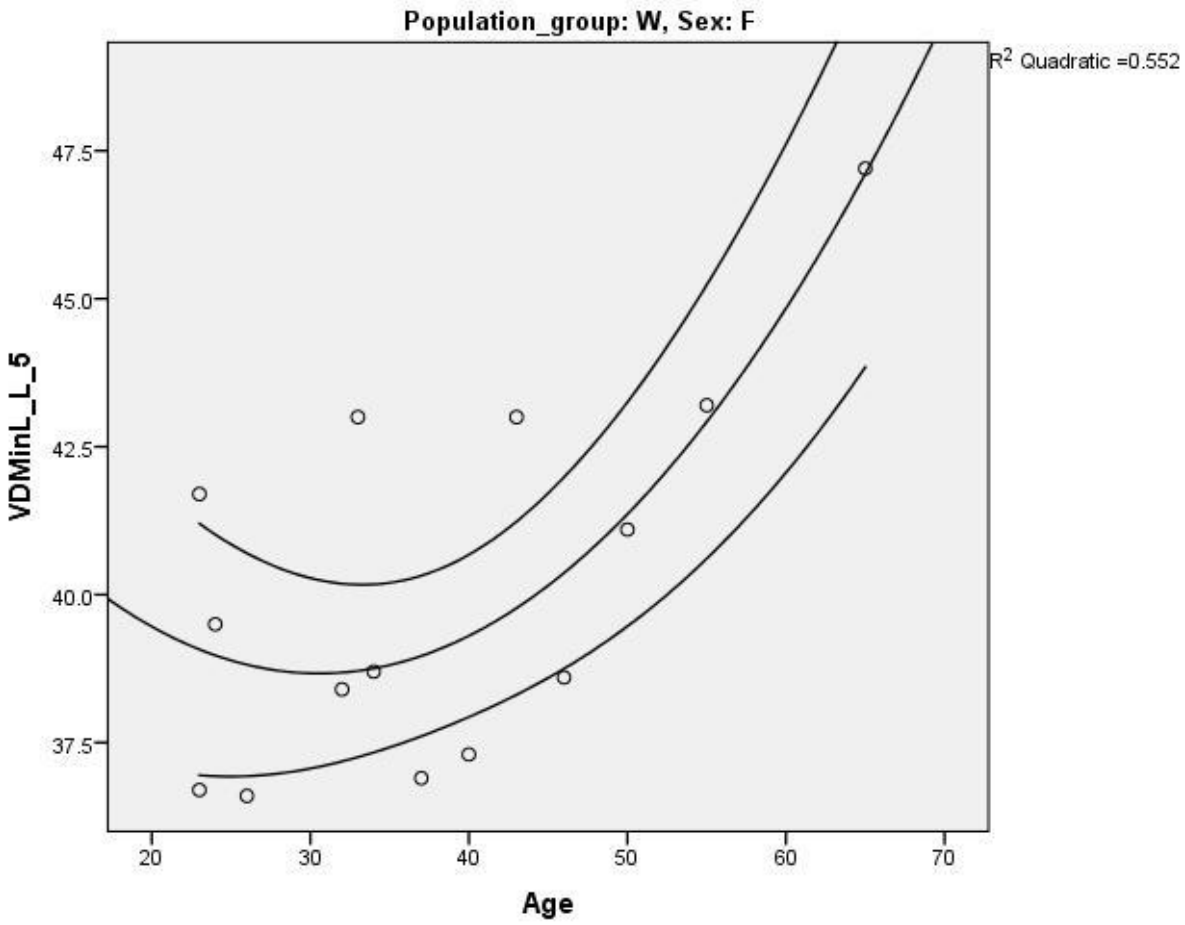

Figure B.4.45: Figure showing the quadratic regression line between the minimum lateral vertebral body diameter (VDMinL) of L5 and age for white females drawn from the scatterplot along with the 95% Confidence interval (lines running parallel to the midline)

Appendix C – LLA and BMD correlations – raw results

Table C.46: Table indicating the r-squared values and associated p-values obtained from the regression analysis for medullary BMD

Variable	VL	P	Linear r^2	p-value	Logarithmic r^2	p-value	Quadratic r^2	p-value	Cubic r^2	p-value	Exponential r^2	p-value
ROI1	L1	BM	0.009	0.611	0.003	0.78	0.024	0.71	0.026	0.86	0.011	0.57
		BF	0.009	0.68	0.019	0.56	0.060	0.57	0.08	0.69	0.014	0.60

Variable	VL	P	Linear r^2	p-value	Logarithmic r^2	p-value	Quadratic r^2	p-value	Cubic r^2	p-value	Exponential r^2	p-value
		WM	0.140	0.26	0.016	0.22	0.250	0.32	0.26	0.30	0.13	0.27
		WF	0.000	0.99	0.000	0.99	0.001	0.99	0.001	0.99	0.002	0.88
	L2	**BM**	0.015	0.50	0.011	0.57	0.015	0.80	0.027	0.86	0.019	0.46
		BF	0.006	0.74	0.005	0.75	0.006	0.94	0.045	0.85	0.004	0.79
		WM	0.218	0.15	0.222	0.14	0.227	0.36	0.230	0.35	0.211	0.16
		WF	0.000	0.99	0.000	0.97	0.002	0.99	0.002	0.99	0.008	0.76
	L3	**BM**	0.000	0.96	0.000	0.98	0.001	0.99	0.053	0.80	0.000	0.99
		BF	0.003	0.76	0.007	0.65	0.014	0.82	0.032	0.82	0.004	0.74
		WM	0.016	0.68	0.033	0.55	0.223	0.28	0.223	0.28	0.031	0.56
		WF	0.002	0.87	0.001	0.94	0.032	0.84	0.027	0.86	0.016	0.67
	L4	**BM**	0.074	0.13	0.075	0.12	0.076	0.31	0.077	0.50	0.082	0.11
		BF	0.034	0.41	0.027	0.47	0.037	0.70	0.040	0.86	0.038	0.39
		WM	0.080	0.35	0.119	0.25	0.370	0.10	0370	0.10	0.100	0.29
		WF	0.000	0.95	0.001	0.92	0.005	0.97	0.005	0.97	0.003	0.85
	L5	**BM**	0.096	0.10	0.088	0.11	0.097	0.25	0.105	0.40	0.102	0.09
		BF	0.023	0.51	0.032	0.43	0.040	0.68	0.041	0.86	0.014	0.60
		WM	0.040	0.51	0.039	0.52	0.040	0.82	0.040	0.81	0.044	0.49
		WF	0.000	0.95	0.002	0.89	0.034	0.83	0.034	0.83	0.000	0.96
ROI2	**L1**	**BM**	0.036	0.29	0.047	0.23	0.046	0.49	0.057	0.63	0.041	0.26
		BF	0.064	0.26	0.049	0.32	0.072	0.49	0.114	0.52	0.074	0.22
		WM	0.006	0.80	0.007	0.79	0.007	0.97	0.007	0.97	0.001	0.94
		WF	0.001	0.94	0.002	0.87	0.043	0.79	0.043	0.79	0.001	0.91
	L2	**BM**	0.040	0.26	0.052	0.20	0.054	0.43	0.062	0.59	0.035	0.29
		BF	0.099	0.16	0.077	0.21	0.110	0.33	0.138	0.43	0.119	0.12
		WM	0.003	0.86	0.005	0.52	0.009	0.96	0.009	0.96	0.000	0.95
		WF	0.023	0.60	0.029	0.56	0.056	0.73	0.057	0.73	0.040	0.49
	L3	**BM**	0.027	0.36	0.042	0.25	0.055	0.43	0.059	0.62	0.026	0.37
		BF	0.064	0.26	0.049	0.32	0.074	0.48	0.100	0.58	0.077	0.21
		WM	0.007	0.78	0.007	0.79	0.008	0.96	0.010	0.95	0.014	0.70
		WF	0.004	0.84	0.007	0.78	0.041	0.79	0.043	0.78	0.011	0.72
	L4	**BM**	0.057	0.18	0.076	0.12	0.084	0.27	0.093	0.41	0.052	0.20
		BF	0.082	0.20	0.077	0.21	0.082	0.44	0.089	0.63	0.087	0.18

Variable	VL	P	Linear r^2	p-value	Logarithmic r^2	p-value	Quadratic r^2	p-value	Cubic r^2	p-value	Exponential r^2	p-value
		WM	0.001	0.92	0.000	0.99	0.040	0.81	0.030	0.86	0.002	0.88
		WF	0.011	0.72	0.013	0.70	0.021	0.89	0.022	0.89	0.024	0.60
	L5	**BM**	0.049	0.24	0.055	0.21	0.060	0.43	0.061	0.65	0.043	0.27
		BF	0.082	0.21	0.090	0.19	0.093	0.42	0.108	0.57	0.101	0.16
		WM	0.001	0.91	0.002	0.88	0.002	0.99	0.004	0.98	0.000	0.97
		WF	0.001	0.94	0.000	0.95	0.001	0.99	0.001	0.99	0.012	0.71
ROI3	**L1**	**BM**	0.074	0.12	0.056	0.19	0.088	0.25	0.088	0.44	0.083	0.11
		BF	0.028	0.45	0.035	0.41	0.059	0.56	0.137	0.44	0.037	0.39
		WM	0.152	0.19	0.085	0.14	0.269	0.21	0.269	0.21	0.155	0.18
		WF	0.014	0.68	0.008	0.75	0.056	0.73	0.050	0.76	0.020	0.63
	L2	**BM**	0.086	0.10	0.073	0.13	0.089	0.25	0.090	0.43	0.086	0.10
		BF	0.093	0.17	0.091	0.17	0.098	0.38	0.154	0.38	0.116	0.12
		WM	0.007	0.79	0.001	0.94	0.230	0.27	0.214	0.30	0.013	0.71
		WF	0.049	0.50	0.045	0.51	0.050	0.79	0.050	0.79	0.050	0.48
	L3	**BM**	0.134	0.04	0.098	0.08	0.159	0.07	0.160	0.16	0.141	0.03
		BF	0.030	0.44	0.044	0.35	0.091	0.40	0.150	0.39	0.041	0.37
		WM	0.016	0.68	0.029	0.58	0.191	0.35	0.198	0.33	0.014	0.70
		WF	0.137	0.26	0.153	0.24	0.205	0.40	0.224	0.36	0.124	0.29
	L4	**BM**	0.135	0.04	0.108	0.06	0.142	0.10	0.143	0.21	0.141	0.03
		BF	0.160	0.07	0.154	0.07	0.165	0.18	0.241	0.16	0.183	0.05
		WM	0.057	0.43	0.083	0.34	0.214	0.30	0.214	0.30	0.066	0.40
		WF	0.000	0.94	0.004	0.83	0.138	0.44	0.141	0.43	0.000	0.97
	L5	**BM**	0.220	0.01	0.181	0.02	0.227	0.03	0.235	0.07	0.218	0.01
		BF	0.112	0.14	0.106	0.15	0.113	0.34	0.158	0.39	0.137	0.10
		WM	0.013	0.71	0.011	0.73	0.013	0.94	0.015	0.93	0.006	0.80
		WF	0.059	0.40	0.079	0.33	0.182	0.33	0.182	0.33	0.037	0.51

Key: VL = Vertebral level; P = Population group; r^2 = The r^2 value; BM = Black male; BF = Black female; WM = White male; WF = White female; ROI1 = Region of interest 1; ROI2 = Region of interest 2; ROI3 = Region of interest 3

Table C.47: Table indicating the r-squared values and associated p-values obtained from the regression analysis for endplate BMD

Variable	VL	P	Linear r^2	p-value	Logarithmic r^2	p-value	Quadratic r^2	p-value	Cubic r^2	p-value	Exponential r^2	p-value
SEP	L1	BM	0.041	0.26	0.026	0.37	0.061	0.37	0.066	0.57	0.027	0.36
		BF	0.000	0.95	0.000	0.99	0.003	0.97	0.004	0.99	0.000	0.99
		WM	0.019	0.67	0.015	0.71	0.028	0.88	0.024	0.90	0.013	0.73
		WF	0.020	0.63	0.017	0.65	0.026	0.87	0.026	0.86	0.010	0.73
	L2	BM	0.000	0.71	0.004	0.72	0.006	0.92	0.008	0.97	0.004	0.72
		BF	0.006	0.72	0.002	0.84	0.018	0.84	0.055	0.79	0.008	0.69
		WM	0.016	0.68	0.008	0.77	0.084	0.65	0.069	0.70	0.016	0.68
		WF	0.105	0.26	0.110	0.25	0.119	0.50	0.123	0.49	0.113	0.24
	L3	BM	0.001	0.86	0.003	0.76	0.006	0.91	0.009	0.97	0.000	0.93
		BF	0.001	0.89	0.001	0.88	0.001	0.99	0.002	0.99	0.003	0.80
		WM	0.010	0.75	0.004	0.85	0.110	0.56	0.101	0.59	0.014	0.70
		WF	0.083	0.32	0.088	0.30	0.095	0.58	0.099	0.56	0.082	0.32
	L4	BM	0.002	0.81	0.000	0.92	0.011	0.92	0.015	0.93	0.004	0.72
		BF	0.018	0.55	0.022	0.51	0.030	0.75	0.034	0.89	0.022	0.51
		WM	0.119	0.25	0.112	0.26	0.128	0.50	0.133	0.49	0.099	0.29
		WF	0.052	0.43	0.055	0.42	0.060	0.71	0.061	0.71	0.042	0.48
	L5	BM	0.001	0.89	0.000	0.99	0.004	0.94	0.005	0.99	0.002	0.79
		BF	0.002	0.83	0.001	0.89	0.009	0.92	0.012	0.98	0.005	0.76
		WM	0.001	0.91	0.002	0.88	0.030	0.86	0.038	0.83	0.001	0.91
		WF	0.095	0.28	0.107	0.26	0.128	0.47	0.131	0.46	0.077	0.34
IEP	L1	BM	0.034	0.31	0.056	0.19	0.094	0.23	0.094	0.41	0.027	0.36
		BF	0.000	0.95	0.001	0.87	0.019	0.84	0.023	0.93	0.004	0.78
		WM	0.014	0.70	0.010	0.74	0.024	0.89	0.022	0.90	0.008	0.77
		WF	0.011	0.72	0.012	0.71	0.015	0.92	0.015	0.92	0.012	0.71
	L2	BM	0.042	0.25	0.053	0.20	0.062	0.39	0.062	0.59	0.040	0.26
		BF	0.017	0.57	0.010	0.66	0.020	0.83	0.107	0.55	0.015	0.59
		WM	0.006	0.79	0.006	0.80	0.007	0.97	0.007	0.97	0.008	0.78
		WF	0.005	0.81	0.002	0.89	0.093	0.59	0.118	0.50	0.003	0.84
	L3	BM	0.090	0.10	0.073	0.14	0.090	0.25	0.171	0.15	0.098	0.08

Variable	VL	P	Linear r^2	p-value	Logarithmic r^2	p-value	Quadratic r^2	p-value	Cubic r^2	p-value	Exponential r^2	p-value
		BF	0.007	0.72	0.010	0.65	0.012	0.90	0.012	0.91	0.005	0.76
		WM	0.010	0.74	0.018	0.67	0.092	0.62	0.093	0.61	0.017	0.67
		WF	0.000	0.99	0.000	0.94	0.040	0.80	0.046	0.77	0.001	0.90
	L4	**BM**	0.008	0.61	0.010	0.58	0.013	0.82	0.017	0.92	0.011	0.57
		BF	0.003	0.80	0.005	0.75	0.005	0.96	0.032	0.90	0.000	0.99
		WM	0.006	0.81	0.004	0.84	0.018	0.92	0.019	0.91	0.012	0.72
		WF	0.230	0.08	0.264	0.06	0.361	0.09	0.375	0.08	0.199	0.11
	L5	**BM**	0.010	0.59	0.021	0.42	0.036	0.58	0.042	0.75	0.009	0.61
		BF	0.015	0.60	0.007	0.72	0.042	0.68	0.043	0.86	0.014	0.62
		WM	0.000	0.97	0.002	0.88	0.063	0.72	0.050	0.77	0.000	0.97
		WF	0.037	0.51	0.038	0.50	0.044	0.78	0.049	0.76	0.037	0.51

Key: VL = Vertebral level; P = Population group; r^2 = The r^2 value; BM = Black male; BF = Black female; WM = White male; WF = White female; SEP = Superior endplate; IEP = Inferior endplate

Table C.48: Table indicating the r-squared values and associated p-values obtained from the regression analysis for border BMD

Variable	VL	P	Linear r^2	p-value	Logarithmic r^2	p-value	Quadratic r^2	p-value	Cubic r^2	p-value	Exponential r^2	p-value
AB	**L1**	**BM**	0.019	0.44	0.018	0.46	0.019	0.75	0.020	0.90	0.018	0.45
		BF	0.066	0.25	0.100	0.15	0.156	0.20	0.157	0.37	0.057	0.29
		WM	0.005	0.83	0.011	0.73	0.069	0.70	0.069	0.70	0.013	0.71
		WF	0.004	0.82	0.003	0.85	0.009	0.95	0.008	0.96	0.001	0.93
	L2	**BM**	0.067	0.15	0.040	0.26	0.095	0.22	0.097	0.39	0.071	0.13
		BF	0.034	0.41	0.052	0.31	0.108	0.34	0.147	0.40	0.038	0.39
		WM	0.073	0.37	0.043	0.50	0.336	0.13	0.320	0.15	0.085	0.33
		WF	0.275	0.05	0.271	0.06	0.276	0.17	0.277	0.17	0.256	0.07
	L3	**BM**	0.036	0.29	0.025	0.38	0.054	0.43	0.084	0.50	0.040	0.27
		BF	0.061	0.27	0.082	0.20	0.139	0.24	0.251	0.15	0.070	0.23
		WM	0.000	0.94	0.007	0.79	0.249	0.24	0.225	0.28	0.000	0.97
		WF	0.220	0.09	0.202	0.11	0.228	0.24	0.228	0.24	0.207	0.10
	L4	**BM**	0.045	0.24	0.038	0.28	0.049	0.47	0.066	0.57	0.052	0.20

Variable	VL	P	Linear r^2	p-value	Logarithmic r^2	p-value	Quadratic r^2	p-value	Cubic r^2	p-value	Exponential r^2	p-value
		BF	0.065	0.25	0.076	0.21	0.080	0.45	0.081	0.67	0.068	0.24
		WM	0.000	0.99	0.002	0.89	0.127	0.51	0.106	0.57	0.001	0.91
		WF	0.025	0.59	0.033	0.54	0.061	0.71	0.061	0.71	0.005	0.81
	L5	**BM**	0.121	0.05	0.086	0.10	0.138	0.12	0.152	0.20	0.130	0.04
		BF	0.043	0.37	0.063	0.27	0.110	0.35	0.131	0.48	0.054	0.31
		WM	0.017	0.67	0.018	0.66	0.021	0.90	0.024	0.89	0.021	0.64
		WF	0.241	0.08	0.253	0.07	0.364	0.19	0.267	0.18	0.207	0.10
PB	**L1**	**BM**	0.002	0.80	0.003	0.77	0.003	0.96	0.005	0.99	0.122	0.73
		BF	0.114	0.12	0.087	0.18	0.140	0.24	0.140	0.43	0.098	0.16
		WM	0.239	0.09	0.235	0.09	0.245	0.25	0.252	0.23	0.253	0.08
		WF	0.008	0.76	0.008	0.77	0.010	0.95	0.012	0.94	0.017	0.66
	L2	**BM**	0.000	0.94	0.000	0.95	0.016	0.79	0.033	0.80	0.000	0.96
		BF	0.043	0.35	0.042	0.36	0.043	0.66	0.056	0.79	0.048	0.33
		WM	0.205	0.12	0.228	0.10	0.237	0.26	0.237	0.26	0.215	0.11
		WF	0.021	0.62	0.029	0.56	0.069	0.68	0.069	0.67	0.001	0.93
	L3	**BM**	0.008	0.62	0.003	0.77	0.019	0.75	0.022	0.88	0.013	0.52
		BF	0.041	0.36	0.040	0.37	0.042	0.67	0.048	0.82	0.049	0.32
		WM	0.064	0.40	0.075	0.36	0.085	0.64	0.085	0.64	0.074	0.37
		WF	0.059	0.40	0.054	0.42	0.073	0.66	0.082	0.63	0.003	0.84
	L4	**BM**	0.001	0.88	0.000	0.91	0.034	0.59	0.034	0.79	0.003	0.75
		BF	0.075	0.22	0.076	0.21	0.077	0.47	0.079	0.68	0.071	0.23
		WM	0.089	0.32	0.100	0.29	0.099	0.59	0.099	0.59	0.096	0.30
		WF	0.055	0.42	0.060	0.40	0.058	0.72	0.058	0.72	0.010	0.73
	L5	**BM**	0.033	0.32	0.015	0.50	0.073	0.33	0.074	0.54	0.051	0.21
		BF	0.001	0.91	0.006	0.74	0.066	0.54	0.074	0.72	0.000	0.94
		WM	0.003	0.87	0.007	0.79	0.042	0.81	0.042	0.81	0.012	0.72
		WF	0.269	0.06	0.234	0.08	0.343	0.10	0.339	0.10	0.175	0.14

Key: VL = Vertebral level; P = Population group; r^2 = The r^2 value; BM = Black male; BF = Black female; WM = White male; WF = White female; AB = Anterior border; PB = Posterior border

Appendix D.1 – Linear correlations: Morphemetrics and LLA

Table D.1.49: Table indicating the Pearson's correlation r-values, r^2 values, and associated p-values obtained from the linear regression analysis for transverse- and spinous process lengths and angle

VL	P	TPL			SPL		
		r	r^2	p-value	r	r^2	p-value
L1	BM	-0.119	0.014	0.509	0.144	0.021	0.424
	BF	0.387	0.150	0.075	0.304	0.092	0.169
	WM	0.159	0.025	0.603	0.146	0.021	0.634
	WF	-0.205	0.042	0.483	0.370	0.137	0.193
L2	BM	-0.064	0.004	0.724	0.131	0.017	0.467
	BF	0.300	0.090	0.175	0.321	0.103	0.145
	WM	0.261	0.068	0.390	0.239	0.057	0.432
	WF	-0.020	0.0004	0.947	0.061	0.004	0.837
L3	BM	-0.196	0.038	0.274	0.055	0.003	0.761
	BF	0.224	0.050	0.315	0.179	0.032	0.424
	WM	0.156	0.024	0.611	0.077	0.006	0.803
	WF	-0.406	0.165	0.150	-0.136	0.018	0.644
L4	BM	-0.098	0.010	0.588	-0.011	0.0001	0.952
	BF	-0.525	0.276	0.012	0.086	0.007	0.702
	WM	-0.147	0.022	0.631	0.038	0.001	0.902
	WF	-0.255	0.065	0.379	-0.220	0.048	0.449
L5	BM	-0.132	0.017	0.471	-0.175	0.031	0.339
	BF	-0.100	0.010	0.667	0.222	0.049	0.333
	WM	0.274	0.075	0.415	-0.273	0.075	0.368
	WF	-0.230	0.053	0.429	-0.407	0.166	0.149

Key: VL = Vertebral level; P = Population group; BM = Black males; BF = Black females; WM = White males; WF = White females; TPL = Transverse process length; SPL = Spinous process length

Table D.1.50: Table indicating the Pearson's correlation r-values, r^2 values, and associated p-values obtained from the linear regression analysis for spinal canal dimensions and angle

VL	P	SCDAP			SCDL		
		r	r^2	p-value	r	r^2	p-value
L1	BM	-0.156	0.024	0.386	-0.238	0.057	0.182
	BF	-0.210	0.044	0.348	0.474	0.225	0.026
	WM	-0.233	0.054	0.444	0.132	0.017	0.668
	WF	-0.396	0.157	0.161	-0.589	0.347	0.027
L2	BM	0.066	0.004	0.721	-0.213	0.045	0.234
	BF	0.282	0.080	0.215	0.374	0.140	0.087
	WM	-0.410	0.168	0.186	0.242	0.059	0.425
	WF	-0.086	0.007	0.769	-0.250	0.063	0.389
L3	BM	-0.002	0.000004	0.993	-0.221	0.049	0.216
	BF	0.043	0.002	0.848	0.300	0.090	0.175
	WM	0.173	0.030	0.573	0.115	0.013	0.708
	WF	-0.188	0.035	0.769	-0.251	0.063	0.387
L4	BM	0.030	0.001	0.870	-0.134	0.018	0.459
	BF	0.066	0.004	0.770	-0.052	0.003	0.818
	WM	-0.020	0.0009	0.948	-0.087	0.008	0.777
	WF	-0.154	0.024	0.599	-0.061	0.004	0.835
L5	BM	0.046	0.002	0.804	-0.088	0.008	0.631
	BF	0.273	0.075	0.300	-0.238	0.057	0.299
	WM	0.165	0.027	0.590	-0.053	0.003	0.864
	WF	0.077	0.006	0.793	0.032	0.001	0.914

Key: VL = Vertebral level; P = Population group; BM = Black males; BF = Black females; WM = White males; WF = White females; SCDAP = Spinal canal AP diameter; SCDL = Spinal canal lateral diameter

Table D.1.51: Table indicating the Pearson's correlation r-values, r^2 values, and associated p-values obtained from the linear regression analysis for pedicle dimensions and angle

VL	P	PDH			PDDL		
		r	r^2	p-value	r	r^2	p-value
L1	BM	-0.049	0.002	0.787	-0.207	0.043	0.248
	BF	0.050	0.003	0.827	0.245	0.060	0.271
	WM	-0.049	0.002	0.873	0.293	0.086	0.331
	WF	-0.480	0.230	0.082	0.019	0.0004	0.949
L2	BM	-0.064	0.004	0.724	-0.020	0.0004	0.912
	BF	0.162	0.026	0.471	0.271	0.073	0.223
	WM	-0.258	0.067	0.394	0.269	0.072	0.374
	WF	-0.080	0.006	0.787	0.189	0.036	0.517
L3	BM	-0.174	0.030	0.332	-0.007	0.00005	0.969
	BF	0.082	0.007	0.717	0.087	0.008	0.699
	WM	-0.102	0.010	0.740	0.400	0.160	0.176
	WF	-0.268	0.072	0.355	0.124	0.015	0.673
L4	BM	0.230	0.053	0.198	-0.018	0.0003	0.919
	BF	0.053	0.003	0.815	-0.131	0.017	0.560
	WM	-0.145	0.021	0.636	0.502	0.252	0.097
	WF	-0.343	0.118	0.230	0.178	0.032	0.543
L5	BM	0.299	0.089	0.096	-0.134	0.018	0.463
	BF	-0.111	0.012	0.631	-0.021	0.0004	0.928
	WM	0.121	0.015	0.694	0.412	0.170	0.162
	WF	-0.547	0.299	0.043	-0.270	0.073	0.350

Key: VL = Vertebral level; P = Population group; BM = Black males; BF = Black females; WM = White males; WF = White females; PDH = Pedicle height; PDDL = Pedicle lateral diameter

Table D.1.52: Table indicating the Pearson's correlation r-values, r^2 values, and associated p-values obtained from the linear regression analysis for vertebral body lateral diameter dimensions and angle

VL	P	VDMaxL			VDMinL		
		r	r^2	p-value	r	r^2	p-value
L1	BM	-0.261	0.068	0.142	-0.310	0.096	0.079
	BF	0.333	0.111	0.130	0.367	0.135	0.093
	WM	0.516	0.266	0.071	0.251	0.063	0.408
	WF	-0.407	0.166	0.149	-0.374	0.140	0.187
L2	BM	-0.110	0.012	0.541	-0.306	0.094	0.079
	BF	0.385	0.148	0.077	0.357	0.127	0.103
	WM	0.528	0.279	0.064	0.365	0.133	0.220
	WF	-0.105	0.011	0.720	-0.175	0.031	0.550
L3	BM	-0.177	0.031	0.324	-0.277	0.077	0.083
	BF	0.303	0.092	0.171	0.275	0.076	0.215
	WM	0.574	0.329	0.040	0.416	0.173	0.158
	WF	-0.225	0.051	0.440	-0.407	0.166	0.149
L4	BM	-0.049	0.002	0.786	-0.298	0.089	0.092
	BF	0.259	0.067	0.245	0.105	0.011	0.642
	WM	0.396	0.157	0.181	0.299	0.089	0.321
	WF	-0.167	0.028	0.567	-0.480	0.230	0.083
L5	BM	-0.242	0.059	0.182	-0.217	0.047	0.234
	BF	0.250	0.063	0.274	-0.065	0.004	0.780
	WM	0.284	0.081	0.347	0.145	0.021	0.637
	WF	-0.246	0.061	0.397	-0.499	0.249	0.069

Key: VL = Vertebral level; P = Population group; BM = Black males; BF = Black females; WM = White males; WF = White females; VDMaxL = Maximum vertebral body lateral diameter; VDMinL = Minimum vertebral body lateral diameter

Table D.1.53: Table indicating the Pearson's correlation r-values, r^2 values, and associated p-values obtained from the linear regression analysis for vertebral body AP diameter dimensions and angle

VL	P	VDMaxAP			VDMinAP		
		r	r^2	p-value	r	r^2	p-value
L1	BM	-0.072	0.005	0.690	-0.072	0.005	0.690
	BF	0.103	0.011	0.648	0.241	0.058	0.279
	WM	0.308	0.095	0.306	0.223	0.050	0.465
	WF	-0.161	0.026	0.581	-0.159	0.025	0.587
L2	BM	-0.092	0.008	0.609	-0.179	0.032	0.318
	BF	0.024	0.001	0.915	0.166	0.028	0.459
	WM	0.038	0.001	0.903	-0.003	0.00001	0.992
	WF	-0.078	0.006	0.791	-0.198	0.039	0.496
L3	BM	-0.106	0.011	0.557	-0.203	0.041	0.257
	BF	-0.012	0.0001	0.959	0.048	0.002	0.833
	WM	0.247	0.061	0.416	0.107	0.011	0.279
	WF	-0.172	0.030	0.555	-0.163	0.027	0.579
L4	BM	-0.337	0.114	0.055	-0.343	0.118	0.051
	BF	-0.002	0.000004	0.994	0.053	0.003	0.816
	WM	0.228	0.052	0.453	0.239	0.057	0.431
	WF	-0.101	0.010	0.732	-0.225	0.051	0.440
L5	BM	-0.078	0.006	0.677	0.063	0.004	0.733
	BF	0.384	0.147	0.085	0.281	0.079	0.217
	WM	0.576	0.332	0.040	0.663	0.440	0.014
	WF	0.168	0.028	0.565	0.314	0.099	0.275

Key: VL = Vertebral level; P = Population group; BM = Black males; BF = Black females; WM = White males; WF = White females; VDMaxAP = Maximum vertebral body AP diameter; VDMinAP = Minimum vertebral body AP diameter

Table D.1.54: Table indicating the Pearson's correlation r-values, r^2 values, and associated p-values obtained from the linear regression analysis for vertebral body height dimensions and angle

VL	P	VHa			VHp		
		r	r^2	p-value	r	r^2	p-value
L1	BM	0.256	0.066	0.151	-0.005	0.00003	0.980
	BF	0.003	0.000009	0.991	-0.148	0.022	0.511
	WM	0.237	0.056	0.435	-0.255	0.065	0.400
	WF	0.308	0.095	0.284	-0.183	0.033	0.532
L2	BM	0.325	0.106	0.065	-0.030	0.001	0.869
	BF	0.169	0.029	0.453	-0.058	0.003	0.797
	WM	0.186	0.035	0.543	-0.020	0.0009	0.947
	WF	0.002	0.000004	0.994	-0.472	0.223	0.088
L3	BM	0.076	0.006	0.676	-0.115	0.013	0.525
	BF	-0.208	0.043	0.354	-0.169	0.029	0.453
	WM	0.597	0.356	0.040	0.006	0.0004	0.984
	WF	-0.314	0.099	0.274	-0.369	0.136	0.194
L4	BM	0.313	0.098	0.077	-0.020	0.00004	0.910
	BF	0.064	0.004	0.778	-0.213	0.045	0.342
	WM	0.406	0.165	0.168	0.094	0.009	0.761
	WF	-0.265	0.070	0.361	-0.310	0.096	0.281
L5	BM	0.083	0.007	0.650	0.003	0.00001	0.987
	BF	0.052	0.003	0.822	-0.303	0.092	0.182
	WM	0.518	0.268	0.070	0.399	0.159	0.177
	WF	-0.299	0.089	0.299	-0.149	0.022	0.611

Key: VL = Vertebral level; P = Population group; BM = Black males; BF = Black females; WM = White males; WF = White females; VHa = Anterior vertebral body height; VHp = Posterior vertebral body height

Appendix D.2 – Linear correlations: BMD and age

Table D.2.55: Table indicating the Pearson's correlation r-values, r^2 values, and associated p-values obtained from the linear regression analysis for medullary BMD and age

VL	P	ROI1			ROI2			ROI3		
		r	r^2	p-value	r	r^2	p-value	r	r^2	p-value
L1	BM	-0.160	0.026	0.381	-0.194	0.038	0.280	-0.408	0.166	0.018
	BF	-0.761	0.580	0.00006	-0.444	0.197	0.039	-0.485	0.235	0.022
	WM	-0.322	0.104	0.334	-0.415	0.172	0.159	-0.459	0.211	0.115
	WF	-0.719	0.517	0.004	-0.637	0.406	0.014	-0.649	0.421	0.012
L2	BM	-0.512	0.262	0.002	-0.030	0.001	0.867	-0.269	0.072	0.131
	BF	-0.522	0.272	0.015	-0.389	0.151	0.066	-0.662	0.438	0.001
	WM	-0.584	0.341	0.036	-0.583	0.340	0.036	-0.675	0.456	0.011
	WF	-0.730	0.533	0.003	-0.742	0.551	0.002	0.013	0.0002	0.968
L3	BM	-0.031	0.001	0.866	-0.070	0.005	0.698	-0.557	0.310	0.001
	BF	-0.404	0.163	0.062	-0.418	0.175	0.053	-0.493	0.243	0.020
	WM	-0.479	0.229	0.098	-0.337	0.114	0.260	-0.402	0.162	0.173
	WF	-0.724	0.524	0.003	-0.791	0.569	0.001	0.092	0.008	0.788
L4	BM	-0.611	0.373	0.0002	-0.095	0.009	0.601	-0.525	0.276	0.002
	BF	-0.395	0.156	0.069	-0.466	0.217	0.029	-0.580	0.336	0.005
	WM	-0.447	0.200	0.126	-0.578	0.334	0.039	-0.245	0.060	0.419
	WF	-0.716	0.513	0.004	-0.739	0.546	0.003	-0.511	0.261	0.062
L5	BM	-0.518	0.268	0.003	0.085	0.007	0.657	-0.403	0.162	0.027
	BF	-0.589	0.350	0.004	-0.587	0.345	0.005	-0.654	0.428	0.001
	WM	-0.360	0.130	0.227	-0.547	0.299	0.053	-0.561	0.315	0.046
	WF	-0.723	0.523	0.003	-0.845	0.714	0.0001	-0.428	0.183	0.126

Key: VL = Vertebral level; P = Population group; BM = Black males; BF = Black females; WM = White males; WF = White females; ROI = Region of interest

Table D.2.56: Table indicating the Pearson's correlation r-values, r^2 values, and associated p-values obtained from the linear regression analysis for cortical endplate BMD and age

VL	P	SEP			IEP		
		r	r^2	p-value	r	r^2	p-value
L1	BM	0.324	0.105	0.066	0.059	0.003	0.746
	BF	-0.358	0.128	0.102	-0.360	0.130	0.100
	WM	-0.191	0.036	0.552	-0.178	0.032	0.560
	WF	-0.491	0.241	0.075	-0.453	0.205	0.104
L2	BM	-0.044	0.002	0.808	-0.219	0.048	0.220
	BF	-0.377	0.142	0.084	-0.169	0.029	0.452
	WM	-0.306	0.094	0.310	-0.083	0.007	0.788
	WF	-0.455	0.207	0.102	-0.463	0.214	0.096
L3	BM	-0.175	0.031	0.330	-0.303	0.092	0.091
	BF	-0.378	0.143	0.083	-0.440	0.194	0.040
	WM	-0.394	0.155	0.183	-0.048	0.002	0.877
	WF	-0.441	0.194	0.114	-0.518	0.268	0.058
L4	BM	-0.346	0.120	0.049	-0.256	0.066	0.151
	BF	-0.457	0.209	0.032	-0.299	0.089	0.177
	WM	-0.006	0.000	0.983	-0.200	0.040	0.513
	WF	-0.538	0.289	0.047	-0.141	0.020	0.631
L5	BM	-0.050	0.003	0.787	-0.170	0.029	0.353
	BF	-0.312	0.097	0.168	-0.356	0.127	0.113
	WM	-0.233	0.054	0.443	-0.459	0.211	0.115
	WF	-0.474	0.225	0.087	-0.357	0.127	0.210

Key: VL = Vertebral level; P = Population group; BM = Black males; BF = Black females; WM = White males; WF = White females; SEP = Superior endplate; IEP = Inferior endplate

Table D.2.57: Table indicating the Pearson's correlation r-values, r^2 values, and associated p-values obtained from the linear regression analysis for cortical border BMD and age

VL	P	AB			PB		
		r	r^2	p-value	r	r^2	p-value
L1	BM	-0.050	0.003	0.780	-0.072	0.005	0.691
	BF	-0.450	0.203	0.036	-0.331	0.110	0.132
	WM	-0.719	0.517	0.006	-0.212	0.045	0.487
	WF	-0.686	0.471	0.007	-0.252	0.064	0.385
L2	BM	-0.142	0.020	0.431	-0.066	0.004	0.717
	BF	-0.576	0.332	0.005	-0.403	0.162	0.063
	WM	-0.186	0.035	0.543	-0.321	0.103	0.285
	WF	-0.309	0.095	0.282	-0.458	0.210	0.100
L3	BM	-0.268	0.072	0.132	-0.278	0.077	0.117
	BF	-0.562	0.316	0.007	-0.284	0.081	0.200
	WM	-0.344	0.118	0.249	-0.034	0.001	0.912
	WF	-0.417	0.174	0.138	-0.710	0.504	0.004
L4	BM	-0.273	0.075	0.124	-0.163	0.027	0.365
	BF	-0.630	0.397	0.002	-0.407	0.166	0.060
	WM	-0.167	0.028	0.586	-0.141	0.020	0.646
	WF	-0.673	0.453	0.008	-0.553	0.306	0.040
L5	BM	-0.356	0.127	0.046	0.049	0.002	0.788
	BF	-0.753	0.567	0.00008	-0.476	0.227	0.029
	WM	-0.013	0.000	0.966	-0.204	0.042	0.504
	WF	-0.510	0.260	0.063	-0.534	0.285	0.049

Key: VL = Vertebral level; P = Population group; BM = Black males; BF = Black females; WM = White males; WF = White females; AB = Anterior border; PB = Posterior border

Appendix D.3 – Linear correlations: Mosprhometrics and age

Table D.3.58: Table indicating the Pearson's correlation r-values, r^2 values, and associated p-values obtained from the linear regression analysis for transverse- and spinous process lengths and age

VL	P	TPL			SPL		
		r	r^2	p-value	r	r^2	p-value
L1	BM	-0.103	0.011	0.567	0.132	0.017	0.464
	BF	-0.091	0.008	0.687	-0.055	0.003	0.807
	WM	0.124	0.015	0.687	0.496	0.246	0.085
	WF	-0.074	0.005	0.802	0.081	0.007	0.783
L2	BM	-0.234	0.055	0.190	0.097	0.009	0.590
	BF	0.227	0.052	0.309	0.129	0.017	0.567
	WM	0.362	0.131	0.225	0.581	0.338	0.037
	WF	-0.162	0.026	0.579	0.286	0.082	0.322
L3	BM	0.031	0.001	0.865	0.151	0.023	0.403
	BF	0.299	0.089	0.176	0.243	0.059	0.276
	WM	0.050	0.003	0.872	0.770	0.593	0.002
	WF	0.066	0.004	0.823	-0.058	0.003	0.844
L4	BM	0.062	0.004	0.730	-0.041	0.002	0.823
	BF	0.270	0.073	0.224	0.186	0.035	0.408
	WM	0.231	0.053	0.448	0.458	0.210	0.116
	WF	0.015	0.0001	0.959	0.027	0.001	0.926
L5	BM	-0.012	0.000	0.949	0.056	0.003	0.763
	BF	0.110	0.012	0.634	0.274	0.075	0.230
	WM	-0.011	0.0001	0.974	0.427	0.182	0.146
	WF	-0.016	0.0003	0.957	0.250	0.063	0.388

Key: VL = Vertebral level; P = Population group; BM = Black males; BF = Black females; WM = White males; WF = White females; TPL = Transverse process length; SPL = Spinous process length

Table D.3.59: Table indicating the Pearson's correlation r-values, r^2 values, and associated p-values obtained from the linear regression analysis for spinal canal dimensions and age

VL	P	SCDAP			SCDL		
		r	r^2	p-value	r	r^2	p-value
L1	BM	-0.051	0.003	0.779	-0.095	0.009	0.598
	BF	0.028	0.001	0.903	0.073	0.005	0.745
	WM	0.075	0.006	0.807	0.294	0.086	0.329
	WF	0.137	0.019	0.642	0.022	0.0005	0.940
L2	BM	0.245	0.060	0.177	-0.125	0.016	0.488
	BF	0.263	0.069	0.250	0.181	0.033	0.419
	WM	0.003	0.0001	0.992	0.279	0.078	0.356
	WF	0.169	0.029	0.563	0.046	0.002	0.875
L3	BM	0.041	0.002	0.822	-0.087	0.008	0.631
	BF	0.081	0.007	0.720	0.080	0.006	0.724
	WM	-0.268	0.072	0.376	-0.111	0.012	0.719
	WF	0.319	0.102	0.267	0.389	0.151	0.169
L4	BM	-0.003	0.0007	0.985	-0.088	0.008	0.628
	BF	-0.062	0.004	0.784	0.345	0.119	0.116
	WM	-0.027	0.001	0.931	0.027	0.001	0.931
	WF	0.121	0.015	0.680	-0.004	0.00002	0.989
L5	BM	0.170	0.029	0.352	0.043	0.002	0.816
	BF	-0.216	0.047	0.348	0.255	0.065	0.264
	WM	-0.234	0.055	0.443	-0.129	0.017	0.675
	WF	0.238	0.057	0.413	0.320	0.102	0.265

Key: VL = Vertebral level; P = Population group; BM = Black males; BF = Black females; WM = White males; WF = White females; SCDAP = Spinal canal AP diameter; SCDL = Spinal canal lateral diameter

Table D.3.60: Table indicating the Pearson's correlation r-values, r^2 values, and associated p-values obtained from the linear regression analysis for pedicle dimensions and age

VL	P	PDH			PDDL		
		r	r^2	p-value	r	r^2	p-value
L1	BM	-0.137	0.019	0.446	-0.092	0.008	0.612
	BF	0.120	0.014	0.593	0.154	0.024	0.494
	WM	-0.256	0.066	0.398	0.031	0.001	0.920
	WF	0.292	0.085	0.311	-0.139	0.019	0.636
L2	BM	-0.310	0.096	0.079	0.084	0.007	0.643
	BF	-0.012	0.0001	0.959	0.200	0.040	0.373
	WM	-0.026	0.001	0.934	-0.039	0.002	0.898
	WF	0.289	0.084	0.316	-0.123	0.015	0.674
L3	BM	-0.220	0.048	0.219	0.116	0.013	0.519
	BF	-0.027	0.001	0.905	0.171	0.029	0.447
	WM	0.024	0.001	0.938	-0.209	0.044	0.492
	WF	0.355	0.126	0.213	-0.254	0.065	0.380
L4	BM	-0.166	0.028	0.356	0.058	0.003	0.749
	BF	-0.155	0.024	0.492	0.013	0.0002	0.955
	WM	-0.561	0.315	0.046	0.130	0.017	0.687
	WF	0.224	0.050	0.441	-0.331	0.110	0.248
L5	BM	-0.066	0.004	0.720	-0.058	0.003	0.753
	BF	0.165	0.027	0.475	0.071	0.005	0.759
	WM	0.046	0.002	0.881	0.283	0.080	0.349
	WF	-0.011	0.0001	0.971	-0.012	0.0001	0.968

Key: VL = Vertebral level; P = Population group; BM = Black males; BF = Black females; WM = White males; WF = White females; PDH = Pedicle height; PDDL = Pedicle lateral diameter

Table D.3.61: Table indicating the Pearson's correlation r-values, r^2 values, and associated p-values obtained from the linear regression analysis for vertebral body lateral diameter dimensions and age

VL	P	VDMaxL			VDMinL		
		r	r^2	p-value	r	r^2	p-value
L1	BM	-0.080	0.006	0.659	-0.115	0.013	0.525
	BF	0.445	0.198	0.038	0.417	0.174	0.054
	WM	0.593	0.352	0.033	0.388	0.151	0.190
	WF	0.384	0.147	0.175	0.363	0.132	0.203
L2	BM	0.054	0.003	0.766	-0.060	0.004	0.739
	BF	0.449	0.202	0.036	0.458	0.210	0.032
	WM	0.451	0.203	0.122	0.397	0.158	0.179
	WF	0.610	0.372	0.021	0.499	0.249	0.070
L3	BM	0.107	0.011	0.553	-0.017	0.0003	0.924
	BF	0.402	0.162	0.063	0.441	0.194	0.040
	WM	0.571	0.326	0.042	0.562	0.316	0.045
	WF	0.579	0.335	0.030	0.523	0.274	0.055
L4	BM	0.037	0.001	0.838	-0.100	0.010	0.581
	BF	0.609	0.371	0.003	0.535	0.286	0.010
	WM	0.477	0.228	0.099	0.533	0.284	0.061
	WF	0.487	0.237	0.077	0.539	0.291	0.047
L5	BM	0.247	0.061	0.172	0.040	0.002	0.829
	BF	0.604	0.365	0.004	0.523	0.274	0.015
	WM	0.544	0.296	0.055	0.575	0.331	0.040
	WF	0.708	0.501	0.005	0.639	0.408	0.014

Key: VL = Vertebral level; P = Population group; BM = Black males; BF = Black females; WM = White males; WF = White females; VDMaxL = Maximum vertebral body lateral diameter; VDMinL = Minimum vertebral body lateral diameter

Table D.3.62: Table indicating the Pearson's correlation r-values, r^2 values, and associated p-values obtained from the linear regression analysis for vertebral body AP diameter dimensions and age

VL	P	VDMaxAP			VDMinAP		
		r	r^2	p-value	r	r^2	p-value
L1	BM	0.002	0.000004	0.991	-0.121	0.015	0.502
	BF	0.354	0.125	0.106	0.120	0.014	0.595
	WM	0.417	0.174	0.157	0.342	0.117	0.253
	WF	0.275	0.076	0.342	0.268	0.072	0.355
L2	BM	0.055	0.003	0.760	-0.073	0.005	0.688
	BF	0.355	0.126	0.104	0.246	0.061	0.270
	WM	0.353	0.125	0.237	0.430	0.185	0.163
	WF	0.385	0.148	0.174	0.240	0.058	0.408
L3	BM	-0.141	0.020	0.434	-0.219	0.048	0.221
	BF	0.449	0.202	0.036	0.368	0.135	0.092
	WM	0.471	0.222	0.104	0.392	0.154	0.185
	WF	0.258	0.067	0.373	0.333	0.111	0.245
L4	BM	-0.029	0.001	0.873	-0.100	0.010	0.580
	BF	0.573	0.328	0.005	0.466	0.217	0.029
	WM	0.434	0.188	0.138	0.382	0.146	0.198
	WF	0.125	0.016	0.670	0.117	0.014	0.690
L5	BM	0.073	0.005	0.698	0.039	0.002	0.834
	BF	0.586	0.343	0.005	0.400	0.160	0.072
	WM	0.635	0.403	0.020	0.481	0.231	0.096
	WF	-0.274	0.075	0.343	-0.258	0.067	0.373

Key: VL = Vertebral level; P = Population group; BM = Black males; BF = Black females; WM = White males; WF = White females; VDMaxAP = Maximum vertebral body AP diameter; VDMinAP = Minimum vertebral body AP diameter

Table D.3.63: Table indicating the Pearson's correlation r-values, r^2 values, and associated p-values obtained from the linear regression analysis for vertebral body height dimensions and age

VL	P	VHa			VHp		
		r	r^2	p-value	r	r^2	p-value
L1	BM	-0.312	0.097	0.077	-0.225	0.051	0.209
	BF	0.012	0.0001	0.959	-0.159	0.025	0.480
	WM	-0.054	0.003	0.860	-0.197	0.039	0.519
	WF	-0.321	0.103	0.264	0.018	0.0003	0.950
L2	BM	-0.184	0.034	0.305	-0.252	0.064	0.157
	BF	-0.036	0.001	0.874	0.019	0.000	0.932
	WM	-0.123	0.015	0.689	0.209	0.044	0.493
	WF	-0.187	0.035	0.522	0.038	0.001	0.897
L3	BM	-0.242	0.059	0.175	-0.291	0.085	0.100
	BF	-0.283	0.080	0.202	-0.064	0.004	0.778
	WM	-0.106	0.011	0.744	0.037	0.001	0.909
	WF	-0.121	0.015	0.681	-0.087	0.008	0.767
L4	BM	-0.258	0.067	0.148	-0.256	0.066	0.151
	BF	-0.314	0.099	0.154	-0.062	0.004	0.784
	WM	0.157	0.025	0.609	0.006	0.00004	0.986
	WF	-0.181	0.033	0.536	-0.269	0.072	0.353
L5	BM	-0.378	0.143	0.033	-0.164	0.027	0.369
	BF	-0.349	0.122	0.121	-0.396	0.157	0.076
	WM	0.356	0.127	0.232	0.308	0.095	0.305
	WF	-0.416	0.173	0.139	-0.406	0.165	0.149

Key: VL = Vertebral level; P = Population group; BM = Black males; BF = Black females; WM = White males; WF = White females; VHa = Anterior vertebral body height; VHp = Posterior vertebral body height

Appendix E.1 – Raw data for CT observer analysis: BMD and LLA

Table E.1.64: Table indicating the inter- and intra-observer measurements used to perform observer analyses for the Lumbar lordosis angle

Case ID	Age	P	Sex	LLA	IA	IE
2796360	36	B	M	21.8	24.2	24.5
8313270	27	B	M	32.4	32.7	34.5
474590	59	W	M	18.9	18.2	18.2
8213390	39	B	M	30.1	31.6	30.6
696271	27	B	F	22.0	19.8	28.5
3080371	37	W	F	13.2	14.4	19.9
376411	41	B	F	42.9	45.3	44.7
2622521	52	B	F	48.5	50.6	54.5

Key: P = Population group; B = Black; W= White; M = Male; F = Female; LLA = Original lumbar lordosis angle measurement; IA = Intra-observer measurements; IE = Interobserver measurements. All measurements are in degrees

Table E.1.65: Table indicating the inter- and intra-observer measurements used to perform observer analyses for the medullary BMD

VL	Case ID	Age	P	Sex	ROI1	IA	IE	ROI2	IA	IE	ROI3	IA	IE
L1	**2796360**	36	B	M	213	197	196	185	175	181	244	238	256
	8313270	27	B	M	263	231	280	215	215	222	277	257	275
	474590	59	W	M	154	151	250	168	166	162	168	167	266
	8213390	39	B	M	250	240	331	234	238	245	274	265	274
	696271	27	B	F	198	194	245	174	166	215	267	271	293
	3080371	37	W	F	243	245	242	167	168	184	225	230	193
	376411	41	B	F	213	221	223	241	252	270	264	262	242
	2622521	52	B	F	171	175	130	126	126	131	163	164	197
L2	**2796360**	36	B	M	221	207	197	173	172	191	237	227	265
	8313270	27	B	M	240	239	273	218	219	234	260	247	279
	474590	59	W	M	160	159	151	152	153	147	199	161	163
	8213390	39	B	M	257	258	285	247	244	257	266	266	280
	696271	27	B	F	166	204	217	193	177	220	257	258	296
	3080371	37	W	F	243	238	238	170	156	177	207	209	211

VL	Case ID	Age	P	Sex	ROI1	IA	IE	ROI2	IA	IE	ROI3	IA	IE
	376411	41	B	F	233	228	223	253	249	260	281	280	271
	2622521	52	B	F	166	163	143	120	119	126	136	136	142
L3	**2796360**	36	B	M	214	230	221	166	154	168	244	246	256
	8313270	27	B	M	234	260	346	216	224	233	273	257	246
	474590	59	W	M	158	147	150	163	159	157	219	179	172
	8213390	39	B	M	262	246	302	238	241	252	260	258	318
	696271	27	B	F	188	189	206	177	168	187	276	231	243
	3080371	37	W	F	242	245	182	154	152	175	234	238	241
	376411	41	B	F	220	220	233	232	226	250	228	227	232
	2622521	52	B	F	189	172	147	113	118	121	135	141	143
L4	**2796360**	36	B	M	207	210	204	183	171	173	208	201	198
	8313270	27	B	M	258	230	266	226	225	254	250	248	253
	474590	59	W	M	143	145	134	154	142	167	177	181	178
	8213390	39	B	M	253	248	282	243	237	256	265	263	295
	696271	27	B	F	216	214	182	190	181	192	234	245	251
	3080371	37	W	F	203	192	281	162	174	174	233	258	169
	376411	41	B	F	225	237	213	219	219	224	252	259	244
	2622521	52	B	F	189	194	210	109	111	122	119	121	130
L5	**2796360**	36	B	M	193	190	200	173	174	183	209	214	183
	8313270	27	B	M	238	236	287	223	223	232	260	249	267
	474590	59	W	M	231	216	141	159	148	189	175	177	184
	8213390	39	B	M	250	247	299	242	238	275	268	265	358
	696271	27	B	F	250	242	200	205	186	208	196	222	212
	3080371	37	W	F	225	219	219	176	176	193	197	197	226
	376411	41	B	F	218	220	233	213	215	222	231	259	260
	2622521	52	B	F	154	150	139	112	102	124	111	115	181

Key: ROI = Region of interest; VL = Vertebral level; P = Population group; B = Black; W = White M = Male; F = Female; IE = Interobserver measurements; IA = Intra-observer measurements. All measurements are in Hounsfield units (HU)

Table E.1.66: Table indicating the inter- and intra-observer measurements used to perform observer analyses for the cortical BMD

VL	Case ID	Age	P	Sex	SEP	IA	IE	IEP	IA	IE	AB	IA	IE	PB	IA	IE
L1	**2796360**	36	B	M	421	434	304	582	550	541	466	468	457	429	480	437
	8313270	27	B	M	437	437	263	564	586	398	602	463	463	691	690	628
	474590	59	W	M	360	449	345	373	436	369	510	342	255	239	413	193
	8213390	39	B	M	534	535	544	572	485	481	650	514	444	707	718	640
	696271	27	B	F	366	392	389	303	475	296	440	421	406	414	566	309
	3080371	37	W	F	421	462	390	437	427	261	497	360	303	677	617	645
	376411	41	B	F	296	320	260	380	458	338	426	493	462	396	505	405
	2622521	52	B	F	467	450	304	464	549	359	374	307	240	496	451	410
L2	**2796360**	36	B	M	501	503	503	566	580	583	567	448	208	537	549	494
	8313270	27	B	M	508	483	493	606	636	431	460	487	407	826	799	769
	474590	59	W	M	375	388	347	468	617	512	367	368	406	317	586	336
	8213390	39	B	M	590	502	585	534	531	364	486	559	409	857	793	879
	696271	27	B	F	394	420	240	444	442	394	467	469	350	375	616	290
	3080371	37	W	F	532	475	455	614	489	559	502	387	255	690	690	649
	376411	41	B	F	275	331	307	496	492	423	340	462	319	302	577	394
	2622521	52	B	F	452	456	328	648	653	561	316	350	303	486	507	479
L3	**2796360**	36	B	M	521	505	482	513	531	439	562	468	414	777	771	636
	8313270	27	B	M	648	664	662	703	737	633	476	456	408	881	881	803
	474590	59	W	M	385	462	337	580	566	422	372	436	280	417	725	374
	8213390	39	B	M	609	609	558	607	604	531	484	484	387	812	812	711
	696271	27	B	F	327	372	226	452	476	329	447	481	368	382	627	454
	3080371	37	W	F	424	433	253	520	567	441	387	359	308	519	534	470
	376411	41	B	F	416	456	378	461	482	475	411	481	372	286	619	258
	2622521	52	B	F	415	493	333	589	572	505	395	332	346	643	688	601
L4	**2796360**	36	B	M	440	485	380	587	586	458	567	567	473	598	618	506
	8313270	27	B	M	684	705	408	684	688	447	460	463	430	827	827	750
	474590	59	W	M	424	462	152	544	613	374	367	444	330	337	578	376
	8213390	39	B	M	528	524	288	551	551	275	486	491	358	823	747	755
	696271	27	B	F	350	447	277	380	472	174	467	444	467	459	768	337
	3080371	37	W	F	378	485	337	467	506	404	502	437	428	467	511	356

VL	Case ID	Age	P	Sex	SEP	IA	IE	IEP	IA	IE	AB	IA	IE	PB	IA	IE
	376411	41	B	F	317	460	225	385	461	334	340	439	314	333	539	376
	2622521	52	B	F	493	594	290	554	483	377	316	378	229	555	514	514
L5	**2796360**	36	B	M	427	437	341	511	630	496	466	509	452	566	540	514
	8313270	27	B	M	617	601	320	722	723	335	602	567	493	639	597	565
	474590	59	W	M	371	485	174	347	462	213	510	511	520	350	606	301
	8213390	39	B	M	586	582	419	633	694	514	650	613	547	842	852	806
	696271	27	B	F	311	353	278	390	428	307	440	484	440	558	584	445
	3080371	37	W	F	443	503	298	422	428	106	497	503	373	421	473	346
	376411	41	B	F	411	432	284	440	473	185	426	448	461	405	618	363
	2622521	52	B	F	389	443	352	439	539	177	374	353	207	447	667	351

Key: VL = Vertebral level; P = Population group; B = Black; W = White M = Male; F = Female; SEP = Original superior endplate measurement; IEP = Original inferior endplate measurement; AB = Original anterior border measurement; PB = Original posterior border measurement; IE = Interobserver measurements; IA = Intra-observer measurements. All measurements are in Hounsfield units (HU)

Appendix E.2 – Raw data for CT observer analysis: Morphometrics

Table E.2.67: Table indicating the inter- and intra-observer measurements used to perform observer analyses for the pedicle measurements

VL	Case ID	Age	P	Sex	PDDL	IA	IE	PDH	IA	IE
L1	**2796360**	36	B	M	7.9	8.2	7.4	15.9	17.0	15.8
	8313270	27	B	M	7.7	6.7	7.4	17.8	17.9	16.5
	474590	59	W	M	11.6	11.4	8.4	18.9	19.2	19.2
	8213390	39	B	M	11.7	11.5	9.4	19.7	19.4	18.2
	696271	27	B	F	7.8	8.7	8.5	18.0	17.3	12.8
	3080371	37	W	F	9.4	10.9	7.4	17.9	17.6	17.3
	376411	41	B	F	10.6	9.4	7.5	16.9	17.3	13.9
	2622521	52	B	F	8.4	8.6	7.1	15.6	14.8	16.3
L2	**2796360**	36	B	M	9.5	9.7	7.4	16.3	16.6	16.3
	8313270	27	B	M	8.6	8.1	7.6	17.2	18.7	14.7
	474590	59	W	M	10.6	11.0	8.8	19.4	19.1	15.5

VL	Case ID	Age	P	Sex	PDDL	IA	IE	PDH	IA	IE
	8213390	39	B	M	12.0	12.3	9.5	19.5	19.2	18.1
	696271	27	B	F	8.1	8.6	7.7	15.4	16.9	14.6
	3080371	37	W	F	9.8	10.2	8.5	16.7	17.5	11.1
	376411	41	B	F	11.9	10.7	8.7	16.9	17.5	16.3
	2622521	52	B	F	9.6	9.0	6.9	15.4	14.3	13.7
L3	**2796360**	36	B	M	10.1	11.1	9.4	16.2	15.1	16.6
	8313270	27	B	M	11.3	11.2	10.0	17.1	17.7	14.2
	474590	59	W	M	13.9	12.6	10.7	20.2	18.9	14.7
	8213390	39	B	M	13.1	13.1	11.2	20.5	20.3	14.8
	696271	27	B	F	10.6	10.8	10.2	17.6	16.6	16.6
	3080371	37	W	F	10.2	11.3	8.9	16.3	17.4	17.4
	376411	41	B	F	11.2	11.5	9.9	15.8	17.5	15.8
	2622521	52	B	F	12.3	11.8	9.4	13.4	15.0	11.6
L4	**2796360**	36	B	M	13.5	13.4	11.7	13.8	16.2	13.5
	8313270	27	B	M	13.8	13.2	11.8	17.0	17.4	14.5
	474590	59	W	M	14.0	13.8	13.2	17.7	18.0	18.0
	8213390	39	B	M	14.8	15.0	13.1	19.4	20.5	28.5
	696271	27	B	F	12.9	12.9	11.3	15.9	16.7	12.3
	3080371	37	W	F	12.4	13.1	10.6	15.7	17.0	12.2
	376411	41	B	F	11.3	12.8	11.9	14.6	15.6	15.0
	2622521	52	B	F	13.3	12.7	11.6	12.9	12.0	13.3
L5	**2796360**	36	B	M	17.9	17.3	15.7	14.6	14.9	11.4
	8313270	27	B	M	16.6	16.3	15.8	13.8	14.4	13.7
	474590	59	W	M	15.8	16.3	15.0	15.1	15.1	12.6
	8213390	39	B	M	17.4	17.7	16.2	18.2	17.8	17.9
	696271	27	B	F	16.1	16.6	15.6	15.5	14.3	14.3
	3080371	37	W	F	15.2	15.6	15.4	14.0	14.6	12.9
	376411	41	B	F	16.5	15.7	15.5	12.6	12.8	14.0
	2622521	52	B	F	16.9	18.1	15.8	11.1	12.3	12.7

Key: VL = Vertebral level; P = Population group; B = Black; W= White; M = Male; F = Female; PDDL = Original lateral pedicle diameter measurement; PDH = Original pedicle height measurement; IA = Intra-observer measurements; IE = Interobserver measurements. All measurements are in millimetres

Table E.2.68: Table indicating the inter- and intra-observer measurements used to perform observer analyses for the transverse and spinous process lengths

VL	Case ID	Age	P	Sex	TPL	IA	IE	SPL	IA	IE
L1	**2796360**	36	B	M	79.1	79.0	69.3	35.6	37.6	37.1
	8313270	27	B	M	70.7	69.9	67.1	36.0	36.3	32.9
	474590	59	W	M	81.7	80.0	77.9	38.5	38.3	34.8
	8213390	39	B	M	77.2	77.0	80.8	38.3	39.3	37.7
	696271	27	B	F	62.1	62.3	65.7	32.0	35.4	27.0
	3080371	37	W	F	67.2	66.7	70.7	30.2	28.9	27.4
	376411	41	B	F	68.1	68.2	74.2	30.9	33.5	29.7
	2622521	52	B	F	72.7	73.2	60.3	34.3	32.7	31.1
L2	**2796360**	36	B	M	86.5	85.0	70.9	42.0	41.1	39.5
	8313270	27	B	M	73.4	72.1	75.1	41.7	41.9	34.8
	474590	59	W	M	92.1	92.1	85.3	43.5	41.4	39.0
	8213390	39	B	M	87.0	86.8	89.0	43.9	44.5	40.3
	696271	27	B	F	78.6	81.7	77.7	34.2	37.0	30.9
	3080371	37	W	F	77.3	77.2	77.7	31.0	32.5	31.9
	376411	41	B	F	87.3	84.4	84.2	33.5	34.3	31.3
	2622521	52	B	F	80.7	81.8	71.8	32.5	35.4	35.1
L3	**2796360**	36	B	M	96.5	98.3	82.0	44.1	43.2	39.9
	8313270	27	B	M	83.4	83.2	78.6	41.9	45.4	37.6
	474590	59	W	M	113.0	114.0	107.6	40.8	42.3	44.3
	8213390	39	B	M	95.5	95.3	101.0	44.6	45.1	40.2
	696271	27	B	F	103.0	103.0	97.6	37.9	38.7	30.4
	3080371	37	W	F	84.5	83.9	86.9	30.1	33.0	34.8
	376411	41	B	F	96.2	95.7	91.6	31.0	34.5	33.4
	2622521	52	B	F	91.3	89.3	101.0	34.8	35.9	37.0
L4	**2796360**	36	B	M	91.4	92.8	84.5	42.5	43.4	43.4
	8313270	27	B	M	86.7	85.3	79.0	39.9	43.0	32.0
	474590	59	W	M	102.0	103.0	94.7	38.3	39.8	41.3
	8213390	39	B	M	93.9	93.1	101.0	44.1	43.9	43.2
	696271	27	B	F	92.1	93.7	86.7	36.1	37.4	37.4
	3080371	37	W	F	89.9	89.5	83.0	25.4	28.8	29.8
	376411	41	B	F	86.7	85.2	82.8	25.0	26.9	26.8

VL	Case ID	Age	P	Sex	TPL	IA	IE	SPL	IA	IE
	2622521	52	B	F	84.8	85.3	91.0	30.3	32.6	32.6
L5	**2796360**	36	B	M	94.7	94.9	82.6	35.4	38.6	30.2
	8313270	27	B	M	78.3	77.8	84.3	33.3	39.0	28.8
	474590	59	W	M	98.1	97.6	92.8	32.1	31.2	36.1
	8213390	39	B	M	101.0	102.0	97.1	36.9	37.8	37.2
	696271	27	B	F	98.4	100.0	87.6	28.1	30.0	29.8
	3080371	37	W	F	89.0	88.9	92.4	24.5	21.4	21.7
	376411	41	B	F	93.3	93.7	86.9	24.2	28.1	27.1
	2622521	52	B	F	97.9	102.0	98.5	23.2	24.1	27.8

Key: VL = Vertebral level; P = Population group; B = Black; W = White M = Male; F = Female; TPL = Original transverse process length measurement; SPL = Original spinous process length measurement; IE = Interobserver measurements; IA = Intra-observer measurements. All measurements are in millimetres

Table E.2.69: Table indicating the inter- and intra-observer measurements used to perform observer analyses for the vertebral body heights

VL	Case ID	Age	P	Sex	VHa	IA	IE	VHp	IA	IE
L1	**2796360**	36	B	M	25.5	27.6	25.5	28.9	30.6	28.3
	8313270	27	B	M	26.0	29.3	24.1	27.3	29.6	27.2
	474590	59	W	M	28.9	30.9	26.4	32.0	32.7	29.0
	8213390	39	B	M	30.2	29.4	24.1	34.3	34.3	30.1
	696271	27	B	F	27.6	27.7	23.6	30.2	29.1	25.4
	3080371	37	W	F	25.9	26.4	23.3	28.3	29.6	23.2
	376411	41	B	F	27.5	28.8	24.7	29.5	30.7	26.0
	2622521	52	B	F	28.4	26.1	26.3	27.4	26.9	28.9
L2	**2796360**	36	B	M	27.8	29.3	29.3	30.4	30.4	27.5
	8313270	27	B	M	29.0	30.0	26.5	29.4	31.5	26.7
	474590	59	W	M	29.4	30.2	27.1	34.2	33.2	33.2
	8213390	39	B	M	30.1	28.8	27.8	32.5	33.8	29.8
	696271	27	B	F	28.4	30.3	25.3	29.9	30.2	27.7
	3080371	37	W	F	27.4	29.1	25.7	30.2	30.2	30.2
	376411	41	B	F	29.0	28.4	28.5	30.8	31.5	26.2
	2622521	52	B	F	26.9	28.4	27.0	25.9	26.6	26.6

VL	Case ID	Age	P	Sex	VHa	IA	IE	VHp	IA	IE
L3	**2796360**	36	B	M	28.6	29.1	27.7	30.1	30.4	30.7
	8313270	27	B	M	30.4	31.9	28.3	33.7	32.6	31.6
	474590	59	W	M	31.8	30.9	26.0	33.0	34.2	34.7
	8213390	39	B	M	32.2	31.2	28.1	34.1	33.9	29.8
	696271	27	B	F	30.7	31.0	27.4	31.2	30.5	27.4
	3080371	37	W	F	31.1	32.1	29.4	32.4	31.4	30.8
	376411	41	B	F	29.3	29.3	25.0	29.0	31.1	30.1
	2622521	52	B	F	26.9	28.6	26.9	27.2	28.7	28.4
L4	**2796360**	36	B	M	27.5	30.2	25.2	26.4	29.5	26.6
	8313270	27	B	M	28.3	30.2	28.3	29.4	30.0	27.5
	474590	59	W	M	30.3	31.4	31.4	31.3	29.9	29.5
	8213390	39	B	M	33.6	34.3	32.5	34.4	35.0	34.4
	696271	27	B	F	28.9	29.9	27.0	30.7	28.8	26.1
	3080371	37	W	F	29.4	32.3	25.6	30.8	32.8	30.7
	376411	41	B	F	27.3	29.6	28.2	27.9	29.1	27.4
	2622521	52	B	F	26.9	27.8	28.2	25.1	24.6	28.1
L5	**2796360**	36	B	M	28.9	29.7	29.7	25.7	26.1	24.4
	8313270	27	B	M	30.2	31.6	31.6	27.5	27.1	28.9
	474590	59	W	M	32.4	32.3	28.5	27.8	26.3	23.9
	8213390	39	B	M	32.1	33.5	29.8	31.3	31.1	32.2
	696271	27	B	F	30.9	31.3	29.3	26.0	26.6	24.4
	3080371	37	W	F	32.1	32.7	27.2	27.9	28.5	26.5
	376411	41	B	F	27.0	31.0	26.1	24.7	25.6	28.1
	2622521	52	B	F	28.3	29.8	29.6	24.5	25.7	25.3

Key: VL = Vertebral level; P = Population group; B = Black; W = White M = Male; F = Female; VHa = Original anterior vertebral body height measurement; PB = Original posterior vertebral body height measurement; IE = Interobserver measurements; IA = Intra-observer measurements. All measurements are in millimetres

Table E.2.70: Table indicating the inter- and intra-observer measurements used to perform observer analyses for the lateral vertebral body diameters

VL	Case ID	Age	P	Sex	VDMaxL	IA	IE	VDMinL	IA	IE
L1	**2796360**	36	B	M	46.1	45.3	46.1	40.5	41.1	39.0

VL	Case ID	Age	P	Sex	VDMaxL	IA	IE	VDMinL	IA	IE
	8313270	27	B	M	45.7	46.2	44.7	40.2	40.0	37.0
	474590	59	W	M	46.7	46.5	49.1	40.2	38.6	37.6
	8213390	39	B	M	49.0	48.1	48.6	41.9	41.7	39.5
	696271	27	B	F	38.5	39.3	39.9	33.9	35.2	32.7
	3080371	37	W	F	36.5	38.4	38.0	33.2	34.5	31.3
	376411	41	B	F	46.2	45.7	37.5	41.3	40.7	31.4
	2622521	52	B	F	37.2	38.3	39.4	33.3	32.7	32.7
L2	**2796360**	36	B	M	46.1	47.5	48.2	41.4	42.0	41.9
	8313270	27	B	M	47.6	47.7	46.1	43.7	42.7	39.6
	474590	59	W	M	46.6	47.9	50.4	42.8	42.8	40.5
	8213390	39	B	M	50.7	49.6	50.9	44.7	45.3	40.1
	696271	27	B	F	39.2	39.6	40.7	35.7	35.8	34.2
	3080371	37	W	F	40.3	40.7	39.9	35.1	35.7	32.5
	376411	41	B	F	46.6	46.3	42.1	41.5	41.2	33.9
	2622521	52	B	F	38.7	39.4	39.1	35.0	34.6	34.4
L3	**2796360**	36	B	M	51.1	49.7	50.8	43.8	42.9	42.3
	8313270	27	B	M	51.8	50.2	48.7	45.3	44.0	39.4
	474590	59	W	M	51.1	50.7	52.7	43.7	44.8	41.9
	8213390	39	B	M	52.2	51.8	53.4	45.1	45.2	42.9
	696271	27	B	F	40.3	39.8	45.1	36.3	36.8	37.5
	3080371	37	W	F	44.3	42.5	43.8	38.7	38.2	36.0
	376411	41	B	F	46.9	47.9	44.2	44.2	43.0	35.8
	2622521	52	B	F	42.8	42.6	44.3	37.8	37.2	36.8
L4	**2796360**	36	B	M	52.7	49.6	53.5	46.7	44.9	44.4
	8313270	27	B	M	52.1	52.8	51.9	45.3	45.0	43.0
	474590	59	W	M	52.1	50.9	51.5	46.6	47.1	45.5
	8213390	39	B	M	52.8	52.6	51.9	46.7	46.4	44.8
	696271	27	B	F	44.1	45.8	46.5	40.4	40.1	41.3
	3080371	37	W	F	44.6	43.4	43.7	42.5	42.2	42.1
	376411	41	B	F	51.6	50.2	45.7	45.9	44.5	38.4
	2622521	52	B	F	44.7	44.4	46.9	39.6	38.7	37.8
L5	**2796360**	36	B	M	56.9	55.9	50.5	45.3	44.3	43.1
	8313270	27	B	M	51.7	52.9	50.1	44.3	45.4	41.6
	474590	59	W	M	56.0	55.1	54.6	43.8	44.5	45.2

VL	Case ID	Age	P	Sex	VDMaxL	IA	IE	VDMinL	IA	IE
	8213390	39	B	M	52.7	53.7	53.8	44.2	45.0	42.4
	696271	27	B	F	46.4	50.8	46.0	40.1	41.1	40.1
	3080371	37	W	F	46.2	45.9	44.9	41.8	41.0	41.4
	376411	41	B	F	57.3	56.2	49.0	49.1	47.5	47.6
	2622521	52	B	F	46.0	46.7	47.3	36.9	41.4	41.1

Key: VL = Vertebral level; P = Population group; B = Black; W = White M = Male; F = Female; VDMaxL = Original maximum lateral vertebral body lateral diameter measurement; VDMinL = Original minimum vertebral body lateral diameter measurement; IE = Interobserver measurements; IA = Intra-observer measurements. All measurements are in millimetres

Table E.2.71: Table indicating the inter- and intra-observer measurements used to perform observer analyses for the AP vertebral body diameters

VL	Case ID	Age	P	Sex	VDMaxAP	IA	IE	VDMinAP	IA	IE
	2796360	36	B	M	34.7	32.6	32.5	30.7	31.0	28.8
	8313270	27	B	M	33.4	31.4	30.5	31.0	29.4	29.4
	474590	59	W	M	30.9	31.9	32.9	28.0	30.2	28.8
	8213390	39	B	M	32.5	32.6	30.6	30.6	30.3	28.2
L1	**696271**	27	B	F	26.3	25.4	28.7	22.3	22.7	24.3
	3080371	37	W	F	29.1	29.2	30.0	26.2	27.8	28.6
	376411	41	B	F	30.4	28.0	30.1	26.5	26.4	27.5
	2622521	52	B	F	32.3	30.7	27.9	29.5	28.7	29.8
	2796360	36	B	M	37.9	36.1	35.4	32.7	33.9	30.8
	8313270	27	B	M	34.2	34.1	33.1	32.9	32.7	32.7
	474590	59	W	M	32.8	32.4	35.3	30.2	31.6	30.8
	8213390	39	B	M	32.6	33.1	33.2	32.3	32.9	27.4
L2	**696271**	27	B	F	28.3	26.7	27.5	24.1	24.4	26.9
	3080371	37	W	F	31.9	31.7	31.8	28.9	30.0	28.9
	376411	41	B	F	31.1	30.1	32.6	29.4	29.2	30.0
	2622521	52	B	F	32.7	31.8	29.0	29.9	30.6	27.6
	2796360	36	B	M	37.9	36.0	35.4	35.1	34.4	30.9
L3	**8313270**	27	B	M	34.9	33.9	33.5	32.2	32.6	28.5
	474590	59	W	M	36.3	36.4	36.6	33.8	34.4	33.2

VL	Case ID	Age	P	Sex	VDMaxAP	IA	IE	VDMinAP	IA	IE
	8213390	39	B	M	34.3	34.6	37.2	33.3	33.4	30.6
	696271	27	B	F	29.2	29.5	29.8	26.1	26.6	29.5
	3080371	37	W	F	33.5	32.4	31.6	31.8	31.0	27.7
	376411	41	B	F	33.5	33.6	34.1	31.1	32.1	30.5
	2622521	52	B	F	32.3	32.9	30.1	30.8	31.1	26.1
L4	**2796360**	36	B	M	36.9	36.6	33.5	34.6	34.0	34.0
	8313270	27	B	M	37.3	34.8	34.3	34.4	31.8	31.8
	474590	59	W	M	36.7	36.6	36.5	34.7	35.2	31.7
	8213390	39	B	M	35.6	34.9	36.7	33.5	33.9	32.3
	696271	27	B	F	32.4	31.2	32.8	29.0	29.1	30.5
	3080371	37	W	F	32.9	33.2	31.6	31.6	32.0	28.6
	376411	41	B	F	35.8	35.6	32.6	34.2	33.7	32.9
	2622521	52	B	F	33.6	33.1	33.2	30.4	31.5	29.8
L5	**2796360**	36	B	M	39.1	37.6	37.6	34.9	35.6	35.7
	8313270	27	B	M	34.7	35.4	34.2	32.7	32.6	31.4
	474590	59	W	M	36.8	37.3	37.2	33.5	35.3	34.5
	8213390	39	B	M	36.6	36.2	37.2	36.0	35.8	32.6
	696271	27	B	F	34.3	33.7	31.9	31.5	30.8	29.6
	3080371	37	W	F	32.2	32.1	35.0	31.8	31.5	32.4
	376411	41	B	F	39.7	38.5	36.7	35.2	38.0	32.0
	2622521	52	B	F	37.7	36.1	36.1	36.4	35.2	33.5

Key: VL = Vertebral level; P = Population group; B = Black; W = White M = Male; F = Female; VDMaxAP = Original maximum lateral vertebral body AP diameter measurement; VDMinAP = Original minimum vertebral body AP diameter measurement; IE = Interobserver measurements; IA = Intra-observer measurements. All measurements are in millimetres

Table E.2.72: Table indicating the inter- and intra-observer measurements used to perform observer analyses for the spinal canal AP and lateral diameters

VL	Case ID	Age	P	Sex	SCDAP	IA	IE	SCDL	IA	IE
L1	**2796360**	36	B	M	15.7	15.8	16.9	24.3	23.8	23.5
	8313270	27	B	M	14.8	15.7	13.8	21.8	23.8	26.0
	474590	59	W	M	13.2	13.7	15.3	21.9	22.7	25.2
	8213390	39	B	M	14.8	15.7	15.0	22.3	22.3	22.9

VL	Case ID	Age	P	Sex	SCDAP	IA	IE	SCDL	IA	IE
	696271	27	B	F	16.7	16.4	17.8	19.3	20.5	20.3
	3080371	37	W	F	21.7	15.1	17.2	19.7	20.4	21.2
	376411	41	B	F	16.8	17.1	18.2	24.6	26.7	25.3
	2622521	52	B	F	13.0	14.0	16.2	20.8	21.9	20.1
L2	**2796360**	36	B	M	14.4	13.7	16.2	23.8	22.2	24.2
	8313270	27	B	M	13.5	14.0	14.3	21.3	23.1	24.0
	474590	59	W	M	11.6	12.3	13.5	20.9	23.2	22.0
	8213390	39	B	M	13.8	13.2	12.6	21.2	22.0	22.2
	696271	27	B	F	15.6	15.4	18.1	19.7	21.4	21.8
	3080371	37	W	F	25.5	16.2	16.6	20.1	23.0	24.0
	376411	41	B	F	16.6	19.1	16.4	25.2	25.0	26.2
	2622521	52	B	F	12.9	14.1	14.1	23.0	23.6	25.0
L3	**2796360**	36	B	M	12.0	12.6	13.8	24.7	23.1	23.9
	8313270	27	B	M	13.9	12.4	13.0	23.5	24.4	26.0
	474590	59	W	M	11.9	11.6	14.9	26.1	24.1	24.6
	8213390	39	B	M	14.3	13.4	13.6	20.6	22.9	23.7
	696271	27	B	F	15.2	14.4	18.4	20.2	21.0	23.4
	3080371	37	W	F	19.7	17.5	16.6	23.9	22.6	24.8
	376411	41	B	F	18.2	17.7	14.2	26.0	28.3	23.5
	2622521	52	B	F	14.3	14.3	17.0	22.6	23.6	20.6
L4	**2796360**	36	B	M	13.5	12.6	13.5	26.1	23.0	23.7
	8313270	27	B	M	11.1	11.5	15.1	24.0	26.4	24.0
	474590	59	W	M	11.9	12.3	14.2	26.4	26.8	26.2
	8213390	39	B	M	15.0	14.2	13.3	22.6	22.8	22.8
	696271	27	B	F	13.6	13.5	13.8	25.8	21.7	25.3
	3080371	37	W	F	12.9	21.8	15.7	26.4	26.3	25.8
	376411	41	B	F	18.2	19.1	18.9	29.6	31.3	31.2
	2622521	52	B	F	14.7	13.4	15.4	24.4	23.8	20.8
L5	**2796360**	36	B	M	13.7	13.1	15.0	25.2	26.5	26.5
	8313270	27	B	M	14.4	14.2	15.7	25.4	23.6	23.6
	474590	59	W	M	15.8	16.0	13.6	29.9	29.9	30.2
	8213390	39	B	M	16.4	17.3	17.0	25.7	26.2	26.2
	696271	27	B	F	15.7	15.4	19.4	26.1	21.5	27.8
	3080371	37	W	F	20.0	22.3	17.7	27.9	26.8	29.2

VL	Case ID	Age	P	Sex	SCDAP	IA	IE	SCDL	IA	IE
	376411	41	B	F	16.5	17.5	15.3	31.1	31.9	28.6
	2622521	52	B	F	16.1	15.9	16.3	29.0	30.2	26.1

Key: VL = Vertebral level; P = Population group; B = Black; W = White M = Male; F = Female; SCDAP = Original spinal canal AP diameter measurement; SCDL = Original spinal canal lateral diameter measurement; IE = Interobserver measurements; IA = Intra-observer measurements. All measurements are in millimetres

Appendix E.3 – Raw data for MRI observer analysis: Sagittal

Table E.3.73: Table indicating the inter- and intra-observer measurements used to perform observer analyses for the pedicle measurements

VL	Case ID	Age	Sex	FH	IA	IE	RD	IA	IE	RP	IA	IE
L1	**314460**	46	M	17.4	18.4	20.3	.0	.5	4.5	11.4	12.2	12.0
	408471	47	F	19.9	18.7	23.1	-4.0	-3.4	2.5	14.0	13.1	11.3
	530410	41	M	15.5	16.0	21.9	-3.7	-2.9	4.8	12.8	10.5	10.9
	659360	36	M	17.4	17.0	22.6	-2.5	-1.7	6.7	11.5	12.0	8.4
L2	**314460**	46	M	22.0	18.7	22.3	1.7	.8	3.3	11.7	12.0	14.1
	408471	47	F	20.0	18.5	23.0	-4.1	-3.4	-2.0	14.0	12.9	18.4
	530410	41	M	15.7	17.0	22.3	-1.9	-2.5	-1.8	8.0	11.8	10.1
	659360	36	M	18.6	19.2	23.5	-3.5	-2.8	-5.7	12.6	13.6	8.9
L3	**314460**	46	M	21.0	19.8	26.5	1.8	2.1	2.3	13.2	13.0	16.2
	408471	47	F	22.4	20.2	25.1	-1.9	-1.3	-2.0	13.8	13.1	15.3
	530410	41	M	18.0	19.3	26.4	-2.7	-3.5	-3.6	11.2	12.9	11.1
	659360	36	M	23.3	22.3	27.2	-5.5	-3.3	-3.2	17.7	15.7	13.5
L4	**314460**	46	M	25.0	25.3	26.7	3.5	2.9	2.8	12.4	13.5	12.9
	408471	47	F	22.2	20.9	23.5	1.7	2.6	1.7	11.1	13.4	8.9
	530410	41	M	19.7	20.3	23.9	-3.8	-3.1	1.7	14.8	15.6	10.7
	659360	36	M	23.0	24.5	27.6	-5.2	-4.5	-6.3	16.7	17.4	10.9
L5	**314460**	46	M	20.0	17.2	20.7	-1.2	-1.2	-1.6	7.8	6.9	11.9
	408471	47	F	21.9	21.0	22.0	4.1	4.3	2.9	11.6	10.1	11.8
	530410	41	M	22.4	21.7	24.4	2.4	2.5	3.8	14.9	11.6	12.5
	659360	36	M	24.9	25.2	27.5	-8.5	-5.7	-4.8	20.1	19.7	21.8

VL	Case ID	Age	Sex	FH	IA	IE	RD	IA	IE	RP	IA	IE
Key: VL = Vertebral level; M = Male; F = Female; FH = Original foraminal height measurement; RD = Original root to disc distance measurement; RP = Original root to pedicle distance; IA = Intra-observer measurements; IE = Interobserver measurements. All measurements are in millimetres												

Table E.3.74: Table indicating the inter- and intra-observer measurements used to perform observer analyses for the superior, middle, and inferior foraminal diameters

VL	Case ID	Age	Sex	SFD	IA	IE	MFD	IA	IE	IFD	IA	IE
L1	**314460**	46	M	9.1	9.9	11.9	9.2	8.4	11.6	8.7	7.4	10.0
	408471	47	F	6.6	7.6	11.3	6.1	7.0	10.3	5.8	5.9	8.8
	530410	41	M	9.2	9.7	15.8	10.1	9.1	13.5	8.4	8.1	11.8
	659360	36	M	8.8	7.6	10.4	7.6	6.0	10.7	5.0	5.3	8.2
L2	**314460**	46	M	8.0	7.7	10.6	8.4	6.7	8.7	7.7	5.2	8.9
	408471	47	F	6.1	4.8	11.2	5.3	4.1	11.3	4.4	4.4	9.4
	530410	41	M	11.0	9.9	15.0	9.7	8.9	15.3	9.2	9.3	13.2
	659360	36	M	7.5	7.8	9.5	7.2	7.1	8.0	4.4	5.5	8.5
L3	**314460**	46	M	8.3	8.4	8.3	7.8	8.1	8.3	5.1	4.0	7.6
	408471	47	F	7.6	6.4	8.4	5.5	4.3	4.0	5.0	4.8	10.6
	530410	41	M	9.1	7.9	10.1	8.2	6.9	8.0	7.2	6.3	11.6
	659360	36	M	8.2	5.8	6.2	5.7	5.0	10.1	5.6	5.6	9.1
L4	**314460**	46	M	7.5	8.3	8.3	5.3	5.6	5.0	5.9	4.3	5.8
	408471	47	F	6.7	4.7	9.7	5.6	3.5	12.7	4.2	3.5	5.2
	530410	41	M	6.0	7.7	8.0	6.9	5.6	13.2	6.3	6.4	10.2
	659360	36	M	6.3	5.5	8.6	6.0	4.2	7.9	5.4	3.9	7.1
L5	**314460**	46	M	7.3	6.8	7.8	5.5	4.8	5.3	0.0	0.0	4.1
	408471	47	F	5.6	5.1	7.5	3.8	3.6	2.0	4.6	3.3	9.9
	530410	41	M	3.5	4.6	5.3	3.1	3.3	3.3	2.0	2.7	9.0
	659360	36	M	4.7	4.5	4.0	4.7	4.8	7.3	3.2	3.6	7.9
Key: VL = Vertebral level; M = Male; F = Female; SFD = Original superior foraminal diameter measurement; MFD = Original middle foraminal diameter measurement; IFD = Original inferior foraminal diameter measurement. IE = Interobserver measurements; IA = Intra-observer measurements. All measurements are in millimetres												

Appendix E.4 – Raw data for MRI observer analysis: Coronal

Table E.4.75: Table indicating the inter- and intra-observer measurements used to perform observer analyses for the measurements form the nerve root to the disc at the medial border of the pedicle (MedD)

VL	Case ID	Age	Sex	MedD L	IA	IE	MedD R	IA	IE
L1	**408471**	47	F	-3.6	-4.0	-4.2	-2.8	-2.8	-2.8
	530410	41	M	-4.1	-5.2	-4.2	-3.1	-4.2	-3.4
	659360	36	M	-6.3	-5.9	-7.8	-4.6	-3.5	-5.7
	2411580	58	M	-4.9	-4.8	-6.4	-4.1	-4.1	-4.1
L2	**408471**	47	F	-4.8	-4.6	-6.9	-3.2	-4.8	-5.1
	530410	41	M	-3.4	-5.0	-2.3	-2.9	-4.6	-2.6
	659360	36	M	-5.9	-6.3	-3.2	-7.2	-7.3	-7.5
	2411580	58	M	-5.4	-5.4	-6.4	-6.8	-6.4	-5.0
L3	**408471**	47	F				-2.9	-3.8	-3.3
	530410	41	M	-6.5	-7.2	-2.2	-2.5	-4.1	-1.2
	659360	36	M	-9.6	-9.1	-6.4	-7.7	-8.0	-7.2
	2411580	58	M	-5.7	-6.0	-3.4	-8.8	-6.9	-10.0
L4	**408471**	47	F	-4.0	-4.5	-5.0	-7.8	-5.1	-10.5
	530410	41	M	-3.9	-3.6	-2.3	-7.2	-6.0	-3.9
	659360	36	M	-8.3	-8.8	-5.4	-8.0	-8.3	-7.5
	2411580	58	M	-5.4	-6.6	-2.4	-2.8	-4.2	-2.2
L5	**408471**	47	F	-7.5	-9.8	-6.2	-8.5	-10.2	-11.6
	530410	41	M	-7.2	-6.5	-6.1	-9.1	-9.5	-9.3
	659360	36	M	-9.8	-8.9	-8.9	-7.5	-8.3	-10.5
	2411580	58	M	-5.4	-4.5	-5.5	-5.8	-4.5	-7.8

Key: VL = Vertebral level; M = Male; F = Female; L = Left side; R = Right side; MedD = Original measurement at the medial border of the pedicle; IA = Intra-observer measurements; IE = Interobserver measurements. All measurements are in millimetres. Measurements with negative values are situated above the superior border of the disc. Empty cells indicate instances where measurements could not be taken

Table E.4.76: Table indicating the inter- and intra-observer measurements used to perform observer analyses for the measurements form the nerve root to the disc at the midline of the pedicle (MidD)

VL	Case ID	Age	Sex	MidD L	IA	IE	MidD R	IA	IE
L1	**408471**	47	F	-2.1	-2.0	-1.4	0.6	1.0	.4
	530410	41	M	-2.6	-1.9	-2.4	-1.2	-1.1	-2.0
	659360	36	M	0.8	1.1	3.1	4.3	3.1	5.0
	2411580	58	M	1.4	1.2	3.4	2.2	1.8	3.5
L2	**408471**	47	F	0.0	0.0	.0	2.9	2.0	.0
	530410	41	M	-1.7	-1.9	-1.3	-2.2	-2.0	-1.2
	659360	36	M	1.3	1.3	4.4	1.5	2.1	5.6
	2411580	58	M	-2.0	-2.7	-2.1	-1.7	-2.2	-4.6
L3	**408471**	47	F				-1.9	-1.6	-2.0
	530410	41	M	-2.9	-2.0	-4.7	-1.0	-1.6	-.7
	659360	36	M	2.3	2.4	2.5	3.7	2.9	4.0
	2411580	58	M	-2.0	-1.7	-2.4	-2.3	-2.2	-2.1
L4	**408471**	47	F	-1.9	-1.3	-1.7	-1.6	-1.1	-1.2
	530410	41	M	-1.3	-2.4	-1.7	-1.9	-2.5	-4.0
	659360	36	M	3.6	3.1	-.9	3.9	4.6	3.4
	2411580	58	M	2.8	3.0	4.8	5.4	4.3	3.8
L5	**408471**	47	F	-3.8	-4.7	-3.4	-4.3	-5.3	-8.6
	530410	41	M	-2.7	-3.5	-2.7	-1.5	-2.0	-1.1
	659360	36	M	-1.6	-1.7	-2.4	2.2	2.8	5.5
	2411580	58	M	-2.0	-3.0	-4.6	1.7	2.5	1.5

Key: VL = Vertebral level; M = Male; F = Female; L = Left side; R = Right side; MidD = Original measurement at the midline of the pedicle; IA = Intra-observer measurements; IE = Interobserver measurements. All measurements are in millimetres. Measurements with negative values are situated above the superior border of the disc. Empty cells indicate instances where measurements could not be taken

Table E.4.77: Table indicating the inter- and intra-observer measurements used to perform observer analyses for the measurements form the nerve root to the disc at the lateral border of the pedicle (LatD)

VL	Case ID	Age	Sex	LatD L	IA	IE	LatD R	IA	IE
L1	**408471**	47	F	4.6	2.7	8.3	5.4	4.0	5.2
	530410	41	M	-1.0	0.0	-1.5	0.4	0.2	.4
	659360	36	M	3.5	3.2	6.1	5.7	4.1	4.6
	2411580	58	M	2.7	3.3	3.4	6.3	4.8	5.5
L2	**408471**	47	F	2.9	2.1	1.1	3.2	3.0	3.8
	530410	41	M	-1.0	-1.2	-1.6	0.7	1.6	.9
	659360	36	M	3.8	4.1	5.8	4.4	5.6	8.9
	2411580	58	M	3.1	3.0	4.3	2.3	3.0	2.1
L3	**408471**	47	F				3.4	3.6	3.4
	530410	41	M	-1.6	-1.4	-1.9	2.5	3.0	4.4
	659360	36	M	5.4	6.3	6.8	7.5	8.0	7.8
	2411580	58	M	5.7	5.4	4.3	4.3	3.9	6.0
L4	**408471**	47	F	3.5	5.6	-2.9	2.7	5.7	2.4
	530410	41	M	4.9	4.4	3.6	5.9	5.5	4.4
	659360	36	M	7.7	8.6	2.9	8.5	9.4	5.5
	2411580	58	M	9.6	10.9	6.4	8.8	8.4	6.4
L5	**408471**	47	F	3.0	3.4	-1.8	2.7	2.9	-1.1
	530410	41	M	4.2	4.6	5.4	8.9	9.8	8.1
	659360	36	M	3.6	3.4	3.9	4.2	5.4	4.0
	2411580	58	M	4.6	4.7	3.6	6.3	5.2	3.6

Key: VL = Vertebral level; M = Male; F = Female; L = Left side; R = Right side; LatD = Original measurement at the lateral border of the pedicle; IA = Intra-observer measurements; IE = Interobserver measurements. All measurements are in millimetres. Measurements with negative values are situated above the superior border of the disc. Empty cells indicate instances where measurements could not be taken

Table E.4.78: Table indicating the inter- and intra-observer measurements used to perform observer analyses for the measurements form the nerve root to the pedicle at the medial border of the pedicle (MedP)

VL	Case ID	Age	Sex	MedP L	IA	IE	MedP R	IA	IE
L1	**408471**	47	F	12.8	12.8	15.1	12.5	12.7	10.0
	530410	41	M	10.3	9.9	10.7	11.2	13.2	10.8
	659360	36	M	14.4	12.1	13.3	14.9	12.3	12.8
	2411580	58	M	12.5	12.6	13.9	11.1	11.1	13.1
L2	**408471**	47	F	13.1	15.5	12.9	11.5	15.3	14.6
	530410	41	M	12.2	13.1	12.2	10.8	10.7	12.0
	659360	36	M	17.2	16.7	14.4	17.5	17.0	15.3
	2411580	58	M	12.2	13.2	12.2	16.1	17.0	15.3
L3	**408471**	47	F				13.6	15.1	15.4
	530410	41	M	15.3	15.8	14.3	14.4	15.2	11.3
	659360	36	M	20.3	19.6	16.4	21.6	21.5	15.7
	2411580	58	M	15.6	15.5	16.5	17.9	17.4	21.5
L4	**408471**	47	F	15.2	17.0	15.7	16.0	17.7	18.1
	530410	41	M	13.3	13.3	14.4	15.9	16.6	16.7
	659360	36	M	18.5	19.4	13.9	23.0	21.9	16.1
	2411580	58	M	19.0	18.8	20.8	20.7	19.1	20.8
L5	**408471**	47	F	15.5	15.1	14.9	13.9	12.8	15.9
	530410	41	M	12.1	13.5	14.2	10.6	11.4	11.2
	659360	36	M	21.3	21.6	17.2	22.1	21.7	18.4
	2411580	58	M	15.1	16.1	15.1	18.7	17.3	23.2

Key: VL = Vertebral level; M = Male; F = Female; L = Left side; R = Right side; MedP = Original measurement at the medial border of the pedicle; IA = Intra-observer measurements; IE = Interobserver measurements. All measurements are in millimetres. Empty cells indicate instances where measurements could not be taken

Table E.4.79: Table indicating the inter- and intra-observer measurements used to perform observer analyses for the measurements form the nerve root to the pedicle at the midline of the pedicle (MidP)

VL	Case ID	Age	Sex	MidP L	IA	IE	MidP R	IA	IE
L1	**408471**	47	F	11.9	9.1	10.4	5.6	8.5	5.1
	530410	41	M	7.8	7.6	8.8	8.4	8.3	6.7
	659360	36	M	6.4	6.4	5.1	6.4	5.3	4.1
	2411580	58	M	6.5	5.7	10.3	5.5	5.1	4.1
L2	**408471**	47	F	13.1	13.4	14.8	10.9	10.1	10.8
	530410	41	M	8.4	8.2	5.7	8.7	8.7	5.0
	659360	36	M	9.5	8.3	7.9	8.5	7.6	6.8
	2411580	58	M	8.8	9.6	11.2	8.2	9.3	4.6
L3	**408471**	47	F				9.9	10.9	8.6
	530410	41	M	10.6	10.1	10.4	12.1	11.2	10.0
	659360	36	M	10.0	9.7	12.0	11.0	10.0	9.2
	2411580	58	M	8.2	9.3	5.1	10.6	10.5	10.4
L4	**408471**	47	F	9.9	9.6	10.5	9.9	7.9	14.7
	530410	41	M	9.7	6.2	10.3	9.6	6.2	11.3
	659360	36	M	10.3	9.6	9.6	10.0	9.5	11.8
	2411580	58	M	12.5	9.4	16.3	11.6	8.4	13.4
L5	**408471**	47	F	10.6	9.6	10.0	11.4	12.6	13.5
	530410	41	M	12.4	10.5	12.0	11.8	9.4	12.6
	659360	36	M	11.3	11.1	13.6	12.9	11.7	13.9
	2411580	58	M	8.2	10.0	10.3	9.6	10.9	11.3

Key: VL = Vertebral level; M = Male; F = Female; L = Left side; R = Right side; MidP = Original measurement at the midline of the pedicle; IA = Intra-observer measurements; IE = Interobserver measurements. All measurements are in millimetres. Empty cells indicate instances where measurements could not be taken

Table E.4.80: Table indicating the inter- and intra-observer measurements used to perform observer analyses for the measurements form the nerve root to the pedicle at the lateral border of the pedicle (LatP)

VL	Case ID	Age	Sex	LatP L	IA	IE	LatP R	IA	IE
L1	**408471**	47	F	12.8	12.2	16.8	10.3	9.7	13.1
	530410	41	M	8.6	10.1	7.9	8.6	9.6	8.9
	659360	36	M	10.8	11.0	11.1	7.7	9.9	8.5
	2411580	58	M	7.1	7.3	5.0	6.2	5.7	2.9
L2	**408471**	47	F	13.4	16.2	10.4	10.9	10.8	10.9
	530410	41	M	10.9	10.4	7.0	9.2	9.5	9.7
	659360	36	M	7.7	7.5	1.2	6.9	7.6	6.5
	2411580	58	M	6.5	5.6	4.5	6.5	6.4	7.6
L3	**408471**	47	F				9.9	9.4	9.5
	530410	41	M	10.6	11.2	11.4	8.6	8.5	7.2
	659360	36	M	7.5	6.6	8.0	8.5	7.1	5.5
	2411580	58	M	6.0	6.3	7.9	5.4	6.0	4.3
L4	**408471**	47	F	5.3	5.9	5.7	6.1	7.2	6.7
	530410	41	M	6.2	7.6	6.0	7.9	8.7	10.7
	659360	36	M	6.9	6.8	5.6	7.7	7.6	11.9
	2411580	58	M	5.7	5.1	5.2	2.3	2.7	3.4
L5	**408471**	47	F	7.7	6.2	4.1	12.1	10.6	14.0
	530410	41	M	7.8	7.1	3.4	6.4	6.1	10.8
	659360	36	M	8.2	8.5	11.6	10.8	9.6	12.3
	2411580	58	M	4.0	3.9	3.6	2.6	2.8	3.4

Key: VL = Vertebral level; M = Male; F = Female; L = Left side; R = Right side; LatP = Original measurement at the lateral border of the pedicle; IA = Intra-observer measurements; IE = Interobserver measurements. All measurements are in millimetres. Empty cells indicate instances where measurements could not be taken

Appendix E.5 – Raw data for MRI observer analysis: Transverse

Table E.5.81: Table indicating the inter- and intra-observer measurements used to perform observer analyses for the transverse foraminal diameter (FDT) measurements taken superior to the disc

VL	Case ID	Age	Sex	FDT L	IA	IE	FDT R	IA	IE
L3	**1750490**	49	M	7.0	7.8	5.1	7.4	7.9	6.4
	1858360	36	M	6.9	6.6	3.3	6.8	5.9	5.3
	2411580	58	M	8.2	7.8	6.5	6.6	5.4	6.0
L4	**1750490**	49	M	7.4	7.3	6.5	7.0	7.0	6.4
	1858360	36	M	8.1	7.4	6.2	8.1	7.2	6.8
	2411580	58	M	6.2	6.0	6.1	5.3	4.7	4.9
L5	**530410**	41	M	7.9	7.2	8.8	7.5	6.7	8.8
	726421	42	F	8.5	8.7	6.7	7.6	6.7	6.7
	1750490	49	M	6.8	6.5	5.1	7.2	7.1	5.1
	1858360	36	M	7.1	6.9	5.3	8.2	8.2	5.3
	2411580	58	M	7.0	7.8	5.3	6.6	6.6	5.3

Key: VL = Vertebral level; M = Male; F = Female; L = Left side; R = Right side; FDT = Original transverse foraminal diameter measurement; IA = Intra-observer measurements; IE = Interobserver measurements. All measurements are in millimetres

Table E.5.82: Table indicating the inter- and intra-observer measurements used to perform observer analyses for the root to disc (RD) measurements taken superior to the disc

VL	Case ID	Age	Sex	RD L	IA	IE	RD R	IA	IE
L3	**1750490**	49	M	2.2	2.7	2.4	2.4	3.1	2.1
	1858360	36	M	2.5	3.0	2.9	2.5	3.7	2.6
	2411580	58	M	2.4	2.2	2.7	1.3	1.9	1.6
L4	**1750490**	49	M	2.3	2.2	2.5	2.5	2.2	2.1
	1858360	36	M	4.4	3.8	4.0	4.0	3.7	3.5
	2411580	58	M	2.7	2.5	3.8	2.2	2.4	2.2
L5	**530410**	41	M	2.7	2.5	2.6	2.2	1.2	1.8
	726421	42	F	2.2	2.3	2.4	3.0	3.0	2.5

VL	Case ID	Age	Sex	RD L	IA	IE	RD R	IA	IE
	1750490	49	M	1.9	2.8	1.7	1.4	1.3	1.9
	1858360	36	M	2.8	2.9	1.7	3.2	3.3	3.0
	2411580	58	M	2.5	2.9	2.0	2.2	1.5	1.6

Key: VL = Vertebral level; M = Male; F = Female; L = Left side; R = Right side; RD = Original root to disc measurement; IA = Intra-observer measurements; IE = Interobserver measurements. All measurements are in millimetres

Table E.5.83: Table indicating the inter- and intra-observer measurements used to perform observer analyses for the root to facet joint (RF) measurements taken superior to the disc

VL	Case ID	Age	Sex	RF L	IA	IE	RF R	IA	IE
	1750490	49	M	2.1	1.3	1.9	2.5	1.9	1.9
L3	**1858360**	36	M	3.7	3.2	2.7	2.6	3.0	2.7
	2411580	58	M	2.4	3.1	2.5	2.3	2.7	2.5
	1750490	49	M	1.7	1.5	1.7	.9	1.0	.3
L4	**1858360**	36	M	2.0	2.7	2.6	1.5	1.7	1.7
	2411580	58	M	2.9	2.1	2.8	1.8	1.2	2.0
	530410	41	M	4.2	3.7	4.5	3.5	2.7	4.3
	726421	42	F	2.7	2.6	3.3	3.1	4.1	3.2
L5	**1750490**	49	M	1.3	1.2	2.1	1.8	2.6	2.0
	1858360	36	M	1.4	1.6	2.7	1.5	1.6	2.7
	2411580	58	M	1.0	1.4	2.6	1.3	1.8	1.3

Key: VL = Vertebral level; M = Male; F = Female; L = Left side; R = Right side; RF = Original root to facet joint measurement; IA = Intra-observer measurements; IE = Interobserver measurements. All measurements are in millimetres

Table E.5.84: Table indicating the inter- and intra-observer measurements used to perform observer analyses for the target angle (TA) measurements taken superior to the disc

VL	Case ID	Age	Sex	TA L	IA	IE	TA R	IA	IE
	1750490	49	M	23.2	22.7	24.7	25.3	23.0	22.6
L3	**1858360**	36	M	19.6	23.0	20.1	19.3	22.0	20.0
	2411580	58	M	16.4	16.4	13.8	16.5	17.4	17.3

VL	Case ID	Age	Sex	TA L	IA	IE	TA R	IA	IE
	1750490	49	M	20.1	23.0	22.9	18.9	18.0	17.8
L4	**1858360**	36	M	19.9	20.8	18.8	19.1	19.4	19.9
	2411580	58	M	14.5	15.2	15.0	14.5	13.8	12.7
	530410	41	M	13.3	9.4	10.8	14.8	10.7	11.8
	726421	42	F	20.2	16.3	17.4	20.4	18.7	20.3
L5	**1750490**	49	M	16.4	15.5	14.7	19.3	19.6	18.9
	1858360	36	M	11.5	12.1	12.6	12.8	13.7	10.0
	2411580	58	M	17.2	18.7	18.2	16.1	16.7	11.6

Key: VL = Vertebral level; M = Male; F = Female; L = Left side; R = Right side; TA = Original target angle measurement; IA = Intra-observer measurements; IE = Interobserver measurements. All measurements are in degrees

Table E.5.85: Table indicating the inter- and intra-observer measurements used to perform observer analyses for the transverse foraminal diameter (FDT) measurements taken inferior to the disc

VL	Case ID	Age	Sex	FDT L	IA	IE	FDT R	IA	IE
	1750490	49	M	8.2	7.9	4.5	7.4	7.2	3.8
L3	**1858360**	36	M	7.4	6.0	4.0	7.9	6.9	4.3
	2411580	58	M	7.4	6.9	4.0	8.0	7.4	5.7
	1750490	49	M	6.7	6.8	6.3	6.1	5.8	5.0
L4	**1858360**	36	M	6.8	5.2	6.0	7.5	6.9	6.9
	2411580	58	M	6.4	5.8	6.0	6.3	5.4	3.5
	530410	41	M	5.0	4.3	5.3	5.9	4.9	4.9
	726421	42	F	5.6	4.1	8.4	7.6	6.0	5.3
L5	**1750490**	49	M	7.7	8.9	7.9	6.6	7.5	6.6
	1858360	36	M	6.4	6.4	6.1	6.6	6.7	6.6
	2411580	58	M	8.2	7.2	6.6	9.5	8.9	6.9

Key: VL = Vertebral level; M = Male; F = Female; L = Left side; R = Right side; FDT = Original transverse foraminal diameter measurement; IA = Intra-observer measurements; IE = Interobserver measurements. All measurements are in millimetres

Table E.5.86: Table indicating the inter- and intra-observer measurements used to perform observer analyses for the root to disc (RD) measurements taken inferior to the disc

VL	Case ID	Age	Sex	RD L	IA	IE	RD R	IA	IE
	1750490	49	M	2.3	2.4	2.0	3.3	3.5	3.0
L3	**1858360**	36	M	2.4	2.6	2.3	2.7	2.5	2.5
	2411580	58	M	2.2	2.4	2.1	2.1	2.2	1.9
	1750490	49	M	2.0	2.3	3.0	2.1	2.6	3.5
L4	**1858360**	36	M	2.5	2.8	2.5	2.6	3.0	3.5
	2411580	58	M	1.9	1.7	1.9	1.9	2.2	1.0
	530410	41	M	2.5	2.6	3.0	1.6	1.7	3.2
	726421	42	F	1.7	1.5	1.7	2.1	1.9	2.9
L5	**1750490**	49	M	3.5	3.5	4.5	3.5	2.9	3.0
	1858360	36	M	2.1	3.9	2.0	2.5	3.9	2.8
	2411580	58	M	3.0	3.4	3.7	3.5	3.9	3.0

Key: VL = Vertebral level; M = Male; F = Female; L = Left side; R = Right side; RD = Original root to disc measurement; IA = Intra-observer measurements; IE = Interobserver measurements. All measurements are in millimetres

Table E.5.87: Table indicating the inter- and intra-observer measurements used to perform observer analyses for the root to facet joint (RF) measurements taken inferior to the disc

VL	Case ID	Age	Sex	RF L	IA	IE	RF R	IA	IE
	1750490	49	M	2.9	3.0	2.4	1.5	1.1	2.5
L3	**1858360**	36	M	6.6	4.2	3.0	5.3	3.6	5.5
	2411580	58	M	5.3	4.7	5.0	4.9	4.3	3.3
	1750490	49	M	8.7	7.2	8.4	8.4	7.6	8.6
L4	**1858360**	36	M	1.1	.8	2.2	1.5	1.9	2.9
	2411580	58	M	4.3	4.0	3.9	3.8	3.5	3.3
	530410	41	M	4.3	3.9	2.6	3.8	3.3	4.4
L5	**726421**	42	F	4.2	3.0	5.0	6.1	5.2	3.1
	1750490	49	M	3.7	4.7	1.2	3.3	4.3	1.7

VL	Case ID	Age	Sex	RF L	IA	IE	RF R	IA	IE
	1858360	36	M	2.1	3.7	1.9	1.1	2.8	3.5
	2411580	58	M	6.6	5.4	4.0	5.2	4.4	3.7

Key: VL = Vertebral level; M = Male; F = Female; L = Left side; R = Right side; RF = Original root to facet joint measurement; IA = Intra-observer measurements; IE = Interobserver measurements. All measurements are in millimetres

Table E.5.88: Table indicating the inter- and intra-observer measurements used to perform observer analyses for the target angle (TA) measurements taken inferior to the disc

VL	Case ID	Age	Sex	TA L	IA	IE	TA R	IA	IE
	1750490	49	M	24.6	23.5	20.2	20.4	19.5	22.4
L3	**1858360**	36	M	13.3	16.1	17.3	13.5	17.3	15.9
	2411580	58	M	15.6	15.5	22.8	15.9	16.1	16.7
	1750490	49	M	18.3	17.9	19.7	19.6	18.7	20.1
L4	**1858360**	36	M	15.9	14.8	14.0	18.7	17.3	26.7
	2411580	58	M	13.2	15.5	15.1	15.4	15.7	20.4
	530410	41	M	11.6	11.8	14.7	11.0	9.7	16.4
	726421	42	F	8.3	5.7	7.1	8.5	5.9	13.8
L5	**1750490**	49	M	16.1	13.6	15.7	18.6	16.4	15.4
	1858360	36	M	14.7	14.8	14.5	13.8	12.4	10.5
	2411580	58	M	12.3	12.8	13.4	9.9	9.8	11.1

Key: VL = Vertebral level; M = Male; F = Female; L = Left side; R = Right side; TA = Original target angle measurement; IA = Intra-observer measurements; IE = Interobserver measurements. All measurements are in degrees

ETHICS DOCUMENTATION

Research ethics certificate – Initial application approval

The Research Ethics Committee, Faculty Health Sciences, University of Pretoria complies with ICH-GCP guidelines and has US Federal wide Assurance.
- FWA 00002567, Approved dd 22 May 2002 and Expires 03/20/2022.
- IRB 0000 2235 IORG0001762 Approved dd 22/04/2014 and Expires 03/14/2020.

UNIVERSITEIT VAN PRETORIA
UNIVERSITY OF PRETORIA
YUNIBESITHI YA PRETORIA

Faculty of Health Sciences Research Ethics Committee

27/07/2017

Approval Certificate
New Application

Ethics Reference No: 320/2017

Title: Morphometric properties and bone mineral density of the lumbar spine in a South African population: surgical considerations for spinal fusion.

Dear Miss Anya Konig

The **New Application** as supported by documents specified in your cover letter dated 19/06/2017 for your research received on the 19/06/2017, was approved by the Faculty of Health Sciences Research Ethics Committee on its quorate meeting of 26/07/2017.

Please note the following about your ethics approval:
- Ethics Approval is valid for 2 years
- Please remember to use your protocol number (**320/2017**) on any documents or correspondence with the Research Ethics Committee regarding your research.
- Please note that the Research Ethics Committee may ask further questions, seek additional information, require further modification, or monitor the conduct of your research.

Ethics approval is subject to the following:
- The ethics approval is conditional on the receipt of **6 monthly written Progress Reports**, and
- The ethics approval is conditional on the research being conducted as stipulated by the details of all documents submitted to the Committee. In the event that a further need arises to change who the investigators are, the methods or any other aspect, such changes must be submitted as an Amendment for approval by the Committee.

Additional Conditions:
- Researcher to take note: A further limitation of the study is that it is not known who in the female population was receiving HRT as this may be a confounding factor when assessing bone density of the female population.

We wish you the best with your research.

Yours sincerely

*** Kindly collect your original signed approval certificate from our offices, Faculty of Health Sciences, Research Ethics Committee, Tswelopele Building, Level 4-60*

Dr R Sommers; MBChB; MMed (Int); MPharMed,PhD
Deputy Chairperson of the Faculty of Health Sciences Research Ethics Committee, University of Pretoria

The Faculty of Health Sciences Research Ethics Committee complies with the SA National Act 61 of 2003 as it pertains to health research and the United States Code of Federal Regulations Title 45 and 46. This committee abides by the ethical norms and principles for research, established by the Declaration of Helsinki, the South African Medical Research Council Guidelines as well as the Guidelines for Ethical Research: Principles Structures and Processes, Second Edition 2015 (Department of Health).

☎ 012 356 3084 deepeka.behari@up.ac.za / fhsethics@up.ac.za http://www.up.ac.za/healthethics
✉ Private Bag X323, Arcadia, 0007 - Tswelopele Building, Level 4, Room 60, Gezina, Pretoria

Research ethics certificate – Subsequent project protocol amendment approval

The Research Ethics Committee, Faculty Health Sciences, University of Pretoria complies with ICH-GCP guidelines and has US Federal wide Assurance.
- FWA 00002567, Approved dd 22 May 2002 and Expires 03/20/2022.
- IRB 0000 2235 IORG0001762 Approved dd 22/04/2014 and Expires 03/14/2020.

UNIVERSITEIT VAN PRETORIA
UNIVERSITY OF PRETORIA
YUNIBESITHI YA PRETORIA

Faculty of Health Sciences Research Ethics Committee

1/03/2018

Approval Certificate
Amendment
(to be read in conjunction with the main approval certificate)

Ethics Reference No: 320/2017

Title: Morphometric properties and bone mineral density of the lumbar spine in a South African population: surgical considerations for spinal fusion.

Dear Miss Anya Konig

The **Amendment** as described in your documents specified in your cover letter dated 12/09/2017 received on 19/01/2018 was approved by the Faculty of Health Sciences Research Ethics Committee on its quorate meeting of 28/02/2018.

Please note the following about your ethics amendment:
- Please remember to use your protocol number (**320/2017**) on any documents or correspondence with the Research Ethics Committee regarding your research.
- Please note that the Research Ethics Committe may ask further questions, seek additional information, require further modification, or monitor the conduct of your research.

Ethics amendment is subject to the following:
- The ethics approval is conditional on the receipt of **6 monthly written Progress Reports**, and
- The ethics approval is conditional on the research being conducted as stipulated by the details of all documents submitted to the Committee. In the event that a further need arises to change who the investigators are, the methods or any other aspect, such changes must be submitted as an Amendment for approval by the Committee.

We wish you the best with your research.

Yours sincerely

*** Kindly collect your original signed approval certificate from our offices, Faculty of Health Sciences, Research Ethics Committee, Tswelopele Building, Level 4-60*

Dr R Sommers; MBChB; MMed (Int); MPharMed; PhD
Deputy Chairperson of the Faculty of Health Sciences Research Ethics Committee, University of Pretoria

The Faculty of Health Sciences Research Ethics Committee complies with the SA National Act 61 of 2003 as it pertains to health research and the United States Code of Federal Regulations Title 45 and 46. This committee abides by the ethical norms and principles for research, established by the Declaration of Helsinki, the South African Medical Research Council Guidelines as well as the Guidelines for Ethical Research: Principles Structures and Processes, Second Edition 2015 (Department of Health).

☎ 012 356 3084 deepeka.behari@up.ac.za / fhsethics@up.ac.za http://www.up.ac.za/healthethics
✉ Private Bag X323, Arcadia, 0007 - Tswelopele Building, Level 4, Room 60 / 61, 31 Bophelo Road, Gezina, Pretoria